Perspectives on LHC Physics
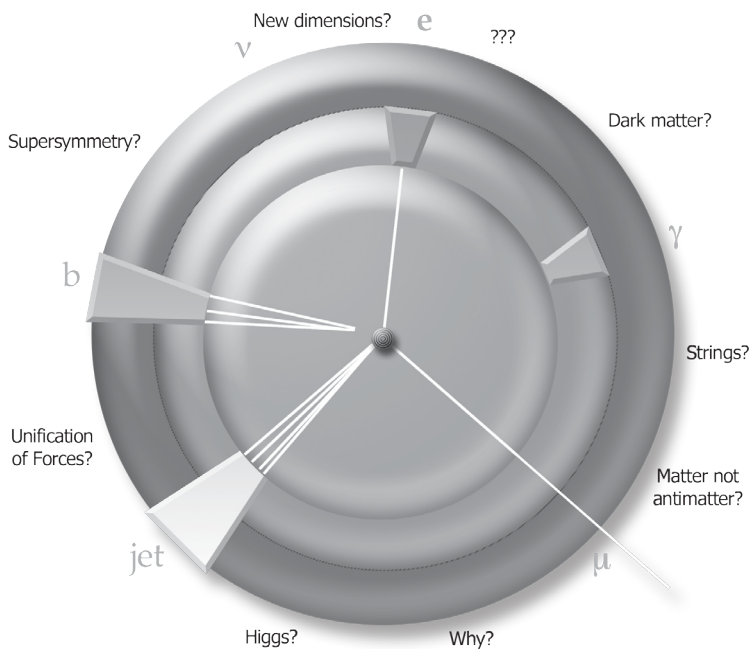
Gordon Kane | Aaron Pierce

Editors

World Scientific

Perspectives on
LHC PHYSICS

This page intentionally left blank

New dimensions?

ν   e   ???

Supersymmetry?

Dark matter?

γ

b

Strings?

Unification
of Forces?

Matter not
antimatter?

jet   μ

Higgs?   Why?

Perspectives on
LHC PHYSICS

Editors

Gordon Kane
Aaron Pierce
University of Michigan, USA

World Scientific

British Library Cataloguing-in-Publication Data
A catalogue record for this book is available from the British Library.

PERSPECTIVES ON LHC PHYSICS

**Sponsoring Consortium for
Open Access Publishing in Particle Physics**

For any available supplementary material, please visit
https://www.worldscientific.com/worldscibooks/10.1142/6686#t=suppl

Printed in Singapore

Preface

By any measure, the Large Hadron Collider is exceptional.

When the LHC begins taking data in 2008, the world's biggest experiment will be underway. The size of the undertaking is massive: thousands of scientists working at an accelerator nearly 30 km in circumference. The detectors responsible for recording the collisions have weights measured in the thousands of tons and are tens of meters on a side. The cost for this experiment is billions of dollars. Detector precision, data rates and storage, are all unprecedented.

Why take on such a massive project? Why do particle physicists, cosmologists, and others around the world so eagerly anticipate these data? It is because this machine may point the way to answer some truly fundamental questions that have puzzled scientists for decades.

Perhaps foremost among these questions is this: what lies beyond the Standard Model of particle physics? For while the Standard Model is a remarkable theory — it has thus far passed every test made at a particle accelerator — we know it must be incomplete. For example, it cannot account for the Dark Matter that we now know pervades out universe. It also provides several theoretical hints that it is not the whole story. The Standard Model's approach to the breaking of electroweak symmetry is a single new particle, the Higgs boson. While economical, this approach appears at odds with the current understanding of naturalness in physics. The LHC should finally provide definitive evidence for the physics that is responsible for the breaking of the electroweak symmetry, whether it be a single Higgs boson, or something more elegant.

The LHC will be the machine that leads us toward the fundamental theories that extend our knowledge beyond the Standard Model, and connects particle physics more strongly to cosmology. No amount of cosmology or astronomy can tell us what the dark matter actually is, or why the universe is made of matter and not equal amounts of matter and antimatter,

but the LHC may give us the data needed to answer these questions. It may also help formulate and test string theory. It is a discovery machine.

In this volume, we have tried to capture some of the excitement surrounding the impending LHC turn-on, the extraordinary detectors and experimental challenges, how the discoveries made there might unfold, and what they might mean for the future of particle physics.

<div align="right">

Gordon Kane and Aaron Pierce
Ann Arbor, Michigan, April 2008

</div>

Contents

10. Naturally Speaking: The Naturalness Criterion and Physics at the LHC   **155**

> *G. F. Giudice*

11. Prospects for Higgs Boson Searches at the LHC   **179**

> *K. Jakobs and M. Schumacher*

This page intentionally left blank

Chapter 1

The LHC — A "Why" Machine and a Supersymmetry Factory

Gordon Kane

Michigan Center for Theoretical Physics
University of Michigan, Ann Arbor, MI, 48109

"*It is as absurd to think about the origin of life*
as it is to think about the origin of matter."

Charles Darwin

The Standard Model of particle physics, and the Standard Model of cosmology are remarkable and elegant achievements. They synthesize four centuries of steady progress in understanding our world. They successfully describe all the physical universe that we see, from the everyday world around us, to the smallest objects and largest ones, back to the beginning of the visible universe and out to its boundaries. Everything we see is formed from fundamental quarks and leptons that interact via the electromagnetic, weak, strong, and gravitational forces. The forms of the forces are determined by symmetry and invariance principles. A few interaction strengths and quark and lepton masses are measured and input to the theory, and the rest can be calculated.

As is well known, even with the great success of the Standard Models there is still much we would like to understand. The Standard Models tell us what is there and how it works to form our world, but it does not tell us why it is that way. We know that about a quarter of the universe is matter, and that about a fifth of the matter is made of quarks and leptons (and that the rest of the matter is not made of quarks and leptons), but we don't know what form the rest of the matter takes. We know the universe is made almost entirely of matter and not antimatter even though it began

in a big bang with equal amounts of matter and antimatter, but we don't know why. There is good evidence that the big bang was preceded by a period of rapid inflation of space-time, but we don't know what the actual physical cause of that inflation was — it is called an "inflaton," and many possible physical causes have been examined, but so far none is convincing. The Standard Model cannot provide these understandings — it is not that the Standard Model has not yet provided them, we know it cannot.

While some information from cosmology can still constrain the answers to these basic questions, *no amount of cosmology can answer these questions.* The CERN Large Hadron Collider (LHC) is a new tool that could provide, through its discoveries, what is needed to construct a more comprehensive theory that leads to the answers to these questions and many others.

More concretely, the LHC will extend testing of the Standard Model, but that is not why we are excited about it. The Standard Model includes Higgs physics that allows the quarks and leptons and the W and Z bosons that mediate the weak force to have mass, but it does not tell us the origins of the Higgs field (of which the Higgs bosons are quanta) and how it works, nor the amounts of mass the particles have. From LEP and Fermilab data there is strong indirect evidence that Higgs bosons do exist. If so, LHC will allow us to detect them. That's exciting.

Similarly, there is strong indirect evidence that nature has a symmetry, called supersymmetry. Quantum theory taught us that there are two kinds of particles, called fermions and bosons. For example, the matter particles (electrons and quarks) are fermions, while the particles whose exchange mediates the forces (photon, gluons, W and Z bosons) are bosons. Our present description of particles and their interactions that shape our world treats the fermions and bosons very differently. Supersymmetry is the surprising idea that the fundamental theory actually treats fermions and bosons in a fully symmetric way — if you interchange them in the basic equations the resulting theory looks just like what you started with. One of its implications is that every particle has a "superpartner," and that makes the theory very testable. If nature is indeed supersymmetric in a way that helps answer the above questions, the superpartners must exist, and some of them can be detected at LHC. There is very strong indirect evidence for superpartners. If the evidence is not misleading coincidences, signals from superpartners should emerge early at LHC. Our space dimensions are bosonic ones in the sense of quantum theory. Supersymmetry also can be formulated by having every space dimension have an associated fermionic

dimension. If we collide particles with enough energy we can knock particles into the fermionic dimension and produce their superpartners. That's why LHC is so important.

If supersymmetry indeed provides the explanation for some of what the Standard Model does not explain, it also implies a rather light Higgs boson exists (one consistent with the indirect evidence for Higgs bosons), and that is another important test. Finding Higgs bosons at LHC is challenging for technical reasons (as is described in other chapters) but detecting the basic signals of the superpartners is likely to be easier since they produce a number of possible effects that can be distinguished from the Standard Model particles. Once the superpartners and the Higgs bosons are observed, their properties will help point the way to the form of the underlying theory and to how it answers the questions of the matter asymmetry and the dark matter and the identity of the inflaton, and much more.

If supersymmetry indeed is part of the correct description of nature at LHC energies there is another remarkable bonus. The supersymmetric theory can be extrapolated to near the Planck scale, so string theories can be written at their naive natural scale and then their predictions for LHC energies can be calculated. Or conversely, data from LHC and associated experiments can be extrapolated to study its implications for string scale physics. We can systematically study physics at 10^{-33} cm, or 10^{19} GeV, or 10^{-43} seconds.

1.1. A "Why" Machine

The Standard Model describes what we see very well. It tells us how things work. In my view arguably the main result that has been learned in the past two decades in particle physics and cosmology is that in order to understand nature at the most fundamental level, and to go beyond the descriptive level, the underlying theory must be formulated in more than three space dimensions. String theory requires for consistency that we live in extra space dimensions, probably wrapped up in a tiny volume of each of our three dimensional space-time points. When we project that world into our three space dimensions there are implications for forces and particles and cosmology. All the questions that are not answered by the Standard Model are at least addressed by string theory. The data from the LHC may allow us to connect the string theories to the additional questions they address, and to test whether the questions are indeed answered.

An optimist can make a defendable argument that the data from LHC and other experiments underway could be sufficient to allow us to point to and test string theories, and answer many of the unanswered questions in such a comprehensive theory. Thus I view the LHC as a "why" machine, one that may lead us to a much greater understanding of why the main things we want to understand about the world are the way they are.

Today everything we know is consistent with an elegant simple picture of the laws of nature. There is an encompassing underlying eleven dimensional M-theory that describes nature at short distances of order the Planck scale. It has solutions with six- or seven-dimensional small submanifolds. Three space dimensions inflate and grow to become our three space dimensions. At the Planck scale there are no particles or forces, but as distances increase families of quarks and leptons emerge, and the familiar forces emerge and appear to act differently. At the short distances nature is supersymmetric, and at larger distances, lower energies, the form the interactions take depends on how the supersymmetry is broken. Although we have some clues today about how supersymmetry is broken, from the absence of various rare decays and from the fact the electroweak symmetry is broken so that quarks and leptons and W's can have mass, we will learn much more from the existence of the superpartners themselves and their properties. That knowledge, combined with an increasing understanding of the theory and with clues from cosmology such as the amount of dark matter, the fact the universe is matter and not antimatter, and properties of inflation encoded in the large scale structure, could provide enough information and hints to allow clever physicists to guess the form of the underlying higher dimensional theory.

Then the theory will suggest additional tests and correlations among different phenomena, and as has always happened historically there will be great progress in understanding. What will be different this time is that the theory will address and provide answers to all the questions we have asked about the natural universe and the law(s) of nature. While some may see this framework as wishful speculation, there is today no reason to reject such a simple outcome, and much to support it. We should not give it up until we have to.

Of course the results from LHC and a few related experiments may turn out not be enough to lead to the underlying theory. Other facilities such as upgrades of the LHC, and/or a linear collider may be necessary, and data from them would certainly make it easier to get to the primary theory. I like the name "primary theory" because it suggests a ladder of effective

theories. Define an effective theory as one in which some quantities (such as quark masses and force strengths) and some principles (such as the rules of quantum theory) are input. The Standard Model of particle physics, and even the supersymmetric Standard Model, are effective theories. The primary theory is not, in that all the needed quantities and principles emerge from one underlying theory.

When I present such arguments most listeners are not immediately convinced. Of course they should not be — there are many alternative approaches to the simple world view, and many different ways the universe and the laws of nature could work. These should be studied, at the very least to learn why they don't work. LHC and related data will allow tests and distinctions. One often heard rebuttal is that historically each step forward has led to more puzzles, so that will not change. There are at least two encouraging rejoinders to this argument. The quest for understanding the laws of nature and the origin of the universe resembles the exploration of the surface of the earth. It went on for many centuries, but then one day it was over, or will soon be over. There were answers, and they were found. It is reasonable to argue the same thing will happen in our quest. There is nothing special about our time — after many centuries finally today all the major questions about the physical universe are being addressed as research questions (rather than philosophical ones). Once they are addressed as research questions usually they are answered within a few decades. The LHC may be the last major expedition needed.

Second, the Standard Model emerged in a similar way. In the late 1960s everyone felt the situation was chaotic and frustrating. Many paths were pursued. Some crucial data was known, such as parity violation, the hadron spectrum, deep inelastic scattering rates and scaling, pion and beta decay, but no coherent picture. The theory had opportunities but was puzzling. Then within a few years everything fell into place for both theory and experiment. It is certainly defendable that we are in a similar era. Some exciting approaches are right and others are not. Data will point toward some approaches and not toward others, but these are not simple yes-no tests. Rather the relevant theorists vote with their choice of what to pursue.

1.2. A Superpartner Factory

For the simple world view described above to be right and fruitful it is essential that the description of nature includes low scale supersymmetry.

Why do we expect that? There are several motivations for a supersymmetric extension of the Standard Model to be the actual description of nature at the energies where we do experiments. While these reasons have mostly been known since the 1980s I have often found that not only more general readers, but also many younger physicists, and many experimenters, and many string theorists, have not had much exposure to them, so I repeat them here in some detail.

- Supersymmetry allows the theory to have two stable but widely separated mass scales, which would in general not be possible in a quantum theory — the infamous so-called "hierarchy problem." These are the scale of the weak interactions, of order 100 GeV, and the natural scale of a fundamental theory of the forces, the Planck scale where gravitational interactions are of the same order as the other forces. Supersymmetry alone does not tell us the numerical value of the weak scale, but it stabilizes it *if some superpartners are about the same mass as the weak scale.*

- The electroweak symmetry is broken, by the Higgs mechanism, to accommodate the quark and lepton and gauge boson masses. In the Standard Model this breaking is imposed in an ad hoc way, but in the supersymmetric extension the breaking of the electroweak symmetry emerges from the theory. Further, it only does so if the supersymmetry is also a broken symmetry, so at a deeper level the two breakings are related and not two separate ones.

- In a quantum theory the effects of a force can be extrapolated to any energy, so the effects of the forces can be examined at higher and higher energies. They become more and more similar, encouraging the view that our understanding of the forces can be unified into one deeper understanding In the Standard Model they become similar but far from equal at any energy, while in the supersymmetric extension they become equal within a few per cent at about 2×10^{16} GeV. A further extrapolation to the Planck scale near 10^{19} GeV is quite plausible (and can be studied in any specific theory). The jargon for this is "gauge coupling unification" because the strengths of the separate forces are determined by the gauge theory couplings.

- It has been known for over two decades that the dark matter of the universe can be accounted for if a stable particle exists with a mass of order the weak scale, 100 GeV or so, and can annihilate

with itself with a cross section of typical weak interaction strength. Generically the lightest of the superpartners (the "LSP") is such a particle. Both Standard Model particles and superpartners are produced in the Big Bang. After a while all the particles have decayed but photons, neutrinos, electrons, up and down quarks, and the LSP. The amount of energy density supplied by the LSP is typically about right to account for the actual dark matter. Indeed, before it was known that dark matter not made of normal matter actually formed most of the dark matter it was predicted that the LSP would provide such dark matter.

- In the Standard Model it is not possible to explain why the universe is matter rather than equal amounts of matter and antimatter. In the supersymmetric extension there are actually several ways to explain this. Each has tests, and the LHC can provide crucial information for some of the tests.

- The LEP collider at CERN taught us four major qualitative results. One is that the number of families with light neutrinos is three. Second is the values of the force strengths to high accuracy so they could be extrapolated to high energies and be seen to unify in the supersymmetric extension of the Standard Model as described above. Third, LEP measured accurately some 20 independent properties of the Z boson and its decays, all of which were predicted by the Standard Model. The Standard Model predictions depended on only one unmeasured parameter, the mass of the Higgs boson. A good fit to all the data could be found if the Higgs boson mass were less than about 165 GeV, implying the Higgs boson existed with a mass in that range. Higgs bosons occur naturally in supersymmetric theories, and in general there is an upper limit of about twice the Z boson mass, about 180 GeV, on the mass of the lightest Higgs boson in supersymmetric theories that stay perturbative to the unification scale. Thus this LEP result is consistent with the supersymmetry prediction. That experimental result is reinforced by the logically independent result that the range of Higgs masses giving the measured W and top quark masses (adding Fermilab data) also has an upper limit of about the same value as the LEP fit.

- The fourth LEP result is that no measurement deviated significantly from the Standard Model prediction. That is natural in a supersymmetric world where the superpartners are either light

enough to be produced directly, or only enter in loops and therefore affect observables at most of order a part in a thousand. All alternative models would naturally have strong interactions at the TeV scale and would typically give significantly larger deviations from the Standard Model. The alternative models can be adjusted and tuned to not disagree with the data, but before the data one would have expected larger effects.

- All the above successes occur simultaneously. Often models can explain one thing but then they get into problems with another. Further, the supersymmetry theory existed (since the mid-1970s) before any of the listed successes. It was not invented to fit or explain any of them. They were recognized as the theory was studied, from about 1980 through the early 1990s.

Thus the motivation for finding that supersymmetry is a part of our description of nature at the TeV scale is very strong. If that is indeed so, then at least some of the superpartners must not be too heavy, and will be produced at LHC. In order to retain the above listed successes probably the partners of the gauge bosons and Higgs ("gauginos") must be at or below about a TeV. The production rates of these particles depend on their masses, which are not yet calculable from what is known about the theory, but the rate for gluinos has a sizable minimum value from the QCD coupling to gluons. For example, a gluino of mass 750 GeV will give about 500 events in the first 100 pb^{-1} of integrated luminosity. If the initial running goes as expected that amount of data could be taken in a few weeks or less. That number of events is sufficient to recognize a signal for new physics, and probably even to allow some initial tests that gluinos have spin 1/2 as predicted, and other tests that what is seen is indeed supersymmetry. After a couple of years and the higher luminosities expected there will be tens of thousands of gluinos. They will decay into other superpartners, and other superpartners will be produced in additional ways, and all can be studied.

The above arguments that supersymmetry must exist at the weak scale are based on indirect evidence, and are not compelling for some people. There are also a few worrisome isssues that could be of concern. They can be summarized by saying that the Z boson mass is too small, the Higgs boson mass is too large, and third that flavor mixing effects should already have been seen. The Z mass seems too small because the theory explains it in terms of superpartner masses, and the relevant superpartner masses

seem to be at least a few times the Z mass, so one is calculating a small number in terms of several that are noticably larger. Effectively one is invoking cancellations to get the small answer, and that usually is not a good thing. The Higgs boson mass is too large in the sense that there is a lower limit on it from data under most conditions, and that lower limit is uncomfortably large in many concrete theories; it should already have been observed. There are a number of ways around this concern, but some require somewhat special circumstances. The third says if one thinks of supersymmetry as a low scale theory then it would be typical for flavor mixing to occur, so decays such as $\mu \rightarrow e + \gamma$ should occur and so far they do not. For me and many other theorists these are interesting puzzles (puzzles of course are meant to be solved) but not nearly as negative as the successes are positive. The first concern, that the smallness of the Z mass needs explaining, is the most significant issue.

1.3. Our String Vacuum

Although I and many of us have great affection for superpartners, we value them not for themselves but for what they can tell us about our world, and about the "why" questions described above. Presumably we live in a string theory vacuum (including M theory — I don't distinguish here). I expect string theory to be the relevant approach not because it is a quantum theory of gravity, but because it can address all the "why" questions. We want to understand the properties of our vacuum qualitatively at least, including the hierarchy between the weak interaction scale and the Planck scale, the origin of supersymmetry and its breaking, the origin of the electroweak symmetry breaking and the Higgs mechanism and their connection to the supersymmetry breaking, the origin and value of the puzzling "μ parameter," parity violation, CP violation (interestingly, parity and CP violation seem to have very different proximate origins in string theory, the first in the presence of chiral representations and the second in complex phases), the origins of quarks and leptons and their mass hierarchies, the origins of the forces, what the dark matter is and how much there is, the matter asymmetry, the physical origin of inflation, and perhaps more. We also want to understand how inevitable these properties are, and their uniqueness. There may be many solutions of string theory that are acceptable vacua, and led by data and the connection via supersymmetry to the natural scales of string theory we may be able to learn about our string vacuum and test such ideas with its predictions.

Learning all of this from hadron collider data will not be simple. But what is observed at LHC *will depend on* the properties of the LSP that is the dark matter, and on the form the extra dimensions take, and other aspects of the underlying theory. Study of the footprints of different theories on plots of observable signatures may allow us to systematically comprehend the essential features of the underlying theory.

The connection of the LHC and its implications to dark energy is less clear, but once there is insight about our vacuum there may be progress in that direction too. Personally I don't think the dark energy is the most important problem in physics. I expect we will first learn about the underlying theory from clues provided by the LHC, and then see how the dark energy arises in that theory. It will not be surprising, I think, if the dark energy is explained from less naive use of quantum theory than we presently use in describing the vacuum, and if the dark energy explanation has little impact on the other important physics questions.

1.4. After the Champagne

The first challenge will be to establish that a signal of new physics is present. That will be done by the experimenters, based on our understanding of the Standard Model.

Then two challenges/opportunities are paramount. First we need to establish that what is seen is indeed supersymmetry or not. I think that will not be difficult. If production of gluinos and/or squarks is large, it will be fairly easy to establish their spins are the needed ones for partners of the Standard Model particles. Additional characteristic signatures and related channels are likely to occur, such as same sign dileptons that arise from the Majorana gauginos, or events with extra missing energy or with larger numbers of jets and/or charged leptons.

The second is to learn about the dark matter of the universe (see Aaron Pierce's chapter). If the LSP is escaping the detectors we can study it, e.g. get information about it mass and determine in what channels it is produced. That may tell us about the main things we need to know to calculate the associated relic density, and perhaps even to learn about the cosmological history of the universe.

Then as data accumulates we will begin to relate what is observed to the underlying theory. If supersymmetry is indeed seen and studied at the LHC it effectively changes the limits of science, and lets us turn from speculation

about the ultimate laws of nature to systematic study of those laws at the shortest distances. Progress may be rapid in that quest too.

The LHC and its results have been anticipated for a long time,

"*Many shall run to and fro, and knowledge shall be increased,*"

Book of Daniel 12:4

This page intentionally left blank

Chapter 2

Dark Matter at the LHC

Aaron Pierce

Michigan Center for Theoretical Physics
450 Church St., Ann Arbor, MI, 48109
atpierce@umich.edu

The majority of the universe is composed of some exotic substance, presumably an unknown particle. There are strong indications that this new particle may be produced at the LHC. We review how we came to believe that the universe was mostly of unknown composition, and discuss a few candidates for the identity of the mysterious Dark Matter.

2.1. Introduction

Of what is the universe made? Perhaps there is no more basic question that fundamental physics might wish to address. We can confidently state that we do not know the answer to this question. This state of affairs is possibly unique in human history. Over two thousand years ago, Empedocles declared that all is made of Earth, Air, Fire and Water. Similar claims were made in Chinese and Indian texts of the same era.

The confident (and incorrect) answer has gone through many iterations since. Particle physicists from the middle of the twentieth century might have felt secure in their knowledge that the vast majority of the universe was comprised of protons and neutrons.

Today the situation is different. We are no longer confident that we know what comprises the universe. Rather, we are assured in our ignorance. How did we come to this state?

2.2. Weighing the Universe, or Why Expect Dark Matter?

As early as 1933, Fritz Zwicky made observations of the Coma Cluster that indicated the possible presence of Dark Matter [1]. Zwicky realized that

the numerous galaxies that made their home in the cluster were moving too fast. The gravitational pull of the luminous matter present in the cluster was insufficient to balance the outward "centrifugal force" of the matter. Without a dark component, the cluster would pull itself apart.

We now know that a similar conundrum exists when the rotation of individual galaxies is considered. The rotation speeds of galaxies themselves can be determined as a function of radius by making red shift measurements, and taking advantage of the optical Doppler effect. Newton's law of gravitation indicates the rate of rotation depends on the enclosed mass. If luminous matter were the whole story, then the rotational speeds of galaxies should begin to fall off with radius beyond the bright core as $v(r) \sim r^{-1/2}$. This is not what is observed — rotation curves remain stubbornly constant at radii far exceeding the luminous core, indicating a dark component of mass. This evidence supports the notion that galaxies posess a halo of Dark Matter.

Both of the above arguments rely on simple kinematics. Velocity measurements, coupled with an understanding of the gravitational force, results in a mass measurement. Arguments with this flavor still have a place in the determination of the amount of Dark Matter in our universe. But to say how much Dark Matter the entire universe contains, one has to go beyond the statement that a given galaxy has a non-luminous component. The key is to make sure that the region of space to which one are applies the kinematic argument represents a fair sample of the universe as a whole. It is thus advantageous to sample as large a region as possible. Remarkably, these measurements are consistent with a host of others that all indicate the need for exotic Dark Matter. We now turn to these alternative measurements.

The most precise determinations of the Dark Matter abundance now come from exquisite measurements of the Cosmic Microwave Background Radiation (CMBR). This radiation, left over from the Big Bang, provides a wealth of information about cosmological parameters. In 1989 the COBE satellite made measurements that indicated the universe is a black body to very high accuracy. This feat resulted in the Nobel Prize in physics in 2006. This strongly suppors the hypothesis that the universe expanded from a hot, dense medium. Shockingly, this experiment is considered a gross measurement by today's standards. More recent experiments, both satellite and balloon borne, have measured the deviations from the pure black body spectrum. These hot and cold spots, present at the 10^{-5} level, were imprinted in the very early universe, as quantum fluctuations from

an inflationary epoch. But before the fluctuations reach our experiments, they are processed by the intervening physics (in both space and time). This processing depends in detail on the underlying cosmological parameters — in particular, the amount of Dark Matter. As the amount of Dark Matter changes, both the observed strengthand the angular size of these flucutations change. By fitting to these paramters, one can extracts an $\Omega_{DM} h^2 = 0.106 \pm 0.008$. Importantly, these same experiments provide a sensitive probe of the combined mass of baryons (ordinary protons and neutrons). Here, they find $\Omega_{baryon} h^2 = 0.0223^{+0.0007}_{-0.0009}$. Thus, one finds that the Universe has nearly six times as much Dark Matter as ordinary matter.

It is important to emphasize that multiple independent measurements have been made of both the Dark Matter and baryon densities. They are all consistent.

As an example, the density of baryons can independently be measured by considering the primordial abundances of the light elements. In the crucible of the hot Big Bang, Deuterium, Helium and Lithium can all be synthesized. The relative abundances depends on well understood, Standard Model physics (for example, nuclear cross sections) and the density of baryons in the universe. So, a measurement of these light element abundances can be converted into a measurement of the baryon density.[a] These measurements imply a baryon density $0.017 < \Omega_{baryon} h^2 < 0.024$, consistent with the above [5].

Another class of measurement takes the measured fluctuations from the CMBR, and asks whether these fluctuations could grow into the large scale structure (galaxies and clusters) that we observe today. The tiny fluctuations grow simply based on gravitational clumping. The type of structure that forms, unsurprisingly, depends on the amount and type of material that is clumping. Current simulations indicate that a universe with a substantial Dark Matter component is consistent with observations. A universe without this Dark Matter grows insufficient structure.

Weak lensing represents another way to measure the Dark Matter directly. Arthur Eddington's expedition of 1919, confirmed Einstein's prediction that gravity bends light by observing starlight bent by the sun during an eclipse. This lensing phenomenon implies that any localization of

---

[a]It should be said that measuring the primordial abundance of these elements is nontrivial. One cannot simply measure the amount of deuterium in the universe today. After all, one would expect substantial processing to take place in stars, converting these light elements to heavier ones. The trick is to look in regions of low metallicity, a tracer for stellar activity.

matter can be observed by the way that it distorts the background sources of light. The effects of Dark Matter have now been observed in this way, see, e.g., [6].

The key point to take away from this discussion is that there are several measurements of the amount of Dark Matter, using different techniques, and they all agree. The fact that all the measurements are consistent lends credence to the hypothesis that the new physics involved is, in fact, Dark Matter, and not, e.g., a modification of the force of gravity.

Recently, a striking observation of the Bullet cluster further buttressed the interpretation of the above measurements as Dark Matter. In 2006, lensing observations were made of two clusters of galaxies that had relatively recently passed through one another [7]. Observations were simultaneously made of the gas that makes up the majority of the visible matter. The collision caused this Dark Matter to be displaced from the visible gas. The result is a system (unlike our own galaxy) where the Dark Matter is no longer co-centered with the visible matter. Precisely because the gravitational effects induced by the Dark Matter do not physically overlap with the visible matter, the measurements of this system are difficult to reconcile with ordinary matter interacting with a modified gravitational law.

2.3. What is the Dark Matter?

It now seems clear that there is Dark Matter. We can point to its effects in a myriad of astrophysical and cosmological settings. We can quantify how much there is with an impressive accuracy. Yet, at present, its identity remains a complete mystery.

What we can say with certainty is that the Dark Matter is *not* — a particle that we already know about in the Standard Model. As discussed in the previous section, we know the the Dark Matter is not made up of baryons, and thus cannot be non-luminous dust or "Jupiters." The remaining possibility for a Dark Matter candidate within the Standard Model was the neutrino. After all, it is electrically neutral, and we know that it exists. However, the neutrino is too light to function effectively as the Dark Matter of the universe. Were it present in the relic abundance indicated by the experiments of the previous section, it would wash out structures on small scales.

So, we must move beyond the Standard Model. But to where? At present, there are many candidates for the Dark Matter. Part of the mission of the Large Hadron Collider is the illumination of the identity of which of

these candidates is realized in nature. Astrophysics has told us that there *is* Dark Matter. Particle physics holds the hope of telling us what that Dark Matter is.

Typically, Dark Matter candidates have been recognized in the following indirect way. A theory of new physics beyond the Standard Model is constructed to solve some other problem, often the gauge hierarchy problem (see, e.g., [4] for a discussion of this issue). Typically this theory predicts a panoply of new particles beyond those already known. Often one of these particles can be recognized as a viable candidate for the Dark Matter, which is viewed as a "check mark" — a piece of corroborating circumstantial evidence for the validity of the theory. This is consistent with the overall reductionist drive of particle physics (some might call it Occam's razor). If there are multiple problems that need solving, nature should choose the most economical solution, thus a theory that can solve multiple problems is favored.

Of course, there is another approach: nature may have chosen a particle that gives the right properties for the Dark Matter, without connecting the Dark Matter to any other problems in particle physics. In this case, aesthetic considerations would argue that the Dark Matter sector should be minimal — perhaps the Dark Matter particle and nothing else. After all, if the Dark sector is not doing anything besides providing Dark matter, shouldn't nature have chosen a simple and elegant way of realizing the Dark Matter?

In either case, it appears that it is likely that the Dark Matter will be found near the weak scale. The argument is an old one, implicit in, e.g., [8]. If we assume that the Dark Matter was in thermal equilibrium with all other species following the Big Bang, we can calculate the amount that is remaining as a "thermal relic" by balancing the expansion rate of the universe against the tendency of the Dark Matter to self-annihilate into ordinary matter. When the rate of expansion is too large, the Dark Matter is no longer able to find other Dark Matter with which it might annihilate. At this point, the amount of Dark Matter freezes out and annihilations become unimportant. Then the amount of Dark Matter is essentially determined. To an reasonable approximation, the equation that summarizes this fight between expansion and annihilation is:

$$\Omega_{DM} h^2 = C \frac{T_0^3}{M_{pl}^3} \frac{1}{\langle \sigma v \rangle} \tag{2.1}$$

where the C is constant that is known and caculable in terms of quantities like, e.g., the number of species of light particles at the freezeout. T_0 is the current CMBR temperature and M_{pl} is the Planck mass. As the thermally averaged cross section, $\langle \sigma v \rangle$, increases, the amount of annihilation increases, and the residual amount of Dark Matter decreases.

To be consistent with the measured amount of Dark Matter, $\Omega_{DM} h^2 = 0.106 \pm 0.008$, the thermally averaged cross section must be $\langle \sigma v \rangle \approx 1$ pb. One can find the approximate value of the mass scale associated with the annihilation by equating

$$\langle \sigma v \rangle \approx \frac{\alpha^2}{m^2}. \tag{2.2}$$

One then finds an $m \approx 100$ GeV. The quantities of Eq. (2.1) are related related to the expansion of the universe (e.g. M_{pl}) and the current energy density in radiation. It is striking that these should conspire to should generate a scale of 100 GeV, already known to be an interesting scale for particle physics. It is possible that the scale generated via Eqs. (2.1), (2.2), could have been an entirely novel scale. The fact that it coincides with the weak scale is striking! Dark Matter may be associated with the physics responsible for electroweak symmetry breaking.

2.4. A Test Case: Supersymmetric Dark Matter

Supersymmetric theories (for reviews see [2], note also [3] in this volume), are the leading theory for new physics beyond the Standard Model at the weak scale. They posit a doubling of all known particles — every observed particle should have a doppleganger particle waiting to be observed at the LHC. If one writes down a (too) simple supersymmetric theory, one finds that the proton would decay in a fraction of a second, not to mention conflict with a cornucopia of experiments that look for rare flavor changing decays. While it is possible to adjust the parameters of this theory to agree with the constraints above, there is a more economical approach. The simple addition to the theory of a discrete symmetry solves, in a single stroke, all these problems, and simultaneously makes the lightest superpartner absolutely stable. So, unlike all the other superpartners created in the thermal bath of the Big Bang, the lightest one has not decayed away.

So, what is the identity of the lightest supersymmetric particle (LSP)? Since is is "dark", it must be electrically neutral. This means that it is the partner to an uncharged particle of the Standard Model. Essentially, this leaves three options. First, the particle can be the partner to the neutrino.

In its simplest incarnation, this possibility is now excluded by underground "direct-detection" experiments designed to look for Dark Matter by observing it bouncing off of nuclei. Second, it can be the partner to the graviton. This possibility has been a subject of renewed study of late [11, 12], and is certainly viable.[b] Thus, we focus on the third logical possibility: the Dark Matter as partner to an admixture of the neutral particles that mediate the forces of the Standard Model (photons, Z bosons, Higgs boson). This mixed particle is known as a neutralino. There is a certain poetry to the possibility that the "dark" matter may well be composed of the doppleganger to light.

2.4.1. *Neutralinos at the LHC*

The relic abundance of the neutralino depends on its precise identity. In many theories, the particle is approximately a bino, the superpartner of the $U(1)_Y$ hypercharge gauge boson of the Standard Model. The bino does not interact via gauge interactions. Thus, if gauge interactions were the entire story, a pure bino would not annihilate, and too much Dark Matter would remain. Fortunately, gauge interactions are not the whole story. For example, if there is a superpartner of one of the quarks or leptons squark that is sufficiently light, interactions of these partners with the bino can effectively reduce the abundance in the early universe. (see, e.g., [9] for a review of these possibilities and their phenomenology).

If the Dark Matter is predominantly Higgsino or wino in character, then it annihilates very effectively via gauge interactions to gauge bosons. There is a danger that too little Dark Matter would remain. Thus, by dialing the mixture of bino and wino/Higgsino, one can get a LSP that correct reproduces the Dark Matter relic abundance. This notion of a well-tempered neutralino was recently discussed in [10].

How does the LSP look at the LHC? Dark Matter escapes the LHC detectors as missing energy. The moment that an excess of events are observed with missing energy, it will be natural to assume that the Dark Matter has been found. After all, an invisible (i.e. dark) particle will have been found near the scale predicted by Eq. (2.1). However, to conclude that the particle (un)observed at the LHC is actually the Dark Matter will require substantially more work. The hope to determine the identity of the Dark Matter

---

[b]In this case, the argument for the correct relic abundance is slightly less direct. The relic abundance is "inherited" from the next to lightest supersymmetric particle (NLSP). The NLSP can have the correct thermal abundance *a la* Eq. (2.1). As long as the gravitino and the NLSP have nearly the same mass, the gravitino will have the correct relic abundance, too.

does not rest on observation of events with Dark Matter particles alone. Instead, one should analyze the full suite of supersymmetric events at the the LHC. Often these events can be long cascade chains — information about the masses and couplings of the particles in the decays will be vital in determining that the new particles are remnants of a supersymmetric theory (and not some other new physics).

Once it is relatively clear that the new physics is supersymmetry, there is still the task of identifying the LSP. Determining whether the LSP is a well-tempered mixture or a bino annihilating with the help of a light sparticle will be a challenge, though certainly not impossible, at least at the qualitative level. For example, the discovery of a light stau or a light stop would be a strong indication that they are important for setting the observed Dark Matter relic abundance. Detailed quantitative statements are more difficult at the LHC, the recent review of [9] discusses some of the challenges of determining the identity of the Dark Matter in the context of supersymmetric models.

2.5. Simple Dark Matter

The theory of the last section was particularly well-motivated because the Dark Matter came from a theory motivated by completely separate considerations. Even absent the presence of a good Dark Matter candidate, people would be excited about supersymmetric theories. The fact that it can naturally explain the Dark Matter is gravy.

But what if those other pieces of evidence (the hierarchy problem [4], the apparent unification of gauge couplings) are a red herring? In this case, one is led towards very different theories of the Dark Matter particle. It is, after all, possible to correctly reproduce the thermal relic abundance (2.1), without the entire superstructure of supersymmetry.

Typically, the collider phenomenology of the theories unmotivated by the hierarchy problem is somewhat limited. This is unsurprising. Due to its high gluon luminosity, the LHC is a machine that excels at producing colored objects. If there is only Dark Matter and no colored matter to be found, then discovery becomes much more challenging.

One possibility is that there could be a single scalar particle coupled to the Higgs boson [13]. This signal of this theory would be a modification of the properties of the Higgs boson — it could dominantly decay "invisibly," and its discovery could occur simultaneously to the discovery of Dark Matter!

Another option, recently championed in [14], is a single multiplet charged under the $SU(2)_L$ weak force. In this case, the Dark Matter again annihilates efficiently via the gauge interactions. To have enough Dark Matter, the new particle must be somewhat heavy, often a couple TeV. Such a particle would be difficult to observe at the LHC, but might be observed at future accelerators (if a machine with sufficient energy will built), or indirectly, via annihilation to gamma rays at the center of our galaxy.

2.6. What If We Don't See Dark Matter at LHC?

If no Dark Matter is observed at the LHC, how do we proceed? One hope is that other experiments designed to observe weak scale Dark Matter will succeed. After all, these experiments rely on rather different approaches in their quest to detect the Dark Matter.

Another possibility is that the whole idea of Dark Matter at the weak scale is incorrect. In this case, one still has to explain the now overwhelming data from the astrophysical experiments that indicates the existence of Dark Matter. The most likely conclusion in this case is that the Dark Matter is made up of some completely different entity, having nothing to do with the TeV scale.

One option is the axion, see [15]. This particle, as recognized by Weinberg and Wilczek, was a consequence of Peccei and Quinn's attempt to solve what is known as the strong CP problem. It passes the test of economy — its existence was posited for purposes other than explaining the Dark Matter. Furthermore, axions now appear to arise quite naturally in string theory constructions.

2.7. Conclusions

The example of Big Bang Nucleosynthesis discussed in Sec. 2.2 is especially useful because it also shows how we can gain confidence about the history of the Early Universe. The calculation had three inputs: known Standard Model particle physics, an unknown parameter (the baryon abundance), and crucially, a standard cosmological history. The output was predictions for the abundance of not one, but several light elements. If these predictions were not consistent for any value of the baryon abundance, then this would have been a signal that our assumption of a standard cosmological history was incorrect. The fact that they do agree tells us that we have a quantitative understanding of the history of the universe back to

the time of BBN. One can imagine doing something similar for the Dark Matter.

Suppose a Dark Matter candidate is discovered at the LHC. Suppose we can glean enough about its properties to compute how much Dark Matter should be left over, assuming a standard thermal history for the universe. We could then compare this value to the observed value for the Dark Matter abundance. Two outcomes are possible. If the observed values agree, that tells us that we understand the thermal history of the universe quantitatively back to the time when the Dark Matter's abundance was being determined, $T_{fr} \sim GeV$. This is approximately three orders of magnitude beyond our current understanding of $T_{BBN} \sim MeV$.

The other outcome is that the two numbers do not agree. Then there are two possibilities. It could be that the particle that looked like the solution to the Dark Matter puzzle was a red herring. It might only make up a small fraction of the current Dark Matter budget. Whether this possibility holds can be tested by looking for the Dark Matter in other experiments (so-called direct and indirect detection) — if the particle found there can definitively be shown to be different from the particle found at the LHC, then we know the LHC particle is not the dominant component of the Dark Matter. The particle found in the new experiments is, and we will need to understand how to study it in more detail. On the other hand, if the particle found in these experiments appears to be one and the same with the particle found at the collider, then we have discovered something very interesting about the history of the universe. Something must have happened to change the abundance of this particle. This would mean that the Standard Big Bang scenario is incorrect, and we have made a fundamental discovery in cosmology.

Acknowledgments

References

[1] F. Zwicky, Die Rotverschiebung von extraglaktischen Neblen, *Helvetica Physica Acta* **6**, 110-127 (1933).

[2] H.P. Nilles, Supersymmetry, Supergravity and Particle Physics, *Phys. Rep.* **110**, 1 (1984); H.E. Haber and G.L. Kane, The Search for Supersymmetry: Probing Physics Beyond the Standard Model, *Phys. Rep.* **117**, 75 (1985); S.P. Martin, *A Supersymmetry Primer*, in *Perspectives on Supersymmetry*, ed. G.L. Kane (World Scientific, Singapore, 1998), p. 1.

[3] G. Kane, this volume.

[4] G. Giudice, this volume.

[5] W. M. Yao *et al.* [Particle Data Group], Review of particle physics, *J. Phys. G* **33**, 1 (2006).

[6] D. J. Bacon, R. J. Massey, A. R. Refregier and R. S. Ellis, Joint Cosmic Shear Measurements with the Keck and William Herschel Telescopes, *Mon. Not. Roy. Astron. Soc.* **344**, 673 (2003), [arXiv:astro-ph/0203134].

[7] D. Clowe, M. Bradac, A. H. Gonzalez, M. Markevitch, S. W. Randall, C. Jones and D. Zaritsky, A direct empirical proof of the existence of dark matter, *Astrophys. J.* **648**, L109 (2006) [arXiv:astro-ph/0608407].

[8] B. W. Lee and S. Weinberg, Cosmological lower bound on heavy-neutrino masses, *Phys. Rev. Lett.* **39**, 165 (1977).

[9] E. A. Baltz, M. Battaglia, M. E. Peskin and T. Wizansky, Determination of dark matter properties at high-energy colliders, *Phys. Rev. D* **74**, 103521 (2006) [arXiv:hep-ph/0602187].

[10] N. Arkani-Hamed, A. Delgado and G. F. Giudice, The well-tempered neutralino, *Nucl. Phys. B* **741**, 108 (2006) [arXiv:hep-ph/0601041].

[11] J. L. Feng, S. Su and F. Takayama, Supergravity with a gravitino LSP, *Phys. Rev. D* **70**, 075019 (2004) [arXiv:hep-ph/0404231].

[12] J. R. Ellis, K. A. Olive, Y. Santoso and V. C. Spanos, Gravitino dark matter in the CMSSM, *Phys. Lett. B* **588**, 7 (2004) [arXiv:hep-ph/0312262].

[13] J. McDonald, Gauge Singlet Scalars as Cold Dark Matter, *Phys. Rev. D* **50**, 3637 (1994) [arXiv:hep-ph/0702143]; C. P. Burgess, M. Pospelov and T. ter Veldhuis, The minimal model of nonbaryonic dark matter: A singlet scalar, *Nucl. Phys. B* **619**, 709 (2001) [arXiv:hep-ph/0011335]. H. Davoudiasl, R. Kitano, T. Li and H. Murayama, The new minimal standard model, *Phys. Lett. B* **609**, 117 (2005) [arXiv:hep-ph/0405097].

[14] M. Cirelli, N. Fornengo and A. Strumia, Minimal dark matter, *Nucl. Phys. B* **753**, 178 (2006) [arXiv:hep-ph/0512090].

[15] F. Wilczek, this volume.

This page intentionally left blank

Chapter 3

LHC's ATLAS and CMS Detectors

Maria Spiropulu[1,*] and Steinar Stapnes[1,2,†]

[1]*Physics Department, CERN*
CH-1211 Geneva, Switzerland
[2]*Department of Physics, University of Oslo*
0316 Blindern, Oslo, Norway
[*]smaria@cern.ch
[†]Steinar.Stapnes@cern.ch

We describe the design of the ATLAS and CMS detectors as they are being prepared to commence data-taking at CERN's Large Hadron Collider. The very high energy proton-proton collisions are meant to dissect matter and space-time itself into its primary elements and generators. The detectors by synthesizing the information from the debris of the collisions are reconstituting the interactions that took place. LHC's ATLAS and CMS experiments (and not only these) are at the closest point of answering in the lab some of the most puzzling fundamental observations in nature today.

3.1. Introduction

The Large Hadron Collider (LHC) [1] is the largest and most complex scientific undertaking ever attempted. Its results will determine the future of the full discipline of high energy physics. The LHC will produce 14 TeV proton-proton collisions in the next year and we expect it will discover a new sector of particles/fields associated with electroweak symmetry breaking and dark matter. The two major experimental observations behind this expectation are:

(1) the masses of the W and Z vector bosons;
(2) the dark matter in the universe.

These, in concert with the theoretical considerations are corroborative evidence for physics mechanisms that broaden the Standard Model.

Both the ATLAS (A large ToroidaL ApparatuS) [2, 3] and the CMS (Compact Muon Solenoid [4–6]) experiments are in the stage of commissioning and integration. The experiments have been collecting cosmic data with the major detectors in place already since 2006 (see for example an event display of a cosmic muon observed at the CMS Magnet and Cosmic Test runs in Fig. 3.1 and a recent one at ATLAS in Fig. 3.2) and finalizing the analysis of beam tests of most-all detector elements. The experiments are also preparing the strategies for the careful understanding and use of the Standard Model data at 14 TeV.
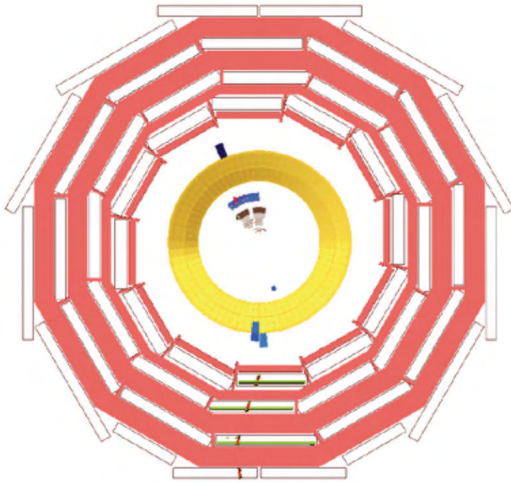
Fig. 3.1.   This "gold plated" event going through all central detectors — the tracker, the hadronic calorimeter, HCAL (top and bottom), the electromagnetic calorimeter ECAL and the muon Drift Tubes — it was recorded in August 2006 in the CMS assembly hall at Point 5; Run No. 2378, event 123 at a magnetic field of 3.8 T.

3.1.1. *LHC: The machine*

The LHC is built in a circular tunnel 27 km in circumference. The tunnel is buried around 50 to 175 m underground and straddles the Swiss and French borders on the outskirts of Geneva as shown in Fig. 3.4. It will circulate the first beams in the summer of 2008 and provide first collisions at high energy soon after.

The LHC is at the edge of the accelerator based energy frontier as illustrated in the "Livingston plot" shown in Fig. 3.3. Note that since the
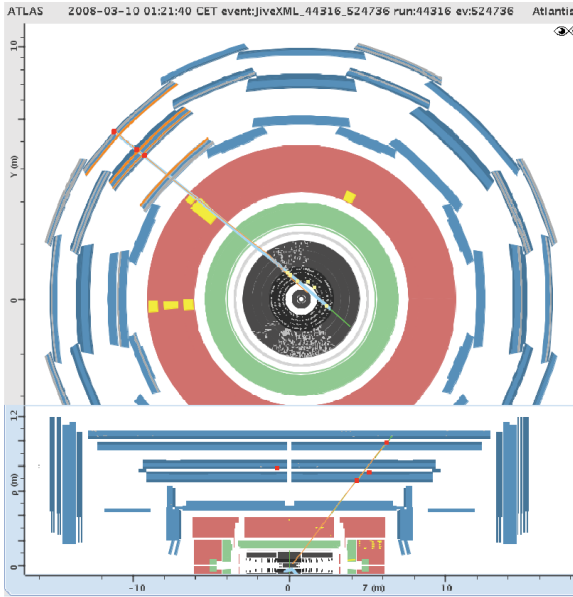
Fig. 3.2.   This cosmic muon event recorded with ATLAS is going through all barrel detectors. The tracker (silicon strip and straw tracker), hadronic calorimeter and muon detectors were read out, while the barrel liquid argon calorimeter (been operated in several periods earlier) and pixel system (being cabled) were not read out. The event was recorded in Mach 2008 at Point 1.

30's (with the 600 MeV Cockcroft-Walton — not shown here) the effective energy increase is more than 11 orders of magnitude while the effective cost per GeV of a typical accelerator is drastically reduced (see also [7]). In accelerator based high energy physics experiments, the type and number of particles brought into collision and their center of mass energy characterize an interaction.

The limitation on the energy for a proton accelerator storage ring is the maximum magnetic field to bend the particles ($R_{\rm ring}(\rm m) = P(\rm GeV)/0.3B(\rm Tesla)$). For an electron storage rings it is the energy lost to synchrotron radiation per revolution ($U \approx 0.0885 E(\rm GeV)^4 R(\rm m)^{-1}$). For relativistic proton beams this is $\approx 7.79^{-15} E(\rm GeV)^4 R(\rm m)^{-1}$. At the LHC this amounts to about 3.6 kW per beam and is absorbed by the cryosystem). The largest electron-positron storage ring was the 27 km LEP ring at CERN in Geneva. It is expected that all future electron-positron machines at higher energy than LEP will be linear.
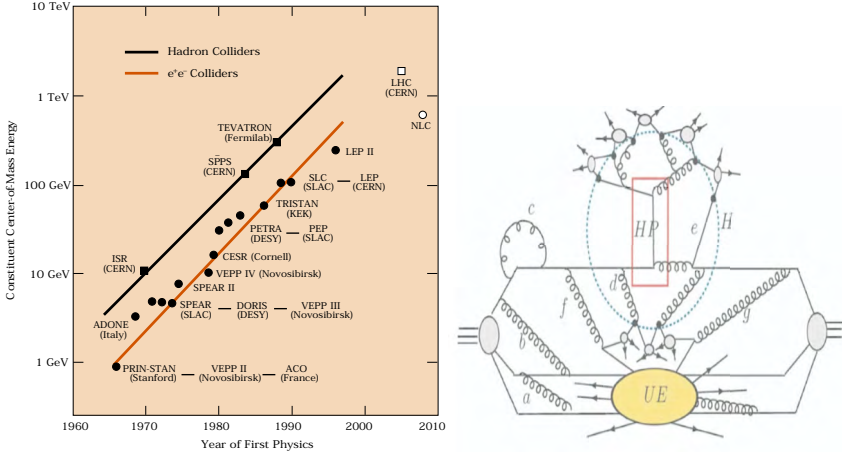
Fig. 3.3. (Left) A variant of the "Livingston plot" showing the energy in the constituent frame of electron-positron and hadron colliders constructed (filled circles and squares) or planned. The energy of hadron colliders has here been derated by factors of 6-10 in accordance with the fact that the incident proton energy is shared among its quark and gluon constituents. (Right) Phases of the hardon-hadron interaction; beads represent hadrons, straight lines quarks and springs gluons. HP indicates the hard process, and UE the underlying event, i.e. the remnants of the protons.

The LHC is colliding proton beams. A monoenergetic proton beam is equivalent to a wide-band parton beam (where parton≡quarks, anti-quarks, gluons), described by momentum distribution dn_i/dp (also referred to as structure function) where i specifies the parton type, i.e. u, d, g, $\bar{u}$, $\bar{d}$. Proton structure functions are measured in deep inelastic scattering experiments. Some of the advantages of hadron collisions include the simultaneous study of a wide energy interval, therefore there is no requirement for precise tuning of the machine energy; the greater variety of initial state quantum numbers, e.g. $u + \bar{d} \rightarrow W^+$, $\bar{u} + d \rightarrow W^-$; the fact that the maximum energy is much higher than the maximum energy of e^+e^- machines; and finally that hadron collisions are the only way to study parton-parton collisions, including gluon-gluon. Some of the disadvantages are the huge cross sections for uninteresting events; the multiple parton collisions in the same hadron collision that result in complicated final states; and that the center-of-mass frame of the colliding partons is not at rest at the lab frame. Figure 3.3(right) [8], illustrates the phases and complexity of a hadron-hadron interaction. In this example HP is the hard process in which a gluon (d) form the left collides with a quark (e) from the right. This

process can be approximately described as an interaction among fundamental freely moving constituents of the proton. The boundary region denoted with a dotted line (H) includes the radiation process that has a "memory" of the hard scattering. The phases of the collision outside the line have no (distinct) memory of the hard scattering. The final state partons radiate and close-by ones merge into color-singlet clusters that are then decaying to physical hadrons (beads around the dotted line). The overall interaction of the remaining hadron fragments is represented with the UE bubble (Underlying Event); initial state gluons such as (f) and (g) are splitting in $q\bar{q}$ pairs that are shared with the underlying event.

An impressive technological challenge of the LHC and the main budget item of the machine are the 1232 superconducting dipoles operating at temperature 1.9 K that bend the two proton beams around the 27 km circumference tunnel. At 7 TeV these magnets have to produce a field of 8.33 Tesla at a current of around 11,700 A. The magnets have two side-by-side apertures (dual-core or "two-in-one" design), one for each of the counter-rotating proton beams [9–11]. Each dipole is 14.3 meters long. The manufacture of the coil that contain the superconducting cable to provide the all-important 8.33 T magnetic field, represents 60% of the magnet production work. The niobium-titanium coils create the magnetic fields to guide the two counter-rotating proton beams in separate magnetic channels, but within the same physical structure. The coils are surrounded by non-magnetic "collars" of austenitic steel, a material that combines the required properties of good thermal contraction and magnetic permeability. The collars hold the coils in place against the strong magnetic forces that arise when the coils are at full field — the force loading 1 m of dipole is about 400 tons. The LHC dipoles comprise 7600 Km superconducting cable that weighs 1200 tons. Each cable is made up of 36 strands of superconducting wire while each strand houses 6300 superconducting filaments of Niobium-titanium (NbTi) — the total length of the filaments is astronomical, more than 10 AU.

The LHC schematic layout given in Fig. 3.4. It has not changed since the original design report [1]. The commissioning of the LHC began with Sector 7-8 in June 2007. During the summer, the quadruple circuits in that sector were powered up to 6500 amps. Sector 4-5 has been cooled down in Feb 2008 and the quadruple and main dipole circuits have been powered up to 10,200 amps in this sector in March 2008. At this intensity of current the magnets are capable of guiding a 6 TeV proton beam. For the cooling of the machine, the LHC cryogenics need ~40,000 leak-tight pipe junctions
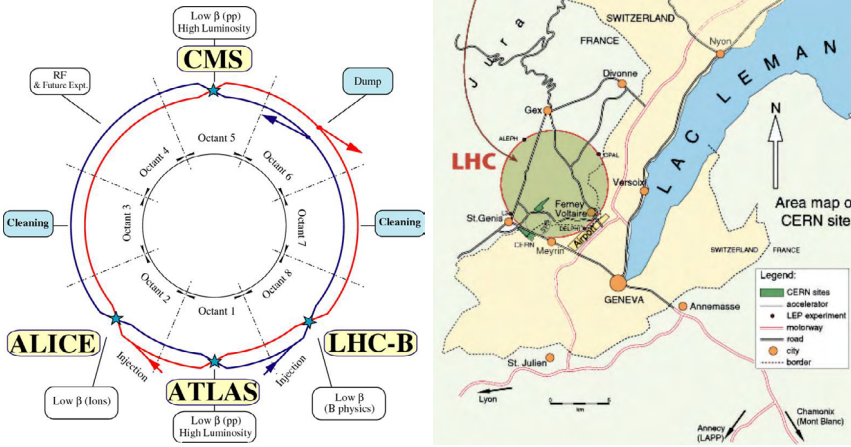
Fig. 3.4.   Overall layout of the LHC machine (left) and geographic location (right).

while 12 million liters of liquid nitrogen will be vaporized during the initial cool-down of 31,000 tons of material and the total inventory of liquid helium will be 700,000 liters.

A complex of older CERN accelerators pre-accelerate the proton bunches from rest to 450 GeV per proton. For each store, 2808 bunches will be injected into each of the twin LHC synchrotron and will be accelerated to 7 TeV per proton. The two beams will be focused and brought into collision at the four interaction points shown in Fig. 3.4. In Fig. 3.5 a graphic of the relative beam sizes around the interaction point (IP1, ATLAS) is given. At the interaction point 100 billion protons are squeezed down to 16 microns.
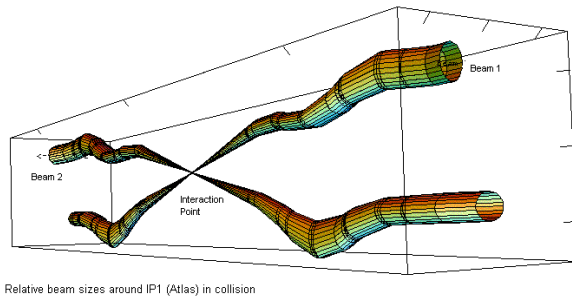
Fig. 3.5.   Relative beam sizes around the ATLAS interaction point

Although there will be 100 billion protons per bunch, most of them will miss each-other, will proceed without scattering and the circulation/collisions of the same bunches will continue for many hours.

3.1.2. *LHC: Figures of challenge*

The power and energy figures for the LHC are very impressive. If we calculate the total energy of each LHC beam we get $2808 \times 1.15 \times 10^{11}$ protons per bunch $\times$ 7 TeV $= 0.185\ M_{\mathrm{Planck}} = 362$ MJ. The accurate steering of the beam at all times is essential.

The *instantaneous luminosity* at the LHC is $\mathcal{L} = \frac{n_b N_L N_R f_{rev}}{A_T^{eff}} \sim$ 10^{34} cm^{-2}s^{-1}, where $f_{rev} = c/27$ km $\sim 10^4$ Hz, $A_T^{eff} = 4\pi\sigma_b^2$ is the effective transverse area of the proton beam and with $\sigma_b = 16$ microns. The total inelastic (non-diffractive) cross section is about 60 millibarns [a] (1 barn=10^{-24} cm^2). The *collision rate*, is $\mathcal{L} \times \sigma \sim 10^9$ Hz: a billion per second.

The rate that the 2808 proton bunches "cross" each-other at each interaction region is 2808 $c/27000 \sim 30 \times 10^6$ Hz. At design luminosity each bunch crossing produces then > 20 proton-proton scatterings! Note that the LHC will operate at bunch crossing rate of 40 MHz (25 ns bunch spacing). However only 80% of the bunches will be filled (allowing e.g. for abort and injection gaps) resulting in an effective bunch crossing rate of 32 MHz.

Fortunately a typical hard scattering of two protons has a large impact parameter and produces relatively low momentum particles in the final state. These are called "minimum bias" collisions. An event with one spectacular hard scattering is unlikely to contain another one. Less fortunate is the fact that minimum bias collisions involve poorly understood nonperturbative QCD. To subtract the minimum bias pollution of the interesting events, a model of the minimum bias physics is needed that will be built based on the actual LHC data. This was done successfully with Tevatron data. Although minimum bias collisions are "soft" (i.e. they produce relatively low momentum particles), their effects are quite significant. A typical LHC event will contain a total of about 1 TeV of "soft" energy from minimum bias collisions. In comparison, the most energetic hard scattering ever recorded prior to LHC was a ~ 1.4 TeV collision at the Tevatron.

---

[a]Using long range inelastic strong interactions modeled by meson exchange as in the original Yukawa theory a back of the envelope calculation with $\sigma = \pi\mathrm{range}^2$ will give an answer very close to this!

The *integrated luminosity* is $\int \mathcal{L}\mathrm{d}t = \mathrm{L}\ \mathrm{cm}^{-2}$ or fb^{-1}. One year is about $\pi \times 10^7$ s. Empirically a collider operates about $1/\pi$ of the time a year and it is customary to take 1 "collider year" to be 10^7 s. The integrated luminosity over a year at the LHC at design luminosity is then $10^{41}\mathrm{cm}^{-2}$ or 100 fb^{-1}. This is to be compared with the total integrated luminosity of about 3 fb^{-1} at the Tevatron after more than 10 years of running. A detailed discussion of the first years of physics at the LHC can be found in Ref. [12].

With bunch crossings every 25 ns and given that in 25 ns the light travels $\sim$7.5 m, much shorter distance than the size of the detectors, the challenge at the LHC is obvious: no electronic system can read the data from an entire detector and decide to do anything with it before the next event comes about. To address this challenge and the large rate of incoming data the experiments need very fast response detectors and readout electronics as well as fast and rigid trigger architecture. *Trigger* refers to the real-time primary selection applied on the raw data or even the analog signals from the detectors. The triggers pipeline the data coming out of the detector subsystems (to buy some time), then decide quickly to allow events that are sufficiently interesting to pass along to the next layer of filtering. There are enough layers of triggers to reduce the original 40 MHz crossing rate down to 100-200 Hz of interesting events that are then permanently recorded, or "written-out" for later analysis ("offline" analysis). A good trigger is a fast trigger that keeps all the interesting events and is re-programmable to respond to detector understanding and possible change of the physics targets. Events that do not pass the trigger are permanently rejected. Note that the first hardware implemented trigger both for ATLAS and CMS is based on the calorimetry and muon detectors. We describe in more detail the trigger layers of ATLAS and CMS in Sec. 3.5.

Trigger notwithstanding the amounts of data that the experiments will collect are unprecedented. There exists no single computing site that could host the LHC data in its entirety. The challenge of the distribution, storage, accessing and analyzing the data of the LHC has spawned new technologies in computer science referred to as grid computing technologies. We discuss the data-flow and computing architecture of ATLAS and CMS in Sec. 3.5.1.

3.2. Detection, Particles and Physics

The large luminosity of the LHC is required so that the detectors have a good chance to capture the data from smaller than the Standard Model cross section processes. Based on the discussion above, even before

describing the two general purpose detectors at the LHC, the requirements on the detector design can be briefly summarized as follows:

- The detectors subsystems must have fast response (20-50 ns), a very challenging requirement for the readout electronics;
- The detectors segmentation should be fine to minimize the chance of overlapping signals from uninteresting events of neighboring bunch crossings. In turn this implies a very large number of readout channels and a high cost;
- The detectors must be resistant to high radiation doses. Special materials and tight quality control is imperative.

Detailed technical reviews of the LHC challenges and the technical design of the detectors such that they meet the requirements can be found in Refs. [13–16].

A high energy proton-proton scattering results in debris of particles that proceed (themselves and/or their decay products, depending on their lifetimne) to interact with the matter that surrounds the interaction region. The detectors and detections techniques are based on the interaction of particles with matter. An extensive review can be found in the Particle Data Book [17]. The the LHC detectors are built to uncover new fundamental dynamics (for example new massive degrees of freedom and their couplings to the known particles) by using the experimentally accessible kinematics (characteristic kinematic observables related to the momentum phase space). The detectors will:

- identify the particles based on their interaction with matter, their decays or their measured mass (from simultaneous measurements of any two of momentum, energy and velocity);
- determine the momentum of the charged particles if charged by measuring their curvature in a a magnetic field if their mass is known;
- determine the origin of the particles and
- determine their polarization and other properties.

In what follows we elaborate on those particles that are characterized already at the trigger level and drive the detector design:

- **electrons** (e): An electron moving through material loses energy by ionizing atoms; the additional electrons are collected so that the position of the high energy particle is determined. If a strong magnetic field is in place, pointing along the direction of the beampipe, an electron

moving away from the beam will curve in the plane orthogonal to the beam. By measuring the curved track, the momentum of the electron and whether it is an electron or a positron (i.e. the charge of the electron) is determined. For electron energies above ∼10 MeV, bremsstrahlung becomes the dominant energy loss mechanism. The photons produced convert back to e^+e^- pairs due to the presence of the material. This cascades into an electromagnetic shower. Such showers are initiated, contained, and detected in devices called calorimeters that are positioned at a larger radius from the interaction point than the tracker. Calorimeters measure the total energy of the initial high energy electron typically that produces a narrow shower with well defined longitudinal and transverse shape. A high energy **photon** is detected as an electron without a track associated to the calorimetric energy deposition. A finely segmented calorimeter, can disambiguate the two particles.

- **hadrons (h)**: High energy pions and kaons live long enough to initiate showers in calorimeters, as do protons and neutrons. These hadronic showers can penetrate farther (and are broader) than electromagnetic showers. Collider detectors have larger hadronic calorimeters surrounding their electromagnetic calorimeters to provide measurements of the hadronic showers. Charged hadrons will also leave tracks in the tracker. Electrons are discriminated from hadrons because their showers are typically mostly contained in the electromagnetic calorimeters. Similarly photons are discriminated from neutral hadrons although high energy neutral pions present a tough case, since they look like two roughly collinear photons. The ensemble of a set of tracks from the charged hadrons and the (approximately circular in the $\eta - \phi$ coordinate system) associated calorimetric depositions both in the electromagnetic and hadronic calorimeters is referred to as a "jet."

- **muons (μ)**: Muons have the same interactions as electrons, but because they are 200 times heavier they do not initiate electromagnetic showers. With a lifetime in the lab frame of $2.2\gamma \times 10^{-6}$ seconds, they are essentially stable particles. Thus high energy muons leave tracks in the tracker, a few hundred MeV in the electromagnetic calorimeter and a few GeV in the hadronic calorimeter. For very high energy muons, the tracker may give a less precise measurement of the momentum. Since there is no energy measurement from the calorimeters the collider detectors require very large muon systems, outside their calorimeters, designed to measure the trajectory and momentum of muons.

- **taus (τ)**: Taus can decay into a muon or electron plus two neutrinos, in which case they are detected as muons or electrons. Taus primarily decay into one or three charged pions with accompanying neutral pions. A high momentum single track or triad of tracks isolated in that there is little energy in the calorimeter around the tau candidate cluster and no other tracks nearby, is a characteristic signature of a hadronically decaying tau.
- **heavy flavor (hf, b, c)**: The mean distance traveled by a B meson before decaying is 0.5 millimeters, while it is 0.3 millimeters for a D meson. With fine tracking devices sufficiently close to the beampipe, it is possible to distinguish the displaced secondary vertices of the charged particles from these decays. In this sense detectors can "see" heavy flavor mesons; this ability is known as "b-tagging" and "charm-tagging." An alternative technique for heavy flavor tagging is to look for muons inside the hadronic jet as semi-leptonic decays of Bs and Ds produce muons.
- **missing energy**: Although neutrinos interact too weakly to be seen in a collider detector, modern detectors can infer the presence of high energy neutrinos by measuring the so-called "missing transverse energy." What is actually measured is missing transverse momentum, applying momentum conservation to all of the observed products of the proton-proton scattering. Since the momentum of the colliding pp pair is almost entirely longitudinal (i.e. along the beam) rather than transverse, the transverse momenta of the scattering products should add up to zero. An imbalance is attributed to an undetected particle (such as a neutrino). Missing energy analyses in hadron colliders have been performed with calorimetric information, and start from calorimetric triggers and not tracking, hence the slight misnomer "missing transverse energy" or *MET*. MET is a vector in the plane transverse to the beam. If the MET vector points to an uninstrumented region in the calorimeters the interpretation of the event is ambiguous. This is one reason why modern collider detectors are constructed to be as hermetic as possible. Note that it is not possible to perform a missing energy analysis in the strict sense of comparing "energy-in" with "energy-out." In a pp collision usually only one parton from each proton undergoes a hard scattering. The energy of this collision is not known — it is less than the full pp center-of-mass energy — and the remnants of the protons (the underlying event) are poorly measured, since they mostly go off down the beam pipe.
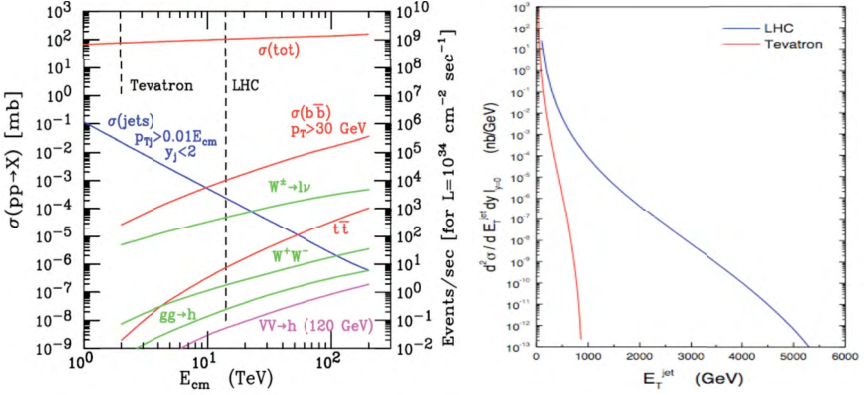
Fig. 3.6.   (Left) Scattering cross sections versus c.m. energy for the SM processes in pp collisions. The Higgs boson mass is taken as 120 GeV [18]. (Right) Comparison of QCD cross section in the Tevatron and the LHC.

Figure 3.6(left), is showing the cross section for various Standard Model processes as a function of the center-of-mass energy of a pp hadron collider in units of millibarn. The scale on the right-hand side gives the event rate for the LHC design instantaneous luminosity 10^{34} cm^{-2} s^{-1} The cross sections grow with the center-of-mass energy E_{cm} due to the larger parton densities at higher energies. The jet-inclusive cross section σ(jets) falls due the energy-dependent imposed jet E_T threshold requirement in the calculation (140 GeV for the LHC center-of-mass energy) and is about 200 nb for the LHC. The $b\bar{b}$ pair production dominated by gluon-gluon scattering is of the order of 1 μb at the LHC (with a cutoff $p_T > 30$ GeV) while the top-quark production – again dominated by gluon fusion is about 1 nb large enough to call the LHC a "top-quark factory."

Higgs production and a multitude of other beyond the Standard Model processes have cross sections in the range of femtobarns to picobarns. These are the processes that the LHC is after and that this entire volume is pondering on. In Figure 3.6(right) the LHC 14 TeV probing length is shown compared to the Tevatron 1.8 TeV one. A detailed discussion of the parton luminosities at the Tevatron and the LHC and their implication can be found in Ref. [19]. As an example and to underline the "power" of the LHC we note that for a 1 TeV gg initiated processes 1 fb^{-1} at the Tevatron is approximately equivalent to 1 nb^{-1} at the LHC while for a 1 TeV qq initiated processes, 1 fb^{-1} at Tevatron is approximately equivalent to 1 pb^{-1} at the LHC.
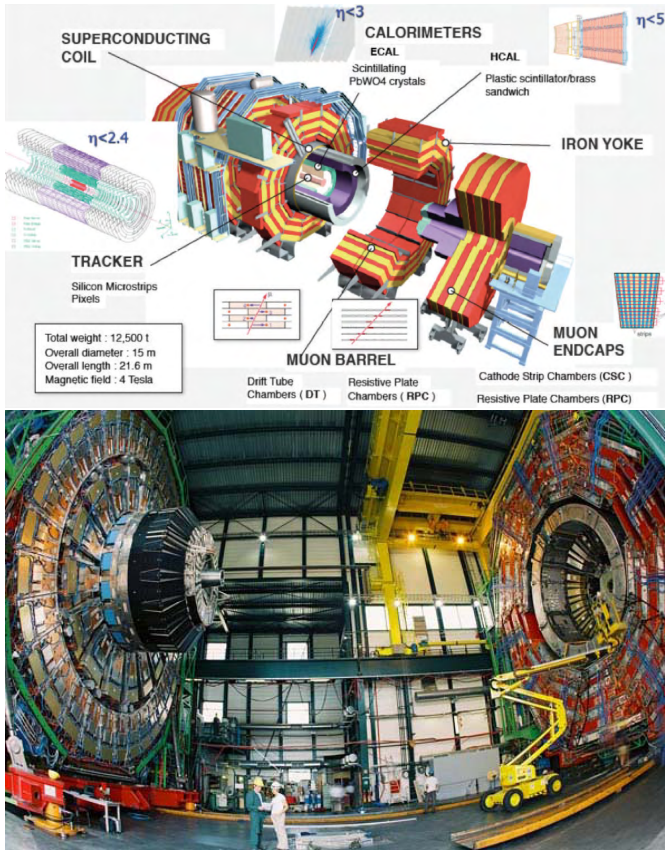
Fig. 3.7.   (Upper) Cut-away view of the CMS detector. The modular design allowed assembly on the surface assembly hall before lowering each module 100 m down the collision hall. The detector weighs approximately 12,500 tons, is 22 m in length and 15 m in diameter. (Lower) On the left the view of the 15 m diameter end-cap "discs" installed with muon chambers; On the right the part of the CMS barrel with the solenoid and the hadron calorimeter visible as well as the muon barrel wheel with . The picture was taken before "closing" the detector for the first time at the assembly for the 2006 magnet test and full slice cosmic data taking. Image reproduced with permission from CERN.

3.3. ATLAS and CMS

The ATLAS and CMS detectors are designed to identify most of the very energetic particles emerging from the proton-proton collisions, and to measure as efficiently and precisely as feasible their trajectories and momenta.
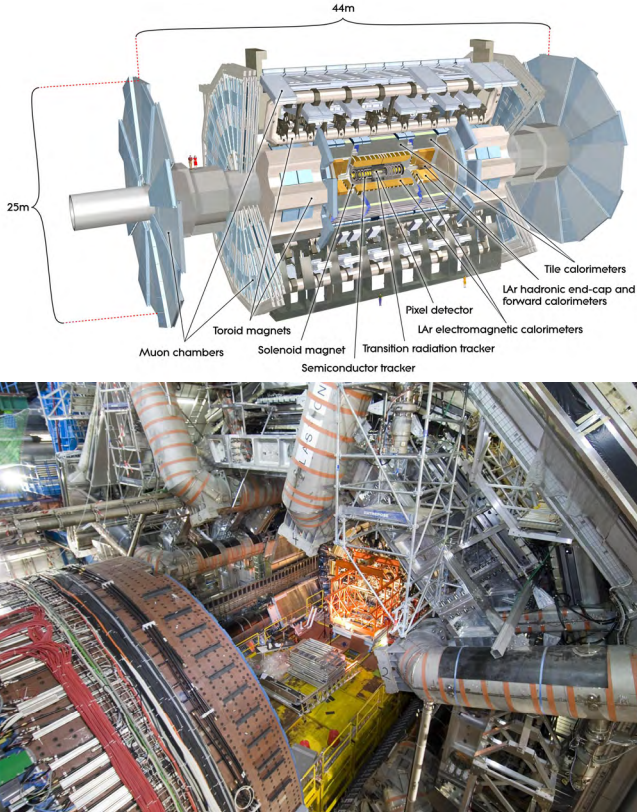
Fig. 3.8.   (Upper) Cut-away view of the ATLAS detector. The dimensions of the de-
tector are 25 m in height and 44 m in length. The overall weight of the detector is
approximately 7,000 tons. (Lower) The components of the ATLAS detector are installed
in the experiment's underground cavern. This picture from April 2007 shows the instal-
lation of the inner detector inside the barrel calorimeter and toroid systems, while the
end-cap calorimeters (in the foreground) are kept in an open position to allow access.
Image reproduced with permission from CERN.

The interesting particles are produced over a wide range of energies (from
a few hundred MeV to a few TeV) and over the full solid angle. They
therefore need to be detected down to small polar angles (θ) with respect
to the incoming beams (a fraction of a degree corresponding to pseudora-
pidities η up to 5, where $\eta = -log[\tan(\theta/2)]$. In addition no detectable
particle should escape unseen. From the discussion above one can roughly
predict what the ATLAS and CMS detectors look like. Moving radially

	ATLAS	CMS
Weight (tons)	7,000	12,500
Diameter (m)	22	15
Length (m)	46	20
Magnetic field for tracking (T)	2	4
Solid angle coverage $\Delta\eta \times \Delta\phi$	$2\pi \times 5.0$	$2\pi \times 5.0$
Cost in M CHF	550	550

outward from the interaction region, they have a tracking system to measure the directions and momenta of all possible charged particles emerging from the interaction vertex; an electromagnetic and a hadronic calorimeter system to absorb and measure the energies of electrons, photons, and hadrons, and outer layers of muon detectors dedicated to the measurement of the directions and momenta of high-energy muons. They also have one or more large magnets, to provide bending fields for the tracker and the muon system. One might imagine that the optimal shape for a hermetic detector is a sphere, but the need of as uniform as possible magnetic fields dictates instead that the main detector is a cylinder or "barrel," centered on the beampipe and the interaction region, supplemented by "end-caps" that provide coverage in the more "forward" regions.

3.3.1. *ATLAS/CMS duality*

A question that naturally arises is why the two general purpose detectors, having a very similar research program and operating in the same collider are so differently designed in terms of dimensions, density and material used for the sub-detectors [20, 21].

In the design phase of the CMS and ATLAS detectors in the early 1990s, the detection of the Higgs boson was used as the driving benchmark for the performance of the proposed designs. The "golden," very clean channel of the Higgs boson decaying to two Z bosons (and eventually 4 muons) determined the baseline design. Specifically the benchmark design requirement is the measurement of the momentum of up to 1 TeV muon to no worse than 10% precision. Because $\frac{\Delta p}{p} \sim \frac{1}{BL^2}$ where B is the magnetic field strength and L is the distance over which the bending of the muon takes place the requirement has in fact more than one solutions: Very large B and compact design in length (CMS) or large L and appropriate magnetic field (ATLAS).

Roughly the muon road from the interaction out to the muon chambers in the two experiments can be summarized as follows:

- at CMS muons travel radially a distance $L=3$ m in the 4 T bending field giving $BL^2 = 36\,\text{Tm}^2$. Out of the solenoid they travel another 3 m and halfway they cross the solenoid return flux in the iron magnet yoke which is about 2 T (with opposite orientation). That gives another $BL^2 \sim 5\,\text{Tm}^2$. The tracker and muons systems within and around the yoke measure the bendings. This explains the otherwise weird "S" path of the muons at CMS as inscribed in the experiment's logo;
- at ATLAS muons travel a distance of 1 meter in the tracker solenoid which is 2 Tesla giving $BL^2 \sim 2\,\text{Tm}^2$. Outside the calorimeters the air-core toroidal magnets provide a bending field of 1 T over a distance of 6 m giving another $BL^2 = 36$ T m^2.[b]

Most-all other design specifications and differences can be derived from this requirement. For example the ATLAS calorimeters can be larger since they don't have to be contained within the solenoid, and the CMS lead tungstate electromagnetic calorimeter is such chosen that it can actually fit in the available space and manage to capture the electromagnetic showers and with appropriate resolution.

3.3.2. *Magnet systems*

ATLAS (Fig. 3.9) has an inner, thin, superconducting solenoid surrounding the inner detector cavity, and large, superconducting, air-core toroids, consisting of independent coils arranged with an eight-fold symmetry, outside the calorimeters. This magnetic system is 22 m in diameter and 26 m in length, with a stored energy of 1.6 GJ. It provides the magnetic field over a volume of approximately 12,000 m^3 (defined as the region where the field exceeds 50 mT). The magnet systems are split into:

- a solenoid that is aligned on the beam axis and provides a 2 T axial magnetic field for the inner detector, while minimizing the radiative thickness in front of the barrel electromagnetic calorimeter;
- a barrel toroid and two end-cap toroids that produce a toroidal magnetic field of approximately 0.5 T and 1 T for the muon detectors in the central and end-cap regions, respectively.

---

[b]Note that the average toroidal field and distances vary significantly in ATLAS depending on the angle so the numbers here are indicative.
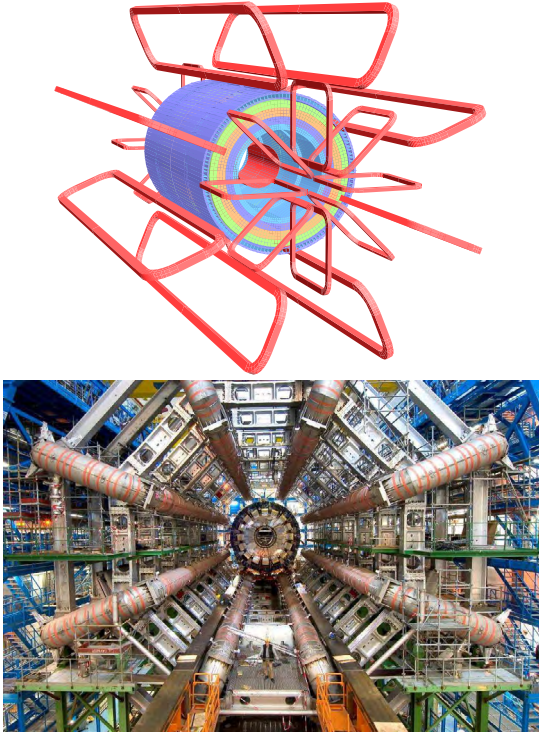
Fig. 3.9. (Upper) Schematic of the geometry of ATLAS magnet windings and tile calorimeter steel. The eight barrel toroid coils, with the end-cap coils interleaved are visible. The solenoid winding lies inside the calorimeter volume. The tile calorimeter is modeled by four layers with different magnetic properties, plus an outside return yoke. For the sake of clarity the forward shielding disk is not displayed. (Lower) The picture shows the eight-fold barrel toroid as installed in the underground cavern. Also visible are the stainless-steel rails carrying the barrel calorimeter with its embedded solenoid that await translation towards their final position in the center of the detector (2005; Image reproduced with permission from CERN).

The first barrel toroid coil was lowered in the cavern in the fall of 2004, immediately followed by the solenoid (embedded inside the liquid argon (LAr) barrel calorimeter). The remaining seven barrel-toroid coils were installed in 2004 and 2005, and the end-cap toroids in the summer of 2007. The position of the central solenoid in front of the electromagnetic calorimeter requires optimization of the material in order to achieve the desired calorimeter performance. As a consequence, the central solenoid and the LAr calorimeter share a common vacuum vessel.

Fig. 3.10.   (Upper) The CMS superconducting solenoid provides a central magnetic field of 4 T; the nominal current is 20,000 A, the weight of the cold mass is 220 tons, its length is 12.5 m and its diameter is 6 m; with stored energy 2.7 GJ it is the highest stored energy solenoid. (Lower) Members of the CMS Magnet and Integration Group and representatives from Saclay stand inside the cryostat of the giant superconducting solenoid during cooling to the interior operating temperature of 4.5 K (February 2006, Image reproduced with permission from CERN).

The superconducting magnet for CMS was designed to reach a 4 T field in a free bore of 6 m diameter and 12.5 m length with a stored energy of 2.6 GJ at full current. The flux is returned through a 10,000 ton yoke of 5 barrel wheels and 2 end-caps, composed of three disks each. The distinctive feature of the 220 ton cold mass is the four layer winding made from a stabilized reinforced NbTi conductor. The ratio between stored energy and

cold mass is critically high (11.6 KJ/kg), causing a large mechanical deformation (0.15%) during energizing– well beyond the values of any solenoidal detector magnets built to-date. The magnet was designed to be assembled and tested at the surface assembly hall prior to being lowered 90 m below ground to its final position in the experimental cavern. After provisional connection to its ancillaries, the CMS magnet has been fully and successfully tested and commissioned during the autumn of 2006 and lowered in the CMS cavern in 2007 where it is due to be cooled-down and powered in May 2008 for the final integration and data-taking.

3.4. ATLAS and CMS: Challenges Addressed

3.4.1. *Inner detectors*

Approximately 1000 particles will emerge from the LHC collision points every 25 ns within $|\eta| < 2.5$, creating a very large track density in the detectors. To achieve the momentum and vertex resolution requirements imposed by the benchmark discovery as well as standard model background physics processes, high-precision measurements must be performed with fine detector granularity in the inner detector volume.

Both the ATLAS and CMS inner detector systems are largely based on silicon detectors, with high granularity pixel systems at the smallest radii, and silicon-strip detectors at larger ones. ATLAS has a straw tracker at the largest radius.

The main challenges for the inner detector parts are the high particle rates, the radiation tolerance needed and the control of aging effects. The ATLAS and CMS trackers had to be designed to withstand high radiation doses (500-1000 kGy) for the innermost pixel layers, and up to 100 kGy for the systems farther away from the interaction point, after 10 years of operation). As a result, the development of the integrated front-end electronics for these systems has been a major challenge and has required several years and design iterations. These circuits are fast, radiation tolerant and low power, and are integrated on low-mass modules where cooling and material limitations are severe. Several iterations of test-beam measurements and rigorous irradiation programs have been necessary to prove that the circuits will function in their final assemblies, as well as after high irradiation. A similarly stringent research and development program was needed for the silicon sensors themselves for which the major difficulty is bulk radiation damage.

Silicon detectors are $p - n$ junction diodes that are operated at reverse bias forming a sensitive region depleted of mobile charge and setting up an electric field that sweeps charge (namely electron-hole pairs) liberated by radiation towards the electrodes. Integrated circuit technology allows the formation of high-density micrometer-scale electrodes on large (10-15 cm in diameter) wafers, providing adequate position resolution. Furthermore, the density of silicon and its small ionization energy result in adequate signals with active layers only 200-300 μm thick, and the charge mobility is such that the signals are also fast (typically tens of nanoseconds).

The ATLAS and CMS inner detectors are contained in central solenoid fields of 2 T and 4 T respectively. They provide efficient tracking of charged particles within the pseudorapidity range $|\eta| < 2.5$, allowing the momentum measurement of charged particles and the reconstruction of primary and secondary vertices.

Considering the flux of charged particles at increasing radii around the LHC beams, three detector regions are defined both in ATLAS and CMS. In the first of these, closest to the interaction point where the particle flux is highest, there are silicon pixel detectors, whose cell sizes of 50×400 μm^2 and 100×150 μm^2 in ATLAS and CMS respectively, give give an occupancy of about 10^{-4} per pixel per bunch crossing. To improve the measurement of secondary vertices (e.g. from b-quark decays and other particles with lifetime) an innermost layer of pixels has been introduced as close to the beam as is practical, at a radius of about 4.5 cm. The pixel systems in ATLAS and CMS are very much larger than any comparable existing system. The ATLAS pixel system covers about 2 m^2 and has 80 million channels; the CMS pixel system is only slightly smaller. Pixel detectors are expensive and have high power density, so at a certain radius and system size, silicon microstrip systems become the preferred technology.

In the intermediate tracking region of ATLAS and CMS, at a radius of 20-55 cm, the particle flux becomes low enough to use silicon microstrip detectors. Barrel cylinders and end-cap discs provide coverage out to about $|\eta| = 2.5$. Strip dimensions of 10-12 cm $\times$ 80-120 μm lead to an occupancy of 1-3% per bunch crossing. Both trackers use stereo angle in some of the strip layers (that is, strips placed at a small angle with respect to the z axis, 40 mrad and 100 mrad for ATLAS and CMS respectively) to improve the resolution in z. In these microstrip systems, it has been essential to find a good balance between the pitch of the cells (resolution and occupancy determinant), radiation effects, capacitive load (noise determinant), material length and costs. In the outermost region (beyond about 55 cm),

the particle flux is sufficiently low to allow the use of larger-pitch silicon microstrips in the CMS tracker, with a maximum cell size of 25 cm × 180 μm while keeping the occupancy to about 1%. There are six layers of such microstrip modules in the barrel, accompanied by nine end-cap discs providing coverage out to about $|\eta| = 2.5$, amounting to 15,400 modules and 9.6 million channels, and spanning a total detector area of more than 200 m^2. For ATLAS, at radii greater than 56 cm, a large number of tracking points (typically 36 per track) is provided by the straw tracker — 300,000 straw-tubes embedded in fiber or foil radiators and filled with a xenon-based gas mixture. This detector allows continuous track following with less material per point, and also has electron identification capabilities.

3.4.2. *Calorimetry*

The ATLAS and CMS calorimeters absorb and measure the energies of electrons, photons and hadrons. In the QCD-dominated environment of the LHC, the ability to reject neutral pions is crucial both for photon and electron identification. Efficient photon and lepton isolation measurements are also important in mutlijet topologies. In the design of the electromagnetic calorimeters for both ATLAS and CMS, the emphasis is on good resolution for photon and electron energy, position and direction measurements, and wide geometric coverage (up to $|\eta|$ close to 3.0). For the hadronic calorimeters, the emphasis is on good jet-energy measurements, and full coverage (to $|\eta| = 5$) to be able to ascribe the observation of significant missing transverse energy to non-interacting particles (such as neutrinos, or light neutralinos from supersymmetric-particle cascade decays). Last but not least, the quantities measured in the calorimeters play a crucial part in the trigger of the experiment as signatures of significant parts of the new physics sought at the LHC.

The ATLAS calorimetry consists of an electromagnetic calorimeter covering the pseudorapidity region $|\eta| < 3.2$, a hadronic barrel calorimeter covering $|\eta| < 1.7$, hadronic end-cap calorimeters covering $1.5 < |\eta| < 3.2$, and forward calorimeters covering $3.1 < |\eta| < 4.9$. Over the pseudorapidity range $|\eta| < 1.8$, a pre-sampler is installed in front of the electromagnetic calorimeter to correct for energy loss upstream. The electromagnetic calorimeter system consists of layers of lead (creating an electromagnetic shower and absorbing particle energy), interleaved with liquid argon (providing a sampling measurement of the energy-deposition) at a temperature of 89 K. The system's "accordion" geometry provides complete azimuthal

symmetry, without uninstrumented regions, and has been optimized for the high sampling rate environment of the LHC. The barrel section is sealed within a barrel cryostat, which also contains the central solenoid, surrounding the inner detector. The end-cap modules are contained in two end-cap cryostats that also contain the end-cap hadronic and forward calorimeters. The hadronic barrel calorimeter is a cylinder divided into three sections: the central barrel and two identical extended barrels. It is again based on a sampling technique, but uses plastic scintillator tiles embedded in an iron absorber. The vertical tile geometry makes it easier to transfer the light out of the scintillator to photomultipliers and achieves good longitudinal segmentation. At larger pseudorapidities, closer to the beam pipe where higher radiation resistance is needed, liquid-argon technology is chosen for all calorimetry, for its intrinsic radiation tolerance. The hadronic end-cap calorimeter is a copper/liquid-argon detector with parallel-plate geometry, and the forward calorimeter is a dense liquid-argon calorimeter with rod-shaped electrodes in a tungsten matrix. The approximately 200,000 signals from all of the liquid-argon calorimeters leave the cryostats through cold-to-warm feedthroughs located between the barrel and the extended barrel tile calorimeters, and at the back of each end-cap. The barrel and extended barrel-tile calorimeters both support the liquid-argon cryostats and act as the flux return for the solenoid.

The electromagnetic calorimeter of CMS is an entirely active hermetic homogeneous calorimeter made of 61,200 lead tungstate ($PbWO_4$) crystals mounted in the central barrel part, closed by 7,324 crystals in each of the two end-caps. A preshower detector is placed in front of the end-caps crystals. The use of high density crystals has allowed the design of a calorimeter that is fast, has fine granularity and is radiation resistant, all important requirements in the harsh LHC environment. One of the driving criteria in the design was the detection of a low mass Higgs boson decaying into two photons and the metric for the performance of the electromagnetic calorimeter has been the di-photon mass resolution. The reasons for the lead tungstate choice are the short radiation length and small Moliere radius leading to a compact calorimeter in size, the short scintillation decay time constant, and its radiation hardness. The electromagnetic calorimeter is placed within the solenoid. Avalanche photodiodes are used as photodetectors in the barrel since they can operate in the 4 T magnetic field, they have a high quantum efficiency over the wavelength of emission, they have stable gain, small enough capacitance and leakage current (reducing the noise) and are radiation hard. The hadron calorimeter surrounds the

electromagnetic calorimeter and acts in conjunction with it to measure the energy and direction of jets and provide hermetic coverage for good missing energy measurement. The hadron calorimeter barrel is radially restricted between the outer extent of the electromagnetic calorimeter (R = 1.77 m) and the inner extent of the magnet coil (R = 2.95 m). This constrains the total amount of material which can be put in to absorb the hadronic shower. In the central region around $\eta = 0$ a hadron shower "tail catcher" is installed outside the solenoid coil to ensure adequate sampling depth. The active elements of the barrel and end-cap hadron calorimeters consist of plastic scintillator tiles with wavelength-shifting fiber readout. Layers of these tiles alternate with layers of copper in the barrel (maximizing the number of hadronic interaction lengths) to form the sampling calorimeter structure. Beyond $|\eta| = 3$, the forward hadron calorimeters placed at 11.2 m from the interaction point extend the pseudorapidity coverage down to $|\eta| = 5.2$ using a Cherenkov-based, radiation-hard technology.

3.4.3. *Muon detectors*

The muon systems in all LHC experiments are large-area gas-based detectors (several thousand square meters of multi-layer chambers each in ATLAS and CMS). The chambers are divided into two basic sets, one intended for precise measurements of muon tracks and the other dedicated to triggering on muons. The sheer size of the systems means that there are significant technical challenges related to the stability and alignment of the chambers and to the careful mapping of the detectors' magnetic fields over large volumes. The radiation levels for the muon chambers are much less severe than for the inner detectors or calorimeters. The designs of the beam pipe and the shielding elements in the forward direction have been carefully optimized to reduce the neutron-induced background rates in the muon chambers.

The ATLAS air-core toroid system, with a long barrel and two inserted end-cap magnets, generates a large-volume magnetic field with strong bending power within a light and open structure. Multiple-scattering effects are therefore minimized, and excellent muon momentum resolution is achieved with three stations of high-precision muon-tracking chambers, covering up to $|\eta| = 2.7$. Over most of the range in pseudorapidity, the measurement of track coordinates (in the principal bending direction of the magnetic field) is performed by monitored drift tubes. This technology provides robust and reliable operation, thanks to the mechanical isolation of each sense wire

from its neighbors in the gas-filled drift volumes of the individual tubes. At large pseudorapidities and close to the interaction point, where the rate and background conditions are more difficult, cathode-strip chambers with higher granularity strip readout are used. The muon trigger system, with a fast time response and covering $|\eta| < 2.4$, comprises resistive-plate chambers in the barrel and thin gap chambers in the end-cap regions. As well as triggering, these chambers provide a measurement of a second track coordinate orthogonal to the one measured by the high-precision chambers. In addition to the muon-chamber measurements, the inner detector measurements in the central solenoid of ATLAS contribute to the combined muon momentum resolution of the experiment.

The CMS muon system has also three functions: muon identification, momentum measurement, and triggering. Good muon momentum resolution and trigger capability are enabled by the high-field solenoidal magnet and its flux-return yoke. The latter also serves as a hadron absorber for the identification of muons. The CMS muon system is designed to have the capability of reconstructing the momentum and charge of muons over the the entire kinematic range of the LHC. CMS uses three types of gaseous particle detectors for muon identification. Due to the shape of the solenoid magnet, the muon system was naturally driven to have a cylindrical, with a central "barrel" section and two planar end-cap regions. The muon system consists of about 25,000 m^2 of detection planes. In the barrel region where the neutron-induced background is small and the 4-T magnetic field is uniform and mostly contained in the steel yoke CMS used drift chambers. The barrel drift tube (DT) chambers cover the pseudorapidity region $|\eta| < 1.2$ and are organized into four stations interspersed among the layers of the flux return plates. In the 2 end-cap regions, where the muon rates and background levels are high and the magnetic field is large and non-uniform, the muon system uses cathode strip chambers (CSC). With their fast response time, fine segmentation, and radiation resistance, these detectors identify muons between $|\eta|$ values of 0.9 and 2.4. There are four stations of cathode strip chambers in each end-cap. The muon detector elements cover the full pseudorapidity interval $|\eta| < 2.4$ with no acceptance gaps and ensure muon identification over the range corresponding to $10° < \theta < 170°$. Note that the muon system and the inner tracker provide independent muon momentum measurements; this redundancy enhances fault finding and permits cross-checking between the systems. A crucial characteristic of the drift tube and cathode strip chamber subsystems is that they can each trigger on the p_T of muons with good efficiency and high background rejection independent

of the rest of the detector. Additional redundancy and complementarity is ensured with a dedicated trigger system consisting of resistive plate chambers in both the barrel and end-cap regions. A total of six layers of RPCs are embedded in the barrel muon system, two in each of the first two stations, and one in each of the last two stations. The redundancy in the first two stations allows the trigger algorithms to function for low momentum tracks that may stop before reaching the outer two stations. In the end-cap region, there is a plane of chambers in each of the first three stations in order for the trigger to use the coincidences between stations to reduce background, improve the time resolution for bunch-crossing identification, and achieve a good p_T resolution. Finally, a sophisticated alignment system measures the positions of the muon detectors with respect to each other and to the inner tracker, in order to optimize the muon momentum resolution.

3.5. Trigger Architecture

At design luminosity, the LHC will produce a billion proton-proton events per second. Data storage and processing capabilities allow 100-200 carefully selected events per second to be recorded for analysis (each of these accompanied by more than 20 overlapping proton-proton events in the same bunch crossing).

The experiments need a trigger system with a rejection factor of nearly 10^7 to select only the most important events in order to carry out the discovery program. The first trigger level is based on custom-built processors and uses a limited amount of the total detector information to make decision in 2.5/3.2 μs (ATLAS/ CMS) and flag the event as worth further processing or not, reducing the data rate to around 100 kHz. Higher trigger levels use a network of several thousand commercial processors and fast switches and networks, access gradually more information and run algorithms that resemble offline data analysis to achieve the final reduction. The total amount of data recorded for each event will be roughly 1.5 megabytes, at a final rate of 150-200 Hz. This adds up to an annual data volume of the order of 10 petabytes for the LHC experiments. The challenges to be faced in real-time data collection and reduction are many.

The synchronization of the individual parts of the detector — and there are several thousand units to time in — will be accurate to better than a nanosecond, taking into account the flight times of particles to the individual sensor elements. At later stages in the event processing, there is the

second synchronization challenge of assembling all of the data fragments for a particular bunch crossing from various parts of the detector into a complete event (event-building).

As we mentioned already, processing and selecting events within the 25 ns available between successive proton bunch crossings is not possible. In addition the sizes of the detectors and the underground caverns where they are installed impose a minimum transit time between the detector read-out electronics and trigger electronics. The first-level trigger calculations themselves need to be sufficiently sophisticated to identify clear physics objects and signatures. The trigger decision is based on the presence of trigger primitive objects in the calorimeters and/or muon detectors, such as photons, electrons, muons and jets above pre-set transverse-energy or transverse-momentum thresholds. It also employs global sums of transverse energy and missing transverse energy. During the transit and processing time (less than 2.5/3.2 μs for ATLAS/CMS), the detector data must be time-stamped and held in buffers.

After an event is accepted by the first-level trigger system, the data from the pipelines are transferred from the detector electronics into readout buffers. The further processing involves signal processing, zero suppression and data compression while the events are examined by a farm of commodity processors consisting of several thousands of central processing units. The event fragments must be directed from the readout buffers to a single processor and buffer node, using fast switches and networks, in order to perform more detailed calculations of the critical parameters of the event and to reduce the final rate further.

3.5.1. *Googles of data and the grid*

Even after a very large online data reduction, huge amounts of data will be recorded at the LHC (tens of petabytes per year). It was obvious already at the very early stages of the design of the LHC experiments that a sophisticated service for sharing computer power and data storage capacity over the Internet was imperative and that the required level of computing resources should be provided by a large number of computing centers working in unison with the CERN on-site computing facilities. Off-site computing centers are vital to the operation of the experiments to an unprecedented extent. The grid infrastructure for data distribution, processing and storage was adopted and further developed [22, 23]. The LHC Computing Grid (LCG) and the Enabling Grids for E-sciencE (EGEE) project which is based in the

European Union and includes sites around the world have been developed to support the experiments at CERN's Large Hadron Collider and constitute the largest computing grids on the planet.

The grid solution is geographically distributed and relies on many "Tiers." The raw data output from the high-level trigger is processed and reconstructed in a "Tier-0" computing facility at CERN, producing reconstructed data. A copy of the raw data plus the reconstructed data is distributed to the "Tier-1" centers around the world. The Tier-1 centers share the archiving of a second copy of the raw data, provide the re-processing capacity and access to the various streams of reconstructed data (corresponding to the trigger paths) and allow data access and processing by the experiments physics analysis groups.

The "Tier-2" centers, each linked to a specific Tier-1 center, are smaller but more numerous and are used largely for analysis and Monte Carlo simulations. Data selection operations run on the Tier-1 data streams and result is more compact secondary datasets tailored for the physics analyses at the Tier-2 centers.

A tertiary level in the hierarchy is provided by individual group clusters and computers used for analysis. In summary:

- The vast amount of data at the LHC cannot be stored at any one single place while researchers around the world need to be able to access and analyze the data.
- Grid computing technologies are used to "enable coordinated resource sharing and problem solving in dynamic, multi-institutional virtual organizations" [22].
- The data from the LHC experiments will be distributed around the globe, according to a multi-tiered model. A primary backup will be recorded on tape at CERN, the Tier-0 center of the LHC Computing Grid project (LCG). After initial processing, this data will be distributed to a series of Tier-1 centers, large computer centers with sufficient storage capacity for a large fraction of the data, and with round-the-clock support for the grid.
- The Tier-1 centers will make data available to Tier-2 centers, each consisting of one or several collaborating computing facilities. Individual scientists will access these facilities through Tier-3 computing resources, which can consist of local clusters in a University Department or even individual PCs, and which may be allocated to LCG on a regular basis.

3.6. To Be Continued

Every day until the day that ATLAS and CMS start collecting the proton-proton data from the LHC collisions is a day closer to discovery. Every day after that, students, post-docs, professors, researchers of all specializations and interests will go to work operating the detectors, collecting and analyzing the data and thinking that "this is the day, it's close, we're there."

Acknowledgments

References

[1] The LHC Study Group, LHC: The large hadron collider conceptual design, *CERN-91-03;CERN-AC-DI-FA-90-06-REV;CERN/AC/95-05(LHC).* (1991).

[2] ATLAS Collaboration, ATLAS : technical proposal for a general-purpose pp experiment at the Large Hadron Collider at CERN, *CERN-LHCC-94-43 ; LHCC-P-2.* (1994).

[3] ATLAS Collaboration, ATLAS detector and physics performance : Technical Design Report, *ATLAS-TDR-015 ; CERN-LHCC-99-015.* (1999).

[4] CMS Collaboration, CMS, the Compact Muon Solenoid : technical proposal, *CERN-LHCC-94-38 ; LHCC-P-1.* (1994).

[5] G. L. Bayatian et al., CMS technical design report, volume I: Physics performance, *CERN-LHCC-2006-001 ; CMS-TDR-008-1.*

[6] G. L. Bayatian et al., CMS technical design report, volume II: Physics performance, *J. Phys.* **G34**, 995–1579, (2007).

[7] M. Spiropulu, Collider experiment: Strings, branes and extra dimensions, *hep-ex/0305019.* (2003).

[8] M. L. Mangano and T. J. Stelzer, Tools for the simulation of hard hadronic collisions, *Ann. Rev. Nucl. Part. Sci.* **55**, 555–588, (2005).

[9] J. P. Blewett, 200-GEV INTERSECTING STORAGE ACCELERATORS, *8th International Conference on High-energy Accelerators.* pp. pp.501–504, (CERN Geneva Switzerland 20 - 24 Sep 1971).

[10] J. Allinger, G. Danby, and J. W. Jackson, High Field Superconducting Magnets for Accelerators and Particle Beams, *IEEE Transactions on Magnetics,MEG-11, no 2.* pp. 463–466. BNL-19575.

[11] R. Palmer and A. V. Tollestrup, Superconducting Magnet Technology for Accelerators, *Ann. Rev. Nucl. Part. Sci.* **34**, 247–284, (1984).

[12] F. Gianotti and M. L. Mangano, LHC physics: The first one-two year(s), *hep-ph/0504221.* (2005).

[13] N. Ellis and T. S. Virdee, Experimental challenges in high luminosity collider physics, *Ann. Rev. Nucl. Part. Sci.* **44**, 609–653, (1994).

[14] J. Engelen, Challenges of the LHC: The detector challenge, *Eur. Phys. J.* **C34**, 61–65, (2004).

[15] S. Stapnes, Detector challenges at the LHC, *Nature.* **448**, 290–296, (2007).

[16] D. Froidevaux and P. Sphicas, General-purpose detectors for the Large Hadron Collider, *Ann. Rev. Nucl. Part. Sci.* **56**, 375–440, (2006).

[17] Yao, W.-M., Review of Particle Physics, *Journal of Physics G.* **33**, 1+, (2006).

[18] T. Han, Collider phenomenology: Basic knowledge and techniques, *hep-ph/0508097.* (2005).

[19] J. M. Campbell, J. W. Huston, and W. J. Stirling, Hard interactions of quarks and gluons: A primer for LHC physics, *Rept. Prog. Phys.* **70**, 89, (2007).

[20] M. Spiropulu, The LHC experiments, *Perimeter Institute Summer School on Particle Physics, Cosmology and Strings.*

[21] J. Lykken, LHC Phenomenology for String Theorists, *RTN Winter School on Strings, Supergravity and Gauge Theories.*

[22] Ian Foster, Carl Kasselman, *The Grid: Blueprint for a New Computing Infrastructure.* (Elsevier, ISBN 1-55860-475-8, 2003).

[23] CERN LHC Grid Computing. LCG Deployment http://lcg.web.cern.ch/LCG.

This page intentionally left blank

Chapter 4

Understanding the Standard Model, as a Bridge to the Discovery of New Phenomena at the LHC

Michelangelo L. Mangano

CERN, PH Department, TH Group,
1211 Geneva 23, Switzerland
michelangelo.mangano@cern.ch

I discuss the basic elements of the process that will lead to the discovery of possible new phenomena at the LHC. We review the status of the tools available to model the Standard Model backgrounds, and the role that such tools can play in the discovery phase, and in the exploration of the features and parameters of such new phenomena.

4.1. Introduction

The Standard Model (SM) of fundamental interactions has by now been successfully tested over the past 30 years, validating its dynamics both in the gauge sector, and in the flavour structure, including a compelling confirmation of the source of the observed violation of parity (P) and combined charge and parity (CP) symmetries. The inability of the SM to account for established features of our universe, such as the presence of dark matter, the baryon asymmetry, and neutrino masses, are not considered as flaws of the SM, but as limitations of it, to be overcome by adding new elements, such as new interactions and new fundamental particles. With this perspective, the LHC is not expected to further test the SM, but to probe, and hopefully provide evidence for, the existence of such new phenomena. Our ability to predict what will be observed at the LHC is therefore not limited by fundamental issues related to left-over uncertainties about the SM dynamics, but by the difficulty of mastering the complex strong-interaction dynamics that underlies the description of the final states in proton-proton collisions [1].

Many years of experience at the Tevatron collider, at HERA, and at LEP, have led to an immense improvement of our understanding of this dynamics, and put us today in a solid position to reliably anticipate in quantitative terms the features of LHC final states. LEP, in addition to testing with great accuracy the electroweak interaction sector, has verified at the percent level the predictions of perturbative QCD, from the running of the strong coupling constant, to the description of the perturbative evolution of single quarks and gluons, down to the non-perturbative boundary where strong interactions take over and cause the confinement of partons into hadrons. The description of this transition, relying on the factorization theorem that allows to consistently separate the perturbative and non-perturbative phases, has been validated by the comparison with LEP data, allowing the phenomenological parameters introduced to model hadronization to be determined. The factorization theorem supports the use of these parameters for the description of the hadronization transition in other experimental environments. HERA has made it possible to probe with great accuracy the short-distance properties of the proton, with the measurement of its partonic content over a broad range of momentum fractions x. These inputs, from LEP and from HERA, beautifully merge into the tools that have been developed to describe proton-antiproton collisions at the Tevatron, where the agreement between theoretical predictions and data confirms that the key assumptions of the overall approach are robust. Basic quantities such as the production cross section of W and Z bosons, of jets up to the highest energies, and of top quarks, are predicted theoretically with an accuracy consistent with the known experimental and theoretical systematic uncertainties. This agreement was often reached after several iterations, in which both the data and the theory required improvements and reconsideration. See, for example, the long saga of the bottom-quark cross section [2], or the almost embarassing — for theorists — case of the production of high transverse momentum J/ψs [3].

While the present status encourages us to feel confident about our ability to extrapolate to the LHC, the sometimes tortuous path that led to this success demands caution in assuming by default that we know all that is needed to accurately predict the properties of LHC final states. Furthermore, the huge event rates that will be possible at the LHC, offering greater sensitivity to small deviations, put stronger demands on the precision of the theoretical tools. In this essay I discuss the implications of these considerations, in the light of some lessons from history, and I discuss the role that theoretical calculations should have in the process of discovering

new physics. I shall not provide a systematic discussion of the state of the art in calculations and Monte Carlo tools (for these, see Refs. [4] and [5], respectively) but rather a personal perspective on aspects of the relation between theory and data analysis that are sometimes neglected. Furthermore, I shall only deal with what we would call "direct discovery", namely the observation of the production of some new particle. Of course the LHC can discover new physics in other ways, for example by measuring $B_s \to \mu^+\mu^-$ decays with a rate different than predicted by the SM, or by measuring the top, W and Higgs masses to be inconsistent with the SM expectation. I shall not cover these aspects, since they are subject to sources of theoretical and experimental uncertainties that are rather complementary to those I intend to focus on.

4.2. Signals of Discovery

Three new elementary particles have been discovered by hadron colliders: the W and Z bosons [6, 7], and the top quark [8, 9]. For the first two, the features of the final states were known in advance with great confidence, and so were the masses and the production rates. The signals stood out of the backgrounds very sharply and cleanly, and their interpretation in terms of W and Z was straightforward. The discovery of the top was harder, but still benefited from the a-priori knowledge that the top *had* to be there somewhere, and of its production and decay properties.

It is likely that the search and discovery of the Higgs boson will follow a similar path. We have reasonable confidence that the Higgs *has* to be there, and we know how it would be produced and decayed, as a function of its mass and even as a function of the possible models alternative to the plain SM implementation of the Higgs mechanism. Search strategies have been set up to cover all expected alternatives, and in many cases a signal will be unmistakable: mass peaks such as those obtained from $H \to \gamma\gamma$, or $H \to ZZ \to 4$ leptons, are easily established as soon as the statistics is large enough to have them stand out of the continuum background, without any need to rely on theoretical modeling.

As we move away from the default Higgs scenarios, into the territory of new physics beyond the SM, life becomes more difficult. One should think of two phases for a discovery: establishing the deviation from the SM, and understanding what this deviation corresponds to. It is crucial to maintain these two phases separate. The fact that a given anomaly is consistent with one possible interpretation does not increase its significance as an indication

of new physics. If we see something odd in a given final state, it is not by appealing to, or freshly concocting, a new physics model that gives rise to precisely this anomaly that makes the signal more likely or more credible. The process of discovery, namely the detection of a deviation from the SM by more than, say, 5 standard deviations of combined statistical and systematic uncertainties, should be based solely on the careful examination of whether indeed this signal violates the SM expectation. Assigning this discrepancy to a slot in the space of possible BSM scenarios is a subsequent step.

We can broadly group the possible deviations from the SM expectation into three, possibly overlapping, classes: mass peaks, shape discrepancies, and excesses in so-called counting experiments.

4.2.1. *Mass peaks*

Whether in a dilepton, diphoton, or dijet final state, a two-body mass peak in the region of hundred GeV and above is the most robust signature one can hope for. Unless one sculpts the signal with a dangerous choice of selection cuts (like looking for a mass peak in the mass region just above the kinematical threshold set by twice the minimum energy of the reconstructed objects), this signal cannot be faked by a detector flaw. For example, things like malfunctioning calorimeter units occasionally giving a fixed signal corresponding to a high-energy deposition, will only fake a mass peak if all events have precisely the same two detector elements giving the signals for the two particles in the mass bin. Random failures by more calorimeter towers would give different two-body invariant masses, because of the different reconstructed kinematics, and would not build up a mass peak! On the other hand if it is always the same two calorimeter towers giving the signal, this is unlikely enough to be immediately spotted as a localized hardware problem rather than as a Z'.

On the theory side, no SM background can give rise to a sharp peak, since, unless you are sitting on top of a W or Z, all sources give rise to a continuum spectrum: either from the obvious DY, or from the decay of separate objects (like WW or $t\bar{t}$ pairs).

An experimental analysis would extract the background directly from the data, by studying the sidebands of the invariant mass distribution below and above the peak, and interpolating under it. The role of the simulation of the SM background is therefore marginal, and will only contribute, possibly, in helping the interpolation and establishing more accurately the

background level for the experimental extraction of the signal excess. The simulation becomes then crucial in the second phase, that of the determination of the origin of the new signal, and of the study of its properties, as discussed later.

Mass peaks are just an example of a general set of self-calibrating signals, for which data themselves offer the most reliable source of background estimate. Other examples include jacobian peaks, or sharp edges in two-body mass distributions, like in the case of dileptons in supersymmetric chain decays of gauginos [10].

4.2.2. *Anomalous shapes of kinematical distributions*

Typical examples in this category are the inclusive transverse energy ($E_{\rm T}$) spectrum of jets, or the missing transverse energy ($\not{E}_T$) distribution in some class of final states (e.g. multijet plus $\not{E}_T$, as expected in most supersymmetric scenarios). A precise knowledge of the SM background shapes is an obvious advantage in these cases. To which extent one can solely rely on such presumed knowledge, however, is a matter worth discussing. To help the discussion it is useful to consider a concrete example from the recent history of hadronic collisions, namely the high-$E_{\rm T}$ jet spectrum measured in run 1 by CDF [11].

For years it has been claimed that a high tail in the jet $E_{\rm T}$ spectrum is a possible signal of an anomalous quark form factor, due for example to the manifestation of quark compositeness. The comparison of CDF's data with the best available theoretical predictions, based on next-to-leading-order (NLO) QCD and the latest parton density functions (PDFs) extracted from HERA, led to a several-σ excess in the region $E_{\rm T} \gtrsim 250$ GeV, compatible with compositeness at a scale just above the TeV. The difference between theory and data was such that no appeal to yet higher order effects could have possibly fixed it. In that respect, the discrepancy would have already been visible using a plain leading-order (LO) calculation, since, aside from an overall K factor, the shapes at LO and NLO were known to agree very well. On the side of PDFs, the same conclusion could be drawn from the analysis of the HERA data. With the lack of flexibility in modifying the behaviour of the partonic NLO cross section, and given the solid understanding of experimental systematics, the PDFs remained however the only possible scapegoat. As it turned out, the supposedly well-known large-x behaviour of the gluon density was driven mostly by the assumed functional form used in the fits, rather than by data directly sensitive to it.

Including the CDF data into the fits, and assigning to them a larger statistical weight, led in fact to new sets [13] that gave equally good descriptions of previous data, as well as explaining away the jet anomaly. The impasse was finally resolved by the subsequent analysis by D0 [12] , which considered the E_T spectrum of jets produced at large rapidity. The production of dijet pairs with a large longitudinal boost but of low invariant mass (therefore in a region free of possible new physics *contamination*) forces the momentum fraction of one of the incoming partons to be close to 1, thus probing the PDFs in the range relevant for the high-E_T, central, production. This measurement confirmed the newly proposed fits, and set the matter to rest.

The lesson for the future is that, more than accurate theoretical calculations, in these cases one primarily needs a strategy for an internal validation of the background estimate. If evidence for some new phenomenon entirely depends on the shape of some distribution, however accurate we think our theoretical inputs are, the conclusion that there is new physics is so important that people will always correctly argue that perhaps there is something weird going on on the theory side, and more compelling evidence has to be given.
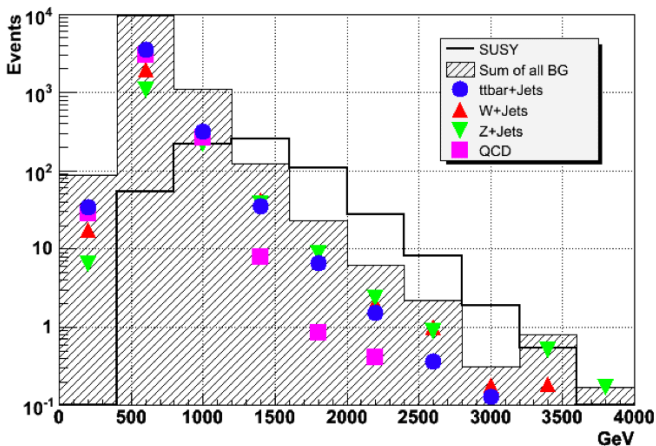
Fig. 4.1. Example of an expected supersymmetry signal and backgrounds in the multijet+$\not{E}_T$ final state [14] .

A place where we shall (hopefully!) encounter this problem at the LHC is the $\not{E}_T$ spectrum in multijet events, the classic signature of escaping neutralinos produced in the chain decay of pair-produced squarks and gluinos. A possible outcome of this measurement is given in Fig. 4.1,

taken from recent ATLAS studies [14]. The variable M_{eff} is defined as the sum of the transverse energies of all hard objects in the event (jets and $\not{E}_T$, in this case). Events are required, among other things, to have at least 4 jets with $E_{\text{T}} > 50\,\text{GeV}$, of which one above 100 GeV, and $\not{E}_T > \max(100\,\text{GeV}, 0.2 \times \text{M}_{\text{eff}})$. The solid histogram is the expected signal, the shaded one is the sum of all backgrounds, including SM processes with real $\not{E}_T$ (such as jets produced in association with a Z boson decaying to neutrinos), and SM processes where the $\not{E}_T$ results from the inaccurate measurement of some jet energies. The signal corresponds to production of squarks and gluinos with a mass of the order of 1 TeV. While the signal has certainly a statistical significance sufficient to claim a deviation from the SM, it is unsettling that its shape is so similar to that of the sum of the backgrounds. The theoretical estimates of these backgrounds have also increased significantly over the last few years, as a result of more accurate tools to describe multijet final states. There is no question, therefore, that unless each of the background components can be separately tested and validated, it will not be possible to draw conclusions from the mere comparison of data against the theory predictions.

I am not saying this because I do not believe in the goodness of our predictions. But because claiming that supersymmetry exists is far too important a conclusion to make it follow from the straight comparison against a Monte Carlo. One should not forget relevant examples from the colliders' history [15, 16], such as the misinterpretation in terms of top or supersymmetry of final states recorded by UA1 with jets, $\not{E}_T$, and, in the case of top, leptons. Such complex final states were new experimental manifestations of higher-order QCD processes, a field of phenomenology that was just starting being explored quantitatively. It goes to the theorists' credit to have at the time played devil's advocate [17], and to have improved the SM predictions, to the point of proving that those signals were nothing but bread and butter W or Z plus multijet production. But the fact remains that claiming discoveries on the basis of a comparison against a MC is dangerous.

So let me briefly discuss the current status of theory predictions for the SM channels relevant for supersymmetry searches. There are three dominant processes: production of jets and a Z boson, with $Z \to \nu\bar{\nu}$ giving the missing energy; production of jets and a W boson, where this decays either to a $\tau\nu$ (the τ faking a jet), or to a $\mu\nu$ or $e\nu$, with the leptons escaping identification; and $t\bar{t}$ pairs, where one of the Ws from the top decays behaves like in the previous case.

$t\bar{t}$ production has been well tested at the Tevatron [18, 19]. Theoretical NLO calculations, enhanced by the resummation of leading and subleading Sudakov logarithms [20], predict correctly the total cross section. The predictions for the LHC are expected to be equally accurate, if not more, since the main source of uncertainty, the PDFs, fall at the LHC in a range of x values where they are known with precision better than at the Tevatron. The kinematical production properties, such as the transverse momentum distribution or the invariant mass of the $t\bar{t}$ pair, are also well described by theory, and Monte Carlo event generators are available to model the full structure of the final states, including both the full set of NLO corrections [21] and the emission of multiple extra jets [22], which is relevant for the backgrounds to supersymmetry.

The processes W+jets and Z+jets are very similar from the point of view of QCD. There are minor differences related to the possibly different initial-state flavour compositions, but the main theoretical systematics, coming from the renormalization-scale sensitivity due to the lack of higher-order perturbative corrections, are strongly correlated. In the case of W/Z+1 and 2 jets, parton-level NLO calculations are available [23]. They are in excellent agreement with the measurements at the Tevatron [24, 25], as shown for example in the case of Z+1 and 2 jets by the CDF results [24] shown in Fig. 4.2. Going to higher jet multiplicities, and generating a realistic representation of the fully hadronic final state, is then possible with LO calculations. Exact, LO matrix-element calculations of multiparton production can be enhanced by merging with shower Monte Carlo codes [26, 27], which add the full perturbative gluon shower and eventual hadronization. An example of the quality of these predictions is given by Fig. 4.3, which shows the ratio of the measured [28] and predicted $W + N$-jet cross sections, for jets with $E_{\mathrm{T}} > 25$ GeV. The theoretical predictions include the LO results from Ref. [29] (labeled as MLM), and from Ref. [30] (labeled as SMPR), while MCFM refers to the NLO predictions for the 1- and 2-jet rates from Ref. [23]. The systematic uncertainties of the individual calculations, mostly due to the choice of renormalization scale, are shown. The LO results, which have an absolute normalization for all N-jet values, are in good agreement with the data, up to an overall K factor, of order 1.4. The prediction for the ratios of the N-jet and $(N-1)$-jet rates is also in good agreement with the data. The NLO calculations embody the K factor, and exactly reproduce the 1- and 2-jet rates.

Thorough comparisons have been performed [31] among a set of independent calculations of W plus multijet final states [29, 32–35]. The
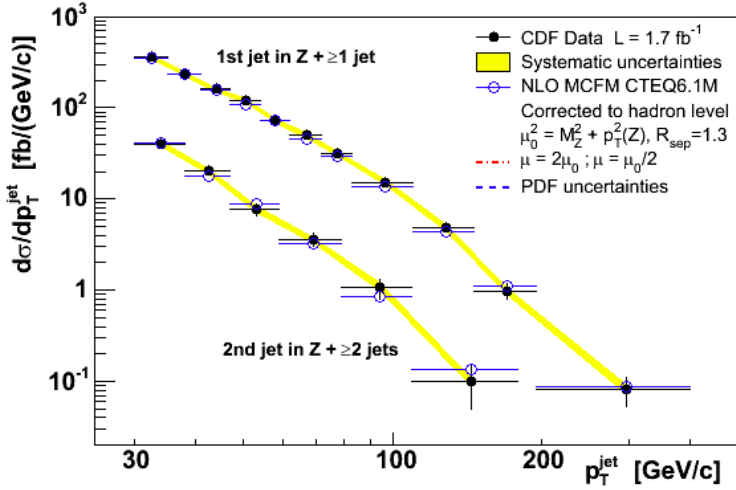
Fig. 4.2.   Jet E_T spectra in Z+jet(s), as measured by CDF at the Tevatron [24].
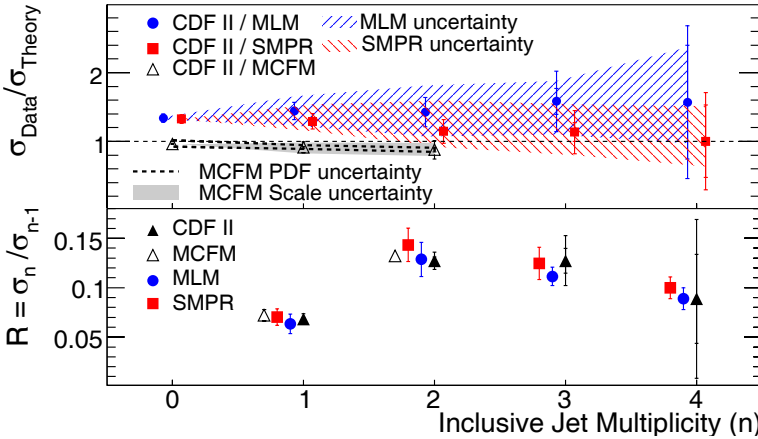
Fig. 4.3.   Comparison between CDF data and theory for $W + N$ jets cross sections [28].

results of the matrix element evaluation for these complex processes are all in excellent agreement; differences in the predictions at the level of hadrons may instead arise from the use of different parton-shower approaches, and of different ways of sharing between matrix elements and shower the task of describing the radiation of hard jets. An example of the spread in the predictions is shown in Fig. 4.4, which shows the E_T spectra of the four
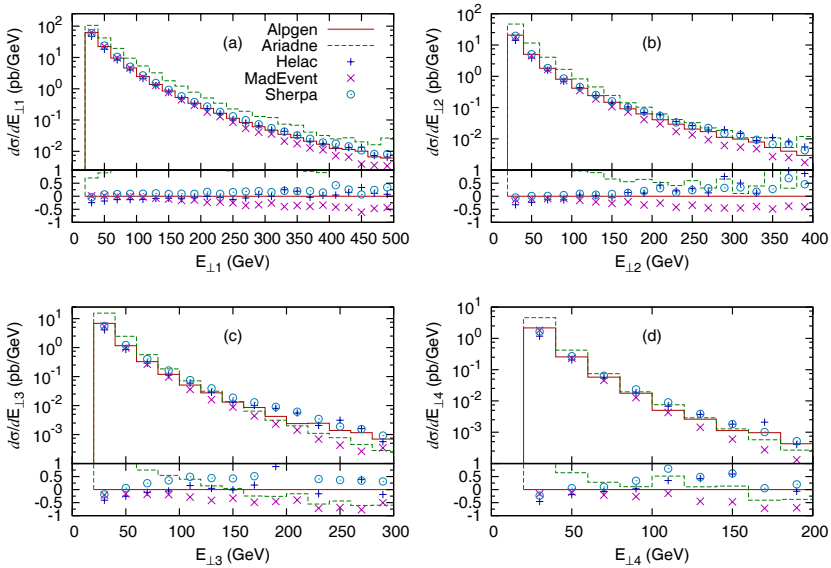
Fig. 4.4.   Predicted jet E_{T} spectra in W+jet(s) final states at the LHC [31].

highest-E_{T} jets in W+multijet events at the LHC. With the exception of the predictions from one of the codes, all results are within $\pm 50\%$ of each other, an accuracy sufficient by itself to establish possible deviations such as those in Fig. 4.1. These differences are of size compatible with the intrinsic uncertainties of the calculations, given for example by the size of the bands in Fig. 4.3. It is expected that they can be removed by tuning the input parameters, like the choice of renormalization scale, by fitting the data. An accurate determination of the normalization and shape of the SM background to a supersymmetric signal could therefore be obtained by analyzing data control samples. The description of the $(Z \rightarrow \nu\bar{\nu})+$ jets process can be validated, and the absolute normalization of the rate tuned, by measuring the signal-free $(Z \rightarrow e^+e^-)+$ jets final states. This information can be then directly used to tune the W+jets predictions; or one can measure directly $(W \rightarrow e\nu)+$ jets in a region where the electron is clearly tagged, and use the resulting tune to extrapolate to the case of τ decays, or to decays where the e and μ are not detected. The fact that the calculations appear to well reproduce the ratios of $\sigma[N-\mathrm{jet}]/\sigma[(N-1)-\mathrm{jet}]$, provides a further handle.

A clear path is therefore available to establish the accuracy of the theoretical tools, and to provide robust background estimates for searches of anomalies in the multijet plus $\not{E}_T$ final states. As always, however, the devil is in the details. As shown by the Tevatron analyses, even the measurement of the background W+multijet cross sections is not an easy task, due to a large contamination from $b\bar{b}$ backgrounds (where both b-hadrons decay semileptonically, one giving rise to a hard and isolated charged lepton, the other to a very energetic neutrino), and $t\bar{t}$ backgrounds, which at the LHC are the dominant source of W+multijet events. It is therefore difficult to anticipate the dimension of the challenge, only the direct contact with to data will tell!

4.2.3. *Counting experiments*

A *counting experiment* is a measurement defined by assigning some selection criteria, counting the number of events passing the cuts, and comparing this against the expected background. Counting experiments are like searches for shape anomalies, since the analysis cuts act on the distribution of some variables. However the expected statistics are too small to allow a meaningful use of the full distributions, and one simply integrates over the full sample passing the cuts. So counting experiments tend to lack a *smoking gun*, a truly compelling evidence that something is wrong, and they require the most robust understanding of backgrounds one can possibly need.

A typical example is given by the analyses that led to the top discovery. Different selections were applied to single out complementary data samples, each characterized by at least one of the expected features of top final states:

- a charged lepton, with $\not{E}_T$, 3 or more jets, and possibly one of them containing either a lepton, or a secondary displaced vertex (SVX), expected features of b-hadron decays;
- a pair of opposite-charge leptons, with invariant mass away from the Z peak is same flavour, and one or two jets, possibly with a b-quark tag.

Each of the objects listed above had to pass some kinematical or quality cuts, in terms of minimum p_T or E_T, or in terms of variables defining the cleanness of the leptonic of SVX tags. The estimate of the backgrounds to a counting experiment is usually very hard. One can always suspect that, even if the background estimates are tested on control samples, the extrapolation in the signal region could fail. For example, backgrounds that are a negligible component of the control samples could sneak into the

signal region, and suddenly dominate the rates. Furthermore, backgrounds could have strong correlations among different variables, and the probability of extrapolating their rate using their relative weight for various variables may not factorize into a product of probabilities. A typical example is the one given earlier for the contribution of $b\bar{b}$ pairs to events with isolated electrons (or muons) and missing transverse energy. The contribution to isolated leptons is proportional to the probability of having a $b\bar{b}$ final state, P_{bb}, times the probability of a suitable decay to a charged lepton, $P_{b\to\ell}$. The contribution to a large $\not{E}_T$ signal is likewise given by $P_{bb} \times P_{b\to\nu}$. But the probability of having both a hard charged lepton and the $\not{E}_T$ is not the product of the two, but is given by $P_{bb} \times P_{b\to\ell} \times P_{b\to\nu}$, which is larger than the product by $\sim 1/P_{bb} \gtrsim 100$.

Analyses of this type require full Monte Carlo codes, where the best possible perturbative input (e.g. multijet matrix elements) is used together with a complete description of the shower, hadronization, particle decays, and underlying event. A good description of a b-hadron decay, based for example on an empirical fit to existing data, may have more value than the inclusion of first-principle NLO corrections to the matrix elements. The challenge for the theorist is to provide a prediction where the accuracy is uniformly distributed over all the delicate areas, rather than concentrated on some specific spots. The calculation must have enough tunable parameters that the predictions can be adjusted to fit the data in the control samples, but not too many that the extrapolation from the control samples to the signal regions may not be trustable. The crucial question that a theorist is called to answer for applications to counting experiments is, in fact, to which extent the predictions of the code tuned on some sample can be trusted when exported to another sample. When codes can be properly tuned, the *portability* issue becomes the dominant source of systematics. Sorting out all of these issues requires a very careful and skilled work, both on the experimental and theoretical side. This sort of explains why it took about 100 pages [8] to document the steps that led to a credible first evidence for the top quark!

The discovery of the Higgs in complex final states, such as the weak-boson fusion channels, with the Higgs decaying to final states without a sharp mass peak, such as $H \to \tau^+\tau^-$ or $H \to b\bar{b}$, and with vetoes on the presence of jets in the central rapidity region, will fall in this category of extremely difficult and hard-to-valiate searches.

An interesting historical example in this class is the famous $e^+e^-\gamma\gamma\not{E}_T$ event seen by CDF in run 1 [36]. The expected SM background for this

event is less than 10^{-6} events. The estimate drops to 10^{-8} if one assumes that the most forward electron (for which the tracking information, and therefore a charge-tag, is missing) is actually a photon. According to *the rules*, this is a 5σ excess, and qualifies for a discovery. After all, even the Ω^- discovery was based on just one, compelling, event. In terms of pure statistics, the $e^+e^-\gamma\gamma\not{E}_T$ is (still today, after 30 times more luminosity has been collected by CDF and D0) even more significant as a deviation from the background (whether caused by physics or instrumental) than the first W observations at UA1 and UA2. Why do we not consider it as evidence of new physics? Because consensus built up in the community that, in spite of the "5σ", the evidence is not so compelling. On one side plausible BSM interpretations have been ruled out [19] by the LEP experiments, which inconclusively explored, for example, scenarios based on gauge-mediated supersymmetry breaking, with $\tilde{e} \to e\tilde{\gamma} \to e\gamma\tilde{G}_{3/2}$. On the other, doubts will always remain that some freaky and irreproducible detector effect may be at the origin of this event. However difficult, the estimate of the physics SM background to this event at the leading-order is relatively straightforward and has been checked and validated. Higher-order effects, not known, cannot be reasonably expected to change the rates by more than a factor of two. I do not think that anyone can seriously argue that the knowledge of the background rates with a NLO accuracy would have changed our conclusions about this event, so I do not think that here theory could have played a more important role. As in other examples of the past (most frequently in the discovery of hadronic resonances, see e.g. the recent case of pentaquarks), theoretical bias (e.g. the availability and appeal of a theoretical framework — or lack thereof — within which to fit the claimed discovery), the possible prejudice towards the robustness of the analysis or of the group that performed it, and other considerations generically labeled as *guts' feeling*, heavily interfere with the purely statistical and systematics assessment of a finding, making its interpretation more difficult. We find a similar situation in other areas of particle physics. The examples of neutrino oscillations and of the muon anomalous magnetic moment come to mind. Davies' solar-neutrino anomaly had been sitting there for years, and no improvement in the solar model was ever going to be good enough for the reality of neutrino oscillations to be uniformly accepted by the community. New data, less sensitive to the details of theory, and providing the opportunity to test more convincingly the model assumptions beyond the shade of any doubt, had to come for Davis' signal to be incorporated in a broader evidence for neutrino oscillations. It is likely that the 3.5σ of BNL's $g_\mu - 2$

experiment [37] will have a similar fate, regardless of how much progress will be made in the theoretical understanding of the hadronic contribution to light-by-light scattering. QCD is simply too vicious for everyone to accept that this anomaly is a conclusive evidence of physics beyond the SM, let alone to commit to an interpretation such as supersymmetry.

4.3. Measuring Parameters

A key element of the discovery programme at the LHC will be improving the accuracy of the SM parameters, and measuring, as precisely as possible, the parameters of the new physics that will hopefully be discovered. The relation between m_{top}, m_W, $\sin\theta_W$ and M_H is an important prediction of the SM, and deviations from it should be accounted for by the effects of new physics. And in presence of new physics, the values of the new particles' masses and couplings will be the starting point to reconstruct the new theory.

This is an area where the ability of theory to describe the final states is crucial. Couplings will be extracted from the determination of production cross sections, branching ratios, or angular distributions. Masses will mostly be obtained via direct kinematical reconstructions. In all cases, an accurate modeling of both the SM backgrounds, which contaminate and deform the signal distributions, and of the signals, will be required.

Cross sections are obtained by counting events. Since the analyses defining a given signal have always selection cuts, to go from event counts to a cross section one has to model the acceptance and efficiency of those cuts. These depend on the details of the production process, something that only a theoretical calculation can provide. This implies that the calculations should not only provide a precise value of the total cross section of a given process, but also of the kinematical distributions that are used in the experimental analysis. For example, in the case of the W or Z cross section one needs the precise form of the p_T and rapidity spectra of the decay leptons [38]. The problem with this is that typical higher-order calculations are more easily done at the total cross section level, to benefit from the full inclusivity of the final state and more easily enforce the cancellation of the divergencies that appear separately in the real and in the virtual corrections. A great amount of work has therefore been invested recently in developing techniques capable of delivering the same perturbative accuracy both at the level of total cross sections and at the level of distributions (for a review of recent developments in higher-order perturbative QCD calculations, see

e.g. Ref. [4]). For example, the full next-to-next-to-leading-order (NNLO) calculation of the lepton distributions in $pp \to (W \to \ell\nu) + X$ was recently completed, in Ref. [39]. Their conclusion is that the inclusion of NNLO corrections is necessary to control the rates at the level of few percent. This is required, for example, for the extraction of the LHC absolute luminosity at a similar level of precision. Such an accurate knowledge of the luminosity is the prerequisite for the precise measurement of all other cross sections, including those of interesting new processes. More recently, even the calculation of rates for some Higgs final states has reached a full NNLO precision for realistic leptonic observables [40].

Purely leptonic observables, where the leptons arise from the decay of non-strongly interacting particles, make it possible to fully integrate over the strongly interacting components of the events and, experimentally, enjoy a reduced dependence on the full hadronic structure. Under these circumstances, the use of parton-level calculations for realistic studies is legitimate (see e.g. Ref. [41] for a discussion of $pp \to H \to WW \to \ell\ell\nu\nu$).

Precision measurements of observables directly sensitive to the hadronic component of the events are typically more demanding. A good example of the difficulties that are encountered in these cases is given by the measurement of the top quark mass. In hadronic collisions the top quark mass can only be measured by reconstructing, directly or indirectly, the total invariant mass of its decay products. Due to the large phase-space available, top quark pairs are always produced well above their kinematical threshold. One cannot therefore use techniques such as those available in e^+e^- collisions, where the mass of a new particle can be deduced from an energy scan at the production threshold. Furthermore, contrary again to e^+e^- collisions where a top-quark pair at threshold is produced without any other object, in the pp case the top pair is always accompanied by both the fragments of the colliding protons, and by the multitude of hadrons that are radiated off as the incoming quarks or gluons that will fuse into $t\bar{t}$ approach each other (initial-state radiation). It is therefore impossible to exactly decide which ones among the many particles floating around originate from the top decays, and have to be included in the determination of the top invariant mass, and which ones do not. As an additional obstacle, the top quark is coloured, it decays before hadronizing, but the detected decay products must be colour-singlet hadrons. This implies that at some stage during the evolution of the quarks and gluons from the top decay they will have to pair up with at least one antiquark drawn from the rest of the event, to ensure the overall colour neutrality of the final state. There is therefore no way,

as a matter of principle, that we can exactly measure on an event-by-event basis the top quark mass. The best that we can do is to model the overall production and decay processes, and to parameterize a set of determined observables as a function of the input top quark mass. For example, such an observable could be the invariant mass of three jets, assuming one of them comes from the evolution of the b quark, and the other two from the decay of the W. This modeling cannot be achieved with parton-level tools, regardless of their perturbative accuracy. A full description of the final state is required, including the non-perturbative modeling of both the fate of the proton fragments and of the transition turning partons into colour-singlet hadrons. With the current level of experimental uncertainties [42] on m_{top}, at the 2 GeV level, we are approaching the level where the theoretical modeling [43] is not validated by a direct comparison with data. At the LHC, where the experimental uncertainties could be reduced below the 1 GeV level, theory will be the dominant source of systematics. Observables will have to be identified that will allow a validation and tuning of this systematics, in the same way that analogous problems had to be addressed for the determination of the W mass at LEP. This is an area where the Tevatron statistics are too small to allow any progress, and all the work will be left to the LHC. Needless to say, all of this work will benefit the precise measurement of the masses of possible new particles decaying to quarks and gluons.

4.4. Conclusions

Advanced MC tools for the description of the SM, and for the isolation of possible new physics at the LHC, are becoming mature. Validation and tuning efforts are underway at the Tevatron, and show that a solid level of understanding of even the most complex manifestations of the SM are well under control. The extrapolation of these tools to the energy regime of the LHC is expected to be reliable, at least in the domain of expected discoveries, where the energies of individual objects (leptons, jets, missing energy) are of order 100 GeV and more. However, the consequences of interpreting possible discrepancies as new physics are too important for us to blindly rely on our faith in the goodness of the available tools. An extensive and coherent campaign of MC testing, validation and tuning at the LHC will therefore be required. Its precise definition will probably happen only once the data are available, and the first comparisons will give us an idea of how far off we are and which areas require closer scrutiny.

Ultimately the burden, and the merit, of a discovery should and will only rest on the experiments themselves! The data will provide the theorists guidance for the improvement of the tools, and the analysis strategies will define the sets of control samples that can be used to prepare the appropriate and reliable use of the theoretical predictions.

Aside from the discovery of anticipated objects like the W, Z and the top, we have never faced with high-energy colliders the concrete situation of a discovery of something beyond the expected. In this respect, we are approaching what the LHC has in store for us without a true experience of discovering the yet unknown, and we should therefore proceed with great caution. All apparent instances of deviations from the SM emerged so far in hadronic or leptonic high-enegy collisions have eventually been sorted out, thanks to intense tests, checks, and reevaluations of the experimental and theoretical systematics. This shows that the control mechanisms set in place by the commonly established practice are very robust.

Occasionally, this conservative approach has delayed in some areas of particle physics the acceptance of true discoveries, as in the case of Davies's neutrino mixing, and as might turn out to be the case for the muon anomaly. But it has never stopped the progress of the field, on the contrary, it has encouraged new experimental approaches, and has pushed theoretical physics to further improve its tools.

The interplay between excellent experimental tools, endowed with the necessary redundancy required to cross-check odd findings between different experiments and different observables, and a hard-working theoretical community, closely interacting with the experiments to improve the modeling of complex phenomena, have provided one of the best examples in science of responsible and professional *modus operandi*. In spite of all the difficult challenges that the LHC will pose, there is no doubt in my mind that this articulated framework of enquiry into the yet unknown mysteries of nature will continue providing compelling and robust results.

Acknowledgements

References

[1] J. M. Campbell, J. W. Huston and W. J. Stirling, Hard interactions of quarks and gluons: A primer for LHC physics, *Rept. Prog. Phys.* **70**, 89 (2007) [arXiv:hep-ph/0611148].

[2] M. L. Mangano, The saga of bottom production in proton antiproton collisions, *AIP Conf. Proc.* **753**, 247 (2005); M. Cacciari, Rise and fall of the bottom quark production excess, arXiv:hep-ph/0407187; M. Cacciari et al., QCD analysis of first b cross section data at 1.96-TeV, *JHEP* **0407** (2004) 033; F. Happacher, P. Giromini and F. Ptohos, Status of the observed and predicted b anti-b production at the Tevatron, *Phys. Rev. D* **73** (2006) 014026; D. E. Acosta *et al.* [CDF Collaboration], Measurement of the J/ψ meson and $b-$hadron production cross sections in $p\bar{p}$ collisions at $\sqrt{s} = 1960$ GeV, *Phys. Rev. D* **71** (2005) 032001.

[3] F. Abe *et al.* [CDF Collaboration], Inclusive J/ψ, $\psi(2S)$ and b quark production in $\bar{p}p$ collisions at $\sqrt{s} = 1.8$ TeV, *Phys. Rev. Lett.* **69** (1992) 3704; S. Abachi *et al.* [D0 Collaboration], J/ψ production in $p\bar{p}$ collisions at $\sqrt{s} = 1.8$ TeV, *Phys. Lett. B* **370** (1996) 239; N. Brambilla *et al.* [Quarkonium Working Group], Heavy quarkonium physics, arXiv:hep-ph/0412158.

[4] L. J. Dixon, Hard QCD Processes at Colliders, arXiv:0712.3064 [hep-ph].

[5] M. A. Dobbs *et al.*, Les Houches guidebook to Monte Carlo generators for hadron collider physics, arXiv:hep-ph/0403045.

[6] G. Arnison *et al.* [UA1 Collaboration], Experimental Observation Of Isolated Large Transverse Energy Electrons With Associated Missing Energy At $S^{1/2}$ = 540-Gev, *Phys. Lett. B* **122** (1983) 103; G. Arnison *et al.* [UA1 Collaboration], Experimental observation of lepton pairs of invariant mass around 95-GeV/c^2 at the CERN SPS collider, *Phys. Lett. B* **126** (1983) 398.

[7] M. Banner *et al.* [UA2 Collaboration], Observation Of Single Isolated Electrons Of High Transverse Momentum In Events With Missing Transverse Energy At The Cern Anti-P P Collider, *Phys. Lett. B* **122** (1983) 476; P. Bagnaia *et al.* [UA2 Collaboration], Evidence for $Z^0 \rightarrow e^+e^-$ at the CERN anti-p p collider, *Phys. Lett. B* **129** (1983) 130.

[8] F. Abe *et al.* [CDF Collaboration], Evidence for top quark production in $\bar{p}p$ collisions at $\sqrt{s} = 1.8$ TeV, *Phys. Rev. D* **50** (1994) 2966; F. Abe *et al.* [CDF Collaboration], Observation of top quark production in $\bar{p}p$ collisions, *Phys. Rev. Lett.* **74** (1995) 2626.

[9] S. Abachi *et al.* [D0 Collaboration], Observation of the top quark, *Phys. Rev. Lett.* **74** (1995) 2632.

[10] I. Hinchliffe, F. E. Paige, M. D. Shapiro, J. Soderqvist and W. Yao, Precision SUSY measurements at LHC, *Phys. Rev. D* **55** (1997) 5520.

[11] F. Abe *et al.* [CDF Collaboration], Inclusive jet cross section in $\bar{p}p$ collisions at $\sqrt{s} = 1.8$ TeV, *Phys. Rev. Lett.* **77** (1996) 438.

[12] B. Abbott *et al.* [D0 Collaboration], Inclusive jet production in $p\bar{p}$ collisions, *Phys. Rev. Lett.* **86** (2001) 1707.

[13] H. L. Lai *et al.*, Improved parton distributions from global analysis of recent deep inelastic scattering and inclusive jet data, *Phys. Rev. D* **55** (1997) 1280.

[14] S. Vahsen [ATLAS Collaboration], presented at the Joint meeting of the Pacific Region Particle Physics Communities, Oct 29 – Nov 3, 2006, Honolulu. S. Yamamoto [ATLAS Collaboration], Strategy for early SUSY searches at ATLAS, arXiv:0710.3953 [hep-ex].

[15] G. Arnison *et al.* [UA1 Collaboration], Associated Production Of An Isolated Large Transverse Momentum Lepton (Electron Or Muon), And Two Jets At The Cern P Anti-P Collider, *Phys. Lett. B* **147** (1984) 493.

[16] G. Arnison *et al.* [UA1 Collaboration], Experimental Observation Of Events With Large Missing Transverse Energy Accompanied By A Jet Or A Photon(S) In P Anti-P Collisions At $S^{1/2}$=540-Gev, *Phys. Lett. B* **139** (1984) 115.

[17] See e.g. S. D. Ellis, R. Kleiss and W. J. Stirling, Missing Transverse Energy Events And The Standard Model, *Phys. Lett. B* **158** (1985) 341.

[18] V. Sorin [CDF and D0 Collaborations], 42nd Rencontres de Moriond on Electroweak Interactions and Unified Theories, La Thuile, Italy, 10-17 Mar 2007, FERMILAB-CONF-07-166-E. Tevatron: top quark production and properties.

[19] W. M. Yao *et al.* [Particle Data Group], Review of particle physics, *J. Phys. G* **33** (2006) 1, and 2007 partial update for 2008.

[20] R. Bonciani *et al.*, NLL resummation of the heavy-quark hadroproduction cross-section, *Nucl. Phys. B* **529** (1998) 424; M. Cacciari *et al.*, The t anti-t cross-section at 1.8-TeV and 1.96-TeV: A study of the systematics due to parton densities and scale dependence, *JHEP* **0404** (2004) 068.

[21] S. Frixione, P. Nason and G. Ridolfi, A Positive-Weight Next-to-Leading-Order Monte Carlo for Heavy Flavour Hadroproduction, *JHEP* **0709**, 126 (2007); S. Frixione, P. Nason and B. R. Webber, Matching NLO QCD and parton showers in heavy flavour production, *JHEP* **0308**, 007 (2003).

[22] M. L. Mangano *et al.*, Matching matrix elements and shower evolution for top-quark production in hadronic collisions, *JHEP* **0701**, 013 (2007).

[23] J. Campbell and R. K. Ellis, Next-to-leading order corrections to W + 2jet and Z + 2jet production at hadron colliders, Phys. Rev. D **65** (2002) 113007; J. Campbell, R. K. Ellis and D. L. Rainwater, Next-to-leading order QCD predictions for W + 2jet and Z + 2jet production at the CERN LHC, *Phys. Rev. D* **68** (2003) 094021 [arXiv:hep-ph/0308195].

[24] T. Aaltonen *et al.* [CDF Collaboration], Measurement of Inclusive Jet Cross Sections in $Z/\gamma^* \to ee+$ jets Production in $p\bar{p}$ Collisions at $\sqrt{s} = 1.96$ TeV, arXiv:0711.3717 [hep-ex].

[25] V. M. Abazov *et al.* [D0 Collaboration], Measurement of the ratios of the $Z/\gamma^* + >= $ n jet production cross sections to the total inclusive Z/γ^* cross section in ppbar collisions at $\sqrt{s} = 1.96$ TeV, Phys. Lett. B **658** (2008) 112.

[26] G. Corcella *et al. JHEP* **01** (2001) 010.

[27] T. Sjöstrand, L. Lönnblad, S. Mrenna and P. Skands [arXiv:hep-ph/0308153].

[28] T. Aaltonen *et al.* [CDF Collaboration], Measurement of the cross section for W-boson production in association with jets in ppbar collisions at $\sqrt{s}$=1.96 TeV, arXiv:0711.4044 [hep-ex].

[29] M. L. Mangano *et al.*, ALPGEN, a generator for hard multiparton processes in hadronic collisions, *JHEP* **0307** (2003) 001.

[30] S. Mrenna and P. Richardson, Matching matrix elements and parton showers with HERWIG and PYTHIA, *JHEP* **0405** (2004) 040.

[31] J. Alwall *et al.*, Comparative study of various algorithms for the merging of parton showers and matrix elements in hadronic collisions, *Eur. Phys. J. C* **53**, 473 (2008).

[32] F. Krauss, A. Schalicke, S. Schumann and G. Soff, Simulating W / Z + jets production at the Tevatron, *Phys. Rev. D* **70** (2004) 114009; F. Krauss, A. Schalicke, S. Schumann and G. Soff, Simulating W / Z + jets production at the CERN LHC, *Phys. Rev. D* **72** (2005) 054017.

[33] N. Lavesson and L. Lönnblad *JHEP* **07** (2005) 054.

[34] F. Maltoni and T. Stelzer *JHEP* **02** (2003) 027.

[35] C. G. Papadopoulos and M. Worek *Eur. Phys. J.* **C50** (2007) 843–856.

[36] F. Abe *et al.* [CDF Collaboration], Searches for new physics in diphoton events in $p\bar{p}$ collisions at $\sqrt{s} = 1.8$ TeV, *Phys. Rev. D* **59** (1999) 092002.

[37] G. W. Bennett *et al.* [Muon G-2 Collaboration], Final report of the muon E821 anomalous magnetic moment measurement at BNL, *Phys. Rev. D* **73** (2006) 072003.

[38] S. Frixione and M. L. Mangano, How accurately can we measure the W cross section?, *JHEP* **0405** (2004) 056.

[39] K. Melnikov and F. Petriello, The W boson production cross section at the LHC through $O(\alpha_s^2)$, *Phys. Rev. Lett.* **96** (2006) 231803.

[40] C. Anastasiou, G. Dissertori and F. Stockli, NNLO QCD predictions for the H →WW→l l ν ν signal at the LHC, *JHEP* **0709** (2007) 018; M. Grazzini, NNLO predictions for the Higgs boson signal in the H→WW→l ν l ν and H→ZZ→4l decay channels, arXiv:0801.3232 [hep-ph].

[41] C. Anastasiou, G. Dissertori, F. Stoeckli and B. R. Webber, QCD radiation effects on the H→WW→l ν l ν signal at the LHC, arXiv:0801.2682 [hep-ph].

[42] CDF and D0 Collaborations, A Combination of CDF and D0 results on the mass of the top quark, arXiv:hep-ex/0703034.

[43] P. Skands and D. Wicke, Non-perturbative QCD effects and the top mass at the Tevatron, *Eur. Phys. J. C* **52**, 133 (2007).

Chapter 5

Thoughts on a Long Voyage

Leonard Susskind

Department of Physics, Stanford University
Stanford, CA 94305-4060

Some thoughts of a former particle physicist.

> *It is an ancient Mariner,*
> *And he stoppeth one of three.*
> *'By thy long beard and glittering eye,*
> *Now wherefore stopp'st thou me?*
> *The Bridegroom's doors are opened wide,*
> *And I am next of kin;*
> *The guests are met, the feast is set:*
> *May'st hear the merry din.'*
> *He holds him with his skinny hand,*
> *'There was a ship,' quoth he.*
> *'Hold off! unhand me, grey-beard loon!'*
> *Eftsoons his hand dropt he.*

Samuel Taylor Coleridge
The Rime of the Ancient Mariner

5.1. The Landscape

Indeed, the feast has been set, but I have been away from the table for a long time. It's been about 25 years since I drifted from particle physics, on a different voyage, to the land of black holes, quantum gravity, string theory, and cosmology. But now the "merry din" has drawn me back, if not as a participant, at least as a very interested observer.

Here's what I think about the seemingly endless period of waiting: Some people may feel that not much happened during the "long wait," but I don't agree. The focus on the "fundamental" questions that I listed above, has hugely changed our (or at least my) perspective on high-energy physics. There is also reason for optimism about the other side of the coin; namely, that the things we learn at the LHC will provide plenty of food for thought about the fundamental questions.

For me the biggest change of perspective involves the Landscape. Let's begin with a biological analogy: Suppose that theoretical biologists had figured out the DNA-theory of biological information-coding long before there was any detailed knowledge of genetics. Actually it's not that far fetched; Von Neumann had guessed a great deal of it in the 1940's. Further, suppose that the only thing these biologists had to work with was a handful of fossil bones from a single creature, out of which they hoped to reconstruct the details of the human genome. It would be very tough for a number of reasons.

The biggest difficulty would be the sheer number of possibilities; the "Landscape of Biological Designs" is unbelievably large, involving numbers far beyond googols. A human DNA molecule has about a billion base pairs so the number of possibilities is something like $4^{1,000,000,000}$. Even if we only counted whole genes the number would be at least $10^{1,000}$. Furthermore, the structure of the few available bones only involves a tiny fraction of the genetic material. It would be very difficult to guess much about the genes which determine the brain, the gall bladder or the eye.

Now turn to String Theory and its rules for compactification. Like the rules governing DNA molecules, the rules for compactification are relatively simple, but the various basic structures — Calabi Yau topology, wrapped branes, orbfolds, orientifolds, and fluxes, like the base pairs of DNA, can be assembled in an astonishing number of ways.

The difficulties that physicists face in reconstructing the Universal (as in universe) DNA are obvious: First of all our experiments are very crude, on a scale many orders of magnitude larger than the DNA structures themselves. Furthermore, in several ways, we are restricted to a minute fraction of the necessary information for figuring out the exact details of the genome. Like the biologists who had a few features of a single creature, we only have access to a few properties of a single bubble of space. The fictitious biologists have a problem: the available bone fragments are only sensitive to a small fraction of the genome and have little or no information about most of the genetic material. The problem for physics is that the experiments that

we can do — those that are actually possible — explore only a small part of the compactification-manifold. Roughly speaking, the standard model may live on a few isolated branes localized in some small region of the Calabi Yau space. Nothing that can be done with our present instruments can excite other, perhaps more distant degrees of freedom. A typical CY manifold together with its fluxes and branes may have a thousand variables, but physics below the GUT scale is only sensitive to a few tens of parameters.

Do we really know that there are many more compactification variables than those that determine the standard model (or the MSSM)? Here is where the cosmological constant comes in. The vacuum energy is the one thing that is sensitive to all the various components of the compactification. From the fact that a vacuum exists with a cosmological constant of order $10^{-123} M_p^4$, one might surmise that the number of vacua is huge, implying that the number of degrees of freedom is much larger than the set of standard-model constants. If all of this is true then we are never going to know the precise genome — topology, branes, fluxes — of our universe. But we probably don't really care.

If we can't find out everything about our own local vacuum, let alone the entire Landcape, what is it that we do want to know? I can't speak for anyone else, but what I want is to be more certain of the basic principles: is string theory right? Is the Landscape correct? Is there a Multiverse? Will black holes cause a breakdown of quantum mechanics? Which features of the world are environmental or anthropic, which are hard wired and which are completely accidental? Why is there a hierarchy of scales? Does supersymmetry play a role as many of us believe? Do axions resolve the CP puzzle? At present we simply don't have enough information to be sure of the principles. But there is little doubt that the LHC will tell us a lot more: it may even bear on some fundamental problems of black hole physics.

5.2. The Hierarchy

The primary focus of the LHC will be on the hierarchy problem: why is there a huge gap between the Planck or GUT scale, and the weak scale? As far as I know there are only two answers on the table. The first is fine tuning: the hierarchy problem would then be similar to the the cosmological constant problem. According to this view the magnitude of the hierarchy varies on the Landscape (and in the multiverse), and a small fraction of Landscape is selected anthropically. Indeed it is hard to imagine life in a universe in which the scale of chemistry is anywhere near the Planck scale.

The anthropic explanation would be the top contender if the LHC discovers *nothing* beyond the standard model.

But there is a big difference between the electroweak hierarchy and the CC. The anthropic explanation of the cosmological constant was a last resort: after at least half a century of thought no one ever found a natural mechanism for insuring that the vacuum energy as small as it is. By contrast, there is a very plausible mechanism that needs no fine tuning for creating a hierarchy between the Planck and weak scales. The trick — I will call it Technicolor — is always the same although it comes in various versions.

According to the Technicolor hypothesis, either directly or indirectly the hierarchy is generated by dynamical evolution (or renormalization group flow) of a small coupling constant, which eventually becomes large enough to go nonlinear. The pattern is familiar from QCD where the coupling g_0^2, defined at some small distance scale r_0, grows as r increases according to

$$g^2(r) = \frac{g_0^2}{1 - cg_0^2 \log(r/r_0)}. \tag{5.1}$$

When r becomes of order $r_0 \exp\left(1/cg_0^2\right)$, the running coupling g^2 becomes of order 1, and nonlinear dynamical effects can spontaneously break symmetries.

The simplest Technicolor theory makes use of a clone of QCD, coupled to the electroweak sector exactly like QCD itself. The only difference is that that the scale of chiral symmetry breaking in the Technicolor sector is raised to the electroweak scale. The spontaneous breaking of chiral symmetry breaks $SU(2) \times U(1)$. To put it another way, the Higgs sector is composed of composites analogous to pions and sigma mesons of QCD.

In its most straightforward version the Technicolor theory is ruled out by a variety of constraints including high precision electroweak data and the difficulty of generating quark masses consistent with the GIM mechanism. From time to time the theory is resurrected in various forms. One very interesting example is the Randall Sundrum model based on a five dimensional ADS-like warped geometry.

The holographic duality between the bulk 5D theory and 4D gauge theory implies that the R-S theory must be equivalent to some version of Technicolor in which the running of the TC coupling is equivalent to the warping of the 5D geometry. The infrared brane at which the Higgs sector is located translates directly to the confinement scale at which the

composite Higgs sector is generated. One should expect that the problems of the simple TC theory will be inherited by the 5D holographic theory. However it is entirely possible that the warped perspective may suggest new solutions of those problems. In any case the existence of a strongly interacting sector, directly generating weak symmetry breaking, should be testable but I have to say that it seems an unlikely possibility to me.

Low energy Supersymmetry offers a far more interesting option. I won't go into any detail about the MSSM — others can do that much better than I — but discuss the implications for the fundamental questions that I have been interested in. First let me point to the very well known fact that low energy Supersymmetry, when combined with "Grand Unification" (of $SU(3) \times SU(2) \times U(1)$ into something like $SU(5)$ or $O(10)$) leads to the miracle of gauge couplings unifying somewhere near the **Planck scale.** If supersymmetry is discovered it will once and for all eliminate the idea that gravity is not crucial to an understanding of elementary particles.

What does low energy Supersymmetry tell us about the DNA of the universe? Among other things it supports the idea of extra dimensions — an idea which in my opinion hardly needs support. From the beginning, in just about every theory of elementary particles, the distinction between different particles is due to their motion in various compact spaces. Isospin space, color space, the phase conjugate to electric charge, are all examples. The topology and other features of these internal spaces is what I call the DNA of the universe.

The discovery of Supersymmetry would add to the list of internal directions of space with an fascinating new kind of "Grassman" dimension that gives rise to the distinction between fermions and bosons. Although Supersymmetry may be possible without string theory; and given the diversity of the Landscape, String Theory may be possible without (low energy) Supersymmetry; it would be hard to not see the experimental discovery of superpartners as an encouraging sign for String Theory.

Another important point about Supersymmetry if it exists, is that it would limit the possible layers of structure between accessible energies and the Planck scale. If physics follows the historical pattern then one might expect new layers of compositness every couple of decades of energy. In a way this would be discouraging: to see to the Planck scale we might have to look around ten corners, so to speak. But Supersymmetry and gauge unification allow very little which can couple directly to the standard model degrees of freedom. In other words the things we see at low energy would be direct reflections of the DNA at much smaller scales.

A major advantage of Supersymmetry — in fact the reason for its original introduction into phenomenology was the fact that it can stabilize the hierarchy.[a] Note that I said stabilize, not explain. In the ordinary standard model the hierarchy is not only unexplained, but it is very unstable. Fixing the weak scale to be 17 orders of magnitude below that Planck scale in the classical Lagrangian is not enough: radiative corrections will pull weak scale up to almost the Planck scale unless the parameters are exquisitely fine tuned. Amazingly, Supersymmetry causes the fermionic and bosonic degrees of freedom to cancel in the large radiative corrections to the Higgs parameters. Thus one can adopt a "set it and forget it" attitude to the Hierarchy; but Supersymmetry does not explain why there is such a large ratio of scales in the original theory.

The most reasonable explanation of the weak hierarchy is that it is linked to the scale of supersymmetry breaking. This requires two not-so-obvious ingredients. The first is that the mass parameter in the Higgs potential (the so called μ-term) should be forbidden by exact Supersymmetry, and therefore only generated at the Supersymmetry breaking scale. That, in itself, requires some juggling that I will come back to.

Secondly, we need a mechanism to break Supersymmery, but only at low energy. As far as I know all of the viable mechanisms go back to the old "hidden sector" idea. The idea is that there is a gauge sector — call it G_H that is decoupled from the Standard Model degrees of freedom. In addition there are other degrees of freedom which bridge the gap, by carrying both Standard Model and Hidden degrees of freedom.

---

[a]Historical note: As far as I know, the origin of the idea that Supersymmetry might explain the stability of the electroweak hierarchy was in Stanford University sometime in 1980. Savas Dimopoulos, Stuart Raby, and I were working on the straightforward version of Technicolor and running into trouble, particularly with strangeness changing neutral currents. The problems were getting bad enough that I suggested that we begin to think about other possibilities. In particular, I recalled a conversation that I had with Ken Wilson a few years earlier. During a brief visit to Cornell, I happened to ask Ken if he had heard anything interesting at some conference he had just returned from. His answer was that the only interesting thing had to do with Supersymmetry. I was surprised and asked what it was that he found interesting. His answer was the Supersymmetry allows scalars to be naturally massless. My response was, so what? Whereupon he mumbled something about the Higgs.
Later on when simple Technicolor was failing, I realized what Ken's point had been, namely, the stability of the hierarchy. I explained the point and Savas, Stuart, and I began to teach ourselves Supersymmetry. Eventually Savas and Stuart presented me with a mixed version of Supersymmetry and Technicolor called Supercolor but I didn't much like it. In retrospect I am sorry that I refused to coauthor it.

According to the hidden sector theory, the primary Supersymmetry breaking is in the hidden sector, and it is then fed to the usual particles through the bridging degrees of freedom. But what causes the breaking of Supersymmetry in the hidden sector, and why does it occur at a scale much below the Planck scale? The likely answer is the hidden sector is a form of Technicolor. But instead of directly precipitating a breaking of electroweak symmetry, it induces a breaking of Supersymmetry, which is then linked to electroweak breaking.

What does the existence of the hidden sector tell us about the DNA of the universe? I think that it mainly reinforces the idea that there is a lot more to the genetic code than just the parts that govern the standard model (or the MSSM). Incidentally, the same could be said about inflation — so far, the inflaton degrees of freedom seem to be quite outside the standard model. All of these diverse sectors may seem very inelegant, but they seem to fit with a complicated genome or compactification.

5.3. Linkages

There are a number of puzzles that are not answered by the pretty package of MSSM coupled to G_H, that many people rightly find disturbing. These puzzles may bear on the question of which features of laws of particle physics are environmental (anthropic?) and which are not.

The first has to do with baryon number conservation or more precisely, the stability of the proton. First let me dispense with the obvious answer: could baryon number be an exact (global)symmetry of nature. There are several things that rather strongly argue against such a symmetry.

(1) The observed baryon excess of the universe is best explained by baryon and CP violation in the early universe.
(2) GUT theories generally have interactions which violate baryon number. Even in the standard model, the baryon current is anomalous.
(3) String theory does not permit the existence of conserved global charges.
(4) To me, the most convincing argument for baryon violation at some scale, comes from black hole physics. A black hole originally composed of a large number of baryons will eventually evaporate by Hawking radiation. For most of its life it is far to cold to emit anything but massless photons and gravitons. Thus the final evaporation products must have far less baryon number than the original collapsing object.

If baryon number is violated, why doesn't the proton decay, say to a positron and a photon, in a typical particle physics time scale? In the MSSM there are dimension 4 operators that would mediate such a rapid decay. The usual answer is that dimension 4 operators can easily be forbidden by an unbroken discrete R-symmetry. But that only raises the question of why R-symmetry is not broken at the Supersymmetry breaking scale? In some portions of the Landscape, that is probably the case.

For dimension 4 operators the most likely answer may be anthropic — our protons had better live for at least the age of the universe for us to be here. So dimension 4 operators are forbidden and the best way to do that is to invoke discrete R-symmetries.

In the standard model there are dimension 6 operators that can mediate proton decay. But if their origin is at the GUT scale they will be too small (at low energy) to be a problem for proton stability. However, as Weinberg pointed out long ago, Supersymmetry creates a new potential problem, namely dimension 5 operators. Typically these lead to a proton lifetime much too long to be explained anthropically. A typical calculation of a dimension 5 decay gives a proton lifetime of order 10^{25} years. But while very long on the anthropic scale, it is much shorter than the observed bound of 10^{34} years. As Banks and Dine have emphasized, there is no known selection principle that would force us to be at a point on the Landscape where the proton lifetime is that long.

Let me come to another puzzle: why is the μ-term (Higgs mass parameter)forbidden above the Supersymmetry breaking scale? Supersymmetry itself does not forbid μ, so a generic version of the MSSM might have μ of order the GUT scale. That would unlink the Supersymmetry breaking scale from the electroweak scale and the hierarchy would be undone.

The usual answer, which I have nothing to add to, is again a new discrete symmetry. Such symmetries are easily found but again, we may ask why nature chose a vacuum with such a discrete symmetry?

This time the answer could easily be anthropic. Life, at least as we know it, cannot exist without a large hierarchy between the Planck and weak scale. Particular discrete symmetries may be rare, requiring rather special arrangements of the DNA. But anthropic selection would require such a symmetry to protect the μ-term.

This raises the question of "linkage." Is it possible that the same symmetry that protects the μ-term might also protect the proton lifetime by eliminating the offending dimension 5 operators? I don't know any general answer but there is at least one example in the literature of such linkage.

5.3.1. *The strong CP problem*

A very puzzling fine-tuning, not explained by either the MSSM or anthropic selection, invovles the strong CP problem. The θ-parameter of QCD breaks CP-invariance unless is is zero. Experimentally, θ is no bigger than 10^{-9}. Straightforward anthropic arguments cannot explain this: even $\theta \sim 1$ would not have much effect on life. The famous elegant solution to this problem is Peccei Quinn symmetry, which in turn entails the existence of an axion field.

The problem is that a variety of observational and theoretical constraints require the axion to be essentially massless in the early universe, even during inflation. This means that at reheating there is no reason why the axion field should be at the minimum of its (eventual) potential. The result is that when the axion becomes massive at the QCD scale, it will slosh around and fill the universe with too much dark matter — unless, by accident the value of the axion was originally very close to zero (the eventual minimum).

It has been suggested that the explanation is anthropic. The argument begins by observing that inflation will "iron" out the axion field so that in our observable patch of space it will be very uniform. If we figure out why it is special at one point, it will be special everywhere in our observable region. But on very large scales inflation will allow the axion to vary, so that on the largest scales, the axion will take on every value in its (periodic) range. This raises the obvious question: is the amount of dark matter due to a generically oscillating axion, anthropically forbidden?

According Tegmark, Aguirre, Rees, and Wilczek, the answer may be yes. These authors argue that any significant increase in the amount of dark matter in the universe would have prevented life from forming, and therefore, we must live in a place where the axion is near its minimum. Indeed, there best guess is that the axion field has to be so close its minimum that CP violation is undetectable.

The conclusion is very attractive. My only problem with it is that it uses very strong assumptions about the conditions necessary for life. For example, the authors claim that too much dark matter would have caused an increase in the rate of stellar encounters which would have disrupted life. Maybe they are right but I wish the argument were more robust.

Will the LHC illuminate this fundamental problem? Supersymmetry provides a very plausible non-axionic candidate for dark matter but it does not eliminate the CP problem. On the other hand if there is no Supersymmetry, the axion becomes the leading dark matter candidate. In neither

case is the CP problem solved. Perhaps the solution of Tegmark, Aguirre, Rees, and Wilczek will become more convincing with time.

Or maybe unexpected developments at the LHC will suggest an alternate solution to the CP problem, but I don't know what it could be.

5.4. Supersymmetry Breaking and the Landscape

It is not easy to find spontaneously broken ground states of a supersymmetric theory. Running to strong coupling by no means guarantees that the "true vacuum" breaks Supersymmetry. Although there are examples, the phenomenon is non-generic.

One of the big course-corrections triggered by the Landscape and the discovery of a positive cosmological constant, is the recognition that our vacuum is probably not absolutely stable. Most likely the only stable vacua in a theory with gravity are supersymmetric, which means they either have vanishing or negative cosmological constant. Certainly this seems to be true in the String Theory Landscape. These facts have dramatically broadened the search for vacua to include metastable states — something that was frowned on in the past. Moreover, it has become clear, particularly from the recent work of Intrilligator, Shih, and Seiberg, that metastable vacua are a very generic feature of strongly coupled supersymmetric theories. I think it is fair to say that low energy supersymmetry almost forces the existence of a Landscape of metastable vacua, and this has enormous implications for fundamental issues of cosmology.

To see the implications, consider the decay mechanism of a metastable vacuum. Vacuum decay is not something that happens globally, i.e., everywhere at once: that would violate causality. Instead, bubbles of more stable vacua nucleate locally. But if the bubble nucleation rate is slower than the Hubble expansion rate, the growing bubbles cannot catch up to one another, so that most of the universe continues to inflate. Thus, the experimental identification of the mechanism of Supersymmetry breaking can inform us about a profound cosmological issue: is the universe eternally inflating and therefore really a multiverse?

5.5. Black Holes at the LHC?

Much of my own effort during the last 25 years concerned the paradoxical quantum properties of black holes. Although the problems raised in the mid 1970's by Stephen Hawking threatened the consistency of quantum

mechanics at high energy, they seemed extremely remote from the day to day issues of experimental physics. Surprisingly, this may not be the case. I am told that approximately ten percent of the LHC running time will be devoted to testing black hole quantum physics.

I am not talking about new theories that place the string or Planck scale at a few TEV's, but rather an old theory, in which the string scale is a fraction of a GEV. String theory started as a theory of hadrons, where it was very successful at explaining the properties of these rather pedestrian particles; including the long sequences of resonances called Regge trajectories; and also the confinement of quarks. Hadrons are certainly strings: there is little doubt of that. But what is the connection between String Theory as a theory of hadrons, and String Theory as a theory of gravity? Originally it was thought that the connection was just an analogy: something like the analogy between an atom and the solar system. But now we know better. The discovery of gauge-theory/gravity duality implies hadrons are fundamental strings in a world of five dimensional quantum gravity.

Ordinary weakly coupled fundamental string theory, of the kind that you read about in String Theory textbooks, is not really a theory of Planck scale phenomena. Rather it is a theory of string-scale phenomena. The Planck scale in string theory is an entirely different scale of energies at which excited strings become so tangled and dense, that interactions become too strong to study by perturbation theory. It is also the scale at which black holes become the dominant form of matter. The parallel between hadronic String Theory and "fundamental" String Theory, requires that hadronic matter should behave like black holes at high energy, albeit, black holes in five dimensions.

Roughly speaking, the 5D picture is something like this: The extra dimension of space is finite in extent, extending from a so-called Planck or ultraviolet brane, to an infrared brane. Think of the UV brane as the ceiling and the IE brane as the floor. The 5D bulk is the region in between, and just as the analogy suggests, there is a gravitational field pulling matter toward the floor.

Hadrons are simple low energy string-like objects that slide along the floor, but when they collide at high energy they create a huge thermally excited tangle of string. The large energy allows the tangle to extend somewhat upward toward the ceiling. Translated into four dimensional terms, the stringy matter becomes thermally excited: the higher the energy, the higher the temperature, or equivalently, the closer to the ceiling. But then the matter cools, spreading out on the floor like a puddle of fluid held

down by gravity. From the four dimensional perspective the puddle is the quark-gluon fluid-like plasma. But the amazing thing is that from the five dimensional viewpoint, the puddle is a black hole, and the surface is its horizon. The puddle always cools to the same temperature, about the de-confinement temperature.

Experiments at RHIC have lent support to the horizon-like behavior of the fluid created in a high-energy heavy ion collision, but the puddle of energy is relatively small and evaporates quickly. I believe that some theoretical studies suggest that at higher energies, the quark-gluon plasma may form larger puddles. The hot fluid does not evaporate in the vertical (floor to ceiling 5th dimension) direction, because gravity pulls the evaporation products back down to the puddle. The evaporation takes place only out the sides, in the horizontal (3D) directions. But at RHIC the puddles are small and have large surface to volume ratio. Thus they decay quickly.

At the LHC the collision between heavy ions will be much higher in energy than at RHIC, and will produce a larger volume of fluid when it cools to the de-confinement temperature. This may give a much better opportunity to study the puddle and compare it with the theoretical predictions of gauge/gravity duality. Although obviously not the primary mission of the LHC, the big machine will be an interesting quantum gravity laboratory.

Thus I hope I have made my case that the long period of waiting, during which many theorists focused on what seemed like very esoteric questions, has not been in vain. We stand now not just to learn more about elementary particles, but to see the subject in a new light with a much deeper appreciation of its connection with the very fundamental questions.

Chapter 6

The "Top Priority" at the LHC

Tao Han

Department of Physics, University of Wisconsin
Madison, WI 53706
than@hep.wisc.edu

The LHC will be a top-quark factory. With 80 million pairs of top quarks and an additional 34 million single tops produced annually at the designed high luminosity, the properties of this particle will be studied to a great accuracy. The fact that the top quark is the heaviest elementary particle in the Standard Model with a mass right at the electroweak scale makes it tempting to contemplate its role in electroweak symmetry breaking, as well as its potential as a window to unknown new physics at the TeV scale. We summarize the expectations for top-quark physics at the LHC, and outline new physics scenarios in which the top quark is crucially involved.

6.1. Brief Introduction

The top quark plays a special role in the Standard Model (SM) and holds great promise in revealing the secret of new physics beyond the SM. The theoretical considerations include the following:

- With the largest Yukawa coupling $y_t \sim 1$ among the SM fermions, and a mass at the electroweak scale $m_t \sim v/\sqrt{2}$ (the vacuum expectation value of the Higgs field), the top quark is naturally related to electroweak symmetry breaking (EWSB), and may reveal new strong dynamics [1].
- The largest contribution to the quadratic divergence of the SM Higgs mass comes from the top-quark loop, which implies the immediate need for new physics at the Terascale for a natural EW theory [2], with SUSY and Little Higgs as prominent examples.

- Its heavy mass opens up a larger phase space for its decay to heavy states Wb, Zq, $H^{0,\pm}q$, etc.
- Its prompt decay much shorter than the QCD scale offers the opportunity to explore the properties of a "bare quark," such as its spin and mass.

Top quarks will be copiously produced at the LHC. The production and decay are well understood in the SM. Therefore, detailed studies of the top-quark physics can be rewarding for both testing the SM and searching for new physics [3].

6.2. Top Quark in The Standard Model

In the SM, the top quark and its interactions can be described by

$$-\mathcal{L}_{SM} = m_t \bar{t}t + \frac{m_t}{v}H\bar{t}t + g_s\bar{t}\gamma^\mu T^a t G^a_\mu + eQ_t\bar{t}\gamma^\mu t A_\mu \tag{6.1}$$

$$+ \frac{g}{\cos\theta_w}\bar{t}\gamma^\mu(g_V + g_A\gamma^5)tZ_\mu + \frac{g}{\sqrt{2}}\sum_q^{d,s,b} V_{tq}\bar{t}\gamma^\mu P_L q W^-_\mu + h.c.$$

Besides the well-determined gauge couplings at the electroweak scale, the other measured parameters of the top quark are listed in Table 6.1.

Table 6.1.   Experimental values for the top quark parameters [4].

m_t (pole)	$|V_{tb}|$	$|V_{ts}|$	$|V_{td}|$
(172.7 ± 2.8) GeV	> 0.78	$(40.6 \pm 2.6) \times 10^{-3}$	$(7.4 \pm 0.8) \times 10^{-3}$

The large top-quark mass is important since it contributes significantly to the electroweak radiative corrections. For instance, the one-loop corrections to the electroweak gauge boson mass can be cast in the form

$$\Delta r = -\frac{3G_F m_t^2}{8\sqrt{2}\pi^2 \tan^2\theta_W} + \frac{3G_F M_W^2}{8\sqrt{2}\pi^2}\left(\ln\frac{m_H^2}{M_Z^2} - \frac{5}{6}\right). \tag{6.2}$$

With the m_t value in Table 6.1, the best global fit in the SM yields a Higgs mass $m_H = 89^{+38}_{-28}$ GeV [4]. The recent combined result from CDF and D0 at the Tevatron Run II gave the new value [5]

$$m_t = 171.4 \pm 2.1 \text{ GeV}. \tag{6.3}$$

The expected accuracy of m_t measurement at the LHC is better than 1 GeV [6], with errors dominated by the systematics.

To directly determine the left-handed V-A gauge coupling of the top quark in the weak charged current, leptonic angular distributions and W polarization information would be needed [7]. No direct measurements are available yet for the electroweak neutral current couplings, $g_V^t = T_3/2 - Q_t \sin^2 \theta_W$, $g_A^t = -T_3/2$ and $Q_t = +2/3$, although there are proposals to study then via the associated production processes $t\bar{t}\gamma$, $t\bar{t}Z$ [8]. The indirect global fits however indicate the consistency with these SM predictions.

6.2.1. *Top-quark decay in the SM*

Due to the absence of the flavor-changing neutral currents at tree level in the SM (the Glashow-Iliopoulos-Maiani mechanism), the dominant decay channels for a top quark will be through the weak charged-currents, with the partial width given by [9]

$$\Gamma(t \to W^+ q) = \frac{|V_{tq}|^2 m_t^3}{16\pi v^2}(1 - r_W)^2(1 + 2r_W)\left[1 - \frac{2\alpha_s}{3\pi}(\frac{2\pi^2}{3} - \frac{5}{2})\right], \quad (6.4)$$

where $r_W = M_W^2/m_t^2$. The subsequent decay of W to the final state leptons and light quarks is well understood. Two important features are noted:

- Since $|V_{tb}| \gg |V_{td}|, |V_{ts}|$, a top quark will predominantly decay into a b quark. While V_{ts}, V_{td} may not be practically measured via the top-decay processes, effective b-tagging at the Tevatron experiments has served to put a bound on the ratio

$$\frac{B(t \to Wb)}{B(t \to Wq)} = \frac{|V_{tb}|^2}{|V_{td}|^2 + |V_{ts}|^2 + |V_{tb}|^2}, \quad (6.5)$$

  that leads to the lower bound for $|V_{tb}|$ in Table 6.1.
- Perhaps the most significant aspect of Eq. (6.4) is the numerics:

$$\Gamma(t \to W^+ q) \approx 1.5 \text{ GeV} \approx \frac{1}{0.5 \times 10^{-24} \text{ s}} > \Lambda_{QCD} \sim 200 \text{ MeV}.$$

  This implies that a top quark will promptly decay via weak interaction before QCD sets in for hadronization [10]. So no hadronic bound states (such as $\bar{t}t, \bar{t}q$, etc.) would be observed. The properties of a "bare quark" may be accessible for scrutiny.

It is interesting to note that in the top-quark rest frame, the longitudinal polarization of the W is the dominant mode. The ratio between the two available modes is

$$\frac{\Gamma(t \to b_L \ W_{\lambda=0})}{\Gamma(t \to b_L \ W_{\lambda=-1})} = \frac{m_t^2}{2M_W^2}. \quad (6.7)$$
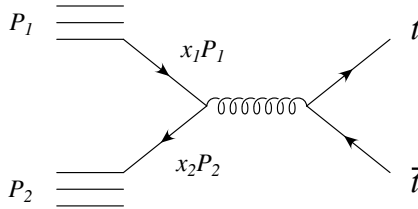
Fig. 6.1.   Top-quark pair production in hadronic collisions via QCD interaction. This figure is taken from Ref. [11].

6.2.2.   *Top-quark production in the SM*

6.2.2.1. *$t\bar{t}$ production via QCD*

Historically, quarks were discovered via their hadronic bound states, most notably for the charm quark via $J/\psi(\bar{c}c)$ and bottom quark via $\Upsilon(\bar{b}b)$. Due to the prompt decay of the top quark, its production mechanisms and search strategy are quite different from the traditional one.

The leading processes are the open flavor pair production from the QCD strong interaction, as depicted in Fig. 6.1. The contributing subprocesses are from

$$q\bar{q}, \ gg \to t\bar{t}. \tag{6.8}$$

The cross sections have been calculated rather reliably to the next-to-leading order [12] and including the threshold resummations [13, 14], as given in Table 6.2.

Table 6.2.   Cross sections, at next-to-leading-order in QCD, for top-quark production via the strong interaction at the Tevatron and the LHC [14]. Also shown is the percentage of the total cross section from the quark-antiquark-annihilation and gluon-fusion subprocesses.

	σ_{NLO} (pb)	$q\bar{q} \to t\bar{t}$	$gg \to t\bar{t}$
Tevatron ($\sqrt{s} = 1.8$ TeV $p\bar{p}$)	$4.87 \pm 10\%$	90%	10%
Tevatron ($\sqrt{s} = 2.0$ TeV $p\bar{p}$)	$6.70 \pm 10\%$	85%	15%
LHC ($\sqrt{s} = 14$ TeV pp)	$803 \pm 15\%$	10%	90%

Largely due to the substantial gluon luminosity at higher energies, the $t\bar{t}$ production rate is increased by more than a factor of 100 from the Tevatron to the LHC. Assuming an annual luminosity at the LHC of 10^{34} cm^{-2} s^{-1} $\Rightarrow$ 100 fb^{-1}/year, one expects to have 80 million top pairs produced.
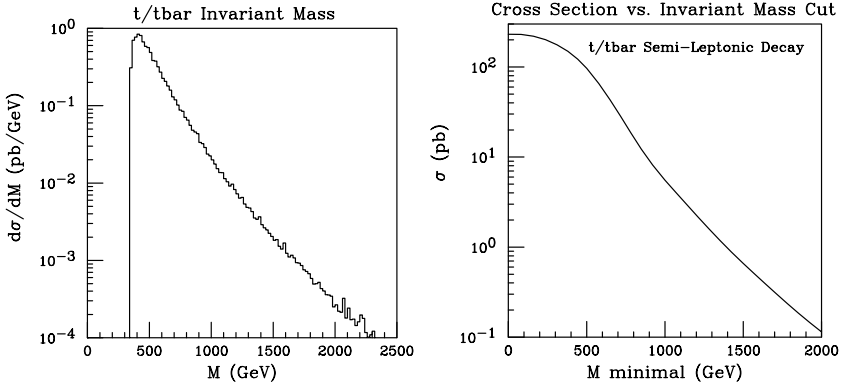
Fig. 6.2.   (a) Invariant mass distribution of $t\bar{t}$ at the LHC and (b) integrated cross section versus a minimal cutoff on $m(t\bar{t})$. Decay branching fractions of one top decaying hadronically and the other leptonically (e, μ) have been included.

It is truly a "top factory." In Fig. 6.2(a), we plot the invariant mass distribution, which is important to understand when searching for new physics in the $t\bar{t}$ channel. Although the majority of the events are produced near the threshold $m(t\bar{t}) \sim 2m_t$, there is still a substantial cross section even above $m(t\bar{t}) \sim 1$ TeV, about 5 pb. This is illustrated in Fig. 6.2(b), where the integrated cross section is given versus a minimal cutoff on $m(t\bar{t})$ and decay branching fractions of one top decaying hadronically and the other leptonically have been included.

It should be noted that the forward-backward charge asymmetry of the $t\bar{t}$ events can be generated by higher order corrections, reaching $10 - 15\%$ at the partonic level from QCD [15] and 1% from the electroweak [16].

6.2.2.2. *Single top production via weak interaction*

As discussed in the last section, the charged-current weak interaction is responsible for the rapid decay of the top quark. In fact, it also participates significantly in the production of the top quark as well [17]. The three classes of production processes, s-channel Drell-Yan, t-channel Wb fusion, and associated Wt diagrams, are plotted in Fig. 6.3. Two remarks are in order:

- The single top production is proportional to the quark mixing element $|V_{tb}|^2$ and thus provides the direct measurement for it, currently [18] $0.68 < |V_{tb}| \leq 1$ at the 95% C.L.
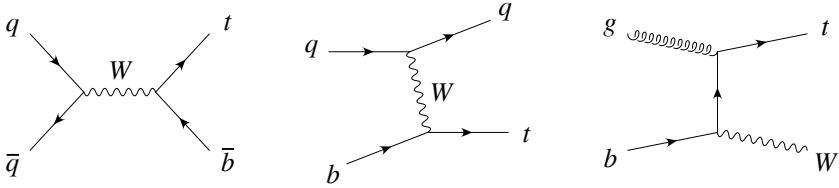
Fig. 6.3.   Single top-quark production in hadronic collisions via the charged-current weak interaction. This figure is taken from Ref. [11].

- The s-channel and t-channel can be complementary in the search for new physics such as a W' exchange [19].

For the production rates [20–24], the largest of all is the t-channel Wb fusion. It is nearly one third of the QCD production of the $t\bar{t}$ pair. Once again, it is mainly from the enhancement of the longitudinally polarized W. The total cross sections for these processes at Tevatron [23] and LHC energies [24] are listed in Table 6.3 [20–22]. We see the typical change of the production rate from the Tevatron to the LHC: A valence-induced process (DY-type) is increased by about an order of magnitude; while the gluon- or b-induced processes are enhanced by about a factor of 100.

Table 6.3.   Cross sections, at next-to-leading-order in QCD, for top-quark production via the charged current weak interaction at the Tevatron and the LHC.

σ(pb)	s-channel	t-channel	Wt
Tevatron ($\sqrt{s} = 2.0$ TeV $p\bar{p}$)	$0.90 \pm 5\%$	$2.1 \pm 5\%$	$0.1 \pm 10\%$
LHC ($\sqrt{s} = 14$ TeV pp)	$10.6 \pm 5\%$	$250 \pm 5\%$	$75 \pm 10\%$

6.2.2.3.   Top quark and Higgs associated production

Of fundamental importance is the measurement of the top-quark Yukawa coupling. The direct probe to it at the LHC is via the processes

$$q\bar{q}, \ gg \rightarrow t\bar{t}H. \tag{6.9}$$

The cross section has been calculated to the next-to-leading-order (NLO) in QCD [25, 26] and the numerics are given in Table 6.4. The cross section ranges are estimated from the uncertainty of the QCD scale.

The production rate at the LHC seems quite feasible for the signal observation. It was claimed [27] that a 15% accuracy for the Yukawa coupling

Table 6.4. Total cross section at the NLO in QCD for top-quark and Higgs associated production at the LHC [26].

m_H (GeV)	120	150	180
σ (fb)	634−719	334−381	194−222

measurement may be achievable with a luminosity of 300 fb^{-1}. However, the potentially large backgounds and the complex event topology, in particular the demand on the detector performance, make the study very challenging [28].

6.3. New Physics in Top-Quark Decay

The high production rate for the top quarks at the LHC provides a great opportunity to seek out top-quark rare decays and search for new physics Beyond the Standard Model (BSM). Given the annual yield of 80 million $t\bar{t}$ events plus 34 million single-top events, one may hope to search for rare decays with a branching fraction as small as 10^{-6}.

6.3.1. *Charged current decay: BSM*

The most prominent examples for top-quark decay beyond the SM via charged-currents may be the charged Higgs in SUSY or with an extended Higgs sector, and charged technicolor particles

$$t \rightarrow H^+ b, \quad \pi_T^+ b. \qquad (6.10)$$

Experimental searches have been conducted at the Tevatron [29], and some simulations are performed for the LHC as well [3, 30]. It is obvious that as long as those channels are kinematically accessible and have a sizable branching fraction, the observation should be straightforward. In fact, the top decay to a charged Higgs may well be the leading channel for $H^{\pm}$ production.

More subtle new physics scenarios may not show up with the above easy signals. It may be desirable to take a phenomenological approach to parameterize the top-quark interactions beyond the SM [7, 31], and experimentally search for the deviations from the SM. Those "anomalous couplings" can be determined in a given theoretical framework, either from loop-induced processes or from a new flavor structure. One can write the

interaction terms as

$$\mathcal{L}_{CC} = \frac{g}{\sqrt{2}} \left(\bar{t}(1+\delta_L)\gamma^\mu P_L q W_\mu^- + \bar{t}\delta_R\gamma^\mu P_R q W_\mu^- \right) + h.c. \quad (6.11)$$

The expected accuracy of the measurements on $\delta_{L,R}$ is about 1% [3, 31], thus testing the top-quark chiral coupling.

6.3.2. *Neutral current decay: BSM*

Although there are no Flavor-Changing Neutral Currents (FCNC) at tree level in the SM, theories beyond the SM quite often have new flavor structure, most notably for SUSY and technicolor models. New symmetries or some alignment mechanisms will have to be utilized in order to avoid excessive FCNC. It is nevertheless prudent to keep in mind the possible new decay modes of the top quark such as the SUSY decay channel

$$t \to \tilde{t}\tilde{\chi}^0. \quad (6.12)$$

Generically, FCNCs can always be generated at loop level. It has been shown that the interesting decay modes

$$t \to Zc, \quad Hc, \quad \gamma c, \quad gc \quad (6.13)$$

are highly suppressed [32, 33] with branching fractions typically $10^{-13} - 10^{-10}$ in the SM, and $10^{-7} - 10^{-5}$ in the MSSM. It has been shown that the branching fractions can be enhanced significantly in theories beyond the SM and MSSM, reaching above 10^{-5} and even as high as 1% [34].

One may again take the effective operator approach to parameterize the interactions. After the electroweak symmetry breaking, one can write them as [35–37]

$$\mathcal{L}_{NC} = \frac{g}{2\cos\theta_w} \sum_{\tau=\pm,q=c,u} \kappa_\tau \bar{t}\gamma^\mu P_\tau q Z_\mu + h.c. \quad (6.14)$$

$$+ g_s \sum_{q=c,u} \frac{\kappa_q^g}{\Lambda} \bar{t}\sigma^{\mu\nu} T^a t G_{\mu\nu}^a + eQ_t \sum_{q=c,u} \frac{\kappa_q^\gamma}{\Lambda} \bar{t}\sigma^{\mu\nu} t A_{\mu\nu} + h.c. \quad (6.15)$$

The sensitivities for the anomalous couplings have been studied at the LHC by the ATLAS Collaboration [38], as listed in Table 6.5.

Table 6.5. 95% C.L. sensitivity of the branching fractions for the top-quark decays via FCNC couplings at the LHC [38].

Channel	10 fb^{-1}	100 fb^{-1}
$t \to Zq$	3.1×10^{-4}	6.1×10^{-5}
$t \to \gamma q$	4.1×10^{-5}	1.2×10^{-5}
$t \to gq$	1.3×10^{-3}	4.2×10^{-4}

6.4. Top Quarks in Resonant Production

The most striking signal of new physics in the top-quark sector is the resonant production via a heavy intermediate state X. With some proper treatment to identify the top decay products, it is possible to reconstruct the resonant kinematics. One may thus envision fully exploring its properties in the c.m. frame.

6.4.1. $X \to t\bar{t}, t\bar{b}$

Immediate examples of the resonant states include Higgs bosons [39], new gauge bosons [40], Kaluza-Klein excitations of gluons [41] and gravitons [42], Technicolor-like dynamical states [1, 3, 43] etc.

The signal can be generically written as

$$\sigma(pp \to X \to t\bar{t}) = \sum_{ij} \int dx_1 dx_2 f_i(M_X^2, x_1) f_j(M_X^2, x_2)$$

$$\times \frac{4\pi^2 (2J+1)}{s} \frac{\Gamma(X \to ij) B(X \to t\bar{t})}{M_X}. \quad (6.16)$$

Thus the observation of this class of signals depends on the branching fraction of $X \to t\bar{t}$ as well as its coupling to the initial state partons. Figure 6.4 quantifies the observability for a bosonic resonance (spin 0,1,2) for a mass up to 2 TeV at the LHC [44] via $q\bar{q}, gg \to X \to t\bar{t}$. The vertical axis gives the normalization factors (ω) for the cross section rates needed to reach a 5σ signal with a luminosity of 10 fb^{-1}. The normalization $\omega = 1$ defines the benchmark for the spin 0, 1 and 2 resonances. They correspond to the SM-like Higgs boson, a Z' with electroweak coupling strength and left (L) or right (R) chiral couplings to SM fermions, and the Randall-Sundrum graviton $\tilde{h}$ with the couplings scaled with a cutoff scale as Λ^{-1} for $\tilde{h}q\bar{q}$, and $(\Lambda \ln(M_{pl}^*/\Lambda))^{-1}$ for $\tilde{h}gg$, respectively. We see that a Z' or a graviton
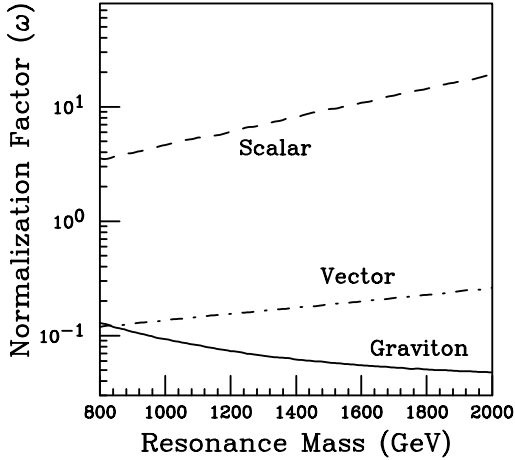
Fig. 6.4. Normalization factor versus the resonance mass for the scalar (dashed) with a width-mass ratio of 20%, vector (dot-dashed) with 5%, and graviton (solid) 2%, respectively. The region above each curve represents values of ω that give 5σ or greater statistical significance with 10 fb^{-1} integrated luminosity.

should be easy to observe, but a Higgs-like broad scalar will be difficult to identify in the $t\bar{t}$ channel.

It is of critical importance to reconstruct the c.m. frame of the resonant particle, where the fundamental properties of the particle can be best studied. It was demonstrated [44] that with the semi-leptonic decays of the two top quarks, one can effectively reconstruct the events in the c.m. frame. This relies on using the M_W constraint to determine the missing neutrino momentum, while it is necessary to also make use of m_t to break the two-fold ambiguity for two possible $p_z(\nu)$ solutions. Parity and CP asymmetries [45] can be studied.

Top-quark pair events at the high invariant mass are obviously important to search for and study new physics. In this new territory there comes a new complication: When the top quark is very energetic, $\gamma = E/m_t \sim 10$, its decay products may be too collimated to be individually resolved by the detector — recall that the granularity of the hadronic calorimeter at the LHC is roughly $\Delta\eta \times \Delta\phi \sim 0.1 \times 0.1$. This is a generic problem relevant to any fast-moving top quarks from heavy particle decays [41, 44, 46] (see the next sections). The interesting questions to be addressed may include:

- To what extent can we tell a "fat top-jet" from a massive QCD jet due to showering?
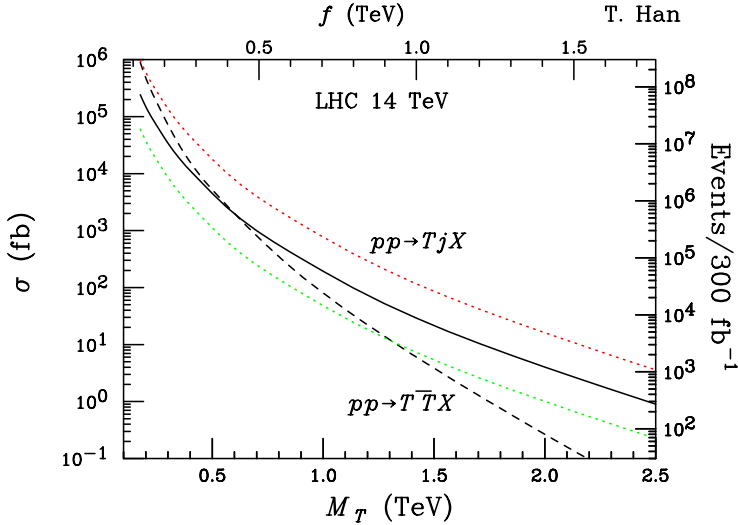
Fig. 6.5. Production of the top-quark partner T in pair and singly at the LHC versus its mass. The Yukawa coupling ratio λ_1/λ_2 has been taken to be 2 (upper dotted curve) 1 (solid) and 1/2 (lower dotted), respectively. The $T\bar{T}$ pair production via QCD includes an NLO K-factor (dashed curve).

- To what extent can we tell a "fat W-jet" from a massive QCD jet?
- Can we make use of a non-isolated lepton inside the top-jet ($b\ell\nu$) for the top-quark identification and reconstruction?
- Can we do b-tagging for the highly boosted top events?

These practical issues would become critical to understand the events and thus for new physics searches. Detailed studies including the detector effects will be needed to reach quantitative conclusions.

6.4.2. $T \to tZ$, tH, bW

In many theories beyond the SM, there is a top-quark partner. These are commonly motivated by the "naturalness" argument, the need to cancel the quadratic divergence in the Higgs mass radiative correction, most severely from the top-quark loop. Besides the scalar top quark in SUSY, the most notable example is the Little Higgs theory [47]. If there is no discrete symmetry, the top partner T will decay to SM particles in the final state, leading to fully a reconstructable fermionic resonance.

It was pointed out [48] that the single T production via the weak charged-current may surpass the pair production via the QCD interaction
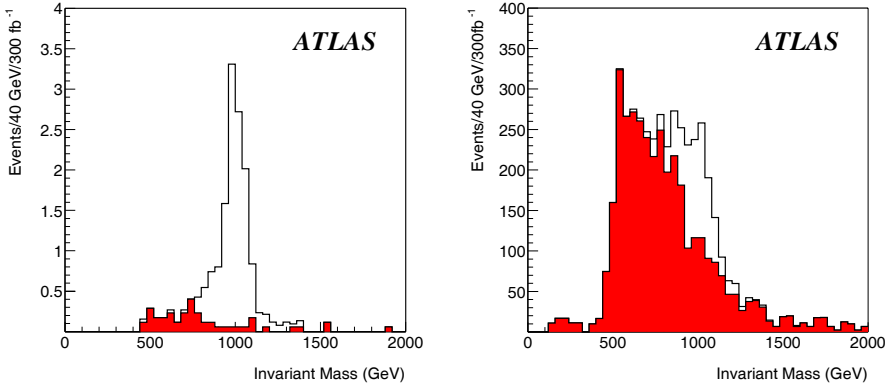
Fig. 6.6.   Observability for the decays (a) $T \to tZ$ and (b) $T \to bW$ at the ATLAS [49].

due to the longitudinal gauge boson enhancement for the former and the phase space suppression for the latter. This is shown in Fig. 6.5. Subsequent simulations [49] performed by the ATLAS collaboration demonstrated the clear observability for the signals above the backgrounds at the LHC for $T \to tZ$, bW with a mass $M_T = 1$ TeV, as seen in Fig. 6.6.

6.5. Top-Rich Events for New Physics

Although the top-quark partner is strongly motivated for a natural electroweak theory, it often results in excessively large corrections to the low energy electroweak observables. In order to better fit the low energy measurements, a discrete symmetry is often introduced, such as the R-parity in SUSY, KK-parity in UED, and T-parity in LH [50]. The immediate consequence for collider phenomenology is the appearance of a new stable particle that may provide the cold dark matter candidate, and results in missing energy in collider experiments.[a]

6.5.1. $T\bar{T}$ pair production

The top partner has similar quantum numbers to the top quark, and thus is commonly assigned as a color triplet. This leads to their production in QCD

$$q\bar{q}, \; gg \to T\bar{T}. \qquad (6.17)$$

[a]Alternatively, the breaking of the R-parity [51] or the T-parity [52] would lead to different collider phenomenology [53].
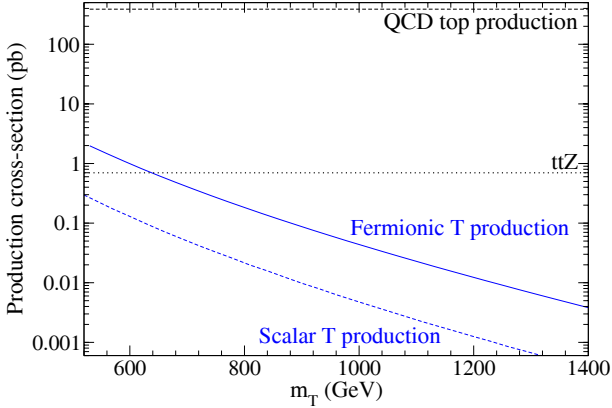
Fig. 6.7. Leading order total cross section for the top partner $T\bar{T}$ production at the LHC versus its mass [54]. Both spin-0 and spin-1/2 top partners are included. The QCD $t\bar{t}$ and the SM $t\bar{t}Z$ backgrounds are indicated by the horizontal lines.

The production cross section is shown in Fig. 6.7 for both spin-0 and spin-1/2 top partners. Although there is a difference of a factor of 8 or so (4 from spin state counting and the rest from threshold effects) in the cross sections, it is still challenging to tell a scalar and a fermionic partner apart [54–56] due to the lack of definitive features.

Due to the additional discrete symmetry, the top partner cannot decay to a SM particle alone. Consequently, $T \to tA^0$, leading to $t\bar{t}$ pair production plus large mixing energy. The crucial parameter to characterize the kinematical features is the mass difference $\Delta M_{TA} = m_T - m_A$. For $\Delta M_{TA} \gg m_t$, the top quark as a decay product will be energetic and qualitatively different from the SM background. But if $\Delta M_{TA} \approx m_t$, then the two will have very little difference, making the signal difficult to separate out. Depending on the top-quark decay, we present two classes of signals.

6.5.1.1. $t\bar{t}$ pure hadronic decay

For both $t\bar{t}$ to decay hadronically [55, 57], the signal will be 6 jets plus missing energy. While it has the largest decay rate, the backgrounds would be substantial as well. With judicious acceptance cuts, the signal observability for $\Delta M_{TA} > 200$ GeV was established, as seen in Fig. 6.8. Possible measurements of the absolute mass scale and its spin of the top partner were considered [54, 55], but the determination remains difficult.
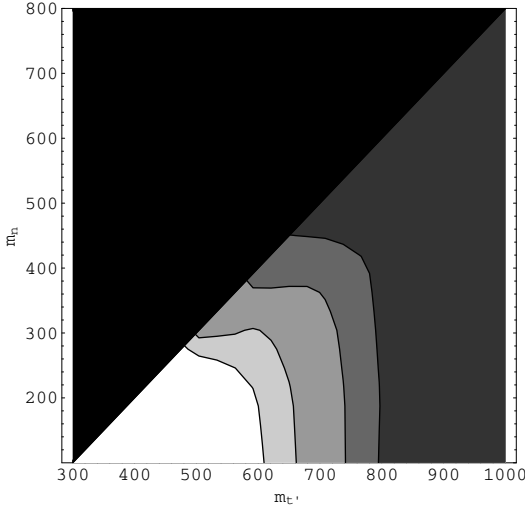
Fig. 6.8.   Contour in $m_{\tilde{t}} - m_N$ for $\tilde{t} \to tN$ for the statistical significance of a scalar $\tilde{t}$ at the LHC with an integrated luminosity of 100 fb^{-1}. Purely hadronic decays are considered.

6.5.1.2. $t\bar{t}$ semi-leptonic decay

If one of the $t\bar{t}$ decays hadronically and the other decays leptonically, the signal may be cleaner. It turns out that if the mass difference ΔM_{TA} is sizable, then requiring large missing transverse energy may be sufficient to suppress the background. However, if $\Delta M_{TA} \sim m_t$, then the $\not{E}_T$ for the signal is not much different from the background. On the other hand, the fact that the $t\bar{t}$ kinematics can be fully reconstructed in the SM implies that the reconstruction for the signal events would be distinctive due to the large missing mass. Indeed, the reconstructed m_t^r based on the $\not{E}_T$ will be far away from the true m_t, and mostly result in an unphysical value. If we impose

$$|m_t - m_t^r| > 110 \text{ GeV}, \tag{6.18}$$

we can reach optimal signal identification. The summary plot for the statistical significance (the number of σ) is given in Fig. 6.9 at the LHC with an integrated luminosity of 100 fb^{-1}, where the left panel is for a fermionic T, and the right is a scalar $\tilde{t}$, both decaying to $t+$ a missing particle.
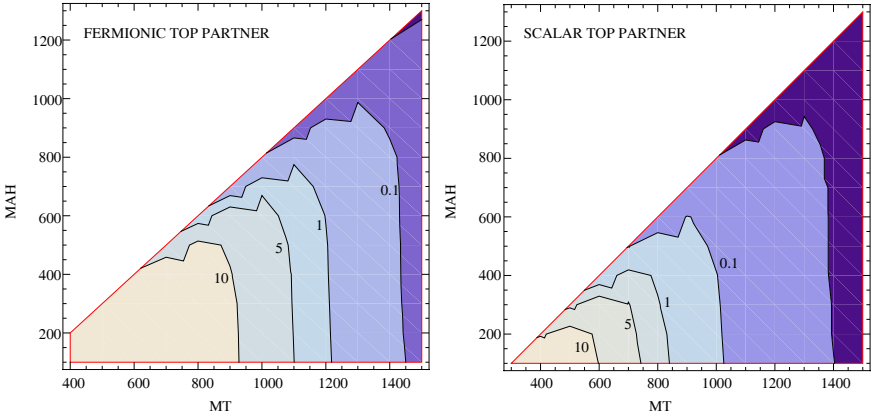
Fig. 6.9.   Contour in $m_T - m_A$ for $T \to tA$ for the statistical significance at the LHC with an integrated luminosity of 100 fb^{-1}. Left panel is for a fermionic T, and the right is a scalar $\tilde{t}$, both decaying to a top plus a missing particle.

6.5.2.   *Exotic top signatures*

Searching for exotic events related to the top quark can be rewarding. First, there exists a variety of natural electroweak models with distinctive top partners that should not be overlooked for collider phenomenology. Second, potentially large couplings of the top quark to new physics may result in multiple top quarks from new particle decays. Finally, the exotic events have less SM background contamination, and thus may stand out for discovery even at the early phase of the LHC. We briefly list a few recent examples:

- Multiple top quarks and b-quarks in the final state may help to search for new heavy particles in the electroweak sector and can be distinctive from the SM backgrounds [58].
- Heavy top partners and other KK fermions in the RS model may lead to unique top-quark and W-boson signatures [59].
- New exotic colored states may predominantly couple to heavy quarks and thus lead to multiple top quarks in the final state [60].
- Composite models for the right-handed top-quark may lead to $t\bar{t}t\bar{t}$ signals at the LHC [61].
- Like-sign top quark pairs may indicate new dynamics [62].

6.6. Summary and Outlook

The LHC will be a true top-quark factory. With 80 million top-quark pairs plus 34 million single tops produced annually at the designed high luminosity, the properties of this particle will be studied to a great accuracy and the deep questions related to the top quark at the Terascale will be explored to an unprecedented level. Theoretical arguments indicate that it is highly likely that new physics associated with the top quark beyond the SM will show up at the LHC. This article only touches upon the surface of the rich top quark physics, and is focused on possible new physics beyond the SM in the top-quark sector. The layout of this article has been largely motivated by experimental signatures for the LHC. Interesting signatures covered here include:

- Rare decays of the top quark to new light states, or to SM particles via the charged and neutral currents through virtual effects of new physics.
- Top quark pair production via the decay of a new heavy resonance, resulting in fully reconstructable kinematics for detailed studies.
- Top quark pair production via the decay of pairly produced top partners, usually associated with two other missing particles, making the signal identification and the property studies challenging.
- Multiple top quarks, b quarks, and $W^\pm$'s coming from theories of electroweak symmetry breaking or an extended top-quark sector.

The physics associated with top quarks is rich, far-reaching, and exciting. It opens up golden opportunities for new physics searches, while brings in new challenges as well. It should be of high priority in the LHC program for both theorists and experimentalists.

References

[1] For a review on new strong dynamics related to the top quark, see *e.g.*, C. T. Hill and E. H. Simmons, *Strong dynamics and electroweak symmetry breaking, Phys. Rept.* **381**, 235 (2003) [Erratum-ibid. **390**, 553 (2004)] [arXiv:hep-ph/0203079]; and references therein.

[2] For a general discussion on the "naturalness", see *e.g.*, G. F. Giudice, Naturally Speaking: *The Naturalness Criterion and Physics at the LHC*, arXiv:0801.2562 [hep-ph], in this book.

[3] For a review on top-quark physics at hadron colliders, see, *e.g.*, A. Quadt, *Top quark physics at hadron colliders, Eur. Phys. J. C* **48** (2006) 835, and references therein.

[4] Particle Data Group, W.-M. Yao et al., *J. Phys. G* **33**, 1 (2006).

[5] E. Brubaker *et al.* [Tevatron Electroweak Working Group], *Combination of CDF and D0 Results on the Mass of the Top Quark,* arXiv:hep-ex/0608032.

[6] A. I. Etienvre, *Top mass measurement at LHC,* PoS **TOP2006** (2006) 023.

[7] G. L. Kane, G. A. Ladinsky and C. P. Yuan, *Using the top quark for testing standard model polarization and CP predictions, Phys. Rev. D* **45**, 124 (1992).

[8] U. Baur, M. Buice and L. H. Orr, *Direct measurement of the top quark charge at hadron colliders, Phys. Rev. D* **64**, 094019 (2001) [arXiv:hep-ph/0106341]; U. Baur, A. Juste, L. H. Orr and D. Rainwater, *Probing electroweak top quark couplings at hadron colliders, Phys. Rev. D* **71**, 054013 (2005) [arXiv:hep-ph/0412021].

[9] M. Jezabek and J. H. Kuhn, *QCD Corrections to Semileptonic Decays of Heavy Quarks, Nucl. Phys. B* **314**, 1 (1989).

[10] I. I. Y. Bigi, Y. L. Dokshitzer, V. A. Khoze, J. H. Kuhn and P. M. Zerwas, *Production and Decay Properties of Ultraheavy Quarks, Phys. Lett. B* **181**, 157 (1986).

[11] S. Willenbrock, *The standard model and the top quark,* arXiv:hep-ph/0211067.

[12] P. Nason, S. Dawson and R. K. Ellis, *The Total Cross-Section for the Production of Heavy Quarks in Hadronic Collisions, Nucl. Phys. B* **303**, 607 (1988); W. Beenakker, H. Kuijf, W. L. van Neerven and J. Smith, *QCD Corrections to Heavy Quark Production in p anti-p Collisions, Phys. Rev. D* **40**, 54 (1989); N. Kidonakis and R. Vogt, *Next-to-next-to-leading order soft-gluon corrections in top quark hadroproduction, Phys. Rev. D* **68**, 114014 (2003) [arXiv:hep-ph/0308222].

[13] E. Laenen, J. Smith and W. L. van Neerven, *Top Quark Production Cross-Section, Phys. Lett. B* **321**, 254 (1994) [arXiv:hep-ph/9310233]; E. L. Berger and H. Contopanagos, *The Perturbative Resummed Series for Top Quark Production in Hadron Reactions, Phys. Rev. D* **54**, 3085 (1996) [arXiv:hep-ph/9603326];

[14] R. Bonciani, S. Catani, M. L. Mangano and P. Nason, *NLL resummation of the heavy-quark hadroproduction cross-section, Nucl. Phys. B* **529**, 424 (1998) [arXiv:hep-ph/9801375]; and references therein.

[15] J. H. Kuhn and G. Rodrigo, *Charge asymmetry in hadroproduction of heavy quarks, Phys. Rev. Lett.* **81**, 49 (1998) [arXiv:hep-ph/9802268].

[16] W. Bernreuther, M. Fuecker and Z. G. Si, *Mixed QCD and weak corrections to top quark pair production at hadron colliders, Phys. Lett. B* **633**, 54 (2006)

[arXiv:hep-ph/0508091]; W. Bernreuther, M. Fuecker and Z. G. Si, *Weak interaction corrections to hadronic top quark pair production, Phys. Rev. D* **74**, 113005 (2006) [arXiv:hep-ph/0610334].

[17] S. S. Willenbrock and D. A. Dicus, *Production Of Heavy Quarks From W-Gluon Fusion, Phys. Rev. D* **34**, 155 (1986); C. P. Yuan, *A New Method to Detect a Heavy Top Quark at the Tevatron, Phys. Rev. D* **41**, 42 (1990); T. Stelzer, Z. Sullivan and S. Willenbrock, *Single top quark production at hadron colliders, Phys. Rev. D* **58**, 094021 (1998) [arXiv:hep-ph/9807340]; Z. Sullivan, *Understanding single-top-quark production and jets at hadron colliders, Phys. Rev. D* **70**, 114012 (2004) [arXiv:hep-ph/0408049].

[18] V. M. Abazov *et al.* [D0 Collaboration], *Evidence for production of single top quarks and first direct measurement of —V(tb)—, Phys. Rev. Lett.* **98**, 181802 (2007) [arXiv:hep-ex/0612052].

[19] Q. H. Cao, J. Wudka and C. P. Yuan, *Search for New Physics via Single Top Production at the LHC, Phys. Lett. B* **658**, 50 (2007) [arXiv:0704.2809 [hep-ph]].

[20] M. C. Smith and S. Willenbrock, *QCD and Yukawa Corrections to Single-Top-Quark Production via $q\bar{q} \rightarrow t\bar{b}$, Phys. Rev. D* **54**, 6696 (1996) [arXiv:hep-ph/9604223].

[21] T. Stelzer, Z. Sullivan and S. Willenbrock, *Single-top-quark production via W-gluon fusion at next-to-leading order, Phys. Rev. D* **56**, 5919 (1997) [arXiv:hep-ph/9705398].

[22] S. Zhu, *Next-To-Leading Order QCD Corrections to $bg \rightarrow tW^-$ at the CERN Large Hadron Collider, Phys. Lett. B* **524**, 283 (2002) [Erratum-ibid. B **537**, 351 (2002)].

[23] Q. H. Cao, R. Schwienhorst and C. P. Yuan, *Next-to-leading order corrections to single top quark production and decay at Tevatron. I: s-channel process, Phys. Rev. D* **71**, 054023 (2005) [arXiv:hep-ph/0409040]; N. Kidonakis, *Single top production at the Tevatron: Threshold resummation and finite-order soft gluon corrections, Phys. Rev. D* **74**, 114012 (2006) [arXiv:hep-ph/0609287].

[24] Q. H. Cao and C. P. Yuan, *Single top quark production and decay at next-to-leading order in hadron collision, Phys. Rev. D* **71**, 054022 (2005) [arXiv:hep-ph/0408180]; N. Kidonakis, *Higher-order soft gluon corrections in single top quark production at the LHC, Phys. Rev. D* **75**, 071501 (2007) [arXiv:hep-ph/0701080].

[25] W. Beenakker, S. Dittmaier, M. Kramer, B. Plumper, M. Spira and P. M. Zerwas, *Higgs radiation off top quarks at the Tevatron and the LHC, Phys. Rev. Lett.* **87**, 201805 (2001) [arXiv:hep-ph/0107081]; W. Beenakker, S. Dittmaier, M. Kramer, B. Plumper, M. Spira and P. M. Zerwas, *NLO QCD corrections to t anti-t H production in hadron collisions, Nucl. Phys. B* **653**, 151 (2003) [arXiv:hep-ph/0211352];

[26] S. Dawson, L. H. Orr, L. Reina and D. Wackeroth, *Associated top quark Higgs boson production at the LHC, Phys. Rev. D* **67**, 071503 (2003) [arXiv:hep-ph/0211438]; S. Dawson, C. Jackson, L. H. Orr, L. Reina and D. Wackeroth, *Associated Higgs production with top quarks at the Large*

Hadron Collider: NLO QCD corrections, Phys. Rev. D **68**, 034022 (2003) [arXiv:hep-ph/0305087].

[27] K. Desch and M. Schumacher, *Model independent determination of the top Yukawa coupling from LHC and LC, Eur. Phys. J. C* **46**, 527 (2006) [arXiv:hep-ph/0407159].

[28] D. Benedetti *et al.*, *Observability Of Higgs Produced With Top Quarks And Decaying To Bottom Quarks, J. Phys. G* **34** (2007) N221.

[29] V. M. Abazov *et al.* [D0 Collaboration], *Direct search for charged Higgs bosons in decays of top quarks, Phys. Rev. Lett.* **88**, 151803 (2002) [arXiv:hep-ex/0102039].

[30] M. Hashemi, *Search for the light charged Higgs in CMS, In the Proceedings of IPM School and Conference on Lepton and Hadron Physics (IPM-LHP06), Tehran, Iran, 15-20 May 2006, pp 0018* [arXiv:hep-ph/0612104].

[31] T. Tait and C. P. Yuan, *Single top quark production as a window to physics beyond the Standard Model, Phys. Rev. D* **63**, 014018 (2001) [arXiv:hep-ph/0007298]; C. R. Chen, F. Larios and C. P. Yuan, *General analysis of single top production and W helicity in top decay, Phys. Lett. B* **631**, 126 (2005), [arXiv:hep-ph/0503040].

[32] G. Eilam, J. L. Hewett and A. Soni, *Rare decays of the top quark in the standard and two Higgs doublet models, Phys. Rev. D* **44**, 1473 (1991) [Erratum-ibid. D **59**, 039901 (1999)]; B. Mele, S. Petrarca and A. Soddu, *A new evaluation of the $t \rightarrow c H$ decay width in the standard model, Phys. Lett. B* **435**, 401 (1998) [arXiv:hep-ph/9805498].

[33] J. J. Cao, G. Eilam, M. Frank, K. Hikasa, G. L. Liu, I. Turan and J. M. Yang, *SUSY-induced FCNC top-quark processes at the Large Hadron Collider, Phys. Rev. D* **75**, 075021 (2007) [arXiv:hep-ph/0702264].

[34] J. L. Diaz-Cruz, H. J. He and C. P. Yuan, *Soft SUSY breaking, stop-scharm mixing and Higgs signatures, Phys. Lett. B* **530**, 179 (2002) [arXiv:hep-ph/0103178]; J. A. Aguilar-Saavedra, *Top flavour-changing neutral interactions: Theoretical expectations and experimental detection, Acta Phys. Polon. B* **35**, 2695 (2004) [arXiv:hep-ph/0409342]; G. Eilam, A. Gemintern, T. Han, J. M. Yang and X. Zhang, *Top quark rare decay $t \rightarrow c h$ in R-parity-violating SUSY, Phys. Lett. B* **510**, 227 (2001) [arXiv:hep-ph/0102037]; F. Larios, R. Martinez and M. A. Perez, *New physics effects in the flavor-changing neutral couplings of the top quark, Int. J. Mod. Phys. A* **21**, 3473 (2006) [arXiv:hep-ph/0605003]; K. Agashe, G. Perez and A. Soni, *Collider signals of top quark flavor violation from a warped extra dimension, Phys. Rev. D* **75**, 015002 (2007) [arXiv:hep-ph/0606293].

[35] R. D. Peccei and X. Zhang, *Dynamical Symmetry Breaking and Universality Breakdown, Nucl. Phys. B* **337**, 269 (1990); T. Han, R. D. Peccei and X. Zhang, *Top Quark Decay Via Flavor Changing Neutral Currents At Hadron Colliders, Nucl. Phys. B* **454**, 527 (1995) [arXiv:hep-ph/9506461].

[36] T. Han, M. Hosch, K. Whisnant, B. L. Young and X. Zhang, *Single top quark production via FCNC couplings at hadron colliders, Phys. Rev. D* **58**, 073008 (1998) [arXiv:hep-ph/9806486].

[37] T. Han, K. Whisnant, B. L. Young and X. Zhang, *Top-Quark Decay Via the Anomalous Coupling $\bar{t}c\gamma$ at Hadron Colliders, Phys. Rev. D* **55**, 7241 (1997) [arXiv:hep-ph/9603247].

[38] J. Carvalho *et al.* [ATLAS Collaboration], *Study of ATLAS sensitivity to FCNC top decays, Eur. Phys. J. C* **52**, 999 (2007) [arXiv:0712.1127 [hep-ex].

[39] H. J. He and C. P. Yuan, *New method for detecting charged (pseudo-)scalars at colliders, Phys. Rev. Lett.* **83**, 28 (1999) [arXiv:hep-ph/9810367]; C. Balazs, H. J. He and C. P. Yuan, *QCD corrections to scalar production via heavy quark fusion at hadron colliders, Phys. Rev. D* **60**, 114001 (1999) [arXiv:hep-ph/9812263].

[40] K. Agashe *et al.*, *LHC Signals for Warped Electroweak Neutral Gauge Bosons, Phys. Rev. D* **76**, 115015 (2007) [arXiv:0709.0007 [hep-ph].

[41] K. Agashe, A. Belyaev, T. Krupovnickas, G. Perez and J. Virzi, *LHC signals from warped extra dimensions, Phys. Rev. D* **77**, 015003 (2008) [arXiv:hep-ph/0612015]; B. Lillie, L. Randall and L. T. Wang, *The Bulk RS KK-gluon at the LHC, JHEP* **0709**, 074 (2007) [arXiv:hep-ph/0701166]; B. Lillie, J. Shu and T. M. P. Tait, *Kaluza-Klein Gluons as a Diagnostic of Warped Models, Phys. Rev. D* **76**, 115016 (2007) [arXiv:0706.3960 [hep-ph].

[42] A. L. Fitzpatrick, J. Kaplan, L. Randall and L. T. Wang, *Searching for the Kaluza-Klein graviton in bulk RS models, JHEP* **0709**, 013 (2007) [arXiv:hep-ph/0701150].

[43] C. T. Hill and S. J. Parke, *Top production: Sensitivity to new physics, Phys. Rev. D* **49**, 4454 (1994) [arXiv:hep-ph/9312324]; C. X. Yue, H. Y. Zhou, Y. P. Kuang and G. R. Lu, *$t\bar{t}$ production rates at the Tevatron and the LHC in topcolor-assisted multiscale technicolor models, Phys. Rev. D* **55**, 5541 (1997) [arXiv:hep-ph/9608294]; T. Han, D. L. Rainwater and G. Valencia, *TeV resonances in top physics at the LHC, Phys. Rev. D* **68**, 015003 (2003) [arXiv:hep-ph/0301039]; D. Choudhury, R. M. Godbole, R. K. Singh and K. Wagh, *Top production at the Tevatron / LHC and nonstandard, strongly interacting spin one particles, Phys. Lett. B* **657**, 69 (2007) [arXiv:0705.1499 [hep-ph]].

[44] V. Barger, T. Han and D. G. E. Walker, *Top Quark Pairs at High Invariant Mass - A Model-Independent Discriminator of New Physics at the LHC, Phys. Rev. Lett.* **100**, 031801 (2008) [arXiv:hep-ph/0612016].

[45] D. Atwood, S. Bar-Shalom, G. Eilam and A. Soni, *CP violation in top physics, Phys. Rept.* **347**, 1 (2001) [arXiv:hep-ph/0006032]; G. Valencia and Y. Wang, *New CP-odd observable in $H \to t\bar{t}$, Phys. Rev. D* **73**, 053009 (2006) [arXiv:hep-ph/0512127].

[46] W. Skiba and D. Tucker-Smith, *Using jet mass to discover vector quarks at the LHC, Phys. Rev. D* **75**, 115010 (2007) [arXiv:hep-ph/0701247]; U. Baur and L. H. Orr, *High p_T Top Quarks at the Large Hadron Collider, Phys. Rev. D* **76**, 094012 (2007) [arXiv:0707.2066 [hep-ph]]; R. Frederix and F. Maltoni, *Top pair invariant mass distribution: a window on new physics,* arXiv:0712.2355 [hep-ph].

[47] For a review, see *e.g.*, *M. Schmaltz and D. Tucker-Smith, Little Higgs review, Ann. Rev. Nucl. Part. Sci.* **55**, 229 (2005) [arXiv:hep-ph/0502182], and references therein.

[48] T. Han, H. E. Logan, B. McElrath and L. T. Wang, *Phenomenology of the little Higgs model, Phys. Rev. D* **67**, 095004 (2003) [arXiv:hep-ph/0301040]; M. Perelstein, M. E. Peskin and A. Pierce, *Top quarks and electroweak symmetry breaking in little Higgs models, Phys. Rev. D* **69**, 075002 (2004) [arXiv:hep-ph/0310039].

[49] G. Azuelos *et al.*, *Exploring little Higgs models with ATLAS at the LHC, Eur. Phys. J. C* **39S2**, 13 (2005) [arXiv:hep-ph/0402037].

[50] H.-C. Cheng and I. Low, *TeV symmetry and the little hierarchy problem, JHEP* **0309**, 051 (2003) [arXiv:hep-ph/0308199].

[51] For a review, see *e.g.*, R. Barbier *et al.*, *R-parity violating supersymmetry, Phys. Rept.* **420**, 1 (2005) [arXiv:hep-ph/0406039], and references therein.

[52] C.T. Hill and R.J. Hill, *Topological Physics of Little Higgs Bosons, Phys. Rev. D* **75**, 115009 (2007) [arXiv:hep-ph/0701044]; C.T. Hill and R.J. Hill, T^- *parity violation by anomalies, Phys. Rev. D* **76**, 115014 (2007) [arXiv:0705.0697 [hep-ph]].

[53] V. Barger, W.-Y. Keung and Y. Gao, *T-Anomaly Induced LHC Signals, Phys. Lett. B* **655**, 228 (2007) [arXiv:0707.3648 [hep-ph]].

[54] T. Han, R. Mahbubani, D. Walker and L.-T. Wang, *Top Quark Pair plus Large Missing Energy at the LHC,* arXiv:0803.3820 [hep-ph].

[55] P. Meade and M. Reece, *Top partners at the LHC: Spin and mass measurement, Phys. Rev. D* **74**, 015010 (2006) [arXiv:hep-ph/0601124].

[56] H. C. Cheng, I. Low and L. T. Wang, *Top partners in little Higgs theories with T-parity, Phys. Rev. D* **74**, 055001 (2006) [arXiv:hep-ph/0510225].

[57] S. Matsumoto, M. M. Nojiri and D. Nomura, *Hunting for the top partner in the littlest Higgs model with T-parity at the LHC, Phys. Rev. D* **75**, 055006 (2007) [arXiv:hep-ph/0612249].

[58] T. Han, G. Valencia and Y. Wang, *Hadron collider signatures for new interactions of top and bottom quarks, Phys. Rev. D* **70**, 034002 (2004) [arXiv:hep-ph/0405055].

[59] C. Dennis, M. Karagoz Unel, G. Servant and J. Tseng, *Multi-W events at LHC from a warped extra dimension with custodial symmetry,* arXiv:hep-ph/0701158; M. Carena, A. D. Medina, B. Panes, N. R. Shah and C. E. M. Wagner, *Collider Phenomenology of Gauge-Higgs Unification Scenarios in Warped Extra Dimensions,* arXiv:0712.0095 [hep-ph]; R. Contino and G. Servant, *Discovering the top partners at the LHC using same-sign dilepton final states,* arXiv:0801.1679 [hep-ph].

[60] B. A. Dobrescu, K. Kong and R. Mahbubani, *Massive color-octet bosons and pairs of resonances at hadron colliders,* arXiv:0709.2378 [hep-ph]; M. Gerbush, T. J. Khoo, D. J. Phalen, A. Pierce and D. Tucker-Smith, *Color-octet scalars at the LHC,* arXiv:0710.3133 [hep-ph].

[61] B. Lillie, J. Shu and T. M. P. Tait, *Top Compositeness at the Tevatron and LHC,* arXiv:0712.3057 [hep-ph].

[62] F. Larios and F. Penunuri, *FCNC production of same sign top quark pairs at the LHC, J. Phys. G* **30**, 895 (2004) [arXiv:hep-ph/0311056]; J. J. Cao, G. L. Liu and J. M. Yang, *Probing topcolor-assisted technicolor from like-sign top pair production at LHC, Phys. Rev. D* **70**, 114035 (2004) [arXiv:hep-ph/0409334]; S. Kraml and A. R. Raklev, *Same-sign top quarks as signature of light stops at the LHC, Phys. Rev. D* **73**, 075002 (2006) [arXiv:hep-ph/0512284].

Chapter 7

LHC Discoveries Unfolded

Joseph Lykken[*] and Maria Spiropulu[†]

Fermi National Accelerator Laboratory
P.O. Box 500, Batavia IL 60510, USA
and
Physics Department, CERN
CH 1211 Geneva 23, Switzerland
[*]*lykken@fnal.gov*
[†]*Maria.Spiropulu@cern.ch*

With the LHC data arriving soon, carrying discoveries, we discuss a strategy for synthesizing a set of early measurements illuminating the dark matter of the universe.

7.1. Escape from Theory Space

Physics is an experimental science that requires theory frameworks to interprete results and render the data meaningful. Theory enables physicists to relate results from disparate experimental approaches and make predictions for new experiments.

Results that contradict well-established theory frameworks are quite properly treated with skepticism. The history of physics is full of experimental "signals" that, upon further review, "went away." But the same history shows that in the end experiment always trumps theory. When theory frameworks fail, paradigm shift occurs, and physicists eventually move on to a deeper level of understanding.

For more than three decades particle physics has been dominated by a theory framework prosaically known as the Standard Model. Many discoveries were made during these decades, almost all of them serving to buttress the soaring collection of ideas that constitute this model. Hundreds of predictions of this model have been verified with great precision in dozens of experiments.

Meanwhile, the majority of particle theorists have been employed concocting new theory frameworks that attempt a deeper level of understanding than is provided by the Standard Model. Most of these Beyond the Standard Model frameworks begin with the same building blocks as the SM: relativistic quantum field theory, gauge symmetry and interactions between fundamental fermions and bosons. One framework, string theory, is so radical in its conception that it has proven difficult to relate it back to the SM. The more typical strategy is to start with the SM and build upwards, inwards or outwards.

The most interesting BSM frameworks are based either upon new symmetries, as is the case for supersymmetry and little Higgs models, or upon new degrees of freedom, most notably the hypothesis of large or warped extra dimensions of space. Within each BSM framework, one can construct a large number of qualitatively different models consistent with all current data. Collectively these models populate the "theory space" of possible physics beyond the Standard Model.

This BSM theory space is many dimensional. Since the models contain new adjustable parameters, such as the masses of new particles, the number of distinct models is formally infinite. This infinity is misleading: in an experimental science the data will not provide a real distinction between models that differ by details that are sufficiently tiny or experimentally irrelevant. Nevertheless the BSM theory space is still dauntingly vast, containing some very large number N of viable possibilities.

Particle physicists have already spent decades tackling the "top-down" problem of mapping these N models into their experimental signatures. Much of this work, especially in recent years, has focused on top-down predictions for experiments at the LHC. The most successful frameworks, such as supersymmetry (SUSY), make dramatic predictions for new particles and interactions that should be visible at the LHC, while simultaneously explaining the current particle physics data set as well as the Standard Model does.

Apart from the already-mentioned exception of string theory, the top-down program of mapping theory space into LHC predictions is fairly straightforward. This approach builds upon the successful program of making detailed predictions from the Standard Model; the main intellectual challenges involve the complexities of QCD. With a twenty year headstart on making LHC predictions, particle physicists have developed powerful tools for simulating LHC collisions initiated by BSM interactions or the production of BSM particles. Given any point in theory space, a diligent

student can use these tools to map that point into fully realized LHC events.

As soon as discoveries are made at the LHC, physicists will face a very different set of challenges. Rather than the top-down approach of applying the Standard Model or a favorite BSM model to make a prediction, we will have to confront the issues of bottom-up physics. These include a host of technical issues for reconstructing "pictures" of events from millions of separate readout channels in the detector. They also include the difficulty of understanding the Standard Model content of LHC events, given the unprecedented complexity and kinematics of 14 TeV proton-proton collisions, as described elsewhere in this volume.

Even when these challenges are addressed, there will remain the LHC Inverse Problem [1–3]: given a finite set of measurements with finite resolutions, how does one map back to the underlying theory responsible for the new phenomena? When N is large, as it certainly is for BSM theory space, it is not a viable strategy to discriminate between N alternative explanations by performing N tests. However, as the game "twenty questions" illustrates, a well-designed series of simple tests can identify the correct alternative in of order $\log(N)$ steps, proceeding along a decision tree such that, at each branching, of order half of the remaining alternatives are eliminated.

The solution to the LHC Inverse Problem is to design and implement this series of simple tests in LHC experiments, such that with high confidence roughly half of the remaining theory space is ruled out at each step. The results of the first few tests will shape the requirements for future tests, so the immediate need is to develop the strategy for the early tests.

As of this writing, particle physicists have not made much progress in this area. Well-developed strategies for early tests on LHC discovery data sets exist for only a few simpler scenarios, such as the resonance production of a new heavy particle that decays back to a pair of muons, electrons, or QCD jets. The lack of progress has a partly sociological origin. During the past few decades, top-down analysis using the Standard Model proved so effective that bottom-up strategies fell into decline. In the more distant past, before the tyranny of the Standard Model took hold, the interpretation of experiments was typically done on the fly. The experiment was performed, data was extracted, and the researchers stood around scratching their heads until they figured out what it meant. With LHC collisions occuring every 25 nanoseconds, producing events of frightening complexity, the "on-the-fly" approach to interpreting LHC signals is not defendable.

In this chapter we describe some recent progress in developing the strategy for early tests to discriminate the origin of one important class of potential LHC discoveries. These are LHC discoveries that could manifest during the first two years of physics running as a "missing energy" signature.

7.2. Dark Matter and Missing Energy

An economical hypothesis for the main constituent of cosmic dark matter is one or more varieties of stable weakly interacting massive particles. Here weakly interacting means that the particles do not carry electric or color charge, and they may or may not carry SM weak charge. As described in more detail by Aaron Pierce in this volume, it is a remarkable fact that standard Big Bang cosmology combined with astrophysical measurements suggest the existence of exotic particles at the TeV energy scale about to be probed by LHC experiments. The LHC and the ATLAS and CMS detectors were designed to discover the Higgs boson and the deeper origins of electroweak symmetry breaking at the Terascale. Nevertheless the LHC also provides an outstanding opportunity to produce WIMP dark matter particles in high energy collisions, and to study their properties in controlled laboratory experiments [4].

WIMP dark matter particles (if they exist) are presumably stable on cosmological timescales for the same reason as the electron: they are the lightest of a family of particles carrying a particular kind of conserved charge or quantum number. Since by definition SM particles don't carry this quantum number, a proton-proton collision at the LHC is "neutral" under this new charge. This has the immediate consequence that WIMP dark matter particles cannot be produced singly in such a collision; they can only be produced (if at all) in pairs.

An equally important implication is that there are probably heavier relatives of the WIMP particles. These particles will be unstable to rapid decays into a stable WIMP plus one or more SM particles, a decay that conserves the new quantum number carried by the WIMP and its heavier parent. There is no reason why all of these heavier parents should be weakly interacting. Those that carry color charge will be copiously produced at the LHC, as long as they have mass less than about 2 TeV. They will be produced in pairs, followed by one or more stages of rapid decays that result in a pair of WIMP dark matter particles together with a collection of energetic SM particles.

Most of these energetic SM particles will be detected and reconstructed in the general purpose LHC detectors ATLAS and CMS. The two dark matter particles will not be directly detected, since they are too weakly interacting to leave a detectable signal in any of the detector subsystems. Instead, the experimental smoking gun of dark matter production at the LHC is missing transverse energy.

To understand this concept, it is useful to peek inside the 7 TeV protons of the LHC colliding beams. Each proton behaves like a bag of constituent elementary particles that Feynman called "partons." These include two u quarks and one d quark, gluons, and a variety of virtual "sea" quarks and antiquarks that wink in and out of existence in the intense gluonic energy field. An LHC proton-proton collision will usually consist of just one parton from one proton colliding with one parton from the other proton: uu, ud, ug, dg, gg, $u\bar{u}$, $u\bar{d}$, ub, $c\bar{s}$, etc. Since each parton only carries a fraction of the total momentum and energy of the proton, this partonic hard scattering is much less energetic than the full 14 TeV carried by the two protons. Most of the energy of these pp collisions is carried off by undetected remnants of the underlying event, which disappear down the beampipe.

The total energy of any particular partonic collision cannot be predicted in advance, neither can the total momentum along the direction of the proton beams. However for precisely controlled and collimated beams, as will obtain for the LHC, the total momentum of each collision in the directions tranverse to the beams is well-known. This transverse momentum is limited by the ability of each parton to rattle around inside of its mother proton. Thus a typical hard scattering with a TeV of total energy will almost always have only about a GeV/c of total transverse momentum.

If LHC detectors could measure the transverse momentum of all the SM particles produced in a collision, a simple vector sum would reveal the presence of unseen particles such as WIMPS carrying off large transverse momentum. In practice LHC detectors only measure momentum directly for charged particles; neutral SM particles are detected in the calorimeters, as energy deposits along a certain three-vector pointing away from the collision. For hermetic calorimeters, this is good enough to establish the existence of large missing transverse energy, defined as the vector sum of all the energy deposits in the plane transverse to the beam. Missing transverse energy implies missing transverse momentum in the underlying collection of SM particles produced from the collision. Missing transverse energy, known dyslexically as MET, is thus an enormously powerful discovery tool for the LHC.

For the case of WIMP dark matter, two undetected WIMPs in a single event contribute missing transverse energy, pointing in different directions in the azimuthal plane tranverse to the beam axis. Suppose for simplicity that the magnitude of the MET from each WIMP were the same. Then, if the azimuthal directions of the WIMPS were completely uncorrelated, the total MET of the event would be larger than the MET of each individual WIMP two-thirds of the time. However in real LHC collisions the azimuthal directions of the WIMPS are in fact anti-correlated; this is because the WIMPS come from decays of other heavy particles that are produced back-to-back in the center-of-mass frame of the original partonic collision. As a result, the MET vectors of the WIMP pair will partially cancel in a majority of events.

In spite of this feature, heavy WIMPS imply spectacular MET signals at the LHC. The large MET arises from two effects. First, the original hard scattering produces a pair of unstable particles that are even heavier than the WIMP. In the fully differential cross section that describes this process, the p_T of these parent particles appears only in the combination

$$m_T = \sqrt{m_{\mathrm{P}}^2 + p_T^2}\,, \tag{7.1}$$

where m_{P} is the parent particle mass, m_T is known as the transverse mass, and the other kinematic variables are dimensionless. By dimensional analysis the fully differential cross section falls off like $1/m_T^4$ (independently of spin and other details) for large p_T, but obviously the suppression is not felt unless p_T is larger than of order m_{P}. So events with heavy particles typically [5] also have p_T roughly of order m_{P}. The resulting WIMPS from decays of these particles also have typically rather large p_T, thus they move off towards the calorimeter at large polar angles from the beam. The energy that they fail to deposit in the calorimeter is at least as large as their mass m_{DM}, which registers as large missing transverse energy since they are moving away from the beam axis. Thus both large m_{P} and m_{DM} conspire to produce large MET. Note that models with larger m_{P} but smaller m_{DM} may produce a distribution of MET that resembles a very different model with smaller m_{P} and larger m_{DM}.

7.3. Missing Energy at the LHC

WIMP dark matter particles are not the only possible source of MET. Indeed the Standard Model contains its own stable weakly interacting particles, known as neutrinos. Few neutrinos will be directly produced in LHC

collisions, but, as we hypothesized for WIMPS, neutrinos can be copiously produced from the decay of heavier unstable particles. For example, top quarks will be strongly produced at the LHC, with a cross section of around 800 picobarns corresponding to roughly 80 million top-antitop pairs produced per year at full LHC luminosity. A top quark decays in less than a yoctosecond (10^{-24} s) to a b quark and a W^+ boson; about one-third of the time the W then decays to an energetic neutrino and a charged lepton (electron, muon or tau). Thus top quark production is a major SM source of large missing transverse energy. More generally, a variety of SM processes can produce W and/or Z bosons, resulting in large MET from the decay of a W to a neutrino or the decay of a Z to a neutrino and an antineutrino. Decays of tau leptons are another possible source of MET in LHC collisions.

This is both a problem and an opportunity. It is a problem because top, W and Z production will create an irreducible Standard Model physics background in LHC experiments to MET signals arising from dark matter particles or other exciting new physics such as large extra dimensions [6]. It is an opportunity because particle experimenters can use neutrinos as a warmup and calibration for missing energy searches.

This opportunity has been thoroughly exploited already in experiments at the Tevatron, with proton-antiproton collisions as 1.8 and 1.96 TeV. Figure 7.1 shows the reconstruction of the transverse mass of W bosons from Tevatron events, produced by combining the 4-vector of an electron with the MET from the same event. The MET is attributed to an unseen neutrino from a leptonic decay of a W. With a large number of events, the transverse mass distribution is seen to have a pronounced (smeared Jacobian) peak at a value slightly lower than the W mass (the transverse mass has the form of an invariant mass without any longitudinal information and has a second order dependence on the boson p_T). This validates the hypothesis that the great majority of these events did indeed contain a heavy particle that decayed into an electron and a single unseen particle. Further study of kinematics and angular distributions shows that the unseen particle is a fermion, and puts a weak upper bound on its mass (a few tens of GeV). Obviously there is a limit to how many detailed properties of neutrinos can be extracted from high energy collisions. Notice however that in this case we learn fundamental information about neutrinos and weak interactions, reconstructing the weak gauge bosons themselves, and extracting their mass with impressive precision. This is precisely what we hope to do for dark matter at the LHC: extract some if its most important properties, and

determine its origin in the larger context of particle physics. In the same sense that we understand that neutrinos exist because of the existence of electrons and of weak interactions, we would like to be able to say that dark matter exists because, for example, there is spontaneously broken supersymmetry with conserved R parity.
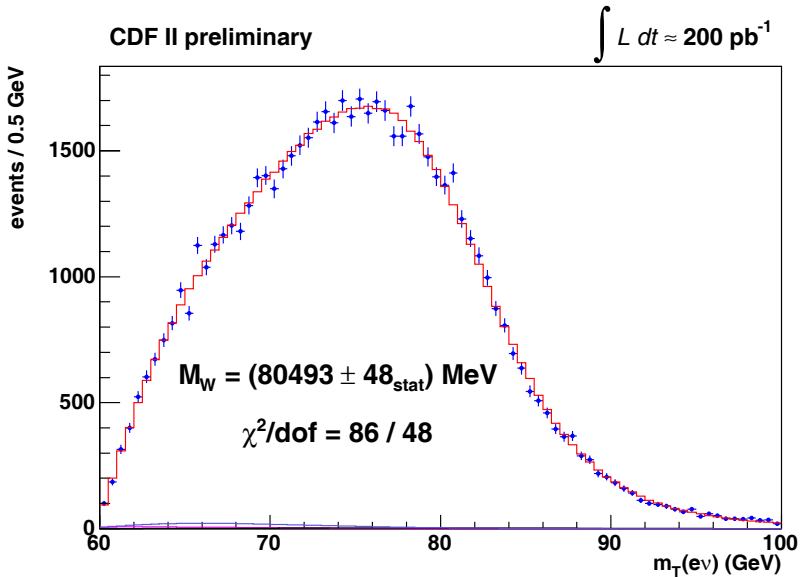
Fig. 7.1.   Distribution of the tranverse mass obtained from electrons and missing transverse energy in events from the CDF detector in Run II of the Tevatron $p\bar{p}$ collider [7, 8]. The distribution is consistent with the hypothesis that the missing energy is from a neutrino produced in a leptonic decay of a W boson. With this hypothesis, the mass of the W is extracted with greater precision than any previous experiment.

Missing energy at the LHC is experimentally challenging. MET searches are plagued by instrumental and spurious backgrounds, including cosmic rays, scattering off beam halo and jet mismeasurement. In analyses of Tevatron data, the great majority of events with putative large MET could be traced to these kinds of backgrounds [9]. Obviously a true MET signal can only be established on a statistical basis, after gaining a strong understanding in the data of top, W and Z production. The motivation of discovering dark matter, even with additional theoretical assumptions like supersymmetry, does not pin down a particular pattern of SM particles that should accompany the MET signal of new physics. Since an early signal implies

strong production, followed by one or more stages of decay to WIMPs, the most conservative assumption is that large MET should be accompanied by multiple energetic QCD jets. We use the phrase *inclusive missing energy signature* to refer to events with both large MET and multiple hard jets. These events may also include energetic leptons, and could be enriched in top, b's, W's or Z's, depending on the details of the underlying physics model.

7.4. A Strategy for Early Discovery with Missing Energy

A detailed strategy for early discovery with the inclusive MET signature was presented in the CMS Physics Technical Design Report [10, 11] and studied with full simulation of the CMS detector. A series of cleanup and analysis cuts were performed on the simulated MET trigger sample, targeting the reduction of both the instrumental and physics backgrounds, while preserving as much signal as possible. Drastic reductions of the backgrounds were achieved while retaining good efficiency for the signal: as high as 25% for supersymmetry models with fairly large m_P and m_{DM}.

For models where the parent particles of the WIMP dark matter are strongly produced, the LHC production cross sections range from about a picobarn for $m_P \simeq 1$ TeV to about a 100 pb for models with masses around 500 GeV. The CMS analysis shows that for many models a MET discovery could be made with the first 100 pb^{-1} of well-understood LHC data.

Supposing, for example, that the new physics signal has a cross section of 20 pb, then an integrated luminosity of 100 pb^{-1} gives 2000 potential signal events. Taking into account trigger efficiencies, the geometrical acceptance of the detector, reconstruction efficiencies for the final state SM particles, and cuts to reduce backgrounds, a well-designed inclusive analysis may preserve 200 to 400 of these signal events. The key to discovery, as discussed in the CMS study, is to reduce the instrumental and SM physics backgrounds to at most a few hundred events in this same data sample; this requires a set of measurements on this sample and related data samples that prove that the backgrounds are understood. There are also systematic effects to worry about, such as the imperfectly measured luminosity and imperfect energy calibrations. In the early running of the LHC experiments, an overall systematic of 10 to 20% is expected. Note that as the basic Standard Model processes become better understood in LHC data, the systematic errors will shrink, since SM processes provide calibrations for energy, luminosity, and various efficiencies. All of these considerations emphasize the

primary importance of getting a strong handle on Standard Model physics in LHC data, as discussed in more detail by Michelangelo Mangano in this volume.
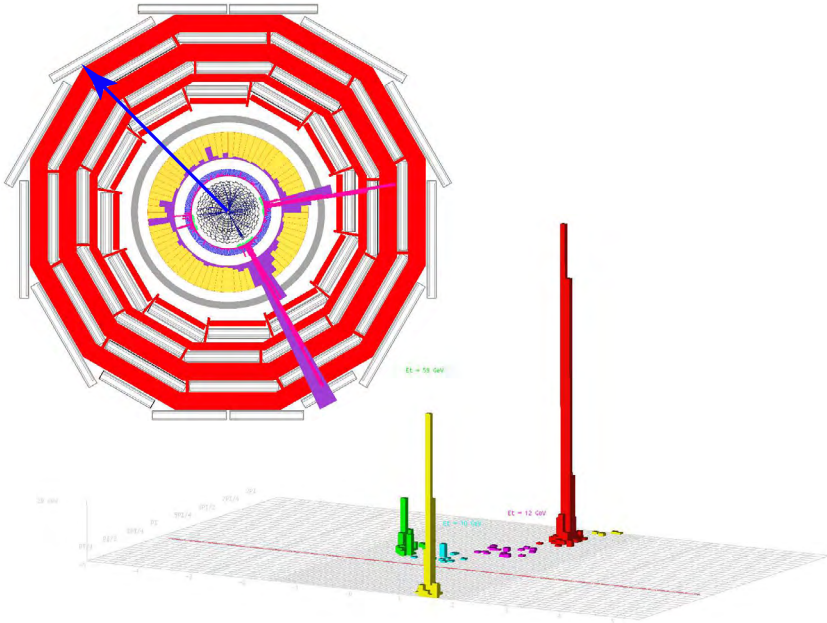
Fig. 7.2.   Event display of SUSY candidate event that survives the requirements of the CMS multijet+missing energy analysis. The three highest E_T jets are 330, 140 and 60 GeV, and the missing transverse energy is 360 GeV. (Right) Lego $\eta - \phi$ calorimeter display; the three leading jets are color coded red-yellow-green, while the red line denotes the azimuthal direction of the missing energy. (Left) Transverse $x - y$ view, showing the energy depositions of the jets in the calorimeter systems as well as the reconstructed tracks and the azimuthal missing energy direction.

Of particular importance for early LHC running will be newly developed "standard candle" calibration methods for normalizations and shapes in the data. A good example of such a standard candle is the production of a Z boson decaying to a pair of muons in association with two or more high energy jets. Because muons do not shower,[a] they deposit at most a couple of GeV of energy while traversing the calorimeters. Thus in a calorimeter measurement of missing transverse energy, a high energy muon looks nearly

---

[a]Actually muons with $p_T \gtrsim 1$ TeV at the LHC sometimes will shower(!), but this does not affect the standard candle calibration.

identical to a neutrino. The muon system outside the calorimeter, and the tracking system inside the calorimeter, do detect the muons and measure their momenta. Thus a study of $Z \rightarrow \mu^+\mu^-$ plus ≥ 2 jets is an excellent calibration of how $Z \rightarrow \nu\bar{\nu}$ plus ≥ 2 jets events will look in the same detector, as well as an absolute calibration of missing transverse energy. Since $Z \rightarrow \nu\bar{\nu}$ plus ≥ 2 jets is one of the most important SM backgrounds to a search for WIMP dark matter particles, this standard candle[b] is of great importance. Even better, it provides an overall normalization for related measurements of W + jets production, another basic SM process related to missing energy searches [9].

7.5. Look-Alikes at the Moment of Discovery

Using the techniques outlined above, it is quite possible that LHC experiments will make a 5σ missing energy discovery with the first 100 pb^{-1} of well-understood data.

At the moment of discovery a large number of theory models will be instantly ruled out because, even within conservative errors for the backgrounds and systematics, they give the wrong excess. However a large number of models will remain as missing energy *look-alikes*, defined as models that predict the same inclusive missing energy excess, within some tolerance, in the same analysis in the same detector, for a given integrated luminosity. The immediate challenge for LHC physicists will then be to begin disambiguating the look-alikes.

For a certain subclass of SUSY models known as minimal supergravity or mSUGRA, the general look-alike problem was studied in Ref. [3] as it might apply to a later mature phase of LHC experiments. Even restricted to the slice of theory space populated by minimal supergravity models, ignoring systematic errors, and applying an uncorrelated χ^2-like statistical analysis to a 1808 correlated observables, this study found that a large number of look-alikes remained unresolved in a simulation equivalent to 10 fb^{-1} of integrated luminosity (1 fb^{-1} = 1000 pb^{-1}).

At the moment of discovery the look-alike problem will be drastically different from the assumptions of this study. The data samples will be much smaller. With small data samples, peaks and edges in invariant mass distributions may not be visible, and most observables related to detailed features of the events will be rate limited. This is particularly true for popular analysis strategies that rely on multiple leptons in the final state.

[b]It is thus only fitting that this terminology was borrowed from the astrophysicists.

The available palette of robust reconstructed physics objects will be limited. For example, it is unlikely that mature τ or b tagging in multijet final states will be fully implemented during the few hundred pb^{-1} era. The observables that *are* available to discriminate the look-alikes will be strongly correlated by systematics and the overall kinematics of the events. In the early running these correlations will be poorly understood, rendering a multivariate analysis highly unreliable.

One possible approach to the look-alike problem after an early LHC discovery would be to build primitive toy models that have only the most generic features required to match gross properties of the discovery data set. This is probably a useful approach, but it is not likely to be the most efficient one. Given twenty-five years of development of full-fledged BSM models, together with powerful software to generate realistic LHC events based on the these models, it would be very strange to give up this impressive machinery at the moment of discovery. In addition, the mapping from a BSM langrangian to the details of a fully simulated LHC event is highly complex; saying that this mapping is implemented in software does not imply that all of its important features are known, let alone intuitively understood. Thus if LHC physicists attempt to reproduce this mapping from the bottom up, their results are likely to be over-simplified and contaminated by theoretical bias.

Instead, we advocate using state-of-the-art simulations of a broad variety of concrete BSM models. LHC simulations can already be performed via a chain of independent modules:

- a model spectrum calculator (e.g. ISASUGRA [12], SUSY-HIT [13] or SPheno [14]) feeding into
- a matrix element calculator (e.g MadGraph [15] or CompHEP [16]), feeding into
- a parton-level event generator (e.g. MadEvent [17]), feeding into
- a showering and hadronizing Monte Carlo (e.g. Pythia [18], Herwig [19], Sherpa [20]), feeding into
- a full LHC detector simulation (e.g. Athena [21] or CMSSW [22]).

The appeal of this approach is that all of these modules except the first can be wholly or substantially validated with Standard Model processes and real LHC data. Thus at the moment of discovery we should already be geared up to make apples-to-apples comparisons of a wide variety of BSM models using simulation chains that are validated and tuned to data.

7.6. Twenty Questions

By focusing on the discrimination of look-alikes, we are pursuing a strategy of simple binary choices: is Model A a significantly better explanation of the discovery dataset than Model B? Each answer carries with it a few bits of important fundamental information about the new physics process responsible for missing energy. Obviously we will need to make many distinct look-alike comparisons before we can hope to build up a clear picture from these individual bits.

Consider how this strategy might play out for answering the basic question "Is it SUSY?" It will almost certainly not be possible to answer this question during the 100 pb^{-1} era. Our strategy will instead answer a series of more modest questions, some of them of the form: "Does SUSY Model A give a significantly better explanation of the discovery dataset than non-SUSY Model B?" None of these individual bits of information by itself is equivalent to answering "Is it SUSY?" However, it is likely that we will be able to build up a picture with several compelling features, e.g.:

- The missing energy probably comes from new particles, not just from neutrinos.
- The missing energy is probably from two particles per event, not one or three or a hundred.
- There is more than one kind of strongly produced parent particle, and they have different color charge.
- The strongly produced parents have several different decay chains.
- Some of these decay chains are enriched in energetic leptons.
- The leptons come from an intermediate exotic particle rather than from W's or Z's.
- etc.

7.7. Spin Discrimination with 100 pb^{-1}

Following a missing energy discovery, we will want to determine the spin of the WIMP, which is tightly correlated with the spin of its parent particles. Spin determination is likewise essential for distinguishing supersymmetry with R parity from non-SUSY BSM frameworks such as Universal Extra Dimensions or little Higgs with T parity, all of which predict a stable WIMP accompanied by a spectrum of heavier "partners" of Standard Model quarks, leptons, gauge bosons and Higgs.

Direct determination of particle spin at a hadron collider is quite challenging, as explained by Lian-Tao Wang in this volume. At the moment of discovery, we will instead rely on indirect information about the spin of the new particles. To see how this works, consider the leading order fully differential cross section to produce a pair of heavy spin $1/2$ quarks with the same mass from a partonic collision of two gluons:

$$\frac{d^4\sigma}{dy_3 dy_4 d^2 p_T}(gg \to Q\bar{Q}) = \frac{\alpha_s^2}{\hat{s}^2} x_1 f_1(x_1) x_2 f_2(x_2) \tag{7.2}$$
$$\times \left(\frac{1}{6\tau_1\tau_2} - \frac{3}{8}\right)\left(\tau_1^2 + \tau_2^2 + \rho - \frac{\rho^2}{4\tau_1\tau_2}\right),$$

In this formula $\hat{s}$ is the square of the total energy of the partonic collision, y_3 and y_4 are the dimensionless rapidities[c] of the heavy quarks and α_s is the QCD strong coupling; x_1 and x_2 are the momentum fractions of the incoming protons carried by the gluons taking part in the partonic collisions, while $f_1(x_1)$ and $f_2(x_2)$ are the probability densities (the pdfs) for these gluon parton fractions to occur in a pp collision. The other variables τ_1, τ_2 and ρ are convenient kinematic variables defined in Ref. [5], related to the particle mass, the p_T and the rapidities.

This can be compared with the analogous cross section to produce a pair of heavy spin 0 squarks from the same partonic initial state: $gg \to \tilde{q}_R \bar{\tilde{q}}_R + \tilde{q}_L \bar{\tilde{q}}_L$; here we include the production of two varieties of squark, denoted $\tilde{q}_R$ and $\tilde{q}_L$, so that the total number of on-shell degrees of freedom are the same as the spin $1/2$ case:

$$\frac{d^4\sigma}{dy_3 dy_4 d^2 p_T}(gg \to \tilde{q}_R \bar{\tilde{q}}_R + \tilde{q}_L \bar{\tilde{q}}_L) = \frac{\alpha_s^2}{\hat{s}^2} x_1 f_1(x_1) x_2 f_2(x_2) \tag{7.3}$$
$$\times \left(\frac{1}{6\tau_1\tau_2} - \frac{3}{8}\right)\left(1 - \tau_1^2 - \tau_2^2 - \rho + \frac{\rho^2}{4\tau_1\tau_2}\right).$$

Obviously these differential cross sections are quite different in detail, even if the spin 0 particles have the same mass as the spin $1/2$ particles.[d] As a result, the total cross section to produce, e.g., a pair of 500 GeV spin $1/2$ quarks at the LHC, is 2.5 times larger than the total cross section to produce a pair of 500 GeV spin 0 squarks (of either variety), from this the most important partonic subprocess. The p_T distributions of these parent particles also differ depending on their spin, thus affecting the kinematical

---

[c]Rapidity is a boost-friendly measure of the polar angle to the beam axis.

[d]Notice also that for equal masses the sum of the two cross sections gives a much simpler expression than either one individually. This is presumably a supersymmetry relation, but to our knowledge it has never been explained in the literature.

distributions of the final state SM particles that are reconstructed for the event.

Even 100 pb^{-1} of LHC data may be sufficient to discriminate between two BSM models that differ *only* by spin. More impressive still is a detailed study showing [23] that a few hundred inverse picobarns of data allow the discrimination of models that differ by spin *and* by other features in their spectra deliberately tuned to make them resemble each other *more* closely in a missing energy analysis.

For example, the smaller cross section for squark production versus production of heavy quarks of the same mass can be partially compensated by introducing by hand some squark-gluino associated production in the SUSY model, without introducing an analogous process in the non-SUSY look-alike. This makes it more difficult to discriminate the SUSY model from the non-SUSY model. In this tuning the gluino should be much heavier than the squark; otherwise due to the gluino's larger color charge squark-gluino (or gluino-gluino) production will dominate. Thus an indirect spin discrimination depends in part on the ability to distinguish lighter squarks from heavier gluinos, using basic kinematic properties reconstructed from the events.

7.8. More Look-Alikes

The only way to develop a library of techniques for discriminating missing energy look-alikes is to look in detail at large numbers of examples. To see how this works in practice, we will briefly review the analysis of five look-alike models presented in Ref. [23]. Simulated events corresponding to 100 pb^{-1} for each model are run through the CMS inclusive missing energy analysis; the models are look-alikes because the number of events after cuts agree within two sigma of the combined statistical and estimated systematic uncertainties. The five models are all MSSM SUSY models, denoted by LM2p, LM5, LM8, CS4d and CS6. The first three, LM2p, LM5 and LM8, are minimal supergravity models [24–26]. The models CS4d and CS6 are not minimal supergravity; they are more general high scale MSSM models based on the compressed supersymmetry idea of Martin [27]. Model CS4d is in fact part of the model line defined in Ref. [27]. Model CS6 is a modification of compressed SUSY where all of the squarks have been made very heavy, $\gtrsim 2$ TeV.

The superpartner mass spectra of the models are displayed in Fig. 7.3. In each case the lightest supersymmetric partner (LSP) is a WIMP dark
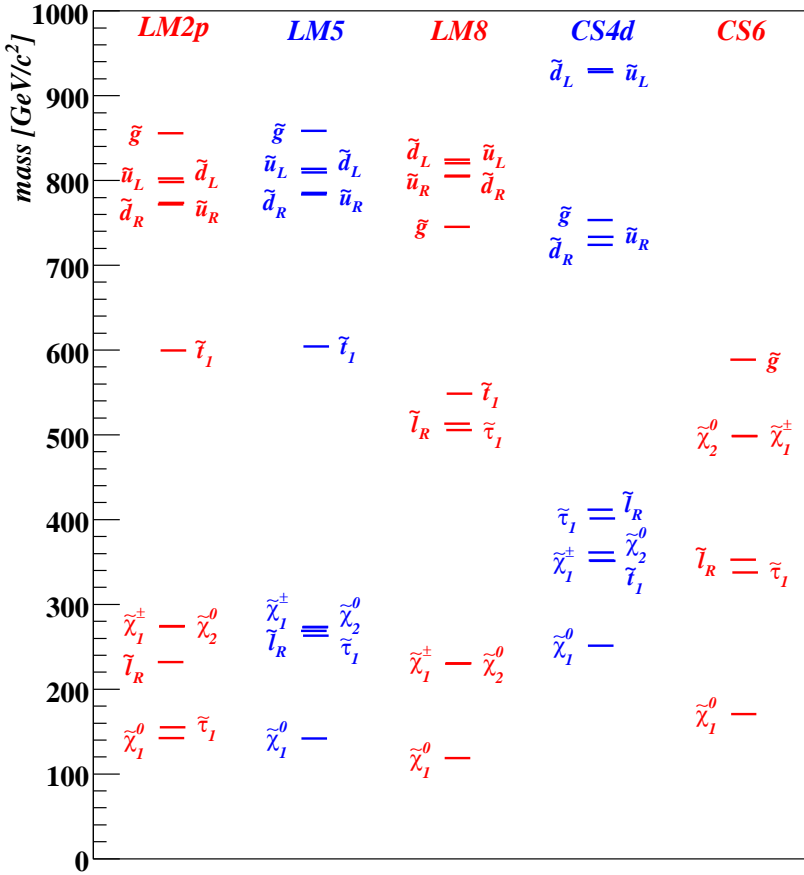
Fig. 7.3.   The mass spectra of the MSSM models LM2p, LM5, LM8, CS4d, and CS6 [23]. Only the most relevant particles are shown: the lighter gauginos $\tilde{\chi}_1^0$, $\tilde{\chi}_2^0$ and $\tilde{\chi}_1^\pm$, the lightest stau $\tilde{\tau}_1$, the right-smuon and selectron denoted collectively as $\tilde{\ell}_R$, the lightest stop $\tilde{t}_1$, the gluino, and the left/right up and down squarks $\tilde{u}_L$, $\tilde{u}_R$, $\tilde{d}_L$ and $\tilde{d}_R$. The very heavy $\simeq 2$ TeV squarks of model CS6 lie outside the displayed range.

matter candidate. Observe that all of the mSUGRA models are more similar to each other than they are to either of the more general MSSM models CS4d and CS6; this shows the limitations of the usual SUSY analyses that do not go beyond mSUGRA. As their name implies, the compressed SUSY models CS4d and CS6 have a compressed gaugino spectrum relative to mSUGRA; this produces either a light gluino (as in CS6) or a heavy LSP (as in CS4d).

The relative frequency of various LHC superpartner production processes is summarized in Table 7.1, for the models both before and after our event selection. As expected, the production fractions are much more similar after the event selection than before it, making the look-alike discrimination more difficult.

Table 7.2 shows the most relevant superpartner decay branching fractions. Table 7.3 shows the most significant inclusive final states. By final state we mean that all unstable superpartners have decayed, while Standard Model particles are left undecayed. We use q to denote any first or second generation quark or antiquark, but list bottom and top quarks separately. The percentage frequency of each final state is with respect to events passing our selection.

Combining the information in these tables, Ref. [23] summarizes the most significant features of the five models as follows:

- **Model LM2p:** 800 GeV squarks are slightly lighter than the gluino, and there is a 155 GeV stau. Dominant production is squark-gluino and squark-squark. Left-squarks decay about two-thirds of the time to quark-chargino, and one-third to quark-LSP; right-squarks decay to quark-LSP. Gluino decay is mostly to quark-squark, with 41% of this bottom-sbottom or top-stop. Charginos decay to the light stau plus a neutrino, while the second neutralino decays to tau-stau. Two-thirds of the final states after event selection have at least one tau.
- **Model LM5:** 800 GeV squarks are slightly lighter than the gluino. Dominant production is squark-gluino and squark-squark. Left-squark decays about two-thirds of the time to quark-chargino, and one-third to quark-LSP; right-squarks decay to quark-LSP. Gluino decay is mostly to quark-squark, with 43% of this bottom-sbottom or top-stop. Charginos decay to a W and an LSP, while the second neutralino decays to a light Higgs and an LSP. After selection 39% of final states have a W boson, and nearly a third have a Higgs.
- **Model LM8:** The 745 GeV gluino is slightly lighter than all of the squarks except $\tilde{b}_1$ and $\tilde{t}_1$. Dominant production is squark-gluino and squark-squark. Left-squarks decay about two-thirds of the time to quark-chargino, and one-third to quark-LSP; right-squarks decay two-thirds to quark-LSP and one-third to quark-gluino. Gluino decay is 81% to top-stop; the 548 GeV stops decay mostly to b-chargino or top-LSP. Charginos decay to W-LSP, and the second neutralino decays to Z-LSP. After selection 45% of final states have two tops, which may or may not

Table 7.1. Summary of LHC superpartner production for the MSSM models LM2p, LM5, LM8, CS4d, and CS6. The relative percentages are shown for each model, both before and after the event selection. The squark–squark percentages shown are excluding the contributions from pair production of the lightest stops, which are shown separately. Note that squark–chargino includes the production of either chargino, and squark-neutralino includes all of the four neutralinos. The category "other" includes weak production as well as the semi-weak associated production of gluinos with charginos or neutralinos. This table is taken from Ref. [23].

	LM2p		LM5		LM8		CS4d		CS6	
	before cuts	after cuts	before cuts	after cuts	before cuts	after cuts	before cuts	after cuts	before cuts	after cuts
squark–squark	33%	36%	32%	38%	22%	33%	19%	34%	0.1%	0.1%
squark–gluino	45%	55%	46%	52%	48%	54%	41%	55%	3.7%	7.4%
gluino–gluino	7.2%	6.4%	7.4%	6.4%	14%	8.3%	11%	8%	95%	92%
stop–stop	2.1%	1.1%	2.1%	0.9%	2.6%	1.5%	26%	1.4%	-	-
squark–chargino	2.1%	0.5%	2.1%	0.7%	1.4%	0.7%	0.2%	0.2%	-	-
squark–neutralino	1.7%	0.4%	1.8%	0.4%	1.2%	0.6%	0.6%	0.2%	-	-
other	9.5%	0.7%	9.3%	0.8%	11%	0.8%	1.9%	0.3%	1.1%	0.1%

Table 7.2. Summary of most relevant superpartner decays for the MSSM models LM2p, LM5, LM8, CS4d, and CS6. The table is taken from Ref. [23].

	LM2p	LM5	LM8	CS4d	CS6
$\tilde{g} \to \tilde{q}q$	45%	45%	-	-	-
$\to \tilde{b}_1 b$	25%	20%	14%	2%	-
$\to \tilde{t}_1 t$	16%	23%	81%	94%	-
$\to q\bar{q}\tilde{\chi}_1^0$	-	-	5%	-	75%
$\tilde{u}_L \to d\tilde{\chi}_1^\pm$	64%	64%	55%	-	-
$\to u\tilde{\chi}_1^0$	32%	32%	27%	-	-
$\to u\tilde{g}$	-	-	-	83%	85%
$\tilde{u}_R \to u\tilde{\chi}_1^0$	99%	99%	62%	92%	-
$\to u\tilde{g}$	-	-	38%	-	85%
$\tilde{b}_1 \to t\tilde{\chi}_1^-$	42%	36%	35%	20%	9%
$\to b\tilde{\chi}_2^0$	29%	23%	22%	14%	5%
$\to b\tilde{\chi}_1^0$	7%	2%	1%	50%	-
$\to b\tilde{g}$	-	-	-	-	85%
$\tilde{t}_1 \to b\tilde{\chi}_1^+$	45%	43%	42%	-	-
$\to t\tilde{\chi}_1^0$	22%	25%	30%	-	4%
$\to t\tilde{g}$	-	-	-	-	96%
$\to bW^+\tilde{\chi}_1^0$	-	-	-	100%	-
$\tilde{\chi}_1^\pm \to W^\pm\tilde{\chi}_1^0$	5%	97%	100%	100%	2%
$\to \tilde{\tau}_1^\pm \nu_\tau$	95%	-	-	-	77%
$\tilde{\chi}_2^0 \to Z\tilde{\chi}_1^0$	1%	11%	100%	100%	-
$\to h\tilde{\chi}_1^0$	3%	85%	-	-	2%
$\to \tilde{\tau}_1\tau$	96%	3%	-	-	77%
$\tilde{\tau}_1 \to \tau\tilde{\chi}_1^0$	100%	100%	88%	98%	100%

have the same sign. Almost half of the final states have a W, more than a third have a Z, and a quarter have both a W and a Z.

- **Model CS4d:** The 753 GeV gluino is in between the right-squark and left-squark masses. The LSP is relatively heavy, 251 GeV, and the ratio of the gluino to LSP mass is small compared to mSUGRA models. Dominant production is squark-gluino and squark-squark. Left-squarks

Table 7.3. Summary of significant inclusive final states for the MSSM models LM2p, LM5, LM8, CS4d, and CS6. By final state we mean that all unstable superpartners have decayed, while Standard Model particles are left undecayed. Here q denotes any first or second generation quark or antiquark, and more generally the notation does not distinguish particles from antiparticles. The percentage frequency of each final state is with respect to events passing our selection. The table is taken from Ref. [23].

	LM2p	LM5	LM8	CS4d	CS6
$qq\,\tilde\chi_1^0\,\tilde\chi_1^0$	76%	72%	57%	43%	99%
$qqq\,\tilde\chi_1^0\tilde\chi_1^0$	39%	31%	29%	10%	79%
$qqqq\,\tilde\chi_1^0\,\tilde\chi_1^0$	9%	5%	14%	5%	77%
$\tau\,\nu_\tau\,qq\,\tilde\chi_1^0\,\tilde\chi_1^0$	34%	2%	4%	-	1%
$\tau\tau\,\tilde\chi_1^0\,\tilde\chi_1^0$	32%	1%	-	-	-
$bb\,q\,\tilde\chi_1^0\,\tilde\chi_1^0$	11%	7%	5%	14%	19%
$b\,t\,W\,q\,\tilde\chi_1^0\,\tilde\chi_1^0$	7%	21%	37%	67%	-
$W\,qq\,\tilde\chi_1^0\,\tilde\chi_1^0$	12%	39%	42%	24%	-
$h\,q\,\tilde\chi_1^0\,\tilde\chi_1^0$	3%	28%	7%	-	-
$tt\,q\,\tilde\chi_1^0\,\tilde\chi_1^0$	11%	13%	45%	-	3%
$Z\,q\,\tilde\chi_1^0\,\tilde\chi_1^0$	3%	6%	36%	10%	-
$Z\,W\,q\,\tilde\chi_1^0\,\tilde\chi_1^0$	1%	6%	25%	5%	-
$bb\,tt\,WW\,\tilde\chi_1^0\,\tilde\chi_1^0$	-	-	1%	13%	-

decay to quark-gluino, while right-squarks decay to quark-LSP. Gluinos decay to top-stop; the 352 GeV stops decay 100% to $bW^+\tilde\chi_1^0$. Two-thirds of the final states contain $btWq\tilde\chi_1^0\tilde\chi_1^0$, and a significant fraction of these contain more b's, t's and W's.

- **Model CS6:** The 589 GeV gluino is much lighter than the 2 TeV squarks, and the ratio of the gluino to LSP mass is small compared to mSUGRA models. Production is 92% gluino-gluino, and gluinos decay predominantly via the three-body mode $qq\tilde\chi_1^0$. The final states consist almost entirely of three or four quarks plus two LSPs, with a proportionate amount of the final state quarks being b's.

7.9. Simple Robust Discriminators

The most robust observables available in the early LHC running will be ratios of inclusive counts, applied to simple reconstructed physics objects in the discovery data sample after all the event selection has been performed. As an example, with some suitable definition of reconstructed jets, one can count the number of events after cuts that have ≥ 3 jets, versus the number of events that have ≥ 4 jets. The ratio of these counts has a reduced sensitivity to systematic errors, and gives a robust measure of jet multiplicity. This observable will help to discriminate models with longer decay chains from those with direct decays to the WIMP final state.

The shapes of kinematic distributions will provide important information for discriminating models, but in the early going we expect rather large uncertainties about the details and overall normalization of these shapes. A good strategy [23] is therefore to extract the shape information in the form of a ratio of inclusive counts. This is done by dividing each distribution into a small number of bins, two in the simplest case. Thus e.g. the MET distribution is divided into a high bin, MET > 320 GeV, and a low bin, 220 GeV < MET $\leq$ 320 GeV (note that events with MET < 220 GeV don't pass the event selection to begin with). The ratio of the number of events in the high MET bin to the total number of events is a robust observable; it discriminates models with larger m_{P} (having smaller cross sections but more MET) from models with smaller m_{P} (having larger cross sections but less MET).

This method also works for other kinds of shape information. For example, a variety of algorithms exist that divide an LHC event into two hemispheres [10] attempting to assign each reconstructed object to one or the other of the two parent particles produced in the original partonic collison. Using such an algorithm, we can define a ratio of inclusive counts, e.g. the count of events where the number of objects in the two hemispheres differs by at least two, divided by the total count of events. This is a robust observable that helps to flag production of more than one kind of parent particle or more than one kind of decay chain.

As previously mentioned, mature τ and b tagging, of the type currently in use in the experiments at the Tevatron, may not be available to LHC experiments at the time of an early missing energy discovery. This does not mean, however, that we will have no ability to discriminate between models on the basis of τs or b jets in the final state. Simple algorithms can be used based on single track jets for hadronic τs and muons inside jets for bs. "Poor man's" tagging schemes of this type will have rather low

efficiencies and high fake rates. Nevertheless, they provide robust ratios of tag counts that discriminate reasonably well. For example, a poor man's tau tag discriminates model LM2p from model LM5, based on the higher tau multiplicty in LM2p.

When a variety of well-chosen robust observables are applied to discriminate the five look-alike models introduced in the previous section, the results are impressive [23]. Although the assumed discovery sample of 100 pb^{-1} is not always enough to discriminate every pair of models, with a few hundred inverse picobarns we begin, not only to disambiguate the lookalikes, but also to reveal combinations of more detailed properties.

7.10. Outlook

As of this writing we are less than a year away from LHC data. Data will allow us to quickly attack the direct LHC problem, namely the understanding of the Standard Model at 14 TeV. The inverse LHC problem is convoluted with this direct one. We will continue to develop simple cogent strategies that address both the direct and the inverse LHC problems. If we succeed, the first iteration of analyses will orient us in the right path to unfold the discoveries.

Acknowledgments

References

[1] P. Binetruy, G. L. Kane, B. D. Nelson, L.-T. Wang, and T. T. Wang, Relating incomplete data and incomplete theory, *Phys. Rev.* **D70**, 095006, (2004).
[2] J. L. Bourjaily, G. L. Kane, P. Kumar, and T. T. Wang, Outside the mSUGRA box. (2005).
[3] N. Arkani-Hamed, G. L. Kane, J. Thaler, and L.-T. Wang, Supersymmetry and the LHC inverse problem, *JHEP.* **08**, 070, (2006).
[4] E. A. Baltz, M. Battaglia, M. E. Peskin, and T. Wizansky, Determination of dark matter properties at high-energy colliders, *Phys. Rev.* **D74**, 103521, (2006).
[5] R. K. Ellis, W. J. Stirling, and B. R. Webber, QCD and collider physics, *Camb. Monogr. Part. Phys. Nucl. Phys. Cosmol.* **8**, 1–435, (1996).

[6] J. L. Hewett and M. Spiropulu, Particle physics probes of extra spacetime dimensions, *Ann. Rev. Nucl. Part. Sci.* **52**, 397–424, (2002).

[7] T. Aaltonen et al., First Measurement of the W Boson Mass in Run II of the Tevatron, *Phys. Rev. Lett.* **99**, 151801, (2007).

[8] T. Aaltonen et al., First Run II Measurement of the *W* Boson Mass. (2007).

[9] A. A. Affolder et al., Search for gluinos and squarks using like-sign dileptons in $p\bar{p}$ collisions at $\sqrt{s} = 1.8$ TeV, *Phys. Rev. Lett.* **87**, 251803, (2001).

[10] G. L. Bayatian et al., CMS technical design report, volume II: Physics performance, *J. Phys.* **G34**, 995–1579, (2007).

[11] M. Spiropulu, SUSY@LHC.CERN.CH. (2008). arXiv:0801.0318 [hep-ex].

[12] F. E. Paige, S. D. Protopopescu, H. Baer, and X. Tata, ISAJET 7.69: A Monte Carlo event generator for p p, anti-p p, and e+ e- reactions. (2003).

[13] A. Djouadi, M. M. Muhlleitner, and M. Spira, Decays of supersymmetric particles: The program SUSY-HIT (SUspect-SdecaY-Hdecay-InTerface), *Acta Phys. Polon.* **B38**, 635–644, (2007).

[14] B. C. Allanach, SOFTSUSY: A C++ program for calculating supersymmetric spectra, *Comput. Phys. Commun.* **143**, 305–331, (2002).

[15] T. Stelzer and W. F. Long, Automatic generation of tree level helicity amplitudes, *Comput. Phys. Commun.* **81**, 357–371, (1994).

[16] E. Boos et al., CompHEP 4.4: Automatic computations from Lagrangians to events, *Nucl. Instrum. Meth.* **A534**, 250–259, (2004).

[17] F. Maltoni and T. Stelzer, MadEvent: Automatic event generation with MadGraph, *JHEP.* **02**, 027, (2003).

[18] T. Sjostrand, S. Mrenna, and P. Skands, PYTHIA 6.4 physics and manual, *JHEP.* **05**, 026, (2006).

[19] G. Corcella et al., HERWIG 6: An event generator for hadron emission reactions with interfering gluons (including supersymmetric processes), *JHEP.* **01**, 010, (2001).

[20] T. Gleisberg et al., SHERPA 1.alpha, a proof-of-concept version, *JHEP.* **02**, 056, (2004).

[21] G. Duckeck et al., ATLAS computing: Technical design report. CERN-LHCC-2005-022.

[22] D. Bonacorsi, The CMS computing model, *Nucl. Phys. Proc. Suppl.* **172**, 53–56, (2007).

[23] J. Hubisz, J. Lykken, M. Pierini, and M. Spiropulu, Missing energy look-alikes with 100 pb-1 at the LHC. FERMILAB-PUB-08-012-T.

[24] A. H. Chamseddine, R. Arnowitt, and P. Nath, Locally Supersymmetric Grand Unification, *Phys. Rev. Lett.* **49**, 970, (1982).

[25] R. Barbieri, S. Ferrara, and C. A. Savoy, Gauge Models with Spontaneously Broken Local Supersymmetry, *Phys. Lett.* **B119**, 343, (1982).

[26] L. J. Hall, J. D. Lykken, and S. Weinberg, Supergravity as the Messenger of Supersymmetry Breaking, *Phys. Rev.* **D27**, 2359–2378, (1983).

[27] S. P. Martin, Compressed supersymmetry and natural neutralino dark matter from top squark-mediated annihilation to top quarks, *Phys. Rev.* **D75**, 115005, (2007).

This page intentionally left blank

Chapter 8

From BCS to the LHC

Steven Weinberg

The University of Texas at Austin, Department of Physics
1 University Station C1600, Austin, TX 7812-0264

Reflections on spontaneous symmetry breaking, and the connection be-
tween condensed matter physics and particle physics, as given in a talk
at a symposium at the University of Illinois in Urbana, celebrating the
50th anniversary of the theory of superconductivity.

It was a little odd for me, a physicist whose work has been mainly on the theory of elementary particles, to be invited to speak at a meeting of condensed matter physicists celebrating a great achievement in their field. It is not only that there is a difference in the subjects we explore. There are deep differences in our aims, in the kinds of satisfaction we hope to get from our work.

Condensed matter physicists are often motivated to deal with phenomena because the phenomena themselves are intrinsically so interesting. Who would not be fascinated by weird things, such as superconductivity, superfluidity, or the quantum Hall effect? On the other hand, I don't think that elementary particle physicists are generally very excited by the phenomena they study. The particles themselves are practically featureless, every electron looking tediously just like every other electron.

Another aim of condensed matter physics is to make discoveries that are useful. In contrast, although elementary particle physicists like to point to the technological spin-offs from elementary particle experimentation, and these are real, this is not the reason we want these experiments to be done, and the knowledge gained by these experiments has no foreseeable practical applications.

Most of us do elementary particle physics neither because of the intrinsic interestingness of the phenomena we study, nor because of the practical

importance of what we learn, but because we are pursuing a reductionist vision. All the properties of ordinary matter are what they are because of the principles of atomic and nuclear physics, which are what they are because of the rules of the Standard Model of elementary particles, which are what they are because ... Well, we don't know, this is the reductionist frontier, which we are currently exploring.

I think that the single most important thing accomplished by the theory of Bardeen, Cooper, and Schrieffer (BCS) was to show that superconductivity is not part of the reductionist frontier [1]. Before BCS this was not so clear. For instance, in 1933 Walter Meissner raised the question whether electric currents in superconductors are carried by the known charged particles, electrons and ions. The great thing showed by Bardeen, Cooper, and Schrieffer was that no new particles or forces had to be introduced to understand superconductivity. According to a book on superconductivity that Leon Cooper showed me, many physicists were even disappointed that "superconductivity should, on the atomistic scale, be revealed as nothing more than a footling small interaction between electrons and lattice vibrations. [2]"

The claim of elementary particle physicists to be leading the exploration of the reductionist frontier has at times produced resentment among condensed matter physicists. (This was not helped by a distinguished particle theorist, who was fond of referring to condensed matter physics as "squalid state physics.") This resentment surfaced during the debate over the funding of the Superconducting SuperCollider (SSC). I remember that Phil Anderson and I testified in the same Senate committee hearing on the issue, he against the SSC and I for it. His testimony was so scrupulously honest that I think it helped the SSC more than it hurt it. What really did hurt was a statement opposing the SSC by a condensed matter physicist who happened at the time to be the President of the American Physical Society. As everyone knows, the SSC project was cancelled, and now we are waiting for the LHC at CERN to get us moving ahead again in elementary particle physics.

During the SSC debate, Anderson and other condensed matter physicists repeatedly made the point that the knowledge gained in elementary particle physics would be unlikely to help them to understand emergent phenomena like superconductivity. This is certainly true, but I think beside the point, because that is not why we are studying elementary particles; our aim is to push back the reductive frontier, to get closer to whatever simple and general theory accounts for everything in nature. It could be

said equally that the knowledge gained by condensed matter physics is unlikely to give us any direct help in constructing more fundamental theories of nature.

So what business does a particle physicist like me have at a celebration of the BCS theory? (I have written just one paper about superconductivity, a paper of monumental unimportance, which was treated by the condensed matter community with the indifference it deserved.) Condensed matter physics and particle physics are relevant to each other, despite everything I have said. This is because, although the knowledge gained in elementary particle physics is not likely to be useful to condensed matter physicists, or vice versa, experience shows that the ideas developed in one field can prove very useful in the other. Sometimes these ideas become transformed in translation, so that they even pick up a renewed value to the field in which they were first conceived.

The example that concerns me here is an idea that elementary particle physicists learned from condensed matter theory — specifically, from the BCS theory. It is the idea of spontaneous symmetry breaking. In particle physics we are particularly interested in the symmetries of the laws of nature. One of these symmetries is invariance of the laws of nature under the symmetry group of three-dimensional rotations, or in other words, invariance of the laws we discover under changes in the orientation of our measuring apparatus.

When a physical system does not exhibit all the symmetries of the laws by which it is governed, we say that these symmetries are spontaneously broken. A very familiar example is spontaneous magnetization. The laws governing the atoms in a magnet are perfectly invariant under three-dimensional rotations, but at temperatures below a critical value, the spins of these atoms spontaneously line up in some direction, producing a magnetic field. In this case, and as often happens, a subgroup is left invariant: the two dimensional group of rotations around the direction of magnetization.

Now to the point. A superconductor of any kind is nothing more or less than a material in which a particular symmetry of the laws of nature, electromagnetic gauge invariance, is spontaneously broken. This is true of high temperature superconductors, as well as the more familiar superconductors studied by BCS. The symmetry group here is the group of two-dimensional rotations. These rotations act on a two-dimensional vector, whose two components are the real and imaginary parts of the electron field, the quantum mechanical operator that in quantum field theories of matter destroys

electrons. The rotation angle of the broken symmetry group can vary with location in the superconductor, and then the symmetry transformations also affect the electromagnetic potentials, a point to which I will return.

The symmetry breaking in a superconductor leaves unbroken a rotation by 180°, which simply changes the sign of the electron field. In consequence of this spontaneous symmetry breaking, products of any even number of electron fields have nonvanishing expectation values in a superconductor, though a single electron field does not. All of the dramatic exact properties of superconductors — zero electrical resistance, the expelling of magnetic fields from superconductors known as the Meissner effect, the quantization of magnetic flux through a thick superconducting ring, and the Josephson formula for the frequency of the ac current at a junction between two superconductors with different voltages — follow from the assumption that electromagnetic gauge invariance is broken in this way, with no need to inquire into the mechanism by which the symmetry is broken.

Condensed matter physicists often trace these phenomena to the appearance of an "order parameter," the non-vanishing mean value of the product of two electron fields, but I think this is misleading. There is nothing special about two electron fields; one might just as well take the order parameter as the product of three electron fields and the complex conjugate of another electron field. The important thing is the broken symmetry, and the unbroken subgroup.

It may then come as a surprise that spontaneous symmetry breaking is nowhere mentioned in the seminal paper of Bardeen, Cooper, and Schrieffer. Their paper describes a mechanism by which electromagnetic gauge invariance is in fact broken, but they derived the properties of superconductors from their dynamical model, not from the mere fact of broken symmetry. I am not saying that Bardeen, Cooper, and Schrieffer did not know of this spontaneous symmetry breaking. Indeed, there was already a large literature on the apparent violation of gauge invariance in phenomenological theories of superconductivity, the fact that the electric current produced by an electromagnetic field in a superconductor depends on a quantity known as the vector potential, which is not gauge invariant. But their attention was focussed on the details of the dynamics rather than the symmetry breaking.

This is not just a matter of style. As BCS themselves made clear, their dynamical model was based on an approximation, that a pair of electrons interact only when the magnitude of their momenta is very close to a certain value, known as the Fermi surface. This leaves a question: How

can you understand the exact properties of superconductors, like exactly zero resistance and exact flux quantization, on the basis of an approximate dynamical theory? It is only the argument from exact symmetry principles that can fully explain the remarkable exact properties of superconductors.

Though spontaneous symmetry breaking was not emphasized in the BCS paper, the recognition of this phenomenon produced a revolution in elementary particle physics. The reason is that (with certain qualification, to which I will return), whenever a symmetry is spontaneously broken, there must exist excitations of the system with a frequency that vanishes in the limit of large wavelength. In elementary particle physics, this means a particle of zero mass.

The first clue to this general result was a remark in a 1960 paper by Yoichiro Nambu, that just such collective excitations in superconductors play a crucial role in reconciling the apparent failure of gauge invariance in a superconductor with the exact gauge invariance of the underlying theory governing matter and electromagnetism. Nambu speculated that these collective excitations are a necessary consequence of this exact gauge invariance.

A little later, Nambu put this idea to good use in particle physics. In nuclear beta decay an electron and neutrino (or their antiparticles) are created by currents of two different kinds flowing in the nucleus, known as vector and axial vector currents. It was known that the vector current was conserved, in the same sense as the ordinary electric current. Could the axial current also be conserved?

The conservation of a current is usually a symptom of some symmetry of the underlying theory, and holds whether or not the symmetry is spontaneously broken. For the ordinary electric current, this symmetry is electromagnetic gauge invariance. Likewise, the vector current in beta decay is conserved because of the isotopic spin symmetry of nuclear physics. One could easily imagine several different symmetries, of a sort known as chiral symmetries, that would entail a conserved axial vector current. But it seemed that any such chiral symmetries would imply either that the nucleon mass is zero, which is certainly not true, or that there must exist a triplet of massless strongly interacting particles of zero spin and negative parity, which isn't true either. These two possibilities simply correspond to the two possibilities that the symmetry, whatever it is, either is not, or is, spontaneously broken, not just in some material like a superconductor, but even in empty space.

Nambu proposed that there is indeed such a symmetry, and it is spontaneously broken in empty space, but the symmetry in addition to being spontaneously broken is not exact to begin with, so the particle of zero spin and negative parity required by the symmetry breaking is not massless, only much lighter than other strongly interacting particles. This light particle, he recognized, is nothing but the pion, the lightest and first discovered of all the mesons. In a subsequent paper with Giovanni Jona-Lasinio, Nambu presented an illustrative theory in which, with some drastic approximations, a suitable chiral symmetry was found to be spontaneously broken, and in consequence the light pion appeared as a bound state of a nucleon and an antinucleon.

So far, there was no proof that broken exact symmetries always entail exactly massless particles, just a number of examples of approximate calculations in specific theories. In 1961 Jeffrey Goldstone gave some more examples of this sort, and a hand-waving proof that this was a general result. Such massless particles are today known as Goldstone bosons, or Nambu-Goldstone bosons. Soon after, Goldstone, Abdus Salam, and I made this into a rigorous and apparently quite general theorem.

This theorem has applications in many branches of physics. One is cosmology. You may know that today the observation of fluctuations in the cosmic microwave background are being used to set constraints on the nature of the exponential expansion, known as inflation, that is widely believed to have preceded the radiation dominated Big Bang. But there is a problem here. In between the end of inflation and the time the microwave background that we observe was emitted, there intervened a number of events that are not at all understood: the heating of the universe after inflation, the production of baryons, the decoupling of cold dark matter, and so on. So how is it possible to learn anything about inflation by studying radiation that was emitted long after inflation, when we don't understand what happened in between? The reason we can get away with this is that the cosmological fluctuations now being studied are of a type, known as adiabatic, that can be regarded as the Goldstone excitations required by a symmetry, related to general coordinate invariance, that is spontaneously broken by the spacetime geometry. The physical wavelengths of these cosmological fluctuations were stretched out by inflation so much that they were very large during the epochs when things were happening that we don't understand, so they then had zero frequency, which means that the amplitude of these fluctuations was not changing, so that the value of the amplitude relatively close to the present tells us what it was during inflation.

But in particle physics, this theorem was at first seen as a disappointing result. There was a crazy idea going around, which I have to admit that at first I shared, that somehow the phenomenon of spontaneous symmetry breaking would explain why the symmetries being discovered in strong interaction physics were not exact. Werner Heisenberg continued to believe this into the 1970s, when everyone else had learned better.

The prediction of new massless particles, which were ruled out experimentally, seemed in the early 1960s to close off this hope. But it was a false hope anyway. Except under special circumstances, a spontaneously broken symmetry does not look at all like an approximate unbroken symmetry; it manifests itself in the masslessness of spin zero bosons, and in details of their interactions. Today we understand approximate symmetries such as isospin and chiral invariance as consequences of the fact that some quark masses, for some unknown reason, happen to be relatively small.

Though based on a false hope, this disappointment had an important consequence. Peter Higgs, Robert Brout and François Englert, and Gerald Guralnik, Dick Hagen, and Tom Kibble were all led to look for, and then found, an exception to the theorem of Goldstone, Salam, and me. The exception applies to theories in which the underlying physics is invariant under local symmetries, symmetries whose transformations, like electromagnetic gauge transformations, can vary from place to place in space and time. (This is in contrast with the chiral symmetry associated with the axial vector current of beta decay, which applies only when the symmetry transformations are the same throughout spacetime.) For each local symmetry there must exist a vector field, like the electromagnetic field, whose quanta would be massless if the symmetry was not spontaneously broken. The quanta of each such field are particles with helicity (the component of angular momentum in the direction of motion) equal in natural units to $+1$ or -1. But if the symmetry is spontaneously broken, these two helicity states join up with the helicity-zero state of the Goldstone boson to form the three helicity states of a massive particle of spin one. Thus, as shown by Higgs, Brout and Englert, and Guralnik, Hagen, and Kibble, when a local symmetry is spontaneously broken, neither the vector particles with which the symmetry is associated nor the Nambu-Goldstone particles produced by the symmetry breaking have zero mass.

This was actually argued earlier by Anderson, on the basis of the example provided by the BCS theory. But the BCS theory is non-relativistic, and the Lorentz invariance that is characteristic of special relativity had played a crucial role in the theorem of Goldstone, Salam, and me, so Anderson's

argument was generally ignored by particle theorists. In fact, Anderson was right: the reason for the exception noted by Higgs *et al.* is that it is not possible to quantize a theory with a local symmetry in a way that preserves both manifest Lorentz invariance and the usual rules of quantum mechanics, including the requirement that probabilities be positive. In fact, there are two ways to quantize theories with local symmetries: one way that preserves positive probabilities but loses manifest Lorentz invariance, and another that preserves manifest Lorentz invariance but seems to lose positive probabilities, so in fact these theories actually do respect both Lorentz invariance and positive probabilities; they just don't respect our theorem.

The appearance of mass for the quanta of the vector bosons in a theory with local symmetry re-opened an old proposal of Chen Ning Yang and Robert Mills, that the strong interactions might be produced by the vector bosons associated with some sort of local symmetry, more complicated than the familiar electromagnetic gauge invariance. This possibility was specially emphasized by Brout and Englert. It took a few years for this idea to mature into a specific theory, which then turned out not to be a theory of strong interactions.

Perhaps the delay was because the earlier idea of Nambu, that the pion was the nearly massless boson associated with an approximate chiral symmetry that is not a local symmetry, was looking better and better. I was very much involved in this work, and would love to go into the details, but that would take me too far from BCS. I'll just say that, from the effort to understand processes involving any number of low-energy pions beyond the lowest order of perturbation theory, we became comfortable with the use of effective field theories in particle physics. The mathematical techniques developed in this work in particle physics were then used by Joseph Polchinski and others to justify the approximations made by BCS in their work on superconductivity.

The story of the physical application of spontaneously broken local symmetries has often been told, by me and others, and I don't want to take much time on it here, but I can't leave it out altogether because I want to make a point about it that will take me back to the BCS theory. Briefly, in 1967 I went back to the idea of a theory of strong interactions based on a spontaneously broken local symmetry group, and right away, I ran into a problem: the subgroup consisting of ordinary isospin transformations is not spontaneously broken, so there would be a massless vector particle associated with these transformations with the spin and charges of the rho

meson. This of course was in gross disagreement with observation; the rho meson is neither massless nor particularly light.

Then it occurred to me that I was working on the wrong problem. What I should have been working on were the weak nuclear interactions, like beta decay. There was just one natural choice for an appropriate local symmetry, and when I looked back at the literature I found that the symmetry group I had decided on was one that had already been proposed in 1961 by Sheldon Glashow, though not in the context of an exact spontaneously broken local symmetry. (I found later that the same group had also been considered by Salam and John Ward.) Even though it was now exact, the symmetry when spontaneously broken would yield massive vector particles, the charged W particles that had been the subject of theoretical speculation for decades, and a neutral particle, which I called the Z particle, which mediates a "neutral current" weak interaction, which had not yet been observed. The same symmetry breaking also gives mass to the electron and other leptons, and in a simple extension of the theory, to the quarks. This symmetry group contained electromagnetic gauge invariance, and since this subgroup is clearly not spontaneously broken (except in superconductors), the theory requires a massless vector particle, but it is not the rho meson, it is the photon, the quantum of light. This theory, which became known as the electroweak theory, was also proposed independently in 1968 by Salam.

The mathematical consistency of the theory, which Salam and I had suggested but not proved, was shown in 1971 by Gerard 't Hooft; neutral current weak interactions were found in 1973; and the W and Z particles were discovered at CERN a decade later. Their detailed properties are just those expected according to the electroweak theory.

There was (and still is) one outstanding issue: just how is the local electroweak symmetry broken? In the BCS theory, the spontaneous breakdown of electromagnetic gauge invariance arises because of attractive forces between electrons near the Fermi surface. These forces don't have to be strong; the symmetry is broken however weak these forces may be. But this feature occurs only because of the existence of a Fermi surface, so in this respect the BCS theory is a misleading guide for particle physics. In the absence of a Fermi surface, dynamical spontaneous symmetry breakdown requires the action of strong forces. There are no forces acting on the known quarks and leptons that are anywhere strong enough to produce the observed breakdown of the local electroweak symmetry dynamically, so Salam and I did not assume a dynamical symmetry breakdown; instead we introduced elementary scalar fields into the theory, whose vacuum

expectation values in the classical approximation would break the symmetry.

This has an important consequence. The only elementary scalar quanta in the theory that are eliminated by spontaneous symmetry breaking are those that become the helicity-zero states of the W and Z vector particles. The other elementary scalars appear as physical particles, now generically known as Higgs bosons. It is the Higgs boson predicted by the electroweak theory of Salam and me that will be the primary target of the new LHC accelerator, to be completed at CERN sometime in 2008.

But there is another possibility, suggested independently in the late 1970s by Leonard Susskind and myself. The electroweak symmetry might be broken dynamically after all, as in the BCS theory. For this to be possible, it is necessary to introduce new extra-strong forces, known as technicolour forces, that act on new particles, other than the known quarks and leptons. With these assumptions, it is easy to get the right masses for the W and Z particles and large masses for all the new particles, but there are serious difficulties in giving masses to the ordinary quarks and leptons. Still, it is possible that experiments at the LHC will not find Higgs bosons, but instead will find a great variety of heavy new particles associated with technicolour. Either way, the LHC is likely to settle the question of how the electroweak symmetry is broken.

It would have been nice if we could have settled this question by calculation alone, without the need of the LHC, in the way that Bardeen, Cooper, and Schrieffer were able to find how electromagnetic gauge invariance is broken in a superconductor by applying the known principles of electromagnetism. But that is just the price we in particle physics have to pay for working in a field whose underlying principles are not yet known.

References

[1] J. Bardeen, L. N. Cooper, and J. R. Schrieffer, Theory of Superconductivity, *Phys. Rev.* **108**, 1175 (1957).
[2] K. Mendelssohn, *The Quest for Absolute Zero* (McGraw-Hill, New York, 1966).

Chapter 9

Searching for Gluinos at the Tevatron and Beyond

Johan Alwall, My-Phuong Le,
Mariangela Lisanti and Jay G. Wacker

SLAC, Stanford University
Menlo Park, CA 94025
and
Physics Department, Stanford University
Stanford, CA 94305

This chapter describes how to perform model-independent searches for new pair-produced color octet particles that each subsequently decay into two jets plus missing energy. The details of this analysis are focussed on the Tevatron, however, all of the lessons can be carried over to the LHC. Current searches are not sensitive to all regions of parameter space because they employ CMSSM-motivated cuts. Optimizing the H_T and $\not{E}_T$ cuts expands the sensitivity of searches for all kinematically allowed decays.

9.1. Introduction

In many theories beyond the Standard Model, there is a new color octet particle that decays into jets plus a stable neutral singlet. This occurs, for example, in supersymmetry [1] and Universal Extra Dimensions [2], as well as Randall-Sundrum and Little Higgs models [3, 4]. As a result, jets plus missing transverse energy ($\not{E}_T$) is a promising experimental signature for new phenomena [5–8]. While jets and missing energy are promising searches, the multitude of different models means that care must be taken in designing searches so that all of these promising models (and hopefully ones that haven't been proposed) so that the searches are sensitive to all of these different models. For instance, in the five parameter, constrained MSSM, gluinos are pair produced which cascade decays to winos that a third of their mass which subsequently decays to the bino which is half

the mass of the wino. In contrast, in Universal Extra Dimensions have a spectrum that is typically much more compact. Representative masses for the first Kaluza-Klein gluon and photon are 650 GeV and 500 GeV, respectively. This 30% mass splitting, in contrast to 600% for the CMSSM, means that the kinematics of the two signals are very different. In this contribution, we explore this difference. In going forward into the LHC era, searches for particles need to be as model independent as possible so that discoveries are not overlooked.

Due to historical prejudices, all searches for jets and missing energy have been based upon the constrained MSSM. The current best limits on searches for non-Standard Model contributions to jets plus missing energy are from the Tevatron and at present, these searches are based upon the CMSSM [6, 7]. Both gluinos and squarks can decay to jets and a bino ($\tilde{B}$), the supersymmetric partner of the photon. The bino is stable, protected by a discrete R-parity, and is manifest as missing energy in the detector. Different jet topologies are expected, depending on the relative masses of the gluinos and squarks.

There are many parameters in the MSSM and setting mass bounds in a multi-parameter space is difficult. This has lead to a great simplifying ansätz known as the CMSSM (or mSUGRA) parameterization of supersymmetry breaking. This ansätz sets all the gaugino masses equal at the grand unified scale. As a result, the ratio between the mass of the gluino and bino is constant ($m_{\tilde{g}} : m_{\tilde{B}} = 6 : 1$). Thus, the mass ratio between the gluino and bino is never scanned when searching through CMSSM parameter space, which means that there is a large region of kinematically accessible gluinos where there are no known limits.

The CMSSM parametrization is not representative of all supersymmetric models. Other methods of supersymmetry breaking, such as anomaly, mirage, and non-Minimal gauge mediation, lead to different low-energy particle spectra where $m_{\tilde{g}} : m_{\tilde{B}}$ is not necessarily constant. A more comprehensive search strategy should be sensitive to all values of $m_{\tilde{g}}$ and $m_{\tilde{B}}$.

In this paper, we describe how model independent mass bounds can be placed on gluino and bino[a] masses. We will treat the gluino as the first new colored particle and will assume that it only decays to the the stable bino: $\tilde{g} \to \bar{q}_1 \tilde{q}^* \to \bar{q}_1 q_2 \tilde{B}$. We show how a set of optimized cuts for $\not{E}_T$ and $H_T = \sum_{\text{jets}} E_T$ can set much tighter mass bounds than current Tevatron searches. Our searches are closely based upon DØ's searches for

---

[a]Throughout this note, we will call the color octet a "gluino" and the neutral singlet the "bino," though nothing more than the color and charge is denoted by these names.

monojets [8], squarks and gluinos [6]. By taking this approach, we hope that our projected sensitivity is close to what is achievable and not swamped by an unforeseen background.

By modeling the source of jets plus missing energy as a gluino with the scalars decoupled from the spectrum, we are making several explicit assumptions. Most obvious is the assumption that the new colored particle is a fermion. The spin of the new color octet and singlet is not known a priori, and the only selection rule is that the octet and singlet must have the same statistics. For fermions there is the additional ambiguity of whether the new particles are Dirac or Majorana. Spin correlations are incredibly difficult to infer and in practice the spin dependence can largely be captured by a simple re-scaling of the entire production cross section. (For a discussion of the difficulties of extracting spin information from the the LHC using angular correlations, see the article by Wang and Yavin in this volume.)

If there are particles that can contribute to t-channel processes, then both the differential and integrated cross sections can be altered by the presence of these other particles. So long as the Tevatron is only kinematically capable of producing the lightest new colored particle, any t-channel particles should be off-shell and the differential production cross section for the gluinos do not have a strong angular dependence. The t-channel particles will change the production cross section; however, since this will be treated as free parameter, there is no loss of generality by considering pure QCD production of the octet.

9.2. Event Generation

9.2.1. *Signal*

The number of jets expected as a result of gluino production at the Tevatron depends on the relative mass difference between the gluino and bino, $m_{\tilde{g}} - m_{\tilde{B}}$. When the mass splitting is much larger than the bino mass, the search is not limited by phase space and four or more well-separated jets are produced, as well as large missing transverse energy. The situation is very different for light gluinos ($m_{\tilde{g}} \lesssim 200$ GeV) that are nearly degenerate with the bino. Such light gluinos can be copiously produced at the Tevatron, with cross sections $\mathcal{O}(10^2$ pb), as compared to $\mathcal{O}(10^{-2}$ pb) for their heavier counterparts ($m_{\tilde{g}} \gtrsim 400$ GeV). Despite their large production cross sections, these events are challenging to detect because the jets
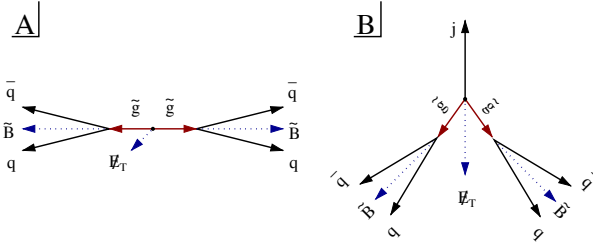
Fig. 9.1. Boosted gluinos that are degenerate with the bino do not enhance the missing transverse energy when there is no hard initial- or final-state radiation. (A) illustrates the cancellation of the bino's $\not{E}_T$. (B) shows how initial- or final-state radiation leads to a large amount of $\not{E}_T$ even if the gluino is degenerate with the bino.

from the decay are soft, with modest amounts of missing transverse energy. Even if the gluinos are strongly boosted, the sum of the bino momenta will approximately cancel when reconstructing the missing transverse energy (Fig. 9.1A). To discover a gluino degenerate with a bino, it is necessary to look at events where the gluino pair is boosted by the emission of hard QCD jets (Fig.9.1B). Therefore, initial-state radiation (ISR) and final-state radiation (FSR) must be properly accounted for.

The correct inclusion of ISR/FSR with parton showering requires generating gluino events with matrix elements. Currently, only Mad-Graph/MadEvent [9] is capable of computing processes of the form

$$p\bar{p} \to \tilde{g}\tilde{g} + Nj, \tag{9.1}$$

where N is the multiplicity of QCD jets. The decay of the gluinos into a bino plus a quark and an antiquark, as well as parton showering and hadronization of the final-state partons, was done in PYTHIA 6.4 [10].

To ensure that no double counting of events occurs between the matrix-element multi-parton events and the parton showers, a version of the MLM matching procedure was used [11]. In this procedure, the matrix element multi-parton events and the parton showers are constrained to occupy different kinematical regions, separated using the $k_\perp$ jet measure:

$$d^2(i,j) = \Delta R_{ij}^2 \min(p_{Ti}^2, p_{Tj}^2)$$
$$d^2(i,\text{beam}) = p_{Ti}^2, \tag{9.2}$$

where $\Delta R_{ij}^2 = 2(\cosh \Delta\eta - \cos \Delta\phi)$ [12]. Matrix-element events are generated with some minimum cut-off $d(i,j) = Q_{\min}^{\mathrm{ME}}$. After showering, the partons are clustered into jets using the k_T jet algorithm with a $Q_{\min}^{\mathrm{PS}} > Q_{\min}^{\mathrm{ME}}$.

The event is then discarded unless all resulting jets are matched to partons in the matrix-element event, $d(\text{parton}, \text{jet}) < Q_{\min}^{\text{PS}}$. For events from the highest multiplicity sample, extra jets softer than the softest matrix-element parton are allowed. This procedure avoids double-counting jets, and results in continuous and smooth differential distributions for all jet observables.

The matching parameters ($Q_{\min}^{\text{ME}}$ and $Q_{\min}^{\text{PS}}$) should be chosen resonably far below the factorization scale of the process. For gluino production, the parameters were:

$$Q_{\min}^{\text{ME}} = 20 \text{ GeV and } Q_{\min}^{\text{PS}} = 30 \text{ GeV.} \qquad (9.3)$$

The simulations were done using the CTEQ6L1 PDF [13] and with the renormalization and factorization scales set to the gluino mass. The matched cross sections were rescaled to the next-to-leading-order (NLO) cross sections obtained using Prospino 2.0 [14].

Finally, we used PGS [15] for detector simulation, with a cone jet algorithm with $\Delta R = 0.5$. As a check on this procedure, we compared our results to the signal point given in [6] and found that they agreed to within 10%.

9.2.2. Backgrounds

The three dominant Standard Model backgrounds that contribute to the jets plus missing energy searches are: $W^{\pm}/Z^0$ + jets, $t\bar{t}$, and QCD. There are several smaller sources of missing energy that include single top and di-boson production, but these make up a very small fraction of the background and are not included in this study.

The $W^{\pm}/Z^0 + nj$ and $t\bar{t}$ backgrounds were generated using Mad-Graph/MadEvent and then showered and hadronized using PYTHIA. PGS was used to reconstruct the jets. MLM matching was applied up to three jets for the $W^{\pm}/Z^0$ background, with the parameters $Q_{\min}^{\text{ME}} = 10$ GeV and $Q_{\min}^{\text{PS}} = 15$ GeV. The top background was matched up to two jets with $Q_{\min}^{\text{ME}} = 14$ GeV and $Q_{\min}^{\text{PS}} = 20$ GeV. Events containing isolated leptons with $p_T \geq 10$ GeV were vetoed to reduce background contributions from leptonically decaying $W^{\pm}$ bosons. To reject cases of $\not{E}_T$ from jet energy mismeasurement, a lower bound of $90°$ and $50°$ was placed on the azimuthal angle between $\not{E}_T$ and the first and second hardest jets, respectively. An acoplanarity cut of $< 165°$ was applied to the two hardest jets. Because the DØ analysis did not veto hadronically decaying tau leptons, all taus were treated as jets in this study.

In general, QCD backgrounds are incredibly hard to simulate and are beyond the scope of PYTHIA and PGS. The QCD background was not simulated in this work. However, to avoid the regions where hadronically produced missing energy becomes the dominant background, a lower limit of $\not{E}_T > 100$ GeV was imposed. Additionally, in the dijet analysis, the azimuthal angle between the $\not{E}_T$ and any jet with $p_T \geq 15$ GeV and $|\eta| \leq 2.5$ was bounded from below by $40°$. This cut was not placed on the three jet or multijet samples because of the large jet multiplicities in these cases.

For each of the $W^\pm/Z^0 + nj$ and $t\bar{t}$ backgrounds, 500K events were generated. The results reproduce the shape and scale of the $\not{E}_T$ and H_T distributions published by the DØ collaboration in [6] for 1fb^{-1}. For the dijet case, where the most statistics are available, the correspondence with the DØ result is $\pm 20\%$. The result is similar for the $t\bar{t}$ background for both the three jet and multijet cuts. The $W^\pm/Z^0 + nj$ backgrounds reproduce the DØ result to within $30 - 40\%$ for the three jet and multijet cases. The increased uncertainty may result from insufficient statistics to fully populate the tails of the $\not{E}_T$ and H_T distributions. PGS inefficiencies at losing a lepton may also contribute to the relative uncertainties for the $W^\pm + nj$ background. Heavy flavor jet contributions were found to contribute 2% to the $W^\pm/Z^0$ backgrounds and are well-below the uncertainties that arise from using PGS and not having NLO calculations for these processes.

9.3. Projected Reach of Searches

The goal of a model-independent gluino search is to have broad acceptance over a wide range of kinematical parameter space. The searches should be sensitive to cases where the gluino and bino are nearly degenerate, as well as cases where the gluino is far heavier than the bino. As already discussed, the number of jets and $\not{E}_T$ depend strongly on both $m_{\tilde{g}}$ and $m_{\tilde{g}} : m_{\tilde{B}}$. Because the signal changes dramatically as the masses of the gluino and bino are varied, it is necessary to design searches that are general, but not closely tied to the kinematics. We divided events into four mutually exclusive searches for $1j + \not{E}_T$, $2j + \not{E}_T$, $3j + \not{E}_T$, $4^+j + \not{E}_T$. For convenience, we keep the $nj + \not{E}_T$ classification fixed for all gluino and bino masses (see Table 9.1). These selection criteria were modeled after those used in DØ's existing search [6].[b] Ultimately, these exclusive searches can be statistically combined to provide stronger constraints.

---

[b]It should be noted, however, that the DØ searches are inclusive because each is designed to look for separate gluino/squark production modes (i.e., $pp \to \tilde{q}\tilde{q}$, $\tilde{q}\tilde{g}$, $\tilde{g}\tilde{g}$).

Table 9.1. Summary of the selection criteria for the four non-overlapping searches. The two hardest jets are required to be central ($|\eta| \leq 0.8$). All other jets must have $|\eta| \leq 2.5$.

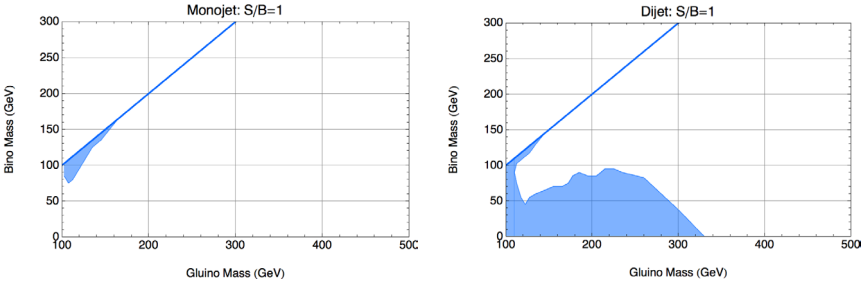|	$1j + \not{E}_T$	$2j + \not{E}_T$	$3j + \not{E}_T$	$4^+j + \not{E}_T$
E_{Tj_1}	≥ 150	≥ 35	≥ 35	≥ 35
E_{Tj_2}	< 35	≥ 35	≥ 35	≥ 35
E_{Tj_3}	< 35	< 35	≥ 35	≥ 35
E_{Tj_4}	< 20	< 20	< 20	≥ 20

Fig. 9.2. The sensitivity of DØ to gluinos degenerate with binos for monojet and dijet searches with $S/B > 1$. The monojet search has better reach, but quickly becomes ineffective when the gluino is not degenerate with the bino.

Two cuts are placed on each search: $H_T^{\min}$ and $\not{E}_T^{\min}$. In the DØ analysis, the H_T and $\not{E}_T$ cuts are constant for each search. The signal (as a function of the gluino and bino masses) and Standard Model background are very sensitive to these cuts. To maximize discovery potential, these two cuts should be optimized for all gluino and bino masses. For a given gluino and bino mass, the significance ($S/\sqrt{S+B}$) is maximized over $H_T^{\min}$ and $\not{E}_T^{\min}$ in each $nj + \not{E}_T$ search. Due to the uncertainty in the background calculations, the S/B was not allowed to drop beneath a minimal value. A conservative limit of $S/B > 1$ was placed and compared to the more aggressive lower limit of $S/B > 0.3$. The resulting 2σ sensitivity plot using the optimized H_T and $\not{E}_T$ cuts is shown in Fig. 9.4.

For light and degenerate gluinos, the $1j + \not{E}_T$ and $2j + \not{E}_T$ searches both have good sensitivity as shown in Fig. 9.2. There is an intermediate degeneracy where the $2j + \not{E}_T$, $3j + \not{E}_T$ and $4^+j + \not{E}_T$ all cover with some success, but there appears to be a coverage gap where no search does particularly well. If one does not impose a S/B requirement, a lot of the gap can be covered, but we feel that our background calculations are not sufficient to probe small S/B. For massive, non-degenerate gluinos, the $3j + \not{E}_T$ and
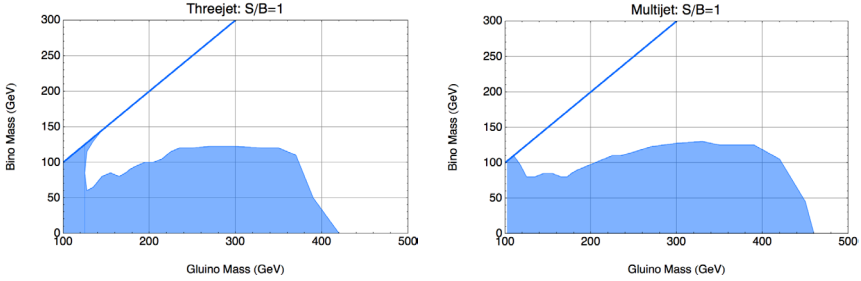
Fig. 9.3.   The sensitivity of DØ to gluinos non-degenerate with binos for the three and four jet searches with $S/B > 1$. The four jet search has better reach at high masses.

$4^+ j + \not{E}_T$ both give good sensitivity, with the $4^+ j + \not{E}_T$ giving slightly more statistical significance as shown in Fig. 9.3.

In the exclusion plot, the $\not{E}_T$ and H_T cuts were optimized for each point in gluino-bino parameter space. However, we found that the exclusion region does not markedly change if the following set of generic cuts are placed for 200 GeV $\lesssim m_{\tilde{g}} \lesssim$ 350 GeV:

$$(H_T, \not{E}_T) \geq (150, 100)_{1j + \not{E}_T}, (150, 100)_{2j + \not{E}_T},$$
$$(150, 100)_{3j + \not{E}_T}, (200, 100)_{4^+ j + \not{E}_T}. \qquad (9.4)$$

As a comparison, the cuts used in the DØ analysis are

$$(H_T, \not{E}_T) \geq (150, 150)_{1j + \not{E}_T}, (300, 225)_{2j + \not{E}_T},$$
$$(400, 150)_{3j + \not{E}_T}, (300, 100)_{4^+ j + \not{E}_T}. \qquad (9.5)$$

The lowered cuts provide better coverage for intermediate mass gluinos, as indicated in Fig. 9.4. For larger gluino masses, the generic cuts are no longer effective and it is necessary to use the optimized cuts, which are tighter than DØ's. While DØ technically has statistical significance in this high-mass region with their existing cuts, their signal-to-background ratio is less than unity. With the admitted difficulties in calculating the Standard Model backgrounds, setting exclusions with a low signal-to-background shouldn't be done and fortunately can be avoided by tightening the H_T and $\not{E}_T$ cuts. A similar phenomenon occurs in the degenerate gluino-bino region; again, tightening the monojet cuts increases the sensitivity.

9.4. Implications for the LHC

The philosophy of this proposed search can be carried over to the LHC. Since jets and missing energy are a particularly difficult channels to search
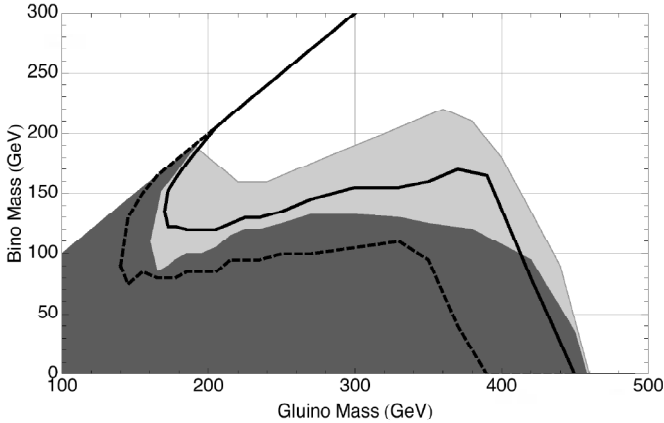
Fig. 9.4. The 95% sensitivity of DØ to discover gluinos. The dark gray region corresponds to $S/B > 1$, while the light gray shows the reach for $S/B > 0.3$. The dashed and solid lines show the corresponding exclusion regions using DØ's non-optimized H_T and $\not{E}_T$ cuts.

in, early on, this channel will not be competitive with many other searches that use leptons. Therefore, by the time that these searches are being considered, there may be big hints as to where to search for the new physics. However, even in the absence of spectacular new signals, these jets plus missing energy searches will become even more important because these signals are arguably the largest channels for producing new physics.

At the LHC, there are potentially some significant differences from the Tevatron case. First, the LHC will increase the center of mass energy from 2 TeV to 14 TeV. This has important implications for the relevant backgrounds. The QCD background that is poorly understood partially arises due to neutrinos in semi-leptonic decays and jet mismeasurement. Semi-leptonic decays are less important at high energies because the fragmentation of heavy quarks becomes softer, meaning that the fraction of the jet energy that the neutrino can carry off decreases. The both CMS and ATLAS have significantly better calorimetry than either CDF or DØ, and this leads to the hope that missing energy from jet mismeasurement will be proportionately better than at current detectors. This leads to the hope that the amount of missing energy arising from physics that is not electroweak or top will be not be significantly more difficult than at the Tevatron.

The backgrounds from pair produced top will be the most challenging to calibrate. Already at the Tevatron, in the four jets plus missing energy

channel, the top background is dominant and the effects from radiation from additional jets is visible. It may be necessarily to increase the missing energy cuts significantly to reduce top backgrounds to manageable levels. For reference, the top cross section at the Tevatron is 7 pb while at the LHC it is expected to be 1000 pb, an increase by over two orders of magnitude.

Weak vector bosons will be an important background to jets plus missing energy. The increase of energy will lead to a dramatic increase in the cross section to produce multiple hard jets in addition to a weak vector boson. For instance, with a jet definition of $E_T \geq 20$ GeV, the cross section for $W^{\pm} + 1j$ will increase by about one order of magnitude, while the cross section for $W^{\pm} + 4j$ will increase by over two two orders of magnitude. The spectrum for the hard jets falls off rapidly in E_T, and by raising the definition of jets from 35 GeV at the Tevatron, to 70 GeV or higher will most likely be necessary. This raising of the jet threshold is not without cost since compressed spectra will have fewer numbers of jets, and thus having larger backgrounds to contend with.

Finally there will be backgrounds that were subdominant at the Tevatron that will become more important at the LHC. One of these is di-boson production plus jets. Another is single top production which was first measured at the Tevatron and will become an important background. There are also new processes that could be important if the new physics have a modest cross section. One such background is four top production that has 100 fb.

The general strategy of cut-based searches should still be possible where one defines the different $nj + \not{E}_T$ samplees and place optimized H_T and $\not{E}_T$ cuts. It might be possible gain in the sensitivity by considering multiple jet energy definitions there could be additional power to discriminate signal from background.

9.5. Conclusions and Outlook

In this chapter, we describe the sensitivity that DØ has in searching for gluinos away from the CMSSM hypothesis in jets + $\not{E}_T$ searches. It was assumed that the gluino only decayed to two jets and a stable bino. However, many variants of this decay are possible and the search presented here can be generalized accordingly.

One might, for example, consider the case where the gluino decays dominantly to bottom quarks and heavy flavor tagging can be used advantageously. Cascade decays are another important possibility. Decay chains

have a significant effect upon the searches because they convert missing energy into visible energy. In this case, additional parameters, such as the intermediate particle masses and the relevant branching ratios, must be considered. In the CMSSM, the branching ratio of the gluino into the wino is roughly 80%. While this cascade decay may be representative of many models that have gluino-like objects, the fixed mass ratio and branching ratio are again artifacts of the CMSSM. A more thorough examination of cascade decays should be considered.

In addition to alternate decay routes for the gluino, alternate production modes are important when there are additional particles that are kinematically accessible. In this chapter, it was assumed that the squarks are kinematically inaccessible at the Tevatron; however, if the squarks are accessible, $\tilde{g}\tilde{q}$ and $\tilde{q}\tilde{q}$ production channels could lead to additional discovery possibilities. For instance, a gluino that is degenerate with the bino could be produced with a significantly heavier squark. The squark's subsequent cascade decay to the bino will produce a great deal of visible energy in the event and may be more visible than gluino pair production.[c]

Ultimately, a model-independent search for jets plus missing energy would be ideal. We believe that our exclusive $nj + \not{E}_T$ searches, with results presented in an exclusion plot as a function of H_T and $\not{E}_T$, would provide significant coverage for all of these alternate channels. This analysis should be carried forward to the LHC to ensure that the searches discover all possible supersymmetric spectra. The general philosophy of parameterizing the kinematics of the decay can be easily carried over. The main changes are in redefining the H_T and $\not{E}_T$ cuts, as well as the definition for the hard jet energy scale. We expect a similar shape to the sensitivity curve seen in Fig. 9.4, but at higher values for the gluino and bino masses. This means that it is unlikely that there will be a gap in gluino-bino masses where neither the Tevatron or the LHC have sensitivity.

Acknowledgments

---

[c]We thank M. Ibe and R. Harnik for this observation.

References

[1] S. Dimopoulos and H. Georgi, Softly Broken Supersymmetry and SU(5), *Nucl. Phys.* **B193**, 150, (1981).

[2] T. Appelquist, H.-C. Cheng, and B. A. Dobrescu, Bounds on universal extra dimensions, *Phys. Rev.* **D64**, 035002, (2001).

[3] L. Randall and R. Sundrum, A large mass hierarchy from a small extra dimension, *Phys. Rev. Lett.* **83**, 3370–3373, (1999).

[4] N. Arkani-Hamed et al., The minimal moose for a little Higgs, *JHEP.* **08**, 021, (2002).

[5] X. Portell, Searches for squarks and gluinos at CDF and D0 detectors, *AIP Conf. Proc.* **842**, 640–642, (2006).

[6] V. M. Abazov et al., Search for squarks and gluinos in events with jets and missing transverse energy using 2.1 fb-1 of ppbar collision data at sqrt(s)=1.96 TeV. (2007).

[7] A. Abulencia et al., Search for Gluino and Squark Production in Multijets Plus Missing ET Final States, *CDF Note.* **9093**, (2007).

[8] A. Abulencia et al., Search for large extra dimensions in the production of jets and missing transverse energy in p anti-p collisions at s**(1/2) = 1.96-TeV, *Phys. Rev. Lett.* **97**, 171802, (2006).

[9] J. Alwall et al., MadGraph/MadEvent v4: The New Web Generation, *JHEP.* **09**, 028, (2007).

[10] T. Sjostrand, S. Mrenna, and P. Skands, PYTHIA 6.4 physics and manual, *JHEP.* **05**, 026, (2006).

[11] J. Alwall et al., Comparative study of various algorithms for the merging of parton showers and matrix elements in hadronic collisions, *Eur. Phys. J.* **C53**, 473–500, (2008).

[12] S. Catani, Y. L. Dokshitzer, M. H. Seymour, and B. R. Webber, Longitudinally Invariant K(T) Clustering Algorithms For Hadron Hadron Collisions, *Nucl. Phys.* **B406**, 187, (1993).

[13] J. Pumplin et al., New generation of parton distributions with uncertainties from global QCD analysis, *JHEP.* **07**, 012, (2002).

[14] W. Beenakker, R. Hopker, M. Spira, and P. M. Zerwas, Squark and gluino production at hadron colliders, *Nucl. Phys.* **B492**, 51–103, (1997).

[15] J. Conway, PGS: Pretty Good Simulator.

Chapter 10

Naturally Speaking: The Naturalness Criterion and Physics at the LHC

Gian Francesco Giudice

Theoretical Physics Division, CERN
CH-1211 Geneva 23, Switzerland

10.1. Naturalness in Scientific Thought

> *Everything is natural: if it weren't, it wouldn't be.*
> Mary Catherine Bateson [1]

Almost every branch of science has its own version of the "naturalness criterion." In environmental sciences, it refers to the degree to which an area is pristine, free from human influence, and characterized by native species [2]. In mathematics, its meaning is associated with the intuitiveness of certain fundamental concepts, viewed as an intrinsic part of our thinking [3]. One can find the use of naturalness criterions in computer science (as a measure of adaptability), in agriculture (as an acceptable level of product manipulation), in linguistics (as translation quality assessment of sentences that do not reflect the natural and idiomatic forms of the receptor language). But certainly nowhere else but in particle physics has the mutable concept of naturalness taken a form which has become so influential in the development of the field.

The role of naturalness in the sense of "æsthetic beauty" is a powerful guiding principle for physicists as they try to construct new theories. This may appear surprising since the final product is often a mathematically sophisticated theory based on deep fundamental principles, and one could believe that subjective æsthetic arguments have no place in it. Nevertheless, this is not true and often theoretical physicists formulate their theories inspired by criteria of simplicity and beauty, i.e. by what Nelson [4] defines as "structural naturalness." When Einstein was asked what he would

have done, had Eddington's observation of the 1919 solar eclipse disproved, rather than confirmed, his theory, he simply replied: *"Then I would have felt sorry for the dear Lord"* [5]. Clearly he was confident that the structural naturalness of general relativity was no frippery.

Structural naturalness is a powerful inspirational principle but, of course, it cannot be used to validate a theory. Moreover, since it is subjected to philosophical influences and to the limited scientific knowledge of the time, sometimes it can even be misleading. From a modern point of view, the solar system is more *naturally* explained by a heliocentric theory, in which planetary motions are described by simple elliptic orbits, rather than by a geocentric theory, which requires the introduction of different epicycles for each planet. But to predecessors and contemporaries of Copernicus a geocentric theory probably appeared more *natural*. Tycho Brahe discarded a heliocentric description of the solar system with the harsh, but rather unconvincing, argument that the Earth is a *"hulking, lazy body, unfit for motion"* [6]. Certainly Aristotelian and biblical influences had their part in forming this belief, but a big role was played by the incorrect scientific notion that we would be able to feel the Earth moving under our feet.

Aristarchus of Samos was the first to postulate that the Sun was at the center of the universe, but the ancient Greeks ruled out the heliocentric model based on the following "naturalness" argument. Assuming proportionality between the period and the radius of planetary orbits, they obtained that Saturn is 29 times as far from the Sun than the Earth, since the period of Saturn was known to be 29 years. Using trigonometry and some astronomical observations, Aristarchus obtained the Sun-Earth distance expressed in terms of the Earth radius $R_\oplus$ previously deduced by Erathostenes with his famous measurement of the inclination of the solar rays in Alexandria when the Sun was at zenith in Syene. This placed Saturn at a distance of 20,000 $R_\oplus$ from the Earth[a] [7]. Since Saturn was the outermost known planet, it was *natural* to assume that the universe was about the same size. But if the Earth orbits around the Sun, we should observe a parallax effect for stars on a celestial sphere of radius 20,000 $R_\oplus$. No stellar parallax could be observed with naked eye (for Alpha Centauri, the closest star, the parallax angle is actually only about one second of arc), and the heliocentric model was rejected. Copernicus dispensed with the parallax objection by refuting the *natural* assumption about stellar distances and required that stars be at least 1,500,000 $R_\oplus$ away from us.

---

[a]The modern value of the minimum distance between Saturn and Earth is 1.9×10^5 $R_\oplus$.

Structural naturalness, because of its subjective character, cannot be quantitatively defined. It is related to what the 1936 medicine Nobel laureate Henry Dale defines as *"the subconscious reasoning which we call instinctive judgement"* [8]. A more precise form of naturalness criterion has been developed in particle physics and it is playing a fundamental role in the formulation of theoretical predictions for new phenomena to be observed at the LHC. This criterion, called "numerical naturalness" by Nelson [4], will be the subject of this essay.

10.2. Drowning by Numbers

> *I am ill at these numbers.*
> William Shakespeare [9]

Our story starts with the observation that the ratio between the Fermi constant G_F and the Newton constant G_N, which characterize respectively the strengths of the weak and gravitational forces, is a very large number[b] [10]

$$\frac{G_F \hbar^2}{G_N c^2} = 1.738\ 59(15) \times 10^{33}. \tag{10.1}$$

The powers of the Planck constant $\hbar$ and of the speed of light c have been introduced in Eq. (10.1) to express the ratio as a pure number.

The human mind has always held in special fascination the pure numbers. Pythagoras went as far as believing that numbers are not just useful tools to describe the properties of nature but rather have special attributes that cause the various qualities of matter. Philolaus, a Pythagorean contemporary of Socrates and Democritus, expressed the idea that five is the cause of color, six of cold, seven of health, eight of love [11]. These mystic properties of numbers are summarized in the motto of the Pythagorean school: *"All is number."*

In a modern context, some numerical constants that appear in equations describing the fundamental laws of physics have often been the object of keen speculation. Sometimes these speculations are mere numerological exercises, but occasionally they are rewarded by a true understanding of deeper physical laws. When in 1885 Balmer first derived [12] a simple formula fitting the data for the frequencies ν of the hydrogen spectral lines

$$\nu = R \left(\frac{1}{n^2} - \frac{1}{m^2} \right) \quad \text{with } m > n \text{ integers}, \tag{10.2}$$

---

[b]The figures in parenthesis give the one standard-deviation uncertainty in the last digits.

he expressed bewilderment for *"agreement which must surprise to the highest degree"* [13], but little did he suspect that Bohr's quantum interpretation [14] was lurking behind it.

There are, however, less fortunate examples. From the very early times of electromagnetism and quantum mechanics, it was immediately recognized the special role of the fine-structure constant α, a pure number constructed out of several fundamental quantities [10]

$$\alpha^{-1} = \frac{4\pi\epsilon_0 \hbar c}{e^2} = 137.035\ 999\ 11(46). \qquad (10.3)$$

Given its importance, there has been no lack of attempts to "derive" α with simple numerical expressions. Early measurements were not even incompatible with the belief that α^{-1} must be an integer [15]. The hope was that finding the right formula for α would have opened the door towards a new theory underlying quantum electrodynamics, and curiously accurate expressions are, among many, $\alpha^{-1} = (8\pi^4/9)(2^4 5!/\pi^5)^{1/4}$ [16], $\alpha^{-1} = 108\pi(8/1843)^{1/6}$ [17], $\alpha^{-1} = 2^{-19/4}3^{10/3}5^{17/4}\pi^{-2}$ [18], $\alpha^{-1} = (137^2 + \pi^2)^{1/2}$ [19]. Even Heisenberg apparently took part in the game, with a less accurate try, $\alpha^{-1} = 2^4 3^3/\pi$ [20]. But, alas, these attempts are not particularly illuminating. Actually, a conceptual derivation of the fine-structure constant can be done in the context of grand unification, but the formula for α is certainly no easy guess for amateur numerologists.[c]

The reason why speculating on the values of the fundamental constants may be meaningful is the reductionist belief in the existence of an underlying theory in which all dimensionless parameters are determined and computable. Einstein was firmly convinced that all forces must have an ultimate unified description and he even speculated on the uniqueness of this fundamental theory, whose parameters are fixed in the only possible consistent way, with no deformations allowed: *"What really interests me is whether God had any choice in the creation of the world; that is, whether the necessity of logical simplicity leaves any freedom at all"* [21]. This reductionist belief has enjoyed a spectacular success during the last century, bringing physics from the state of disconnected subjects (mechanics, optics, electro-

[c]The formula is

$$\alpha = \alpha_s \frac{\sin^2 \theta_W (b_1 - b_3) + \frac{3}{5}\cos^2 \theta_W (b_3 - b_2)}{(b_1 - b_2)} + \text{higher-order terms.}$$

Here, the fine-structure constant α, the strong coupling constant α_s and the weak mixing angle θ_W are evaluated at the same renormalization scale and $b_{1,2,3}$ are the gauge β-function coefficients. Higher-order terms cannot be neglected to achieve a prediction that matches the experimental accuracy.

magnetism, thermodynamics, etc.) into the unified description of the Standard Model which, with a handful of free parameters, can accurately predict the properties of matter from distances down to about 10^{-16} cm to the conditions of the universe one second after the big bang. Nevertheless, it is this handful of free parameters which still escapes our understanding, preventing the fulfillment of Einstein's program. The determination of the ratio between Fermi and Newton constants in Eq. (10.1) is part of this puzzle.

The striking feature of the ratio in Eq. (10.1) is that its numerical value is huge. If the free parameters of the elementary-particle Standard Model are ultimately derived from a more fundamental theory, they may carry information about deeper laws of physics. What we observe as constants of order unity in the Standard Model could have a well-defined mathematical expression, in the more fundamental theory, containing numbers like 2, π or the like.[d] On the other hand, if the constant is measured to be equal to a very large number, its ultimate expression cannot be a simple combination of 2's and π's and we are inclined to think that some important properties of the final theory can be learnt from its value.

The lure of very large numbers is especially addicting. Eddington was stricken by the thought that the number of protons (equal to the number of electrons) in the universe, which he computed [22] to be equal to something like 10^{80}, must be an exact *integer* number N_E. He was convinced that N_E was not an accidental peculiarity of our universe, but rather a fundamental constant of nature. From this he deduced that the gravitational force between an electron and a proton ($G_N m_e m_p / r^2$) in a system of N_E particles is given by the statistical fluctuation ($\sqrt{N_E}$) of the electric force between the two particles (e^2/r^2) and therefore [23]

$$\frac{e^2}{G_N m_e m_p} = \sqrt{N_E}. \tag{10.4}$$

For $N_E = 10^{80}$, this well agrees with the measured value $e^2/G_N m_e m_p = 2.85 \times 10^{40}$. To modern readers (and actually to many of his contemporaries as well) this argument has too much of a kabbalistic flavor. Nevertheless, it inspired Dirac to make his Large Number Hypothesis [24]. Any very large number occurring in nature should be simply related to a single very large number, which he chose to be the age of the universe. Indeed, he constructed three dimensionless numbers which all happen to be very close to 10^{40}: the ratio of the size of the observable universe to the electron radius, the ratio of electromagnetic-to-gravitational force between protons

---

[d]My considerations here refer only to constants which are given by pure numbers; dimensionful constants define the units of measure.

and electrons, and the square root of the number of protons in the observable universe. To satisfy the Large Number Hypothesis, the ratio between any of these three numbers should remain roughly constant during the expansion of the universe. This can be achieved only if some fundamental constants vary with time, in order to maintain the proportionality of the three numbers. From this Dirac argued that the Newton constant G_N should vary during the evolution of the universe, and he predicted its time dependence. This startling result and the fact that Dirac's paper was written during his honeymoon prompted Bohr's remark: *"Look what happens to people when they get married!"* [25]. Indeed, Dirac's prediction was not very successful. His modification of gravity in the past would have changed the energy output of the Sun such that the oceans would have boiled in the pre-Cambrian era, while in fact life developed on Earth much earlier [26].

One lesson that we can learn from Dirac's hypothesis is that the existence of large numbers in nature may have nothing to do with the properties of the fundamental theory, but rather are the result of the cosmological history of our universe. Actually, as was first pointed out by Dicke [27], the largeness of the three numbers examined by Dirac has a very simple explanation, which does not require any time-varying Newton constant. In order to reach the biochemical complexity that we observe on Earth, it is necessary for the universe to produce carbon, nitrogen, oxygen and other heavy elements which are synthesized in main-sequence stellar evolution and then dispersed throughout space by supernova explosions. An estimate of the time required by these processes, together with the information that the universe expands, shows that the three numbers considered by Dirac should indeed be at least as large as we observe them. Actually, they couldn't be much larger either, because otherwise hydrogen-burning stars, like our Sun, would have all burnt out. This means that we should have expressed surprise if Dirac's numbers had turned out to be of order one or much bigger than what they are, but their actual values lie indeed in the most reasonable range. A vast and old universe is an inevitable consequence of having observers like us. It is just a matter of the observer's point of view: although on Earth the Chinese are a million times more common than Mount Athos' inhabitants, if you happen to wonder around the Greek peninsula's monasteries, you will not be surprised to know that you have a much larger probability to encounter an orthodox monk rather than a Chinese person. In short, Dirac's problem appears as a red herring.

Can it be that also the G_F/G_N ratio in Eq. (10.1) is large because of cosmological evolution or because of statistical probability, but carries no

information whatsoever of the theory beyond the Standard Model? I will come back to this question later, but for the moment it is more urgent to understand why the largeness of the number in Eq. (10.1) has anything to do with collider experiments at the LHC.

10.3. A Quantum Complication

> *Anyone who is not shocked by quantum*
> *theory has not understood a single word.*
> Niels Bohr [28]

The really problematic aspect about the G_F/G_N ratio in Eq. (10.1) comes about when we consider the effects of quantum mechanics. In a quantum theory, the vacuum is a very busy place. Particle-antiparticle pairs are constantly produced out of nothing, violating the energy-conservation law by borrowing an amount of energy E from the vacuum for a time t such that $E\,t < \hbar$, according to Heisenberg's uncertainty principle. These "virtual" particles created from the vacuum have the same quantum numbers and properties as ordinary particles, with the exception that their energy-momentum relation is unusual ($E^2 - p^2 \neq m^2$). In the Standard Model, the size of G_F is determined (up to coefficients which are unimportant for our discussion) by the mass of the Higgs boson m_H, according to the relation $G_F \sim m_H^{-2}$. As the Higgs boson propagates in the quantum vacuum, it feels the presence of virtual particles and interacts with them. A characteristic property of the Higgs boson is to interact with any Standard Model particle with a strength proportional to the corresponding particle mass. Indeed, as Lenin once explained, *"The Higgs mechanism is just a reincarnation of the Communist Party: it controls the masses"* [29]. When virtual particles appear in the vacuum, they interact with the Higgs boson with an effective strength determined by the available energy E. Because of quantum corrections, the motion of the Higgs boson in the vacuum populated by virtual particles is affected by an amount proportional to E. As a result, the Higgs-boson squared mass m_H^2 receives an additional contribution

$$\delta m_H^2 = \kappa \Lambda^2, \tag{10.5}$$

where Λ is the maximum energy E accessible to virtual particles and κ is a proportionality constant, which is typically[e] in the range of 10^{-2}.

---

[e]The contribution to κ coming from virtual particles with the quantum numbers of the Standard Model degrees of freedom will be given in Sec. 10.6, see Eq. (10.9). It amounts to $\kappa = 3 \times 10^{-2}$.

A simple analogy can help us understand the result in Eq. (10.5). Let us replace the quantum fluctuations of the vacuum with the more familiar thermal fluctuations of a thermodynamic system of a large number of particles at a temperature T. The particles (which I will call P) in this thermal bath play the role of the virtual particles in the quantum vacuum, and T the role of the maximum available energy Λ. Let us now insert inside the box containing this hot P-particle gas a different particle initially at rest. I will call it H, as it plays the role of the Higgs in my analogy. At some initial time, H has zero velocity and therefore its energy is equal to its mass, which I take it to be much smaller than the temperature ($E_H = m_H \ll T$). However, by statistical-mechanics arguments, we expect that the collisions of the particles P will soon bring H in thermal equilibrium, and therefore its energy will quickly become of order T. This is very similar to what happens in the quantum system, where the Higgs mass is pushed towards Λ, because of quantum-fluctuation effects.

The disturbing aspect of Eq. (10.5) is that it predicts that the Higgs mass m_H ($\sim G_F^{-1/2}$) should be close to the maximum energy allowed by the theory. If the maximum energy is equal to the Planck mass $M_{\rm Pl}$ ($= G_N^{-1/2}$), we find that the ratio G_F/G_N is predicted to be rather close to unity, in strong contradiction with the measured value of 10^{33}, see Eq. (10.1).

One possible way out of the puzzle introduced by Eq. (10.5) is to assume that, once we include all quantum effects, the coefficient κ in Eq. (10.5) is incredibly smaller than its typical value of 10^{-2}. This requires a very precise cancellation of the different contributions to m_H coming from different virtual particles at different energy scales. For instance, if we take $\Lambda = M_{\rm Pl}$, the cancellation in κ must be one part in 10^{32}. This could occur just accidentally, as a result of the particular values chosen by nature for all the numerical constants entering in particle physics. But a purely fortuitous cancellation at the level of 10^{32}, although not logically excluded, appears to us as disturbingly contrived. This is not what Einstein had in mind when he imagined a theory in which logical simplicity leaves no freedom at all.

Just to get a feeling of the level of parameter tuning required, let me make a simple analogy. Balancing on a table a pencil on its tip is a subtle art that requires patience and a steady hand. It is a matter of fine tuning the position of the pencil such that its center of mass falls within the surface of its tip. If R is the length of the pencil and r the radius of the tip surface, the needed accuracy is of the order of r^2/R^2. Let us now compare this with the fine tuning in κ. The necessary accuracy to reproduce G_F/G_N is equal

to the accuracy needed to balance a pencil as long as the solar system on a tip a millimeter wide!

This has led to a widespread belief among particle physicists that such an apparently fantastic coincidence must have some hidden reason. If we do not appeal to any special cancellation and fix κ to its expected value of 10^{-2}, then we can use Eq. (10.5) to extract the maximum energy up to which we can extrapolate our present knowledge of particle physics, and we find $\Lambda \approx$ TeV. Beyond the TeV a new theory should set in, modifying the Higgs mass sensitivity to quantum corrections. The LHC experiments, by studying particle collisions at energies above the TeV, will explore this new energy regime and will be able to tell us if the Standard Model is replaced by a new theory.

10.4. The Naturalness Criterion as a Principle

> *I have never lived on principles.*
> Otto von Bismark

We are now ready to formulate the naturalness criterion. Let us consider a theory valid up to a maximum energy Λ and make all its parameters dimensionless by measuring them in units[f] of Λ. The naturalness criterion states that one such parameter is allowed to be much smaller than unity only if setting it to zero increases the symmetry of the theory [30]. If this does not happen, the theory is unnatural.

There are two fundamental concepts that enter this formulation of the naturalness criterion: symmetry and effective theories. Both concepts have played a pivotal role in the reductionist approach that has successfully led to the understanding of fundamental forces through the Standard Model.

In modern physics, symmetries are viewed as fundamental requirements that dictate physical laws. If a parameter of the theory is equal to zero because of a symmetry, it will remain zero even after we have included all quantum corrections.[g] This is why a small parameter is not necessarily problematic, if it is "protected" by a symmetry according to the naturalness criterion stated above.

In the Standard Model there is no symmetry protecting the Higgs mass and this is the basic cause of the large quantum corrections in Eq. (10.5)

---

[f]Here I am following the usual convention of setting $\hbar = c = 1$.
[g]Anomalous symmetries are exceptions to this rule, but they are not relevant to our discussion.

that bring m_H close to Λ. The absence of a symmetry protecting m_H is linked to the spin-zero nature of the Higgs boson, as can be understood by a simple argument. Massless particles of spin 1/2 or higher have two degrees of freedom. Massive particles of spin[h] 1/2 or higher have more than two degrees of freedom.[i] Therefore there is a conceptual distinction between the massless and massive cases. This distinction is due to the presence of an extra symmetry in the massless theory (gauge symmetry for spin 1, chiral symmetry for spin 1/2). The symmetry allows us to eliminate some degrees of freedom from the massless theory. This argument is valid for any particle with spin 1/2 or higher, but not for spin 0. There exist special symmetries able to protect spin-0 masses (non-linearly realized symmetries, supersymmetry) but they are not present in the Standard Model. This is why the Higgs boson is viewed as "unnatural."

The second ingredient of the naturalness criterion is the use of effective field theories [31]. Effective field theories are an extremely powerful concept. The idea is that, in a quantum field theory, it is possible to compute any physical process involving particles with momenta smaller than a maximum scale Λ by replacing the original theory with a truncated version of it. This effective theory is expressed in terms of local operators that involve only light degrees of freedom. This means that the dynamics of low energies (large distances) can be fully described and computed by encoding the information of high energies (small distances) into a finite number of parameters. Effective field theories are a powerful realization of the reductionist approach. As we increase the distance scale, we increase the complexity of the system and new phenomena emerge. These phenomena are best described by an effective theory, for which knowledge of the full details of the underlying theory is unnecessary, but can be summarized in

---

[h]Spin-1/2 Majorana particles are an exception. However, the symmetry argument applies also to this case, since the Majorana mass term violates the associated fermion number.

[i]This difference between massless and massive particles can be intuitively understood. A photon has two polarizations, the transverse modes along the direction of motion. But for a massive spin-1 particle, we can go to a reference frame where the particle is at rest. In that frame, we cannot distinguish between transverse and longitudinal modes, and therefore rotational invariance requires the existence of three polarization states. An analogous argument is valid for the spin-1/2 case. A massless spin-1/2 particle has a definite chirality. However, for a massive particle, with a boost along the direction of motion we can go to a frame where the chirality is opposite. Therefore relativistic invariance requires the massive particle to possess both chirality states. The argument cannot be repeated for a spin-0 particle, because there is no direction intrinsically defined by the particle itself.

a finite number of parameters. These parameters can be experimentally measured or theoretically derived (and possibly both). The way thermodynamics can be derived from statistical mechanics is a good example of this reductive process.

The naturalness criterion, as stated above, excludes the possibility that the parameters that encode the information of physics at very short distances are correlated with dynamics of the effective theory occurring at large distances. Such a correlation would signal a breakdown of the philosophy underlying the effective-theory approach.[j] If the naturalness criterion is a good guiding principle, we expect to discover new particles at the LHC, associated to the taming of the Higgs-mass quantum corrections. If experiments at the LHC find no new phenomena linked to the TeV scale, the naturalness criterion would fail and the explanation of the hierarchy G_F/G_N would be beyond the reach of effective field theories.

10.5. An Account of Events

> *History is a set of lies agreed upon.*
> Napoléon Bonaparte

The concept of naturalness and its implications for electroweak physics did not spring from a single paper but, rather, they developed through a "collective motion" of the community which increasingly emphasized their relevance to the existence of physics beyond the Standard Model. I will give here a short account of how the naturalness criterion for the Higgs boson mass was developed by theoretical particle physicists.

Starting in 1976, the work by Gildener and Weinberg [33] revealed a conceptual difficulty with the recently discovered grand unified theories, the so-called hierarchy problem. One-loop quantum corrections were found to give contributions to the Higgs mass proportional to the mass of the superheavy states, of the order of $M_{GUT} = 10^{14-16}$ GeV. Keeping a hierarchical separation of scales between M_W and M_{GUT} required fine tuning the parameters of the theory of more than 10^{-24}. This is nothing less than a specific realization of the Higgs naturalness problem, in the presence of a theory with two widely separated scales. Even today some people find

---

[j]This would not mean that the effective-theory approach is useless. It would only mean that certain properties of the theory cannot be captured by low-energy arguments alone. The conjecture of gravity as the weakest force [32], if true, is one example of a theoretical property that cannot be derived using an effective-theory approach.

it easier to understand and to accept the naturalness problem in this context, since one makes no reference to cut-off (and regularization procedure) dependent quantities of the effective theory.[k]

In 1978, Susskind [35] introduced the naturalness problem of the Higgs as a primary motivation for his proposal of technicolor, giving however full credit to Wilson for pointing out the conceptual difficulty linked to the existence of fundamental scalar particles. Indeed, in an article written at the end of 1970, Wilson had clearly expressed the problem, from an effective-theory point of view: *"It is interesting to note that there are no weakly coupled scalar particles in nature; scalar particles are the only kind of free particles whose mass term does not break either an internal or a gauge symmetry. This discussion can be summarized by saying that mass or symmetry-breaking terms must be "protected" from large corrections at large momenta due to various interactions (electromagnetic, weak, or strong). A symmetry-breaking term h_λ is protected if, in the renormalization-group equation for h_λ, the right-hand side is proportional to h_λ or other small coupling constants even when high-order strong, electromagnetic, or weak corrections are taken into account [. . .]. This requirement means that weak interactions cannot be mediated by scalar particles"* [36]. He could not have been more explicit. Nevertheless, in 2004 Wilson completely retracted, while recalling the results he obtained in the early 1970's: *"The final blunder was a claim that scalar elementary particles were unlikely to occur in elementary particle physics at currently measurable energies [. . .]. This claim makes no sense"* [37].

The naturalness criterion, in the way I stated it in Sec. 10.4, was formulated by 't Hooft in lectures held in 1979 [30]. Actually a precursor of this criterion was Gell-Mann's totalitarian principle which states: *"Everything which is not forbidden is compulsory."*[l] It refers to the property, largely confirmed by experimental evidence, that every interaction term not explicitly forbidden by conservation laws must be present. Quantum corrections in an

---

[k]Shaposhnikov [34] concedes that there is a Higgs naturalness problem in presence of M_{GUT}, but he argues that in the absence of any new mass scale between the weak and the Planck scale the problem may not exist since, according to him, the Planck mass could be conceptually different from the field-theoretical ultraviolet cutoff of the effective low-energy theory.

[l]Although the totalitarian principle is indisputably attributed to Gell-Mann, I could not trace the original source. The earliest reference to it that I found is Ref. [38]. In the first version of this essay I stated that the totalitarian principle's expression is borrowed from "The Once and Future King" by T.H. White, published in 1958. I thank Stanley Deser who pointed out to me that the expression is actually coming from "Nineteen Eighty-Four" by G. Orwell, published in 1949.

effective theory appear to enforce the totalitarian principle by giving large contributions to parameters that are not forbidden by a symmetry.

Although by 1979 the Higgs-naturalness problem had been clearly spelled out, supersymmetry as a possible solution is only mentioned in some lectures held by Maiani in that year: *"In a supersymmetric theory, one could hope to obtain that the bare curvature of V_{eff} vanishes and it is not renormalized by radiative corrections [...] No concrete model of this type have been constructed yet"* [39]. Supersymmetric models were being developed for years, most notably by Fayet [40], but with no connection to the naturalness problem. Although the non-renormalization theorems had already been discovered, supersymmetry was seen more as a way to unify gravity and gauge forces [41], rather than a way to address the hierarchy problem. Probably many physicists did not attach great importance to the naturalness problem of the Higgs mass, simply because the Higgs model did not appear to be very compelling, as was expressed by Iliopoulos in the 1979 Einstein Symposium: *"Several people believe, and I share this view, that the Higgs scheme is a convenient parametrization of our ignorance concerning the dynamics of spontaneous symmetry breaking and elementary scalar particles do not exist"* [42].

Things changed by 1981. At the end of 1980 Veltman had published an influential paper emphasizing the problem [43]. In 1981 Witten clearly pointed out how supersymmetry can solve the naturalness problem and explained the crucial role of dynamical supersymmetry breaking [44]. About a month later Dimopoulos and Georgi [45], using the results of Girardello and Grisaru on soft supersymmetry breaking [46], developed a simple and realistic grand unified supersymmetric model. The age of supersymmetric model building had started and an explosion of activity followed. Since then, the Higgs naturalness problem has become one of the most studied puzzles in particle physics and one of the driving motivations to explore physics beyond the Standard Model.

10.6. The Paths Chosen by Nature

> *Can we actually know the universe?*
> *My God, it's hard enough finding*
> *your way around in Chinatown.*
> Woody Allen [47]

How does nature deal with the hierarchy between G_F and G_N? Does nature respect the naturalness criterion? Experiments at the LHC will be

able to shed some light on these questions. In the meantime, we can only use our imagination. Something useful can be learned by studying how nature deals with other problems, which have similar characteristics, but for which we already know the answer.

An interesting analogy was first suggested, to the best of my knowledge, by Murayama [48]. Consider the electron as a sphere of radius r. The electromagnetic energy associated with this configuration is α/r. This energy must be smaller than the total energy of the electron, equal to $m_e c^2$, where m_e is the electron mass. Therefore, we obtain

$$r > \frac{\alpha}{m_e} = 3 \times 10^{-15} \text{ m}. \tag{10.6}$$

In words, the electron radius has to be larger than an atomic nucleus! Things get even worse when we include the magnetic energy of a spinning sphere μ^2/r^3 (where $\mu = e\hbar/(2m_e c)$ is the electron magnetic moment), as done by Rasetti and Fermi [49], immediately after the discovery of the electron spin. In this case, one finds $r > \alpha^{1/3}/m_e$.

The puzzle is the following. Either the different contributions to the total electron energy mysteriously cancel with a high precision, or some new physics sets in before the energy scale $r^{-1} \sim m_e/\alpha$, modifying the electromagnetic contribution to the electron mass at short distances and preserving naturalness. In this example, nature has chosen the second option. Indeed Dirac showed that a new particle with mass m_e, the positron, has to be included in a consistent relativistic quantum theory. As explicitly calculated by Weisskopf [50], the electromagnetic contribution to the electron mass at small distances grows neither like $1/r$ nor like $1/r^3$, but rather like $\alpha\, m_e \ln(m_e r)$. This contribution is less than the electron mass even for distances r as small as the Planck length. In this case, nature has preferred to obey the naturalness criterion.

There are several other examples one can consider where physical quantities computed in the effective theory require either cancellations of contributions sensitive to the small-distance regime, or the appearance of new physics that restore naturalness. In many cases, nature has chosen to preserve naturalness and new particles at the appropriate energy scale modify the theory. For instance, the electromagnetic contribution to the charged to neutral pion mass difference is

$$M_{\pi^+}^2 - M_{\pi^0}^2 = \frac{3\alpha}{4\pi}\Lambda^2, \tag{10.7}$$

where Λ is the ultraviolet momentum cutoff, i.e. the maximum energy of the effective theory of pions. The request that Eq. (10.7) not exceed the measured quantity $M_{\pi^+}^2 - M_{\pi^0}^2 = (35.5 \text{ MeV})^2$, implies that Λ must be smaller than 850 MeV. Indeed, before that mass scale, the ρ meson exists ($M_\rho = 770$ MeV) and the composite structure of the pion softens the electromagnetic contribution.

Another example is the mixing between the K^0 and $\bar{K}^0$ mesons. The mass difference between the K_L^0 and K_S^0 states, as computed in an effective theory valid at energies of the order of the kaon mass, is given by

$$\frac{M_{K_L^0} - M_{K_S^0}}{M_{K_L^0}} = \frac{G_F^2 f_K^2}{6\pi^2} \; \sin^2 \theta_c \, \Lambda^2, \tag{10.8}$$

where $f_K = 114$ MeV is the kaon decay constant and $\sin \theta_c = 0.22$ is the Cabibbo angle. If we require that the result in Eq. (10.8) be smaller than the measured value $(M_{K_L^0} - M_{K_S^0})/M_{K_L^0} = 7 \times 10^{-15}$, we find $\Lambda < 2$ GeV. Indeed, before reaching this energy scale a new particle (the charm quark with mass $m_c \approx 1.2$ GeV) modifies the short-distance behavior of the theory, implementing the so-called GIM mechanism [51]. Incidentally, while the other two examples are *a posteriori* deductions, the case of K^0–$\bar{K}^0$ mixing is historically accurate: this is the actual argument used by Gaillard and Lee [52] to compute the mass of the charm quark before its discovery.

We can formulate the problem of the Higgs mass m_H in the same fashion. Using the Standard Model as an effective theory, we can compute the contributions to m_H due to Higgs interactions. The leading effect is

$$\delta m_H^2 = \frac{3 G_F}{4\sqrt{2}\pi^2} \left(4m_t^2 - 2m_W^2 - m_Z^2 - m_H^2 \right) \Lambda^2, \tag{10.9}$$

where m_t, m_W, m_Z are the masses of the top quark, W and Z gauge bosons, and Λ is the maximum momentum.[m] The request that the contribution in Eq. (10.9) be not larger than 182 GeV (the 95% CL limit from Standard Model fits of present experimental data [53]), implies $\Lambda < 1.0$ TeV. Only

---

[m]Naively one may think that the Higgs naturalness problem disappears for the special value of m_H that cancels the right-hand side of Eq. (10.9) (which happens to be about 200–300 GeV, depending on the value of the renormalization scale). Unfortunately this is not sufficient because Eq. (10.9) gives only the infrared contribution to m_H. Modes with masses of order Λ (outside the domain of the effective theory) give new contributions of the same size. For example, in a softly-broken supersymmetric theory, quadratic divergences are absent, but this is not sufficient to solve the hierarchy problem. It is also necessary that the masses of the new particles lie below the TeV scale.

the LHC will tell us if the naturalness criterion is successful in this case as well, and whether new particles exist with masses below the TeV.

Unfortunately not all examples are successful and there is one important case in which nature does not seem to respect the naturalness criterion. Astronomical observations place bounds on the energy density of the vacuum in our universe which constrain the scale of the cosmological constant to be less than 3×10^{-3} eV. Since quantum corrections to the cosmological constant grow with the maximum energy Λ, the naturalness criterion implies that our theoretical description of particle physics should start failing at an energy scale as low as 3×10^{-3} eV. We have good evidence that this is not the case. Nature could have chosen supersymmetry to deal with this problem in a *natural* way because the cosmological constant vanishes in supersymmetric theories. However, we already know that nature has decided not to take this opportunity, since supersymmetry is not an exact symmetry down to energies of 3×10^{-3} eV.

The issue is more involved, because the cosmological constant becomes a physical observable only when we include gravity, which can be usually ignored when dealing with particle physics processes. If a solution to the cosmological constant exists, it may involve some complicated interplay between infrared and ultraviolet effects (maybe in the context of quantum gravity) or it may just be linked to the cosmological history. At any rate, none of these solutions will be obtained by an effective field theory approach. But then, are we sure that this is not the case also for the Higgs mass? The verdict will be handed down by the LHC.

10.7. Measuring Naturalness

> *I used to measure the heavens,*
> *now I measure the shadows of earth.*
> Johannes Kepler [54]

As new particle physics theories were invented to cope with the naturalness problem of the Higgs mass, and as collider experiments started to set bounds on the existence of the new particles, there was a need to give a quantitative criterion for the degree of naturalness (or unnaturalness) of the new theories. A commonly adopted criterion [55] was to consider the expression of the Z boson mass (which is equivalent, up to constants of order unity, to m_H or to $G_F^{-1/2}$) as a function of the parameters a_i of the underlying theory. Indeed, such an expression should always exist,

since in the new theory the weak scale must be a "calculable" quantity (although calculable only in terms of unknown parameters). The measure of naturalness (or, more precisely, of the amount of fine-tuning) is given by the logarithmic variation of the function $M_Z(a_i)$ with respect to a_i,

$$\Delta \equiv \max \left| \frac{a_i}{M_Z^2} \frac{\partial M_Z^2(a_i)}{\partial a_i} \right|. \tag{10.10}$$

A theory with $\Delta = 10$ suffers from a parameter tuning of no more than 10%, one with $\Delta = 100$ of 1%, and so on.

For example, in the case of supersymmetry, the requirement of less than 10% tuning led to the prediction that supersymmetry had to be discovered at LEP2. This prediction turned out to be wrong. Indeed, today supersymmetric models pass the experimental tests only if their free parameters are tuned at the level of few percent. Actually this is essentially true for all known extensions of the Standard Model that address the Higgs mass problem. Of course, one can argue that the Sun and the Moon have radius and distance from the Earth "tuned" to appear equal in the sky (with a precision of about 5%), for no better reason than producing rare and spectacular eclipses (and permitting us to test general relativity). Even more dramatic numerical coincidences happen in nature. Still, I would hope that the new theory of electroweak interactions, whatever that is, "naturally" solves the naturalness problem.

It may well be that, in some cases, Eq. (10.10) overestimates the amount of tuning. Indeed, Eq. (10.10) measures the sensitivity of the prediction of M_Z as we vary parameters in "theory space". However, we have no idea how this "theory space" looks like, and the procedure of independently varying all parameters may be too simple-minded.[n] In conclusion, although a quantitative measure of naturalness can be of useful guidance to build new theories, it is very easy to slip into purely academic and sterile considerations. As we are drawing closer to the beginning of LHC operations, the real issue is whether the new theory predicts observable phenomena in the TeV domain or not.

---

[n]For instance, some authors have argued that, supersymmetric models become less fine-tuned if one imposes special restrictions on the theoretical parameters at the GUT scale (like $\tilde{m}_t = \tilde{m}_H$ and large $\tan \beta$ [56] or $\tilde{m}_t^2 \approx -4M_{\tilde{g}}^2$ [57]). In the absence of solid theoretical motivations for these restrictions, it is difficult to assess the real benefits of such approaches.

10.8. Anthropic Reasoning

> *A physicist talking about the anthropic principle runs*
> *the same risk as a cleric talking about pornography:*
> *no matter how much you say you are against it,*
> *some people will think you are a little too interested.*
> Steven Weinberg

Is the naturalness of the Higgs mass a good scientific question that will make us understand fundamental properties of nature? There are some questions that at first sight appear pregnant with deep meanings, but then end up to be red herrings. Probably Dirac's question ("Why are these numbers so large?") was one of them because, as we have seen in Sec. 10.2, his explanation in terms of a time-varying G_N was less successful than Dicke's simple observation based on the essential role of contingency in the observation. An alien landing on Mount Athos is warned: do not make wrong conclusions on the mystical inclinations of earthlings, before carefully considering the circumstances of your observation.

In 1595 Kepler asked the apparently good scientific question "Why are there six planets?", and in *Mysterium Cosmographicum* proposed an attractive symmetry-based answer. Planetary orbits lie on successive spheres that circumscribe and inscribe the five Platonic solids.[o] Based on this hypothesis he could predict the ratio of the planetary distances, which matched observations well within the accuracy known at the time. Of course today we known that the number of planets and their distances from the Sun do not carry any significant information on the fundamental laws of physics; hence, another red herring.

Even from these "wrong" questions there is a lesson to be learned. Special incidents may not be an indication of some deep property of the fundamental theory, but just the consequence of the special condition of the observer [58]. However, for this to happen, there must exist a large ensemble of possible incidents, from which the special observer picks a special case. In practice this means that, if we do not want to attach a special significance to our observation, we learn something about the ensemble. From large numbers, we deduce that the universe must expand; from meeting a thousand Orthodox monks, we conclude that the Earth is highly populated;

---

[o]It is interesting to note how the number of space dimensions plays an essential role in this hypothesis. In three dimensions there exist only five regular solids but, in two dimensions, there is an infinite number of regular polygons, and therefore an infinite number of planets.

from the special location of the Earth in the solar system, we deduce that the universe must contain a large number of stars.

In the same way, the measured value of G_F/G_N, which seems special to us, could actually be a very plausible observation in a universe that has developed complex structures, if there exists a multitude of universes with different values of G_F/G_N. In the vast majority of the universes G_F/G_N is of order unity, but those universes do not have the right properties to develop observers. Indeed, the measured value of G_N appears very favorably chosen to sustain non-trivial chemistry [59] (the same can be said about the cosmological constant, since the existence of galaxies is very sensitive to its value [60]). This picture of a multitude of parallel universes, usually referred to as the "*multi*verse" (as opposed to a single *uni*verse), can be realized in the context of string theory and eternal inflation [61]. If true, it would represent the next step in Copernican revolution: not only is the Earth not special, but even the universe in which we live is just one out of many.

Does this scenario imply that the Higgs naturalness problem was a red herring and that the LHC is doomed to find the Higgs particle and nothing else? Quite possible. However, sometimes there are remarkable properties that unexpectedly emerge. Sometimes they are simple coincidences, but sometimes they hide significance of great importance. A most singular episode is related by Barrow [62]. Unattested tradition narrates that William Shakespeare may have contributed to the English renderings of the Psalms in the King James Version of the Bible. An Eton schoolboy noticed that in Psalm 46, written in the year in which Shakespeare (who was born in 1546) was 46 years old, the word "SHAKE" is the 46th from the beginning, and "SPEAR" is the 46th from the end. Coincidence or a hidden signature of the poet?

Supersymmetry at the weak scale was introduced to tame the quantum corrections to the Higgs mass. However, it has been noticed that the supersymmetric particles have exactly the right quantum numbers to unify the gauge couplings at a very large energy scale with surprising precision. Moreover, the massive, neutral, stable Majorana particle that automatically emerges from many supersymmetric theories is exactly what is needed to account for the dark matter observed in our universe. Coincidences or hidden signatures of supersymmetry?

These observations have led to the proposal of Split Supersymmetry [63], in which gauge-coupling unification and dark matter are taken as basic elements, while the solution of the Higgs naturalness problem is abandoned.

This theory has several interesting features and quite distinctive signatures at collider experiments. If confirmed by the LHC, it would provide tangible experimental evidence against the naturalness criterion.

10.9. Naturalness versus Criticality

> *Results without causes are much more impressive.*
>   Sherlock Holmes [64]

There is a different way of looking at the hierarchy problem G_F/G_N. In the Standard Model the weak scale is determined by the vacuum expectation value of the Higgs field, which triggers electroweak symmetry breaking. The order parameter of the phase transition can be expressed in terms of the coefficient μ^2 that enters the Higgs potential. If μ^2 is positive the symmetry remains unbroken, if μ^2 is negative the symmetry is broken, and $\mu^2 = 0$ defines the critical point. This is completely analogous to the Ginzburg-Landau description of ferromagnetism. For temperatures T larger than the critical Curie temperature T_C, the dipoles are randomly oriented, the total magnetization vanishes, and the system is rotationally symmetric. When $T-T_C$ becomes negative, the dipoles are aligned creating a spontaneous magnetization, and the system breaks rotational symmetry.

Because of quantum corrections, we expect $|\mu^2|$ to be close to the maximum energy Λ^2 and, depending on its sign, to break or preserve electroweak symmetry. The hierarchy problem can then be rephrased in the following way [65]: if the critical value separating the two phases is not special from the point of view of the fundamental theory, why are the parameters in the real world chosen such that we live so near the critical condition?

There are systems in nature which have the tendency to evolve into critical states, even if there is no outside agent that forces them in that direction. This process is called self-organized criticality [66]. The prototype example is a sand pile where grains of sand are slowly added. As the pile grows, it reaches a condition where catastrophic sand slides occur after the addition of just a single grain. Avalanches of all sizes obey a power-law distribution and therefore the dynamics of the system can no longer be understood in terms of single grains. There are correlations among distances vastly larger than the size of the grain of sand. The system has arranged itself to be near critical and remains close to the critical condition (as long as we continue to slowly add more sand). There are many, apparently unrelated, phenomena that seem to follow this pattern: from

the distribution of earthquake intensity to extinctions of biological species; from river bifurcations to traffic jams.

Is it possible that a pattern of self-organized criticality with respect to electroweak symmetry brings the Standard Model towards the condition of a large hierarchy G_F/G_N? If anything like this operates in nature, then it will not be captured by an effective-theory approach and it will not respect the naturalness criterion. The microphysics description will fail to properly account for some large-scale correlations, in the same way as individual grains are not useful to describe the avalanches in the sand pile occurring at all scales (between the size of a single grain and the size of the whole pile). To realize such an idea, an ensemble of theories seems to be a necessary ingredient, and therefore we still have to rely on the multiverse. However, the process of selection of our universe will be, in this case, determined by dynamics rather than by anthropic considerations.

10.10. Conclusions

> *"Data! Data! Data!" he cried impatiently.*
> *"I can't make bricks without clay."*
> Sherlock Holmes [67]

The primary goal of the LHC is to discover the mechanism of electroweak symmetry breaking. Indeed, the Standard Model, including only the particles known today, becomes inconsistent at an energy scale of about 1 TeV. The LHC, producing particle collisions with energies above this scale, is bound to probe the mechanism of electroweak breaking, whether it is given by the Higgs or by some alternative dynamics.

There is a second, more subtle, issue related to the existence of a fundamental Higgs boson, which will also be investigated by the LHC. The basic problem is the absence, within the Standard Model, of symmetries protecting the Higgs mass term, and therefore the expectation that the maximum energy up to which the theory can be *naturally* extrapolated is, again, the TeV. A new physics regime should set in at that energy scale, and the hypothetical Higgs boson must be accompanied by new particles associated with the cancellation of the quantum corrections to m_H. This is not a problem of internal consistency of the theory, but an acute problem of naturalness. As such, it does not necessarily guarantee that a new physics threshold really exists in nature. But, if new particles at the TeV scale are indeed discovered, it will be a triumph for our understanding of physics in terms of symmetries and effective field theories.

This is, in conclusion, the naturalness problem that theoretical particle physics is facing today. If you found the subject too speculative, be reassured: time has come for the question to be settled by experimental data.

References

[1] M.C. Bateson, On the Naturalness of Things, from *How Things Are: A Science Toolkit for the Mind*, ed. J. Brockman and K. Matson.

[2] J.E. Anderson, A Conceptual Framework for Evaluating and Quantifying Naturalness, *Conservation Biology*, **5**, (3) 347, (1991).

[3] R. Courant and H. Robbins, *What is Mathematics?*, (Oxford University Press, Oxford 1941).

[4] P. Nelson, Naturalness in Theoretical Physics, *Am. Sci.* **73**, 60 (1985).

[5] A. Einstein, as quoted in I. Rosenthal-Schneider, *Reality and Scientific Truth: Discussions with Einstein, von Laue, and Planck*, (Wayne State University Press, Detroit 1980).

[6] *Tychonis Brahe Dani opera omnia* (J.L.E. Dreyer, ed.) 4, 156, line 17, Copenhagen 1913-1929.

[7] T.S. Kuhn, *The Copernican Revolution*, (Harvard University Press, Cambridge 1957); J.T. Cushing, *Philosophical Concepts in Physics*, (Cambridge University Press, Cambridge 1998).

[8] H.H. Dale, *Brit. Med. J.*, Sep 4th p. 451 (1948).

[9] W. Shakespeare, *Hamlet*, Act II, Scene 2 (1600).

[10] W. M. Yao *et al.* [Particle Data Group], Review of particle physics, *J. Phys. G* **33**, 1 (2006).

[11] D.E. Smith, *History of Mathematics*, (Dover Pub., New York 1923.)

[12] J. Balmer, *Verh. Naturf. Ges. Basel* **7**, 548 (1885).

[13] J. Balmer, *Verh. Naturf. Ges. Basel* **7**, 750 (1885).

[14] N. Bohr, *Phil. Mag.* **26**, 1 (1913).

[15] A.S. Eddington, *Proc. Roy. Soc.* **A 122**, 358 (1930).

[16] A.M. Wyler, *Acad. Sci. Paris Comptes Rendus* **B 269**, 743 (1969); **B 271**, 186 (1971).

[17] H. Aspden and D.M. Eagles, *Phys. Lett.* **A 41**, 423 (1972).

[18] B. Robertson, *Phys. Rev. Lett.* **27**, 1545 (1971).

[19] T.J. Burger, *Nature* **271**, 402 (1978).

[20] W. Heisenberg, as quoted in H. Kragh, *Dirac: A Scientific Biography*, (Cambridge University Press, Cambridge 1990).

[21] A. Einstein, remark to Ernst G. Straus, one of his assistants.

[22] A.S. Eddington, *New Pathways in Science*, (Cambridge University Press, Cambridge 1935).

[23] A.S. Eddington, as quoted in Ref. [62].

[24] P.A.M. Dirac, *Nature* **139**, 323 (1937); *Proc. Roy. Soc.* **A 165**, 199 (1938).

[25] N.H.D. Bohr, as quoted in G. Gamow, *Science* **158**, 766 (1967).

[26] E. Teller, *Phys. Rev.* **73**, 801 (1948).

[27] R.H. Dicke, *Nature* **192**, 440 (1961).

[28] N.H.D. Bohr, as quoted in M.J. Wheatley, *Leadership and the New Science: Discovering Order in a Chaotic World*, (Berrett-Koehler Pub., San Francisco 1999).

[29] V.I. Ulyanov (better known as Lenin), apocryphal. I learned this quote from Luis Alvarez-Gaumé.

[30] G. 't Hooft, in Proc. of 1979 Cargèse Institute on *Recent Developments in Gauge Theories*, p. 135, (Plenum Press, New York 1980).

[31] See *e.g.* A. V. Manohar, Effective field theories, arXiv:hep-ph/9606222; D. B. Kaplan, Five lectures on effective field theory, arXiv:nucl-th/0510023.

[32] N. Arkani-Hamed, L. Motl, A. Nicolis and C. Vafa, The string landscape, black holes and gravity as the weakest force, *JHEP* **0706**, 060 (2007).

[33] E. Gildener, Gauge Symmetry Hierarchies, *Phys. Rev. D* **14**, 1667 (1976); S. Weinberg, Gauge Hierarchies, *Phys. Lett. B* **82**, 387 (1979).

[34] M. Shaposhnikov, Is there a new physics between electroweak and Planck scales?, arXiv:0708.3550 [hep-th].

[35] L. Susskind, Dynamics Of Spontaneous Symmetry Breaking In The Weinberg-Salam Theory, *Phys. Rev. D* **20**, 2619 (1979).

[36] K. G. Wilson, The Renormalization Group And Strong Interactions, *Phys. Rev. D* **3**, 1818 (1971).

[37] K. G. Wilson, The origins of lattice gauge theory, *Nucl. Phys. Proc. Suppl.* **140**, 3 (2005).

[38] O.-M. Bilaniuk and E.C.G. Sudarshan, Particles Beyond the Light Barrier, *Physics Today* **22**, 43, (May 1969).

[39] L. Maiani, in Proc. École d'été de physique des particules, Gif-sur-Yvette 1979.

[40] P. Fayet, in Proc. Europhysics Study Conference in Erice on *Unification of the Fundamental Particle Interactions*, p. 587, (Plenum Press, New York 1980).

[41] J. Ellis, M.K. Gaillard, L. Maiani, B. Zumino, in Proc. Europhysics Study Conference in Erice on *Unification of the Fundamental Particle Interactions*, p. 69, (Plenum Press, New York 1980); B. Zumino, *ibid.* p. 101.

[42] J. Iliopoulos, in *1979 Einstein Symposion Berlin*, p. 89, (Springer-Verlag, Berlin 1979).

[43] M. J. G. Veltman, The Infrared - Ultraviolet Connection, *Acta Phys. Polon. B* **12**, 437 (1981).

[44] E. Witten, Dynamical Breaking Of Supersymmetry, *Nucl. Phys. B* **188**, 513 (1981).

[45] S. Dimopoulos and H. Georgi, Softly Broken Supersymmetry And SU(5), *Nucl. Phys. B* **193**, 150 (1981).

[46] L. Girardello and M. T. Grisaru, Soft Breaking Of Supersymmetry, *Nucl. Phys. B* **194**, 65 (1982).

[47] A.S. Königsberg (better known as W. Allen), *Getting Even*, First Vintage Books Edition, New York 1978.

[48] H. Murayama, Supersymmetry phenomenology, arXiv:hep-ph/0002232.

[49] F. Rasetti and E. Fermi, *Nuovo Cim.* **36**, 226 (1926).

[50] V.F. Weisskopf, *Phys. Rev.* **56**, 72 (1939).

[51] S. L. Glashow, J. Iliopoulos and L. Maiani, Weak Interactions with Lepton-Hadron Symmetry, *Phys. Rev. D* **2**, 1285 (1970).

[52] M. K. Gaillard and B. W. Lee, Rare Decay Modes Of The K-Mesons In Gauge Theories, *Phys. Rev. D* **10**, 897 (1974).

[53] LEP Electroweak Working Group, `http://lepewwg.web.cern.ch`.

[54] J. Kepler, epitaph composed for himself few months before dying (1630).

[55] J. R. Ellis, K. Enqvist, D. V. Nanopoulos and F. Zwirner, Observables In Low-Energy Superstring Models, *Mod. Phys. Lett. A* **1**, 57 (1986); R. Barbieri and G. F. Giudice, Upper Bounds On Supersymmetric Particle Masses, *Nucl. Phys. B* **306**, 63 (1988).

[56] J. L. Feng, K. T. Matchev and T. Moroi, Multi-TeV scalars are natural in minimal supergravity, *Phys. Rev. Lett.* **84**, 2322 (2000).

[57] R. Dermisek and H. D. Kim, Radiatively generated maximal mixing scenario for the Higgs mass and the least fine tuned minimal supersymmetric standard model, *Phys. Rev. Lett.* **96**, 211803 (2006).

[58] J.D. Barrow and F.J. Tipler, *The Anthropic Cosmological Principle*, (Oxford University Press, Oxford 1986).

[59] V. Agrawal, S. M. Barr, J. F. Donoghue and D. Seckel, The anthropic principle and the mass scale of the standard model, *Phys. Rev. D* **57** 5480 (1998).

[60] S. Weinberg, Anthropic Bound On The Cosmological Constant, *Phys. Rev. Lett.* **59** 2607 (1987).

[61] R. Bousso and J. Polchinski, Quantization of four-form fluxes and dynamical neutralization of the *JHEP* **0006**, 006 (2000); L. Susskind, *The Cosmic Landscape: String theory and the illusion of intelligent design*, (Time Warner Books, New York 2005); *Universe or Multiverse?*, B. Carr (ed) (Cambridge University Press, Cambridge, 2007).

[62] J.D. Barrow, *The Constants of Nature*, (Pantheon Books, New York 2002).

[63] N. Arkani-Hamed and S. Dimopoulos, Supersymmetric unification without low energy supersymmetry and signatures for fine-tuning at the LHC, *JHEP* **0506** 073 (2005); G. F. Giudice and A. Romanino, Split supersymmetry, *Nucl. Phys. B* **699** 65 (2004); N. Arkani-Hamed, S. Dimopoulos, G. F. Giudice and A. Romanino, Aspects of split supersymmetry, *Nucl. Phys. B* **709** 3 (2005).

[64] A. Conan Doyle, *The Memoirs of Sherlock Holmes*, The Adventure of the Stockbroker's Clerk (1893).

[65] G. F. Giudice and R. Rattazzi, Living dangerously with low-energy supersymmetry, *Nucl. Phys. B* **757** 19 (2006).

[66] P. Bak, C. Tang and K. Wiesenfeld, Self-organized criticality — an explanation of 1/f noise, *Phys. Rev. Lett.* **59** 381 (1987); P. Bak, *How Nature Works*, (Oxford University Press, Oxford 1997).

[67] A. Conan Doyle, *The Adventures of Sherlock Holmes*, The Adventure of the Copper Beeches (1892).

Chapter 11

Prospects for Higgs Boson Searches at the LHC

Karl Jakobs[*] and Markus Schumacher[†]

[*]*Physikalisches Institut, Universität Freiburg*
79104 Freiburg, Germany
karl.jakobs@uni-freiburg.de

[†]*Fachbereich Physik, Universität Siegen*
57068 Siegen, Germany
markus.schumacher@hep.physik.uni-siegen.de

The investigation of the dynamics responsible for electroweak symmetry breaking is one of the prime tasks of experiments at the CERN Large Hadron Collider (LHC). The experiments ATLAS and CMS have been designed to be able to discover a Standard Model Higgs boson over the full mass range as well as Higgs bosons in extended models. In this chapter, the prospects for Higgs boson searches at the LHC are reviewed. In addition, the potential for the measurement of Higgs boson parameters is discussed.

11.1. Introduction

While the Standard Model of electroweak and strong interactions is in excellent agreement with the numerous experimental measurements, the dynamics responsible for electroweak symmetry breaking are still unknown. Within the Standard Model, the Higgs mechanism [1] is invoked, i.e. a doublet of complex scalar fields is introduced of which a single neutral scalar particle, the Higgs boson, remains after symmetry breaking.

The Higgs boson is the only Standard Model particle that has not been discovered so far. The direct search at the e^+e^- collider LEP has led to a lower bound on its mass of 114.4 GeV/c^2 [2]. Indirectly, high precision electroweak data constrain the mass of the Higgs boson via their sensitivity to loop corrections. Assuming the overall validity of the Standard Model, a

global fit [3] to all electroweak data leads to $m_H = 76^{+33}_{-24}$ GeV/c^2. On the basis of the present theoretical knowledge, the Higgs sector in the Standard Model remains largely unconstrained. While there is no direct prediction for the mass of the Higgs boson, an upper limit of $\sim$1 TeV/c^2 can be inferred from unitarity arguments [4].

Further constraints can be derived under the assumption that the Standard Model is valid only up to a cutoff energy scale Λ, beyond which new physics becomes relevant. Requiring that the electroweak vacuum is stable and that the Standard Model remains perturbative allows to set upper and lower bounds on the Higgs boson mass [5, 6]. For a cutoff scale of the order of the Planck mass, the Higgs boson mass is required to be in the range $130 < m_H < 190$ GeV/c^2. If new physics appears at lower mass scales, the bound becomes weaker, e.g., for $\Lambda = 1$ TeV the Higgs boson mass is constrained to be in the range $50 < m_H < 800$ GeV/c^2.

The Minimal Supersymmetric Standard Model (MSSM) [7] contains two complex Higgs doublets, leading to five physical Higgs bosons after electroweak symmetry breaking: three neutral (two CP-even h, H and one CP-odd A) and a pair of charged Higgs bosons $H^{\pm}$. At tree level, the Higgs sector of the MSSM is fully specified by two parameters, generally chosen to be m_A, the mass of the CP-odd Higgs boson, and $\tan\beta$, the ratio of the vacuum expectation values of the two Higgs doublets. Radiative corrections modify the tree-level relations significantly. Loop corrections are sensitive to the mass of the top quark, to the mass of the scalar particles and in particular to mixing in the stop sector. If the full one-loop and the dominant two-loop contributions are included [8, 9], the upper bound on the mass of the light Higgs boson h is expected to be around 135 GeV/c^2. While the light neutral Higgs boson may be difficult to distinguish from the Standard Model Higgs boson, the other heavier Higgs bosons are a distinctive signal of physics beyond the Standard Model. The masses of the heavier Higgs bosons H, A and $H^{\pm}$ are often almost degenerate.

If the global fit to the electroweak precision data is repeated within the MSSM and constraints from heavy flavour physics and from the abundance of cold dark matter in the universe are included [10], the mass of the lightest Higgs boson can be tightly constraint to be $m_H = 110^{+10}_{-8} \pm 3$ (theo.) GeV/c^2.

At present, the Fermilab Tevatron $p\overline{p}$ collider with a center-of-mass energy of 1.96 TeV continues to be the leading accelerator exploring the energy frontier and its preeminence will continue until the LHC experiments have collected sufficient amounts of good quality and well understood data. Until

the end of 2007 the two experiments CDF and DØ have analysed data corresponding to an integrated luminosity of ~ 1.7 fb^{-1}. So far no evidence for the production of Higgs bosons has been found [11]. The data taking period is expected to be continued until the end of 2009, with a possible extension into the year 2010, leading to an increase in the integrated luminosity to 5.5 or 7.0 fb^{-1}, respectively. Based on the present experience and assuming some improvements in the analysis techniques, both Tevatron experiments combined are expected to reach sensitivity to the production of a Standard Model Higgs boson up to masses of 180 GeV/c^2 at 95% confidence level (C.L.). Within the context of the MSSM, also most of the parameter space can be tested at 95% C.L. However, even with the full integrated luminosity of 7 fb^{-1} and after combining all channels and both experiments, a 5σ discovery will not be possible at the Tevatron, leaving it to the LHC to explore and discover Higgs bosons over the full parameter range of both the Standard Model and the MSSM.

In the following the excellent prospects for Higgs boson searches at the LHC are reviewed (Secs. 11.3 and 11.5), after a brief discussion of the Higgs boson production and decay properties in Sec. 11.2. In Sec. 11.4 the LHC potential for the determination of the Higgs boson properties is briefly described.

11.2. Higgs Boson Production and Decay

At hadron colliders, Higgs bosons can be produced via four different production mechanisms:

- gluon fusion, $gg \to H$, which is mediated at lowest order by a heavy quark loop;
- vector boson fusion (VBF), $qq \to qqH$;
- associated production of a Higgs boson with weak gauge bosons, $qq \to W/Z\ H$ (Higgs Strahlung, Drell-Yan like production);
- associated Higgs boson production with heavy quarks, $gg, qq \to ttH$, $gg, qq \to bbH$ (and $gb \to bH$).

The lowest order production cross sections for the four different processes are shown in Fig. 11.1(left) as a function of the Higgs boson mass [12]. The dominant production mode is the gluon-fusion process, followed by the vector boson fusion process. In the low mass region the latter amounts at leading order to about 20% of the gluon-fusion cross section, whereas it reaches the same level for masses around 800 GeV/c^2.
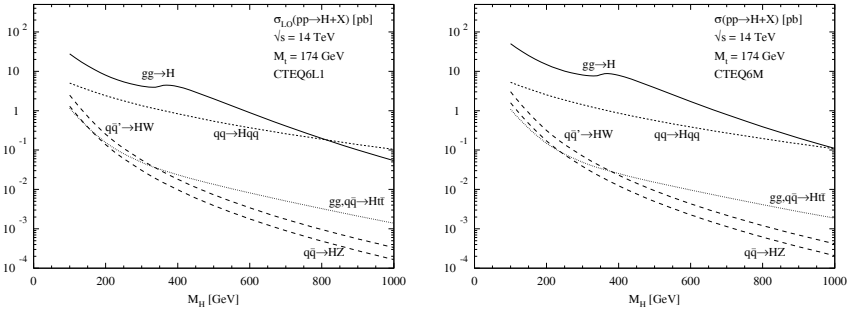
Fig. 11.1.   Leading order (left) and next-to-leading order (right) production cross sections for a Standard Model Higgs boson at the LHC as a function of the Higgs boson mass. In the cross section calculation the CTEQ6L1 structure function parametrization has been used. (The calculations have been performed by M. Spira, Ref. [12].)

For all production processes higher order QCD corrections have been calculated. Already more than ten years ago, the next-to-leading order (NLO) QCD corrections to the gluon-fusion process have been calculated and have been found to be large, increasing the leading order cross section by 50-100% [13]. These large corrections stimulated the calculation of the next-to-next-to-leading order (NNLO) corrections, to which many authors contributed [14–17] and which meanwhile has been completed in the heavy top-quark limit ($m_t \rightarrow \infty$). The results for the total cross section show a modest increase between the NLO and NNLO calculation at the level of 10–20%, indicating that a nicely converging perturbative series seems to be emerging. Also for the other processes next-to-leading order corrections are available. It should be noted that in the Standard Model, the cross section for producing a Higgs boson in association with b quarks is relatively small. However, in a supersymmetric theory with a large value of $\tan\beta$, the b-quark Yukawa coupling can be strongly enhanced and Higgs boson production in association with b quarks becomes the dominant production mechanism. For a detailed summary of the theroetical aspects the reader is referred to Ref. 18.

The branching fractions of the Standard Model Higgs boson are shown in Fig. 11.2(left) as a function of the Higgs boson mass. They have been calculated taking into account both electroweak and QCD corrections [19]. When kinematically accessible, decays of the Standard Model Higgs boson into vector boson pairs WW or ZZ dominate over all other decay modes. Above the kinematic threshold, the branching fraction into $t\bar{t}$ can reach up
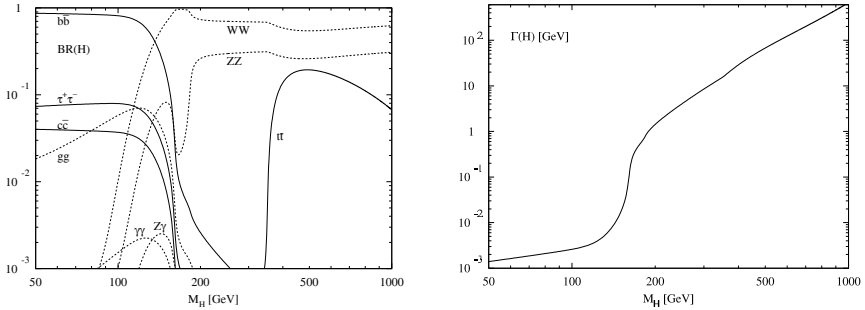
Fig. 11.2. Branching fractions (left) and total decay width (right) of the Standard Model Higgs boson as a function of Higgs boson mass (from Ref. [19]).

to 20%. All other fermionic decays are only relevant for Higgs boson masses below 2 m_W, with $H \to b\bar{b}$ dominating below 140 GeV/c^2. The branching fractions for $H \to \tau\tau$ and $H \to gg$ both reach up to about 8% at Higgs boson masses between 100 and 120 GeV/c^2. Decays into two photons, which are of interest due to their relatively clean experimental signature, can proceed via fermion and W loops with a branching fraction of up to $2 \cdot 10^{-3}$ at low Higgs boson masses.

Compared to experimental mass resolution, the total decay width of the Standard Model Higgs boson is negligible at low masses and becomes significant only above the threshold for decays into ZZ, as shown in Fig. 11.2(right).

Within the MSSM, branching fractions of five physical Higgs bosons have to be considered as a function of their masses as well as $\tan\beta$ and the SUSY breaking parameters. The neutral Higgs bosons decay dominantly into $b\bar{b}$ and $\tau\tau$ at large $\tan\beta$ or for masses below 150 GeV/c^2 (up to 2 m_t for the CP-odd Higgs boson A). Decays into WW, ZZ and photons are generally suppressed by kinematics as well as the Higgs boson couplings and become relevant only in the decoupling limit $m_A \to \infty$, where the light CP-even Higgs boson h effectively behaves like a Standard Model Higgs boson while all other MSSM Higgs bosons are heavy. Charged Higgs bosons preferably decay into tb if accessible. For masses below $m_t + m_b$, the decay $H^\pm \to \tau\nu$ dominates, with small contributions from $H^\pm \to cb$ and $H^\pm \to cs$. In addition, both charged and heavy neutral Higgs bosons can decay into lighter Higgs bosons: $H^\pm \to Wh$, WA as well as $H \to hh, AA, ZA$ and $A \to Zh$. Generally, the branching fractions of these decay modes are significant only at small $\tan\beta$. It should be noted that supersymmetric

particles are considered to be heavy enough to play a negligible role in the phenomenology of Higgs boson decays in the following.

11.3. Search for the Standard Model Higgs Boson

The Standard Model Higgs boson is searched for at the LHC in various decay channels, the choice of which is given by the signal rates and the signal-to-background ratios in the different mass regions. The search strategies and background rejection methods have been established in many studies over the past ten years [20, 21]. Originally, inclusive final states have been considered, among them the well established $H \rightarrow \gamma\gamma$ and $H \rightarrow ZZ^{(*)} \rightarrow \ell\ell\,\ell\ell$ decay channels. More exclusive channels have been considered in the low mass region by searching for Higgs boson decays in $b\bar{b}$ or $\gamma\gamma$ in association with a lepton from a decay of an accompanying W or Z boson or a top quark. The search for a Standard Model Higgs boson in the intermediate mass region can be extended by using the vector boson fusion mode and exploiting forward jet tagging, which had been proposed in the literature several years ago [22]. In this Section, a brief summary of the Standard Model Higgs boson discovery potential at the LHC is given.

Due to the enormous progress in the calculation of higher order QCD corrections for signals and backgrounds over the past few years, the LHC physics studies have started to use these calculations. Only in cases where the corrections for the major backgrounds are not available or in older studies, performance figures are evaluated by using Born-level predictions for both signals and backgrounds.

In addition, more detailed and better understood reconstruction methods have been established by the experimental collaborations. They are partially based on testbeam measurements of various detector components or rely on extensive Monte Carlo simulations of the detailed detector response [23].

11.3.1. *Inclusive Higgs boson searches*

Several important channels for Higgs boson discovery at the LHC have been discussed extensively in the literature. Among those channels are the $H \rightarrow \gamma\gamma$ decay mode, the gold plated decay channel $H \rightarrow ZZ^{(*)} \rightarrow 4\ell$ as well as the decay channel $H \rightarrow WW^{(*)} \rightarrow \ell\nu\ell\nu$. If no additional particles except the Higgs boson decay products are searched for, the production

via gluon fusion provides the largest contribution to the signal event yields.

11.3.1.1. $H \to ZZ^{(*)}$ decays

The decay channel $H \to ZZ^* \to \ell\ell\,\ell\ell$ provides a rather clean signature in the intermediate mass region 115 GeV/c^2 $< m_H < 2\,m_Z$. In addition to the irreducible backgrounds from ZZ^* and $Z\gamma^*$ production, there are large reducible backgrounds from $t\bar{t}$ and $Zb\bar{b}$ production. Due to the large production cross section, the $t\bar{t}$ events dominate at production level, whereas the $Zb\bar{b}$ events contain a genuine Z boson in the final state and are therefore more difficult to reject. In addition, there is background from ZZ continuum production, where one of the Z bosons decays into a τ pair, with subsequent leptonic decays of the τ leptons, and the other Z decays into an electron or muon pair. It has been shown that in both LHC experiments the reducible backgrounds can be suppressed well below the level of the irreducible background from $ZZ^* \to 4\ell$. Calorimeter and track isolation together with impact parameter measurements can be used to achieve the necessary background rejection [20, 21]. The expected distribution of signal events for a Higgs boson with a mass of 130 GeV/c^2 in the CMS experiment is shown in Fig. 11.3 on top of the background. Already for a low integrated luminosity of 10 fb^{-1} the signal is clearly visible. Assuming an integrated luminosity of 30 fb^{-1}, the $H \to ZZ^* \to 4\ell$ signal can be observed with a significance of more than 5σ in the mass range $130 < m_H < 180$ GeV/c^2, except for a narrow region around 170 GeV/c^2, where the branching ratio is suppressed due to the opening up of the WW decay mode.

For Higgs boson masses in the range 180 GeV/c^2 $< m_H < 700$ GeV/c^2, the $H \to ZZ \to 4\ell$ decay mode is the most reliable one for the discovery of a Standard Model Higgs boson at the LHC. The expected background, which is dominated by the continuum production of Z boson pairs, is smaller than the signal. In this mass range the Higgs boson width grows rapidly with increasing m_H, and dominates over the experimental mass resolution for $m_H > 300$ GeV/c^2. The momenta of the final-state leptons are high and their measurement does not put severe requirements on the detector performance.

For larger values of m_H, the Higgs boson signal becomes very broad and the signal rate drops rapidly. In the high mass region, the decay modes $H \to ZZ \to \ell\ell\,\nu\nu$ and $H \to ZZ \to \ell\ell\,jj$ provide additional discovery potential [20, 21] and allow to extend the 5σ-discovery range up to ~ 1 TeV/c^2.
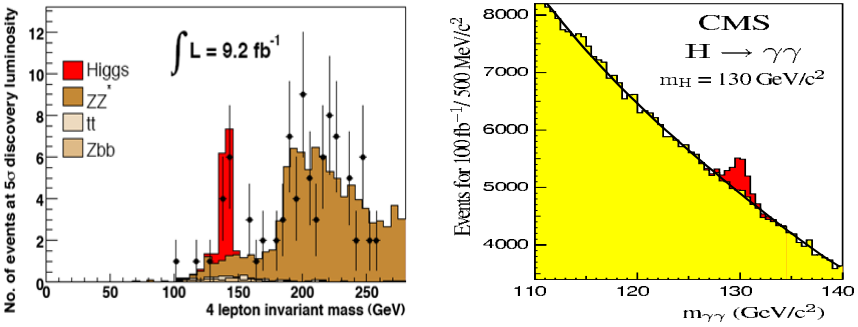
Fig. 11.3. (Left) Expected $H \to ZZ^* \to 4\ell$ signal above the background for $m_H = 140$ GeV/c^2 and for an integrated luminosity of 9.2 fb^{-1} (signal significance of 5σ) in the CMS experiment. (Right) Reconstructed $\gamma\gamma$ invariant mass distribution of a $H \to \gamma\gamma$ signal (dark) with $m_H = 130$ GeV/c^2 and the background (light) for an integrated luminosity of 100 fb^{-1} in the CMS experiment.

11.3.1.2. $H \to \gamma\gamma$ decays

The decay $H \to \gamma\gamma$ is a rare decay mode, which is only detectable in a limited Higgs boson mass region between 80 and 150 GeV/c^2, where both the production cross section and the decay branching ratio are relatively large. Excellent energy and angular resolution are required to observe the narrow mass peak above the irreducible prompt $\gamma\gamma$ continuum. In addition, there is a large reducible background resulting from direct photon production or from two-jet production via QCD processes. Using a realistic detector simulation, it has been demonstrated [20, 21] that the required rejection can be achieved and that the residual jet-jet and γ-jet backgrounds can be brought well below the irreducible $\gamma\gamma$ background.

It should be stressed that due to the large amount of material in the central detectors of the LHC experiments (from ~40% of a radiation length at $\eta \sim 0$ to 140% towards the barrel-endcap-transition region), a large fraction of converted photons appears and results in a degraded $\gamma\gamma$ mass resolution as compared to unconverted photons.

On the theoretical side, the large K factors for the gluon fusion process lead to an improved signal significance. In addition, it is anticipated that multivariate analysis strategies like neural networks and likelihood methods can be used to increase the signal significance. For a Higgs boson with a mass of 130 GeV/c^2, for example, a signal significance of around 6σ is expected for both experiments, assuming data corresponding to an integrated

luminosity of 30 fb^{-1} and NLO cross sections. Despite the intrinsically better energy resolution of the CMS calorimeter the expected performance for a Higgs boson discovery in the $\gamma\gamma$ decay mode is found to be comparable between the two experiments. As an example of signal reconstruction above background, the expected signal from a Higgs boson with a mass of 130 GeV/c^2 in the CMS experiment is shown in Fig. 11.3(right), assuming an integrated luminosity of 100 fb^{-1}.

11.3.1.3. $H \to WW^{(*)}$ decays

For Higgs boson masses around 170 GeV/c^2, for which the ZZ^* branching ratio is suppressed, the discovery potential can be enhanced by searching for the $H \to WW^{(*)} \to \ell\nu\ell\nu$ decay [20, 21, 24]. In this mode it is not possible to reconstruct a Higgs boson mass peak. Instead, an excess of events above the expected backgrounds can be observed and used to establish the presence of a Higgs boson signal. Usually, the transverse mass computed from the leptons and the missing transverse momentum, $M_T = \sqrt{2P_T^{\ell\ell}\not{E}_T(1 - \cos\Delta\phi)}$, is used to discriminate between signal and background (see Fig. 11.4(left)). The WW, $t\bar{t}$ and single-top production processes constitute severe backgrounds and the signal significance depends critically on their absolute knowledge. In addition, a so called jet veto is applied, i.e. it is required that there is no jet activity in the central region of the detector. An estimate of the signal significance relies therefore heavily on a reliable Monte Carlo description of this jet activity. It is anticipated that after relaxing cuts, the Monte Carlo predictions for those backgrounds can be normalized to the data in regions where only a small fraction of signal events is expected.

It has recently been shown that the $gg \to WW$ background contribution increases the background in particular in the regions of phase space selected by the selection criteria, i.e. at small values of $\Delta\phi$ between the two final-state leptons [25]. Although this background constitutes only 5% of the $qq \to WW$ background before cuts, its fraction increases to about 30% after the final selection criteria.

Due to the large signal rate this channel may provide for an early discovery if the backgrounds can be reliably controlled. The CMS experiment claims that for a Higgs boson with a mass of 165 GeV/c^2 a signal with a 5σ significance can already be claimed with data corresponding to an integrated luminosity of only $\sim$2 fb^{-1}.

11.3.2. *Higgs boson searches using vector boson fusion*

In recent studies it has been demonstrated that, not only in the high mass but also in the intermediate mass range, the discovery potential can be significantly increased by performing a search for Higgs boson production in the vector boson fusion mode [21, 22, 26]. Although the contribution to the cross section in the intermediate mass range amounts at leading order only to about 20% of the total production cross section, the additional event characteristics can be exploited to suppress the large backgrounds. In vector boson fusion events, the Higgs boson is accompanied by two jets in the forward regions of the detector, originating from the initial quarks that emit the vector bosons. On the other hand, central jet activity is suppressed due to the lack of colour exchange between the initial state quarks. This is in contrast to most background processes, where colour flow appears in the t-channel. Jet tagging in the forward region of the detector together with a veto of jet activity in the central region are therefore powerful tools to enhance the signal-to-background ratio.

The performance of the detectors for forward jet tagging has been studied in a detailed simulation [21, 26]. In the study presented in Ref. 26, the two tag jets are searched for over the full calorimeter coverage ($|\eta| < 4.9$). A large separation in pseudorapidity between the two reconstructed jets can be used to discriminate between signal and backgrounds from QCD production.

As pointed out above, a veto against jets in the central region will be an important tool to suppress background from QCD processes. It should be noted that a reliable estimate of the jet veto efficiency is difficult to obtain and might be affected by sizeable uncertainties.

11.3.2.1. $qqH \rightarrow qqWW^{(*)}$

According to Monte Carlo studies, the LHC experiments have a large discovery potential in the $H \rightarrow WW^{(*)} \rightarrow \ell\nu\ell\nu$ decay mode [21, 26]. The additional signatures of tag jets in the forward and of a low jet activity in the central regions of the detector allow for a significant reduction of the background. This results in a better signal-to-background ratio compared to the inclusive $H \rightarrow WW^{(*)}$ channel, which is dominated by the gluon fusion process. As a consequence, the signal sensitivity is less affected by systematic uncertainties on the predictions of the background. As an example, the reconstructed transverse mass distribution for a Higgs boson signal with a mass of 160 GeV/c^2 is shown on top of the backgrounds from $t\bar{t}$,
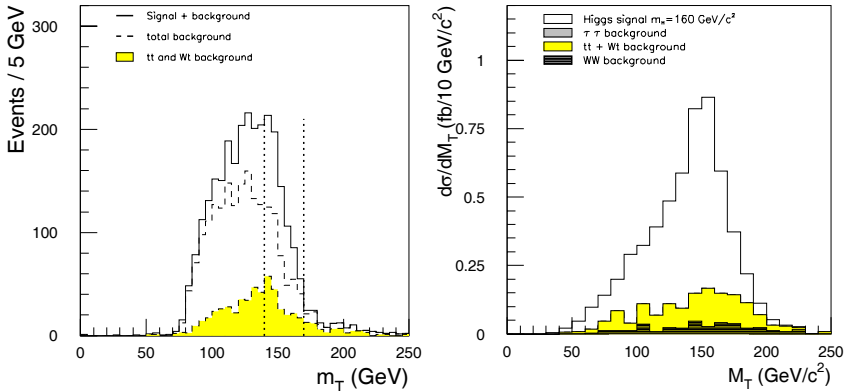
Fig. 11.4. (Left) Transverse mass distribution for the summed $H \to WW^* \to \ell\nu\,\ell\nu$ signal ($m_H = 150$ GeV/c^2) for the inclusive analysis and total background for the ATLAS experiment, for an integrated luminosity of 30 fb^{-1}. The distribution for the background alone is also shown separately. The shaded histogram represents the contributions from the Wt and $t\bar{t}$ backgrounds. The dashed lines indicate the selected signal region. (Right) Distribution of the transverse mass for the vector boson fusion analysis for a Higgs boson with a mass of 160 GeV/c^2 and the backgrounds in the $e\mu$-channel after all cuts for the ATLAS experiment.

Wt, and WW production in Fig. 11.4(right). Since neutrinos appear in the final state, the transverse mass is used for the mass reconstruction. After all cuts, a signal-to-background ratio in the order of 3:1 is found, such that this channel alone has a good discovery potential for a Higgs boson with a mass around 160 GeV/c^2. This compares favourably with the $gg \to WW^{(*)}$ channel discussed in Sec. 11.3.1.3.

It is interesting to note that an application of looser kinematical cuts on the final-state leptons allows for a better discrimination between the signal and background shape [26]. In this case, the background extends to higher M_T values and a background normalization outside the signal region is possible. The presence of a signal can also be demonstrated in the distribution of $\Delta\phi$, the difference in azimuthal angle between the two leptons in the final state. As discussed in Ref. [27], this distribution can be used for both a demonstration of the consistency of the signal with a spin-0 hypothesis and for an additional background normalization.

11.3.2.2. $qqH \to qq\tau\tau$

It has been shown that in the mass region $110 < m_H < 140$ GeV/c^2 the ATLAS and CMS experiments are sensitive to the $\tau\tau$ decay mode

of the Standard Model Higgs boson in the vector boson fusion chan-
nel [20, 26]. Searches for $H \rightarrow \tau\tau$ decays using the double leptonic de-
cay mode $qqH \rightarrow qq\ \tau\tau \rightarrow qq\ \ell\nu\bar{\nu}\ \ell\nu\bar{\nu}$ and the lepton-hadron decay mode
$qqH \rightarrow qq\ \tau\tau \rightarrow qq\ \ell\nu\bar{\nu}\ had\ \nu$ seem to be feasible. In these analyses,
Z+jet production with $Z \rightarrow \tau\tau$ constitutes the principal background. The
$\tau\tau$ invariant mass can be reconstructed using the collinear approximation.
In signal and background events, the H and Z bosons are emitted with
significant P_T, which contributes to large tau boosts and causes the tau
decay products to be nearly collinear in the laboratory frame. Assuming
that the tau directions are given by the directions of the visible tau decay
products (leptons or hadrons from tau decays respectively), the tau mo-
menta and therefore the $\tau\tau$ invariant mass can be reconstructed. As an
example, the distributions of the reconstructed $\tau\tau$ invariant masses for the
$e\mu$ and ℓ-had final states are shown in Fig. 11.5 for Higgs boson masses
of 120 and 135 GeV/c^2, respectively. A discovery based on a combination
of the $\ell - \ell$ and ℓ-had final states would require an integrated luminosity
of about 30 fb^{-1}. It should however be stressed that this assumes that
the background from $Z \rightarrow \tau\tau$ decays in the signal region is known with a
precision of $\pm 10\%$. More studies are needed to establish that this preci-
sion can indeed be achieved. The detection of the $H \rightarrow \tau\tau$ decay mode is
particularly important for a measurement of the Higgs boson couplings to
fermions and for Higgs boson searches in MSSM scenarios [27].

11.3.3. *Higgs boson searches using the associated* $t\bar{t}H$ *production*

For low Higgs boson masses the discovery potential might be increased
by searching for the $H \rightarrow b\bar{b}$ decay mode, which has the largest branching
ratio in this mass range. Due to the huge backgrounds from QCD jet
production in this decay mode, only the associated production modes can
be used. It has already been demonstrated that the discovery potential
for a Standard Model Higgs boson in the WH production mode at the
LHC is marginal [20]. Also the extraction of a Higgs boson signal in the
$t\bar{t}H$, $H \rightarrow b\bar{b}$ channel appears to be difficult [21] and is extremely sensitive
to the precise knowledge of the large backgrounds. The strategy is to
fully reconstruct the two top quarks which calls for an excellent b-tagging
capability of the detectors. A critical item is the knowledge of the shape of
the main residual background from $t\bar{t}jj$ and $t\bar{t}b\bar{b}$ production.
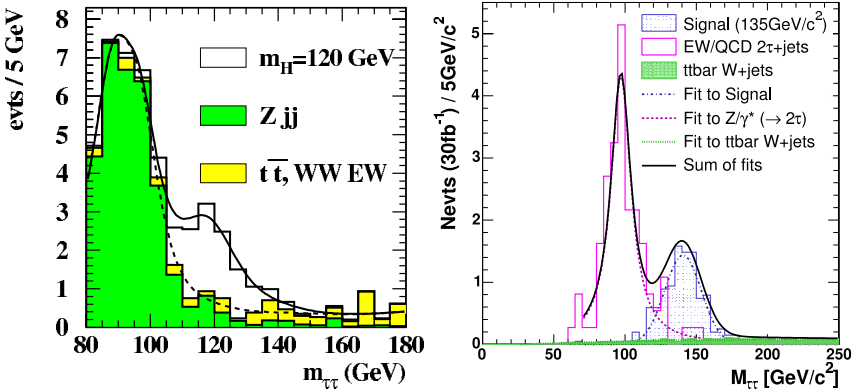
Fig. 11.5.   The reconstructed $\tau\tau$ invariant masses for a Higgs boson signal of 120 GeV/c^2 in the $e\mu$ channel in the ATLAS experiment (left) and for 135 GeV/c^2 in the ℓ-had channel in the CMS experiment (right). The signals are shown above all backgrounds after application of all cuts except the mass window cuts around the Higgs boson masses for integrated luminosities of 30 fb^{-1}.

The CMS collaboration has recently updated their studies using a more realistic simulation of the b-tagging performance of the detector [28]. In addition, explicit matrix element calculations based on the ALPGEN Monte Carlo [29] have been used to estimate the above mentioned backgrounds. It has been found that the $t\bar{t}jj$ background dominates, in addition there is a large $t\bar{t}b\bar{b}$ background and a combinatorial background (ambiguities in the association of the tagged b jets to the top quarks and Higgs boson) from the signal itself. The problem is illustrated in Fig. 11.6 where the reconstructed invariant $b\bar{b}$ mass distribution for the $t\bar{t}H \to \ell\nu b\,qqb\,bb$ signal with $m_H = 115$ GeV/c^2 and for background events is shown for the CMS experiment assuming an integrated luminosity of 30 fb^{-1}. As mentioned above, the signal significance depends strongly on the uncertainty on the absolute knowledge of the background. Only for background uncertainties below 5% — which is difficult to reach — a signal significance exceeding 2σ can be reached [28]. It is expected that the ATLAS collaboration will present updated results soon.

11.3.4.   *Combined signal significance*

The combined ATLAS Higgs boson discovery potential over the full mass range, $100 < m_H < 1000$ GeV/c^2, assuming an integrated luminosity of

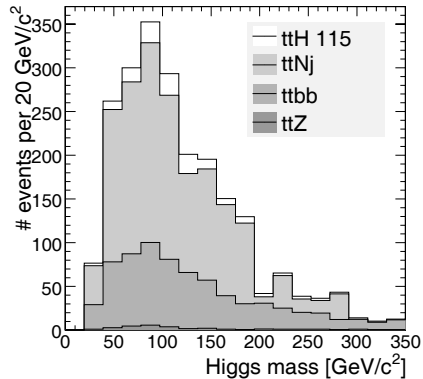Fig. 11.6. Reconstructed $b\bar{b}$ invariant mass distribution of a $ttH \rightarrow \ell\nu b\, qqb\, bb$ signal (light) with $m_H = 115$ GeV/c^2 and the background (shaded) in the CMS experiment for an integrated luminosity of 30 fb^{-1}.

30 fb^{-1} is shown in Fig. 11.7(left). The full mass range up to $\sim$1 TeV/c^2 can be covered with a signal significance of more than 5σ with several discovery channels available at the same time. The vector boson fusion channels play an important role for the discovery of a Higgs boson at the LHC. It should be noted that in the ATLAS evaluation no K-factors have been included. Updated results from the ATLAS collaboration are expected to be published soon.

A similar performance has also been established for the CMS experiment. The corresponding discovery potential is shown in Fig. 11.7(right). In this updated plot the $t\bar{t}H$ channel has no longer been included as a discovery channel.

The various discovery channels available at the LHC are complementary both from physics and detector aspects. The gluon and vector boson fusion channels test different production mechanisms. This complementarity also provides sensitivity to non-standard Higgs models, such as fermiophobic models [30].

Also from the experimental point of view the Higgs boson discovery potential at the LHC is robust. The searches are complementary in the sense that different detector components are important for different channels. The $H \rightarrow \gamma\gamma$ decays require excellent electromagnetic calorimetry. In the identification of vector boson fusion the measurement of jets, in particular the reconstruction of the forward tag jets, is essential.
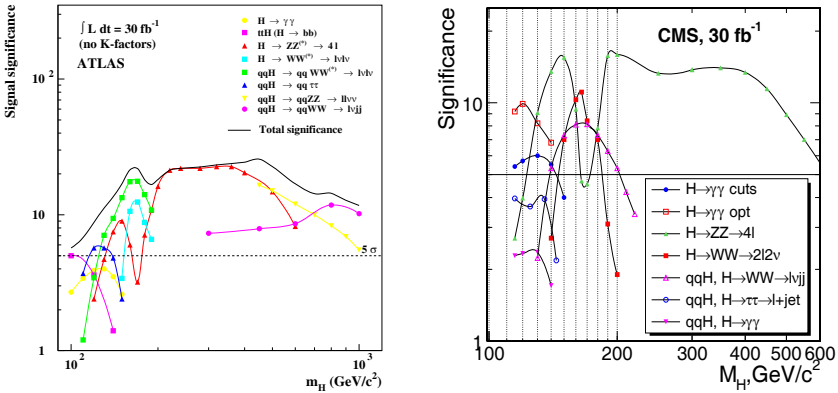
Fig. 11.7. ATLAS (left) and CMS (right) sensitivities for the discovery of a Standard Model Higgs boson for an integrated luminosity of 30 fb^{-1} over the full mass region. The signal significances are shown for individual channels, as well as for the combination of channels. Systematic uncertainties on the backgrounds have been included. The ATLAS results do not include K factors for higher order QCD corrections.

11.4. Determination of Higgs Boson Properties

The discovery of a new particle is only the first step in exploring the mechanism responsible for electroweak symmetry breaking and generation of particle masses. The confirmation of the Higgs mechanism requires the determination of quantum numbers, widths and couplings. The mass of the Higgs boson fixes completely its profile in the Standard Model. The observation of deviations from the predictions may hint towards new physics and allow to discriminate between the Higgs sector of the Standard Model and possible extensions as realised, e.g. in supersymmetric theories.

11.4.1. *Mass and total decay width*

The mass of a Higgs boson can best be measured in the decay channels $H \rightarrow \gamma\gamma$ and $H \rightarrow ZZ^{(*)} \rightarrow 4\ell$. The expected accuracy in the CMS experiment after collecting data corresponding to 30 fb^{-1} is better than 0.3% for masses smaller than about 300 GeV/c^2 taking into account statistical errors only [21]. For the ATLAS experiment, assuming an integrated luminosity of 300 fb^{-1} and taking into account in addition a systematic uncertainty on the absolute energy scale of leptons and photons of 0.1%, the precision is expected to be 0.1% for Higgs boson masses below 400 GeV/c^2 and the precision degrades to around 1% for a mass of 600 GeV/c^2 [20]. In addition,

the measurement of the mass will be possible with a larger uncertainty using the $H \to WW^{(*)}$ and $H \to \tau\tau$ decay modes.

The total decay width of the Higgs boson can only be determined directly if the mass resolution in the decay channel under consideration is comparable or smaller than the decay width itself. This restricts the direct measurement of the width in the $H \to ZZ \to 4\ell$ decay mode to larger masses. For Higgs boson masses above 270 GeV/c^2 a measurement precision of better than 8% is expected for data corresponding to 300 fb^{-1}. For Higgs boson masses below 200 GeV/c^2 the width can only be determined indirectly using additional theoretical assumptions from a global fit to all observable Higgs boson events rates [31].

11.4.2. *Partial decay widths and couplings*

In a completly model independent way only the ratios of partial widths can be extracted from the signal event rates at the LHC as no decay mode independent observation is possible and the total decay width cannot be extracted for mass values below 200 GeV/c^2 [31]. The strength of the LHC is based on the simultaneous information which, for a given Higgs boson mass, is available in the various production and decay modes. A Study has been performed where the full information of all accessible production and decay channels is used to fit the coupling parameters [31]. In this study, the correlations among the various channels as well as experimental and theoretical systematic uncertainties are taken into account.

Under the assumption that only one scalar CP-even Higgs boson exists, relative branching ratios, which are identical to ratios of partial decay widths, can be measured. The decay $H \to WW^{(*)}$ is used as normalization since it can be measured over the full intermediate mass range with a relatively small error. In Fig. 11.8(left) the expected relative errors on the measurement of ratios of Higgs boson branching ratios are shown, assuming an integrated luminosity of 300 fb^{-1}. In particular the ratios Γ_Z/Γ_W can be measured with an accuracy of the order of 10–20% for Higgs boson masses above 130 GeV/c^2.

If additional theoretical assumptions are made, information from the production can be used as well, and in particular a measurement of the top-Yukawa coupling becomes possible via the strong dependence of the gluon fusion and $t\bar{t}H$ production cross sections on this coupling [31]. Assuming that only the known particles of the Standard Model couple to the Higgs boson and that no couplings to light fermions are extremely enhanced, all
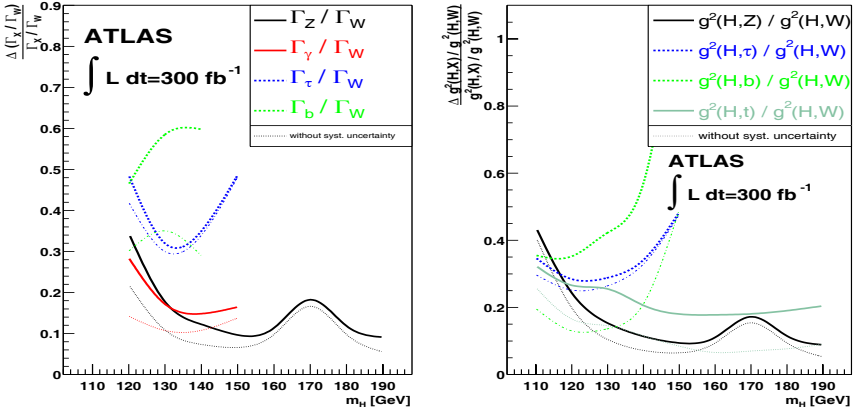
Fig. 11.8. The expected relative errors for the measurement of relative branching ratios (left) and relative couplings (right), normalized to those of the $H \to WW^{(*)}$ decay and assuming an integrated luminosity of 300 fb^{-1} for one experiment. The dashed lines give the expected relative error without systematic uncertainties.

accessible Higgs boson production and decay modes at the LHC can be expressed in terms of the Higgs boson couplings g_W, g_Z, g_t, g_b and g_τ. The production cross sections depend on the square of these couplings. The exact dependence has to be calculated theoretically and put into the fit with corresponding systematic errors. Similarly, the Higgs boson branching ratios are proportional to g^2/Γ, and again, the proportionality factors are taken from theory. In Fig. 11.8(right) the relative errors on the measurement of relative couplings are shown for an integrated luminosity of $300\,\text{fb}^{-1}$ for one experiment. Due to the large contributions of the gluon fusion and $t\bar{t}H$ production modes, the ratio of the top-Yukawa coupling to the Higgs boson coupling to W bosons can be well constrained with an estimated uncertainty of the order of 10 to 20%.

11.4.3. *Spin and CP quantum number*

The spin and CP quantum number of the Higgs boson can be inferred from the angular distributions of the leptons in the $H \to ZZ \to 4\ell$ decay mode [21, 32, 33]. The CMS collaboration has considered the case that the observed scalar boson ϕ is a mixture of a CP-even (H) and CP-odd (A) boson according to $\phi = H + \xi A$. The precision of the determination of ξ is shown in Fig. 11.9(left). Using the same observables the ATLAS collaboration has found that the hypothesis of non Standard Model CP and

spin combinations can be distinguished from the Standard Model values for masses above 250 GeV/c^2 and integrated luminosities above 100 fb^{-1} [33].
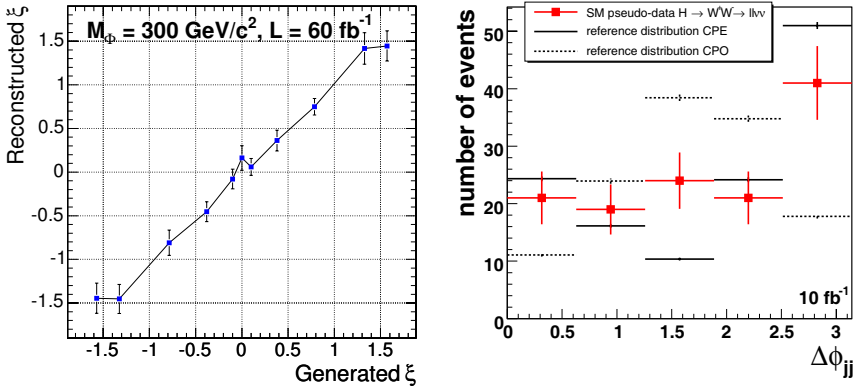

Fig. 11.9.   (Left) Expected precision for the determination of ξ (see text) for a boson ϕ with a mass of 300 GeV/c^2 in the CMS experiment assuming an integrated luminosity of 60 fb^{-1}. (Right) Expected distribution of $\Delta\phi_{jj}$ in vector boson fusion events with $H \to WW \to \ell\nu\ell\nu$ ($m_H = 160 \text{ GeV/c}^2$) in the ATLAS experiment including background for an integrated luminosity of 10 fb^{-1}.

The coupling of a scalar boson to vector bosons can be parametrised in a model independent way via three terms: a CP-even Standard Model-like contribution, which only exists if the scalar field has a non-vanishing vacuum expectation value, and CP-even and CP-odd anomalous terms. The contributions and admixtures can be determined in the vector boson fusion process using the azimuthal separation $\Delta\phi_{jj}$ of the tagging jets [34]. The expected spectra are shown in Fig. 11.9(right) for the different coupling hypotheses assuming a Higgs boson with a mass of 160 GeV/c^2 in the WW decay mode. For an integrated luminosity of 10 fb^{-1} anomalous purely CP-even or CP-odd effective couplings can be excluded with a significance of approximately 5σ. For a Higgs boson with a mass of 120 GeV/c^2 a sensitivity of 2σ can be reached for an integrated luminosty of 30 fb^{-1} using the $H \to \tau\tau$ decay mode [35].

11.5. Search for MSSM Higgs Bosons

When considering the MSSM Higgs sector the following questions are to be addressed at LHC: (i) can at least one Higgs boson be observed for the

entire model parameter space and (ii) can the MSSM be distinguished from the Standard Model by either the observation of additional Higgs bosons or via a determination of Higgs boson properties.

11.5.1. *Search for heavy MSSM Higgs bosons*

In the search for the light, Standard Model-like Higgs boson h the same channels as in the search for the Standard Model Higgs boson will be used. Heavier Higgs bosons will be searched for in additional final states. In the MSSM the associated production of neutral Higgs bosons in association with a pair of b-quarks is enhanced by $\tan\beta$ and the decay modes $H/A \to \mu\mu$ and $H/A \to \tau\tau$ provide discovery channels [20, 21]. As an example the $H/A \to \tau\tau$ signal is shown in Fig. 11.10(left), as expected in the CMS experiment on top of the background, which is dominated by Z+jet and $t\bar{t}$ events. The 5-σ discovery contours for such a search in various final states is shown in Fig. 11.10(right). Decays into τ leptons also dominate the search for charged Higgs bosons at the LHC. They can either be produced in the decay of a top quark for low masses or in the process $gb \to tH^{\pm}$ for larger masses.
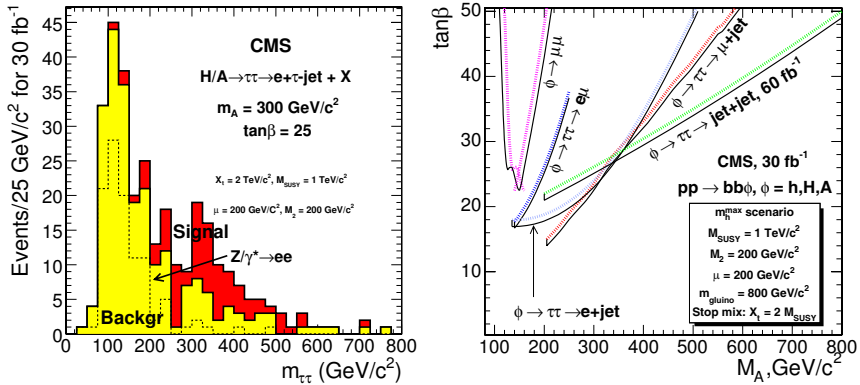

Fig. 11.10. (Left) The invariant $\tau\tau$ mass distribution for bbH/A production with $H/A \to \tau\tau \to e - had + X$. (Right) The 5σ discovery contour from the bbH/A associated production process.

11.5.2. *Discovery potential in various benchmark scenarios*

Different benchmark scenarios have been proposed for the interpretation of MSSM Higgs boson searches [36]. In the MSSM, the masses and couplings

of the Higgs bosons depend, in addition to $\tan\beta$ und m_A, on the SUSY parameters through radiative corrections. In a constrained model, where unification of the SU(2) and U(1) gaugino masses is assumed, the most relevant parameters are A_t, the trilinear coupling in the stop sector, the Higgs mass parameter μ, the gaugino mass term M_2, the gluino mass m_g and a common scalar mass M_{SUSY}. Instead of the parameter A_t, the stop-mixing parameter $X_t := A_t - \mu\cot\beta$ can be used. In particular the phenomenology of the light Higgs bosons h depends on the MSSM scenario, for which the following have been considered in a recent ATLAS study [37]:

(1) m_h-max scenario: the SUSY parameters are chosen such that for each point in the $(m_A, \tan\beta)$-parameter space a Higgs boson mass close to the maximum possible value is obtained. For fixed M_2, μ, m_{SUSY} and m_g this is achieved by adjusting the value of X_t.

(2) No mixing scenario: in this scenario vanishing mixing in the stop sector is assumed, i.e. $X_t = 0$. This scenario typically gives a small mass for the lightest CP-even Higgs boson h and is less favourable for the LHC.

(3) Gluophobic scenario: the effective coupling of the light Higgs boson h to gluons is strongly suppressed for a large area of the $(m_A, \tan\beta)$-plane. This requires large mixing in the stop sector and a small stop mass, leading to cancellations between top-quark and stop loops such that the production cross section for gluon fusion is strongly suppressed.

(4) Small α scenario: The parameters are chosen such that the effective mixing angle α between the CP-even Higgs bosons is small for a particular part of the $(m_A, \tan\beta)$-parameter space. This results in a reduced branching ratio into $b\bar{b}$ and $\tau\tau$ for large $\tan\beta$ and intermediate values of m_A.

The exact parameters for the four scenarios can be found in Refs. [36, 37]. In the evaluation of the discovery potential for the light Higgs boson h all production modes, i.e. the gluon fusion, the vector boson fusion as well as the associated $b\bar{b}h$, $t\bar{t}h$ (ATLAS) production have been used. The decay modes $h \to \gamma\gamma$, $h \to ZZ$, $qqh \to qq\tau\tau$, $qqh \to qqWW$, $qqh \to qq\gamma\gamma$, $b\bar{b}h \to b\bar{b}\,\mu\mu$ and $t\bar{t}h$ with $h \to b\bar{b}$ have been considered (for details see Ref. [37]). For the heavier Higgs bosons the decay modes mentioned above have been used. The discovery potential for the light CP-even Higgs boson in the m_h-max and in the small α scenarios is shown in Fig. 11.11 for an integrated luminosity of 30 fb^{-1}. The findings for the nomixing and the gluophobic scenarios are similar to the m_h-max scenario; only the contours from the LEP exclusion and vector boson fusion channels are shifted to higher values

of $\tan\beta$. At leading order the discovery potential is dominated by vector boson fusion with $h \rightarrow \tau\tau$ with some contributions from $bbh \rightarrow bb\mu\mu$ in the low M_A region. Since many complementary channels are available at the LHC, the loss in sensitivity due to suppressed couplings in certain benchmark scenarios can be compensated for by other channels. In the small α scenario, for example, the effect of the suppressed branching ratio into τ leptons is nicely compensated for by the bosonic decay modes of h. For large integrated luminosities, the $h \rightarrow \gamma\gamma$ and $h \rightarrow ZZ^* \rightarrow 4\ell$ channels provide additional sensitivity. In the uncovered area at low M_A
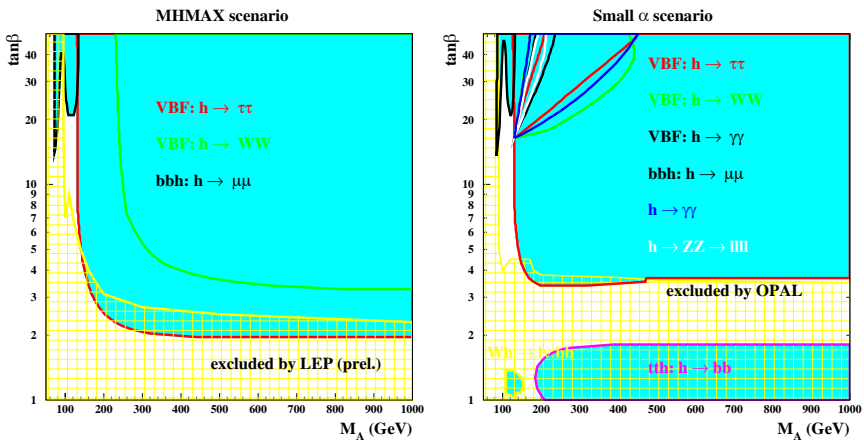

Fig. 11.11. The 5σ discovery contours for the light CP-even MSSM Higgs bosons h with ATLAS for an integrated luminosity of 30 fb^{-1} in the m_h-max (left) and small α scenario (right). The cross hatched yellow region is excluded by searches at LEP.

the searches for heavier Higgs bosons have sensitivity, such that at least one MSSM Higgs boson would be discovered at the LHC already with a moderate integrated luminosity of 30 fb^{-1}. For the heavier Higgs bosons, the production cross sections and decay branching ratios are similar for the various benchmark scenarios, in particular for large values of m_A and hence the findings are almost identical. The overall discovery potential after collecting 30 fb^{-1} is shown in Fig. 11.12(left). In the whole model parameter space in all considered benchmark scenarios at least one Higgs boson can be discovered and for a significant part of the parameter space more than one Higgs boson can be observed allowing to distinguish between the Higgs sector of the SM and its MSSM extension via direct observation. However,

a large area at intermediate $\tan \beta$ is left where only the light Higgs boson h can be discovered. A further increase in integrated luminosity will only marginally reduce that region [38]. Some sensitivity to heavier Higgs bosons might, however, be provided via their decays into SUSY particles [27] for very specific choices of SUSY model parameters.

The observation of the light Higgs boson h in various search channels might allow a discrimination between the Standard Model Higgs sector and its extensions via the measurement of, e.g. ratios of branching ratios in the same production mode, which is advantageous as several systematic uncertainties cancel. The sensitivity of a discrimination between the Standard Model and the MSSM has been estimated using the ratio R of branching ratios measured in the vector boson fusion production mode: $R = BR(h \rightarrow \tau\tau)/BR(h \rightarrow WW)$. The red (black) area in Fig. 11.12(right) displays the regions in which Δ, defined as $\Delta = (R_{MSSM} - R_{SM})/\sigma_{exp}$ is larger than 1 (2). Here σ_{exp} denotes the expected error on the ratio R in this particular point of MSSM parameter space. Only statistical uncertainties have been taken into account and M_h is assumed to be known with high precision. A similar study, based on the analysis used in the determination of the Higgs boson couplings, reaches the same conclusion [31].

Finally it should be noted that Higgs boson decays into Standard Model particles can be strongly suppressed in certain MSSM scenarios. An example has been presented in Ref. [39], where the light Higgs boson decays predominantly into light bottom squarks leading to multijet final states. In such scenarios the detection of a light Higgs boson might be difficult at hadron colliders.

All studies discussed above have been performed assuming CP conservation in the Higgs sector. Although CP conservation is present at Born level, CP violating effects might be introduced via complex SUSY breaking parameters. As a consequence the mass eigenstates are mixtures of the CP eigenstates and a light Higgs boson with a mass below 60 GeV/c^2 may have escaped detection at LEP [40]. Preliminary studies in the so called CPX scenario [41], which maximises the CP mixing effects, indicate that there may exist uncovered regions in parameter space for low H_1 masses [40]. The exact size, shape and position of these holes depends on the precise value of the top-quark mass and on the details of the theoretical calculations [40]. A similar situation may occur in the context of the Next-to-Minimal-Supersymmetric Standard Model (NMSSM) [42]. It needs to be studied whether these scenarios can be covered at the LHC by exploiting additional search channels.
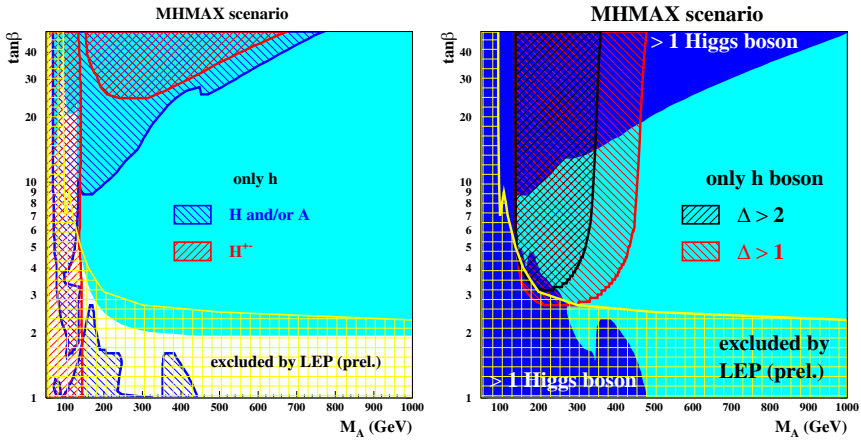
Fig. 11.12. (Left) The overall 5σ discovery potential for MSSM Higgs bosons with ATLAS at the LHC for an integrated luminosity of 30 fb^{-1} in the m_h-max scenario. In the shaded area (cyan) only the light CP-even Higgs boson h can be observed. In the blue left-hatched area the heavy neutral Higgs bosons H and/or A, and in the red right-hatched area the charged Higgs bosons $H^{\pm}$ can be detected. The cross hatched yellow region is excluded by searches at LEP. (Right) Sensitivty for the discrimination between the Standard Model and the MSSM from the measurement of Δ (see text) in the m_h-max scenario. The discovery contours are shown for a luminosity of 300 fb^{-1}, for the vector boson fusion channels only 30 fb^{-1} are assumed.

11.6. Conclusions

It has been demonstrated in numerous experimental studies that the experiments at the CERN Large Hadron Collider have a huge discovery potential for the Standard Model Higgs boson. If the Higgs mechanism is realized in nature the corresponding Higgs boson should not escape detection at the LHC. The full mass range can be explored and the Higgs boson can be detected in several decay modes. In addition, the parameters of the resonance can be measured with adequate precision to establish Higgs-boson like couplings to bosons and heavy fermions. For both the discovery and the parameter measurements the vector boson fusion mode plays an important role.

In the Minimal Supersymmetric Standard Model, Higgs bosons can be detected across the entire parameter space with a significance of more than 5σ for established CP-conserving benchmark scenarios.

References

[1] P.W. Higgs, Phys. Rev. Lett. **12** (1964) 132 and Phys. Rev. **145** (1966) 1156;
    F. Englert and R. Brout, Phys. Rev. Lett. **13** (1964) 321;
    G.S. Guralnik, C.R. Hagen and T.W. Kibble, Phys. Rev. Lett. **13** (1964) 585.

[2] ALEPH, DELPHI, L3 and OPAL Collaborations, Phys. Lett. **B565** (2003) 61.

[3] The LEP Collaborations ALEPH, DELPHI, L3 and OPAL, the LEP Electroweak Working Group, the SLD Electroweak and Heavy Flavour Groups, arXiv:0712.0929 (2007); updated numbers from the LEP Electroweak Working Group, August 2007,
    http://lepewwg.web.cern.ch/LEPEWWG.

[4] B.W. Lee et al., Phys. Rev. Lett. **38** (1977) 883;
    M. Quiros, *Constraints on the Higgs boson properties from the effective potential*, hep-ph/9703412;
    A. Ghinculov and T. Binoth, Acta Phys. Polon. **B30** (1999) 99.

[5] L. Maiani, G. Parisi and R. Petronzio, Nucl. Phys. **B136** (1979) 115;
    N. Cabibbo et al., Nucl. Phys. **B158** (1979) 295;
    R. Dashen and H. Neunberger, Phys. Rev. Lett. **50** (1983) 1897;
    D.J.E. Callaway, Nucl. Phys. **B233** (1984) 189;
    M.A. Beg et al., Phys. Rev. Lett. **52** (1984) 883;
    M. Lindner, Z. Phys. **C31** (1986) 295.

[6] G. Altarelli and G. Isidori, Phys. Lett. **B337** (1994) 141;
    J.A. Casas, J.R. Espinosa and M. Quiros, Phys. Lett. **B342** (1995) 171, Phys. Lett. **B383** (1996) 374;
    B. Grzadkowski and M. Lindner, Phys. Lett. **B178** (1986) 81;
    T. Hambye and K. Riesselmann, Phys. Rev. **D55** (1997) 7255.

[7] H.P. Nilles, Phys. Rep. **110** (1984) 1;
    H.E. Haber and G.L. Kane, Phys. Rep. **117** (1985) 75;
    S.P. Martin, in *Perspectives on supersymmetry*, Ed. G.L. Kane, World Scientific, (1998) 1, hep-ph/9709356.

[8] S. Heinemeyer, W. Hollik and G. Weiglein, Eur. Phys. J. **C9** (1999) 343;
    S. Heinemeyer and G. Weiglein, J. High Energy Phys. **10** (2002) 72;
    G. Degrassi, S. Heinemeyer, W. Hollik, P. Slavich and G. Weiglein, Eur. Phys. J. **C28** (2003) 133.

[9] For a recent review, see: S. Heinemeyer, J. Mod. Phys. **A21** (2006) 2659.

[10] O. Buchmüller et al. *Predictions for the lightest Higgs boson mass in the cMSSM using indirect experimental constraints*, arXiv:0707.3447.

[11] The TEVNPH working group, for the CDF and DØ experiments, *Combined CDF and DØ upper limits on Standard Model Higgs boson production*, arXiv:0712.2383.

[12] M. Spira, private communication.

[13] A. Djouadi, M. Spira and P.M. Zerwas, Phys. Lett. **B264** (1991) 440;
    S. Dawson, Nucl. Phys. **B359** (1991) 283;
    D. Graudenz, M. Spira and P.M. Zerwas, Phys. Rev. Lett. **70** (1993) 1372;

M. Spira, A. Djouadi, D. Graudenz and P.M. Zerwas, Phys. Lett. **B318** (1993) 347 and Nucl. Phys. **B453** (1995) 17;
S. Dawson and R.P. Kauffman, Phys. Rev. **D49** (1994) 2298.

[14] R.V. Harlander, Phys. Lett. **B492** (2000) 74;
R.V. Harlander, W.B. Kilgore, Phys. Rev. **D64** (2001) 013015;
S. Catani, D. de Florian, M. Grazzini, *JHEP* **0105** (2001) 025.

[15] R.V. Harlander, W.B. Kilgore, Phys. Rev. Lett. **88** (2002) 201801.

[16] C. Anastasiou, K. Melnikov, Nucl. Phys. **B646** (2002) 220.

[17] V. Ravindran, J. Smith and W.L. van Neerven, Nucl. Phys. **B665** (2003) 325.

[18] A. Djouadi, *The anatomy of electroweak symmetry breaking, I and II*, hep-ph/0503172 and hep-ph/0503173;
R. Harlander, Acta Phys. Polonica **B38** (2007) 693.

[19] A. Djouadi, J. Kalinowski and M. Spira, Comput. Phys. Commun. **108** (1998) 56;
A. Djouadi, M. Spira and P. M. Zerwas, Z. Phys. **C70** (1996) 427.

[20] ATLAS Collaboration, *Detector and Physics Performance Technical Design Report*, CERN/LHCC/99-15 (1999).

[21] CMS Collaboration, *CMS Physics Technical Design Report, Vol II: Physics Performance*, CERN/LHCC/2006-021 (2006), J. Phys. G: Nucl. Part. Phys. **34** (2006) 995.

[22] D.L. Rainwater and D. Zeppenfeld, J. High Energy Phys. **12** (1997) 5;
D.L. Rainwater, D. Zeppenfeld and K. Hagiwara, Phys. Rev. **D59** (1999) 014037;
T. Plehn, D.L. Rainwater and D. Zeppenfeld, Phys. Rev. **D61** (2000) 093005;
D.L. Rainwater and D. Zeppenfeld, Phys. Rev. **D60** (1999) 113004, [Erratum-ibid. **D61** (2000) 099901];
N. Kauer, T. Plehn, D.L. Rainwater and D. Zeppenfeld, Phys. Lett. **B503** (2001) 113.

[23] R. Brun and F. Carminati, CERN Program Library Long Writeup W5013 (1993).

[24] M. Dittmar and H.K. Dreiner, Phys. Rev. **D55** (1997) 167.

[25] T. Binoth, M. Ciccolini, N. Kauer and M. Krämer, J. High Energy Phys. **03** (2005) 065;
M. Dührssen, K. Jakobs, P. Marquardt and J.J. van der Bij, J. High Energy Phys. **05** (2005) 064.

[26] S.Asai et al., Eur. Phys. J. **C32** (2003) 209, hep-ph/0402254.

[27] V. Büscher and K. Jakobs, Int. J. Mod. Phys. **20** (2005) 2523.

[28] D. Benedetti et al., J. Phys. G: Nucl. Part. Phys. **34** (2007) 221.

[29] M. Mangano et al., J. High Energy Phys. **07** (2003) 001.

[30] see for example: L. Brücher, R. Santos, Eur. Phys. J. **C12** (2000) 87 and references therein.

[31] M. Dührssen, *Prospects for the measurement of Higgs boson coupling parameters in the mass range from 110 - 190* GeV/c^2, ATLAS note, ATL-PHYS-2003-030;
M. Dührssen et al., Phys. Rev. **D70** (2004) 113009.

[32] J. R. Dell'Aquila and C. A. Nelson, Phys. Rev, **D33** (1986) 101;
A. Skold and P. Osland, Phys. Lett. **B329** (1994) 305;
S. Y Choi, D. J. Miller, M. M Muhllleitner and P. M. Zerwas, Phys. Lett. **B553** (2003) 6;
R. M. Godbole, D. J. Miller and M. M. Muhlleitner, JHEP **0712** (2007) 031;
P. S. Bhupal, A. Djouadi, R. M. Godbole, M. M. Muhlleitner and S. D. Rindani, arXiv:0707.2878.

[33] C. P. Buszello et al., Eur. Phys. J. **C32** (2004) 209.

[34] T. Plehn, D. Rainwater and D. Zeppenfeld, Phys. Rev. Lett. **88** (2002) 051801.

[35] C. Ruwiedel et al., Eur. Phys. J. **C51** (2007) 385.

[36] M. Carena, S. Heinemeyer, C.E. Wagner and G. Weiglein, Eur. Phys. J. **C26**, (2003) 601.

[37] M. Schumacher, *Investigation of the discovery potential for Higgs bosons in the CP-conserving MSSM with the ATLAS detector at the LHC*, hep-ph/0410112.

[38] G. Azuelos et al., J. Phys. G: Nucl. Part. Phys. **28** (2002), 2453.

[39] E.L. Berger, C.W. Chiang, J. Jiang, T.M.P. Tait and C.E.M. Wagner, Phys. Rev. **D66** (2002) 095001.

[40] E. Accomando et al., *Workshop on CP studies and non-standard Higgs physics*, arXiv:hep-ph/0608079.

[41] M. Carena et al., Phys. Lett. **B495** (2000) 155.

[42] H. P. Nilles, M. Srednicki and D. Wyler, Phys. Lett. **B124** (1983) 337;
J. M. Frere, D. R. T. Jones and S. Raby, Nucl. Phys. **B222** (1983) 11;
J. R. Ellis, J. F. Gunion, H. E. Haber, L. Roszkowski and F. Zwirner, Phys. Rev. **D39** (1989) 844;
M. Drees, Int. J. Mod. Phys **A4** (1989) 3635;
U. Ellwanger, M. Rausch de Traubenberg and C. A. Savoy, Phy. Lett. **B315** (1993) 331;
S. F. King and P. L. WHite, Phys. Rev. **D52** (1995) 4183;
U. Ellwanger, J.G. Gunion and C.Hugonie, JHEP **0507** (2005), 041.

Chapter 12

A Review of Spin Determination at the LHC

Lian-Tao Wang[*] and Itay Yavin[†]

Joseph Henry Laboratories, Princeton University
Princeton, New Jersey 08544
[*]*lianwang@princeton.edu*
[†]*iyavin@princeton.edu*

Spin measurement is crucial in distinguishing major scenarios of TeV scale new physics once it is discovered at the LHC. We give a brief survey of methods of measuring the spin of new physics particles at the LHC. We focus on the case in which a long lived massive neutral particle is produced at the end of every cascade decay and escape detection. This is the case for R-parity preserving supersymmetry, Little Higgs models with T-parity, extra-dimensional models with KK-parity, and a large class of similar models and scenarios. After briefly commenting on measuring spin by combining mass and rate information, we concentrate on direct measurement by observing angular correlations among decay products of the new physics particles. We survey a wide range of possible channels, discuss the construction of possible correlation variables, and outline experimental challenges. We also briefly survey the Monte-Carlo tools which are useful in studying such correlations.

12.1. Introduction

Most models of TeV scale new physics are motivated by solving the hierarchy problem. Therefore, the most crucial ingredient of all of them is the mechanism of cancelling the quadratically divergent correction to the Higgs mass within the Standard Model. In order to achieve this, a set of new physics particles with the same or similar gauge quantum numbers as the Standard Model particles are introduced, whose couplings to the Higgs are related to those of the Standard Model particles. This "partner"-like structure of new physics is very generic in large classes of new physics

scenarios. Well-known examples include the set of superpartners in low energy supersymmetry [1] (for a recent review see Ref. [2]), KK excitations in extra-dimensional models [3], as well as similar states in little Higgs models [4] (Ref. [5] provides a brief review).

Due to the similarities in gauge quantum numbers, initial LHC signatures of new partners are very similar, as they can decay into the same set of observable final state particles. The mass spectra of different scenarios can be chosen to produce similar dominant kinematical features, such as the p_T distribution of the decay product. For example, a typical gluino decay chain in supersymmetry is $\tilde{g} \to q\bar{q} + \tilde{N}_2$ followed by $\tilde{N}_2 \to \ell\ell + \tilde{N}_1$. A similar decay chain in universal extra-dimension models [3] with KK-gluon ($g^{(1)}$), KK-W ($W_3^{(1)}$) and KK-photon ($\gamma^{(1)}$), $g^{(1)} \to q\bar{q}W_3^{(1)}$ followed by $W_3^{(1)} \to \ell\bar{\ell}\gamma^{(1)}$, gives identical final states since both $\tilde{N}_1$ and γ^1 are neutral stable particles which escape detection. The mass spectra of both supersymmetry and UED can be adjusted in such a way that the p_T of the jets and leptons are quite similar.

Some of the similarities in the LHC signature are actually the result of equivalences in low energy effective theory at collider scales. For example, it is known that "theory space" motivated little Higgs models are equivalent to extra-dimensional models in which Higgs is non-local in the bulk, via deconstruction [6–8]. Therefore, they can actually be described by the same set of low energy ($\sim$ TeV) degrees of freedom. An important feature of this class of models is that the partners typically have the same spin as their corresponding Standard Model particles.

However, the difference between this set of models and low energy supersymmetry is physical and distinguishable with a sufficiently precise measurement. In particular, the spin of superpartners differ from their Standard Model counter parts by half integers. Therefore, a crucial measurement to set these scenarios apart is to measure the spin of any new physics particles.

The conventional way of measuring the spin of a new particle involves reconstruction of its rest frame using its decay products and studying the angular distribution about the polarization axis. For example, in process $e^+e^- \to Z \to \mu^+\mu^-$, the $1 + \cos^2\theta$ distribution of the muon direction in the rest frame of the Z reveals its vector nature. Unfortunately, in most new physics scenarios of interest such a strategy is complicated by the generic existence of undetectable massive particles. Motivated by electroweak precision constraints and the existence of Cold Dark Matter, many such scenarios incorporate some discrete symmetry which guarantees the existence of a lightest stable neutral particle. Well-known examples of such

discrete symmetries include R-parity in supersymmetry, KK-parity of universal extra-dimension models (UED) [3], or similarly, T-parity in Little Higgs Models [9–12]. The existence of such a neutral particle at the end of the decay chain results in large missing energy events in which new physics particles are produced. This fact helps to separate them from the Standard Model background. On the other hand, it also makes the spin measurement more complicated because it is generically impossible to reconstruct the momentum, and therefore the rest frame, of the decaying new physics particles.

There are two different approaches to measuring spin. First, given the same gauge quantum numbers, particles with different spin usually have very different production rates, due to the difference between fermionic and bosonic couplings and the number of degrees of freedom. Such an approach could be useful, in particular initially, for colored particles due to their large (hence more measurable) production rates. However, a crucial ingredient in such a strategy is the measurement of the masses of particles produced, as rate can only provide definitive information once the mass is fixed. Such an effort is made more difficult owing to the existence of missing massive particles. There is some residual model dependence since, for example, a couple of complex scalars can fake a dirac fermion.

The second approach, is the direct measurement of spin through its effect on angular correlations in decay products. In the absence of a reconstructed rest frame, one is left to consider Lorentz invariant quantities which encode angular correlations. As we will see later in this review, spin correlations typically only exist in certain type of decays. Furthermore, new physics particles are frequently pair produced with independent decay chains containing similar particles. Therefore, a valid spin correlation measurement requires the ability to identify a relatively pure sample of events where we can isolate certain decay chains and suppress combinatorics effectively. Therefore, except for very special cases, we expect this measurement will require large statistics. At the same time, as will be clear from our discussion, using the appropriate variables and correctly interpreting the measured angular distribution frequently requires at least a partial knowledge of the spectrum and the gauge quantum numbers. Obtaining information about the spectrum and the quantum numbers is likely to require a somewhat lower integrated luminosity than spin measurements do. Therefore, the order with which we uncover the properties of new particles is congruent to the order with which we must proceed in the first place to correctly establish these properties. Thus, we should clearly focus on

mass scales, branching ratios and gauge quantum numbers first, once new physics is discovered at the LHC, while keeping an unbiased perspective towards the underlying model. More refined measurements, such as the ones described in this review, will enable us to tell the different models apart thereafter. Such measurements can be useful and even more powerful in a linear collider as was recently proposed in Ref. [13]. In this review we will concentrate on methods applicable to the LHC.

In principle, the production of particles with different spins leads to distinguishable angular distributions. This was investigated in the context of linear colliders in Ref. [14]. A similar measurement using the process $pp \to \tilde{\ell}\tilde{\ell}^\star$ at the LHC has been studied in Ref. [15]. An analogues measurement in the production of colored states is more challanging. First, typically several different initial states and partial waves can contribute to the same production process. Therefore, it is difficult to extract spin information from the resulting angular distribution in a model independent way. Second, as commented above it is difficult to reconstruct the direction of the original particles coming out of the production vertex. As a result, angular distributions are further washed out.

In the rest of this review, we will survey both of these approaches with slightly heavier emphasis given to the angular correlation technique. For concreteness, we will compare supersymmetry with another generic scenario in which the partners, such as gluon partner g', W-partner W', quark partner q', etc., have the same spin as their corresponding Standard Model particles. As was pointed out above, this generic scenario effectively parameterizes almost all non-SUSY models which address the hierarchy problem.

Spin measurement at the LHC is still a relatively new field where only first steps towards a comprehensive study have been taken. We will briefly summarize these developments in this review. We will focus here on the theoretical foundations and considerations relevant for the construction of observables. The potential for measuring spin in many new decay channels remains to be studied. Important effects, such as Standard Model background and large combinatorics, deserve careful further consideration. We outline these issues in connection to particular channels below.

12.2. Rate and Mass Measurement

The total cross section might serve as an initial hint to the spin of the new particles discovered [16]. Due to differences in the number of degrees of freedom, the couplings, spin-statistics and angular momentum conservation,

particles with different spin have very different cross-sections. Two examples of such differences are shown in Fig. 12.1. Therefore, if we could measure the mass of the new physics particles, it will provide us with a good measurement of the spin. Notice that many factors, such as the uncertainties in Parton Distribution Functions, total integrated luminosity, as well as the detector and cut efficiencies have to be taken into account to extract production rates at the LHC. Such difficulties could in principle be addressed with more detailed study and probably higher statistics. A sizable error bar on the production rate, say a factor of two, will not seriously affect these results since the rate in different scenarios are very different (see Fig 12.1) due to the quantized nature of the spin.
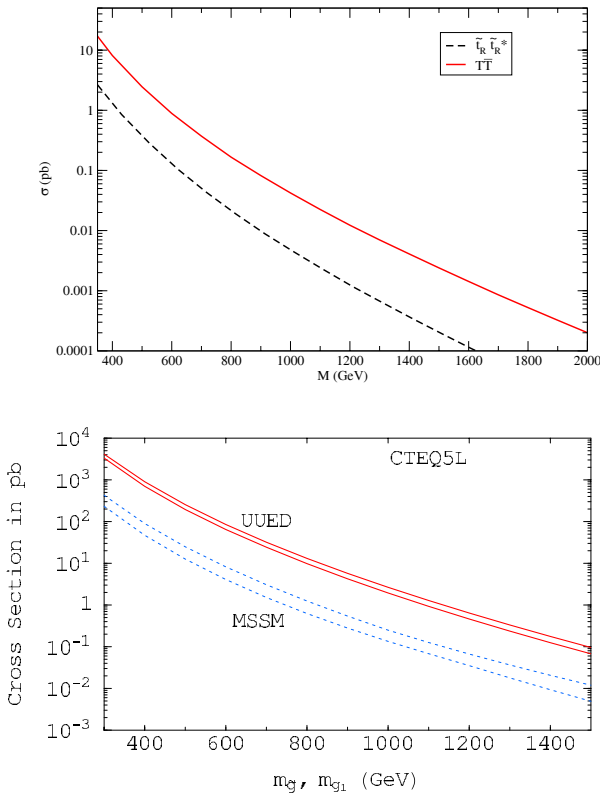

Fig. 12.1. Examples of the production rates of new physics particles. Top panel: the rate of Dirac fermion top partner vs right-handed stop (complex scalar) [12]. Bottom panel: the rate of KK-gluon vs gluino (Majorana fermion) [16].

Certain model dependence is inevitable in this approach. For example, a fermion can be faked by two closely degenerate scalars. A potentially more serious problem is the model dependence in extracting production rates from observations. What we actually measure is the production rate multiplied by a some branching ratio into the particular set of final states we observe. Such branching ratios could easily vary by one order of magnitude over the parameter space of a certain scenario. Therefore, a straightforward extraction of rate information can only be achieved in the cases where the branching ratio is simple and largely model independent. This is in principle well motivated since there are many examples in which a single channel dominates a one step decay process. It is also true when the coupling is simple and known, such as the decay of some colored particle. However, in more complicated cases and longer decay chains, more information is necessary to extract information about the production rate.

Moreover, such a determination is only possible if we could measure the masses of the particle using kinematical information. As demonstrated in Refs. [12, 17], typical "transverse" kinematical observables are not sensitive to the absolute mass of particles. One can only deduce the mass difference between the decaying particle and the neutral particle escaping the detector. If this is all the information one can extract, there are clearly ambiguities in interpreting data in terms of an underlying model. For example, suppose supersymmetry is the correct model for TeV scale new physics, and we have observed gluino production at the LHC, $pp \rightarrow \tilde{g}\tilde{g}$, followed by $\tilde{g} \rightarrow q\bar{q}+$ LSP. By assuming supersymmetry, we can find the gluino mass $M_{\tilde{g}}$ and LSP mass M_{LSP} which give rise to the measured rate and mass difference $\Delta m = M_{\tilde{g}} - M_{\mathrm{LSP}}$. However, there is also, for example, a UED scenario in which KK-gluon with higher mass have the same production rate. It follows a similar decay chain $g^1 \rightarrow q\bar{q}+$ LKP. We can adjust the mass of the LKP so that $M_{g^1} - M_{\mathrm{LKP}} \sim \Delta m$ at which point this model results in the same experimental observables at the LHC. Notice that in order for this degeneracies to exist, the only requirement is that the observables are only functions of Δm, even if the functions are different for different scenarios. Of course, we expect detailed measurement at the LHC to yield more than just the mass difference. With some assumptions regarding the underlaying model there are more subtle kinematical observables which, in combination with the rate information, could determine the spin [17]. To what extent this could be generalized to a broader classes of new physics particles deserves further study.

Recently, several methods have been proposed to measure the mass of new physics particles directly [18–24]. A detailed discussion of these methods is beyond the scope of this review. Combined with a rate measurement, such determination of mass will certainly provide an important measurement of the spin within the context of a certain (possibly well motivated) model. We expect such information to be complementary to the angular correlations we are about to discuss next. The detailed comparison between them with the effect of fully realistic Standard Model background and detector effects included has yet to be carried out.

12.3. Angular Correlations in a General Decay Topology

The decay topology we will be interested in is shown in Fig. 12.2: A heavy partner, X, decays into a SM particle with momentum p_1 and another partner Y. Y subsequently decays into a second SM particle with momentum p_2 and a third heavy partner, Z which may or may not be stable. For most of the discussion we will assume that Y is produced on-shell, but it is important to keep in mind that this same topology may still apply even for 3-body decays where the intermediate particle is off-shell (we will explore this possibility in Sec. 12.7). If Y is indeed on-shell, it is straightforward to show that the differential decay width is simply a polynomial in $t_{12} = (p_1 + p_2)^2$ of degree $2s$, with s being the spin of Y (for details see [25]),

$$\frac{d\Gamma_{X \to p_1\ p_2\ Z}}{dt_{12}} = a_0 + \ldots + a_{2s}t_{12}^{2s} \qquad \text{where} \quad t_{12} = (p_1 + p_2)^2. \quad (12.1)$$

We have chosen to use the variable $t_{12} = m_{12}^2$, rather than invariant mass m_{12}. While they are equivalent in principle, distribution of t_{12} is more convenient to interpret since it is linear in $\cos\theta_{12}$.

The observed distribution often deviates from this simple relation because of both experimental and theoretical reasons. First, if the intermediate particle Y is not polarized, there is no hope of seeing any angular correlations, i.e. the polynomial is simply a constant. Second, if it is a fermion then polarizing it is not enough and we need its decay to distinguish handedness. This leads us to some simple necessary conditions for the existence of angular correlations [25]:

- If the intermediate particle Y is a vector-boson then $M_Y \ll M_X$ so that it is longitudinally dominated and hence polarized.

- If the intermediate particle is a Dirac fermion then both vertices in the topology of Fig. 12.2 must be at least partially chiral.[a]
- If the intermediate particle is a Majoranna fermion then one must be able to determine the charge of the outgoing particles, p_1 and p_2 (even if only statistically).
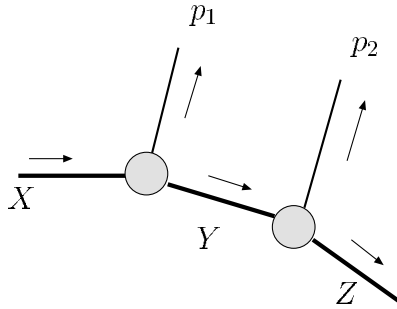

Fig. 12.2. The topology for a generic decay where spin information may be found. A heavy particle X decays into a SM particle with momentum p_1 and a heavy partner Y of spin s. Y subsequently decays into another SM particle with momentum p_2 and an invisible particle Z. If Y is on-shell then the differential decay width for this process is a polynomial of order $2s$ in the relativistically invariant variable $t_{12} = (p_1 + p_2)^2$.

Based on these simple rules it is straightforward to list the different decay channels that may contain spin effects in the MSSM and other scenarios. In what follows, we divide these channels into those which probe the spin of the Electroweak gauge-bosons and Higgs sector partners and those which probe the spin of the matter sector partners. In certain cases additional information of the spin correlations can be used to determine the spin of the external particles, X and Y in Fig. 12.2. As we show below it can lead to a full spin determination of every new physics particle involved in a decay chain.

12.4. Mis-Pairing and Background

Common to all attempts of establishing angular correlations is the problem of mis-pairing. The generic process shown in Fig. 12.2 is usually a part of a longer decay chain involving more final state particles. Moreover,

---

[a]We will see below that there is possibly an additional subtle kinematical suppression if the fermion consequently decays into a heavy vector boson, but this is non-generic.

this decay chain itself is only one of two branches in pair production. For example, the full event may look like Fig. 12.3, which is a process commonly discussed in connection with spin determination and elaborated upon in Sec. 12.5. If we are interested in the spin of $\tilde{N}_2$ we would like to correlate the adjacent outgoing jet and lepton, e.g. q_1 and l_{near}. However, in general there are no sharp kinematical differences between the near and far leptons along the same decay chain. Similarly, it is not easy to tell which is the correct jet to pair with the lepton. Therefore, an experimental histogram of the invariant mass variable t_{12} is unlikely to follow the simple polynomial presented of Eq. (12.1). Instead we will get some shape which is composed of the polynomial structure coming from the correct pairing together with a more complicated behavior associated with the wrong pairing. This is in principle not a problem since one can fit to the result of a simulation, however, it does lead to a reduction in the relative statistical significance of the correct pairing and must be taken into account. This problem is shared by all the channels we discuss below and we will refrain from the refrain where it is self-evident.
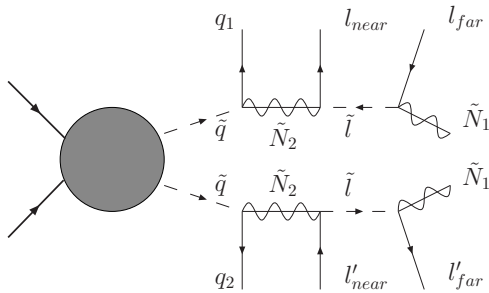

Fig. 12.3. A typical SUSY decay chain where the identification of the right pairing required for spin determination could be difficult.

We will not discuss the problems associated with Standard Model background in this review and assume that it was reduced with a strong set of cuts on missing energy, number of leptons and etc. However, even if all the events contain new physics we may still have events with different underlying topology contributing the same visible final states. We refer to such ambiguities as same model background. Before investigating spin effects we must first ascertain that the event topology is well understood. Otherwise the resulting correlations will carry little significance.

12.5. Spin Determination of Electroweak Gauge-Boson Partners

In this section we cover potential channels which may reveal the spin of heavy partners of the EW gauge-bosons and scalars (in SUSY those would be the winos, binos and higgsinos). Considering the hierarchy problem it is necessary to have the $W^\pm$ gauge-boson partners at the EW scale since the $W^\pm$ gauge-boson loop contribution to the corrections to the Higgs mass are the largest after the top quark loops. We begin with the least model dependent channel and follow with channels which involve more assumptions about the spectrum.

12.5.1. *Charged boson partner's spin — Jet-$W^\pm$ correlations*

The first channel we discuss is the minimal one in that it only assumes the presence of quark partners, charged EW bosons' partners and a stable lightest particle. This channel was first presented and investigated in Ref. [25] and later also in Ref. [26]. The relevant topology is shown in Fig. 12.4 for both SUSY and same-spin scenarios.

The differential decay width for the two processes is a polynomial in $t_{qW} = (p_q + p_W)^2$, where p_q is the momentum of the outgoing quark and p_W is that of the outgoing W gauge-boson. It is of degree 1 (2) for the SUSY (same-spin) scenario and is given by,

$$\frac{d\Gamma_{SUSY}}{dt_{qW}} = C_1(|a_L|^2 - |a_R|^2)t_{qW} + C_0 \,,$$

$$\frac{d\Gamma_{same-spin}}{dt_{qW}} = C'_2 t_{qW}^2 + C'_1 t_{qW} + C'_0$$

(12.2)

where $a_{L,R}$ are the left and right coupling of the $\tilde{N}_1^0 - \tilde{C}^+ - W^+$ vertex and the C_i's are dimensionful factors which depend only on the masses of the different particles in the decay and can be found in Ref. [25]. The expression for $d\Gamma_{SUSY}/dt_{qW}$ in Eq. (12.2) makes it evident that in the SUSY case angular correlations vanish in the non-chiral limit where $|a_L| = |a_R|$.

There are several experimental difficulties associated with this channel. First, if the $W^\pm$ decays leptonically then one must correlate the resulting lepton with the outgoing jet. Since it is impossible to fully reconstruct the gauge-boson the distribution is no longer governed by the simple formula in Eq. (12.2) (if the gauge-boson is strongly boosted in the lab frame one
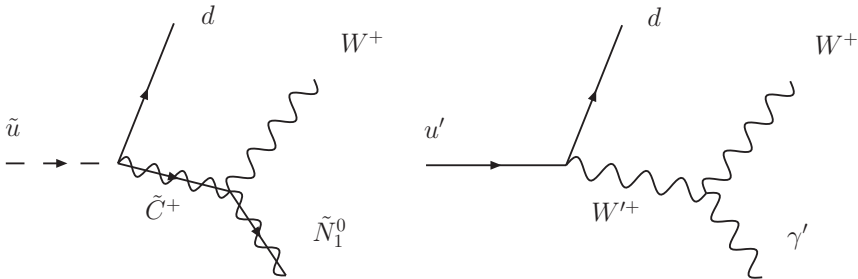
Fig. 12.4.   Topology for the decay of an up-type quark partner into a down-type quark, a W^+ gauge-boson and an invisible stable particle. On the left is the SUSY decay chain and on the right is the corresponding decay chain in a theory with same-spin partners.

may be able to extract its four-vector at least approximately). Nonetheless, preliminary studies seem to indicate that the distinction between SUSY and same-spin scenarios is still very pronounced [25].

Second, if the $W^\pm$ decays hadronically then it is important to establish how well can the $W^\pm$ be reconstructed and its momentum correlated with that of the outgoing jet. This will require a more realistic study and simulations and such an effort will benefit greatly from any help from the experimental community.

Figure 12.5 contrasts the Jet-$W^\pm$ correlation in SUSY against same-spin scenarios with quark partners at 1 TeV, vector boson partners at 500 GeV and an LSP at 100 GeV. This simulation was done including background from the same model (no SM background, though) and without any knowledge of the correct pairing. In every event one tries to reconstruct the $W^\pm$ from two of the 4 jets and then form the invariant mass t_{qW} with the two remaining jets. If more than one pairing reconstructs W it is regarded as failure and the event is discarded. The cuts involve $\displaystyle{\not}P_T > 200$ GeV and $|\eta| < 4.0$. Jets were defined with a cone size of $\Delta R = 0.4$. The linear behavior vs. the the quadratic behavior is still visible on top of the background coming from the wrong pairing and contamination from other event topologies.

This example also serves as a remainder that any observable suggested as a possible determinant of spin better result in robust differences in distributions' shapes. Any discriminator that relies on small discrepancies is unlikely to survive when the experimental limitations are properly taken into account.
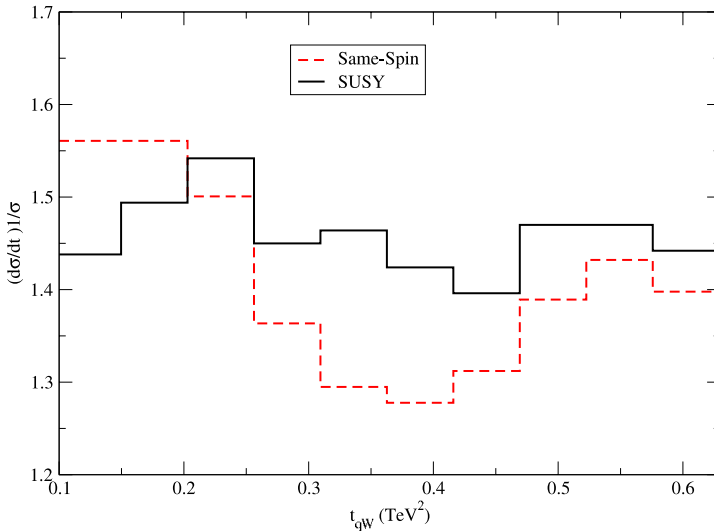
Fig. 12.5.   Considering only signal events with 2-jets and a hadronic $W^{\pm}$ this is a histogram of the invariant mass t_{qW} (see text for details concerning the reconstruction) for the two prototype models: SUSY (solid-black), Same-Spin (dashed-red). The histogram is normalized to unit area and the normalized statistical error is approximately $\sqrt{N} \sim 0.04$. The quadratic behavior of the same-spin scenario is clearly distinguished from the linear behavior associated with SUSY.

12.5.2.   *Charged boson partner's spin — Jet-Z^0 correlations*

If the spectrum contains two light charged EW bosons' partners (e.g. both Higgsino and Wino are light) then the topology shown in Fig. 12.6 is possible. With sizable branching ratio, this is a very promising decay channel because the Z^0 gauge-boson can be unambiguously reconstructed together with its four-momentum.   The differential decay width follows that of Eq. (12.2) and the prospects of determining spin using this channel are now under investigation [27]. In addition, if the underlaying model is indeed SUSY, the slope in Eq. (12.2) is sensitive to the value of $\tan \beta$. This is easy to understand if one recalls that for an intermediate Dirac fermion both interaction vertices need to be at least partially chiral. The $\tilde{q} - \tilde{C}_2 - q$ vertex is certainly chiral if the intermediate chargino is mostly a wino. The $\tilde{C}_2 - \tilde{C}_1 - Z$, however, is only chiral if $\tan \beta \neq 1$. In fact it is straightforward to show that the slope of the distribution is directly related to $\tan \beta$ and vanishes as $\tan \beta \to 1$. Since, this measurement is in principle very clean, it may offer extra information in addition to the spin of the chargino state.
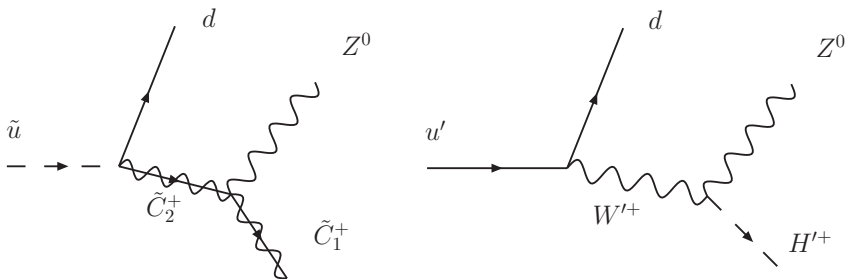
Fig. 12.6. Topology for the decay of an up-type quark partner into an up-type quark, a Z^0 gauge-boson and a charged partner. On the left is the SUSY decay chain and on the right is the corresponding decay chain in a theory with same-spin partners.

12.5.3. *Neutral boson partner's spin*

In an early and interesting paper [28], Barr has pointed out that the inherent charge asymmetry of a proton-proton collider may lead to certain angular correlations which carry spin information. This channel is known to be useful for mass determination and its sensitivity to spin was pointed out earlier in Ref. [29] and references therein. The decay topology for the SUSY case is shown in Fig. 12.7. Experimentally, the far lepton cannot be distinguished from the near lepton and one must average over both contributions. Barr found that it is possible to define an asymmetry parameter which is sensitive to the spin of the intermediate neutralino $\tilde{N}_2$,

$$\mathcal{A} = \left(\frac{d\Gamma}{dt_{ql^+}} - \frac{d\Gamma}{dt_{ql^-}} \right) \bigg/ \left(\frac{d\Gamma}{dt_{ql^+}} + \frac{d\Gamma}{dt_{ql^-}} \right) \qquad (12.3)$$

(The original asymmetry defined by Barr was with respect to the invariant mass rather than $t_{ql\pm}$, but these two definition are isomorphic).

This decay chain was further investigated by [14, 30–32] and contrasted against the corresponding decay chain in the scenario with Universal Extra Dimensions (UED) [3, 33]. As in the previous cases, this asymmetry has the opposite sign if the initial state is an anti-squark. Therefore, this observable relies on the LHC begin a proton-proton collider and is sensitive to the quark-anti-quark asymmetries in the parton distribution functions.

We remark that this channel demands the existence of light lepton partners in the spectrum. Leptonic partners at the EW scale are certainly not required in order to solve the hierarchy problem. For example, they are not present in Little Higgs models. They exist in Supersymmetric theories and
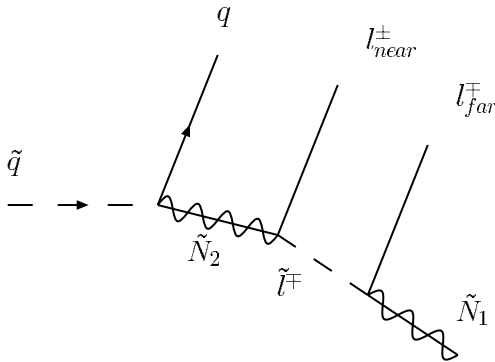
Fig. 12.7. Topology for the cascade decay of a quark into two leptons and neutral stable partner. The correlation of the quark with the near lepton reveals the spin of the intermediate neutralino $\tilde{N}_1$. However, experimentally it is hard to distinguish between the far and near lepton and one must average over both. The resulting distribution is asymmetric in the correlation of the quark with a positive versus negative leptons.

RGE effects tend to cause them to be lighter than the quark partners, but they may not necessarily be lighter than the neutralinos. Nonetheless, if they are light and the decay chain of Fig. 12.7 is allowed, it will teach us an enormous amount regarding the underlying model.

Some of the experimental difficulties associated with this channel were pointed out above already (mis-pairing and same model background). In addition, the necessity for a charge asymmetry means that gluino pair production events will tend to contaminate the signal and reduce the sensitivity due to the absence of charge asymmetry to begin with. This is also true for squark pair production if dominated by gluon-gluon initial state. In connection with this difficulty, Ref. [34] had the interesting proposal to overcome this using the distinction between b and $\bar{b}$. It may even lead to a measurement of the gluino spin with enough luminosity. However, so far this possibility has only been investigated for the parameter point SPS1a which is particularly friendly for hadron collider studies. It remains uncertain whether these conclusions can be extended to more generic spectra.

12.6. Spin Determination of Standard Model Matter Partners

In SUSY, the matter partners are scalars and therefore carry no spin information. In scenarios with same spin partners, angular correlations in

decays involving the intermediate heavy fermions are certainly possible and the conditions for such effects were elucidated in Ref. [35]. It was also noted that, in combination with the measurements discussed above, one may obtain information on the spin of the initial and final partners in the cascade. We now briefly review these findings.

The general decay topology is shown in Fig. 12.8 where the SUSY decay of a gluino is shown alongside the corresponding decay in the same-spin scenario. The differential decay width is in general given by,

$$\frac{d\Gamma_{SUSY}}{dt_{f\bar{f}}} = C_0 \qquad\qquad \frac{d\Gamma_{same-spin}}{dt_{f\bar{f}}} = C'_1 t_{f\bar{f}} + C'_0 \qquad (12.4)$$

where $t_{f\bar{f}} = (p_f + p_{\bar{f}})^2$ and the coefficients C'_1 and C'_0 are presented in Table 12.1.

As mentioned above, when the intermediate partner is a Dirac fermion the necessary conditions for the existence of angular correlations (i.e. for the coefficient C'_1 in Eq. (12.4) to be non-zero) are that both interaction vertices in Fig. 12.8 are at least partially chiral. As we will now show, it is possible to satisfy this condition with very few assumptions about the same-spin model.

First, we will assume that the members of this new sector have the same quantum numbers as the known quarks and leptons (this assumption is not necessary, but will simplify the discussion). As throughout this review, we
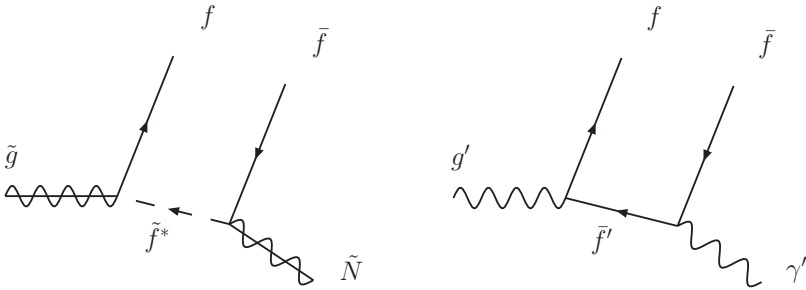

Fig. 12.8. Topology for a decay involving an intermediate matter partner. On the left is the SUSY decay of a gluino into two SM fermions and a neutralino. Since the intermediate particle is a scalar there are no angular correlations between the two outgoing fermions. On the right is the decay in a scenario with same spin partners. A heavy gluon-like particle decays into two SM fermions and a heavy neutral gauge-boson. The outgoing fermions do exhibit angular correlations owing to the fermionic nature of the intermediate heavy matter partner.

will assume that some Z_2 parity symmetry is present. In what follows we use the quark sector to demonstrate our results, but similar conclusions hold for the lepton sector as well.

SM	Heavy partners		$SU(2) \times U_Y(1)$
q_L	$Q'_L = \begin{pmatrix} u'_L \\ d'_L \end{pmatrix}$	$Q'_R = \begin{pmatrix} u'_R \\ d'_R \end{pmatrix}$	$\left(2, \frac{1}{6}\right)$
u_R	U'_R	U'_L	$\left(1, \frac{2}{3}\right)$
d_R	D'_R	D'_L	$\left(1, -\frac{1}{3}\right)$

We denote the heavy fermionic modes by $Q'_{L,R}$, $U'_{L,R}$ and $D'_{L,R}$. Here, $Q' = (u', d')$ is an $SU(2)$ doublet while U' and D' are singlets; note that Q'_L, U'_R and D'_R are partners to SM fermions while Q'_R, U'_L and D'_L have no Standard Model counterparts.

At this stage, the coupling to the SM matter is via heavy bosons (g', W' and etc.) because of the Z_2 parity. Since the SM matter sector is chiral it forces the new interaction to be chiral as well. The coupling to the heavy gluon g', for example, is schematically,

$$\mathcal{L}_{int} = \overline{Q}'_L \slashed{g}' q_L + \overline{U}'_R \slashed{g}' u_R + \overline{D}'_R \slashed{g}' d_R + h.c. \qquad (12.5)$$

where q_L is the SM electroweak doublet and u_R and d_R are the singlets.

However, for the new fermions to be parametrically heavy they must have Dirac masses in addition to the usual Yukawa coupling to the Higgs. Therefore, after EW symmetry breaking, their mass matrix is given by (in here we ignore the flavor structure to simplify the discussion),

$$\mathcal{L}_{mass,up} = \begin{pmatrix} u'_L & U'_L \end{pmatrix} \begin{pmatrix} M_Q & \lambda v \\ \lambda v & M_U\, e^{i\varphi} \end{pmatrix} \begin{pmatrix} u'_R \\ U'_R \end{pmatrix} \qquad (12.6)$$

where $v = 246$ GeV, λ is a Yukawa coupling of the new states, and φ is some phase which in general cannot be rotated away. A similar mass matrix holds for the down sector. After diagonalizing the mass matrix the mixing angle is given by,

$$\tan\theta = \frac{2\lambda v \sqrt{M_Q^2 + 2M_Q M_U \cos\varphi + M_U^2}}{\left(M_Q^2 - M_U^2\right) + \sqrt{\left(M_Q^2 - M_U^2\right)^2 + 4\lambda^2 v^2 \left(M_Q^2 + 2M_Q M_U \cos\varphi + M_U^2\right)}}.$$

$$(12.7)$$

Below, we concentrate on two limiting cases of this relation which result in very different angular correlations.

12.6.1. *Non-degenerate spectrum*

When the diagonal terms in the mass matrix are sufficiently separated, $M_Q - M_U \gg \lambda v$, the mixing between the states is small and the phase plays no role,

$$\tan \theta \sim \frac{\lambda v}{\Delta M} \quad \ll \quad 1 \tag{12.8}$$

where $\Delta M = M_Q - M_U$. When the mixing is small the interactions with the SM in Eq. (12.5) remain chiral after rotation into the mass eigenstate basis. This leads to an important conclusion: any model with heavy fermionic partners of the SM matter sector protected by some Z_2 parity (KK-parity, T-parity etc.), with a non-degenerate spectrum, exhibits angular correlations in decays.

12.6.2. *Degenerate spectrum*

We now turn to examine a degenerate spectrum, so that $M_Q - M_U \ll \lambda v$. Such a spectrum can result from any symmetry that relates left and right mass parameters. In this case the phase φ carries significance. When $\varphi = 0$ the mixing is large,

$$\tan \theta = \frac{\lambda v}{\Delta M + \sqrt{\Delta M^2 + \lambda^2 v^2}} \to 1 - \frac{\Delta M}{\lambda v}. \tag{12.9}$$

The coupling of the mass eigenstates to the SM is no longer chiral,

$$\mathcal{L}_{int} = \overline{U}'_1 \slashed{g}' u + \overline{U}'_2 \gamma_5 \slashed{g}' u \quad + \quad \mathcal{O}\left(\frac{\Delta M}{\lambda v}\right) + h.c. \tag{12.10}$$

and similarly for the other gauge couplings. Therefore, since the interactions with the SM, Eq. (12.10), are no longer chiral we expect angular correlations in decays to vanish (up to corrections of order $\mathcal{O}(\Delta M/\lambda v)$).

In the UED model, not only are the masses degenerate by construction, but also the phase is fixed by 5-d Lorentz invariance $\varphi = \pi$ as shown in Ref. [35]. In this case, unless λ is unnaturally large, the mixing is always small,

$$\tan \theta = \frac{\lambda v}{\overline{M} + \sqrt{\overline{M}^2 + v^2 \lambda^2}} \to \frac{\lambda v}{2\overline{M}} \quad \ll \quad 1 \tag{12.11}$$

where $\overline{M} = (M_Q + M_U)/2$. Therefore, as can be seen from Eq. (12.5), the interactions of the SM with U_1' and U_2' remain chiral and angular correlations should be present in decays.

This observation leads to the following conclusion: *if angular correlations are not present, or are strongly suppressed, UED model can be ruled out, but it is still possible that matter sector partners are fermions.*

12.6.3. *Slope information*

If the vertices are chiral and angular correlations are therefore present then one may extract more information out of such measurements than just the spin of the intermediate matter partner. In Table 12.1 the other possible spin assignments for the external particles in a decay involving an intermediate Dirac fermion are shown.[b] All these distributions have an edge at,

$$t_{f\bar{f}}^{(edge)} = \frac{\left(M_{g'}^2 - M_Q^2\right)\left(M_Q^2 - M_{\gamma'}^2\right)}{M_Q^2}. \tag{12.12}$$

However, depending on the spin of the external particles the slope is different and the behavior near the edge is modified. The slopes presented in the table assume no significant Left-Right mixing, such as UED or the non-degenerate case discussed above. A determination of the slope together with a measurement of the ratio $M_Q/M_{\gamma'}$ (from kinematical edges and cross-sections) can identify the spin of the external particle up to a two fold ambiguity.
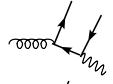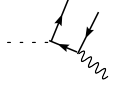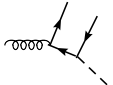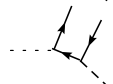
For example, if one measures a positive slope and $M_Q^2/M_{\gamma'}^2 > 2$ then one can conclude that the gluon partner is a vector-boson, but whether γ' is a scalar or a vector-boson is left unresolved. On the other hand, a positive slope together with $M_Q^2/M_{\gamma'}^2 > 2$ leads one to conclude that γ' is a scalar, but the spin of the gluon partner can be either zero or unity.

12.6.4. *Long cascade decays and total spin determination*

The cascade decay in Fig. 12.10 is an example for a decay chain where the spin of all the partners may be determined unambiguously. Suppose one measures the slope of the $b\bar{b}$ pair to be negative with $M_{B'}^2/M_{Z'}^2 < 2$ and that of the dilepton pair, $\ell^-\ell^+$, to be negative with $M_{L'}^2/M_{\gamma'}^2 < 2$ as well.

[b]The reader will undoubtedly notice that the slope vanishes as $M_Q^2 \to 2M_{\gamma'}^2$, when γ' is a vector-boson. This subtle kinematic suppression arises because the outgoing vector-boson γ' is unpolarized in this limit.

Table 12.1. If angular correlations exist between the outgoing $f - \bar{f}$ or dilepton pair, then the sign of the slope of the distribution (whether $C_1' > 0$ or $C_1' < 0$) may reveal the spin of the external particles as well as the intermediate one. In the first row we consider a scenario where the external particles are both vector-bosons (VFV). In the second row the incoming partner is a scalar whereas the outgoing partner is a vector-boson (SFV) and so forth.

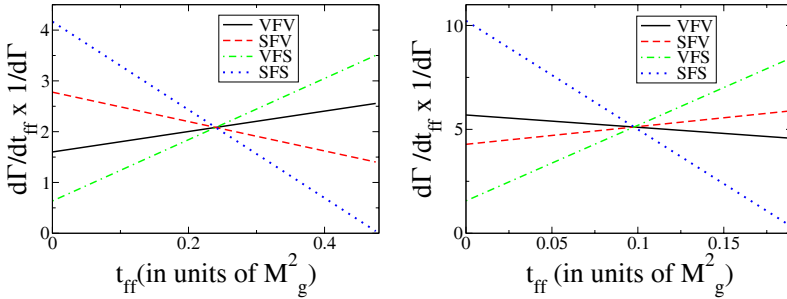| Scenario	Slope C_1'	Intercept C_0'
	$\left(2M_{g'}^2 - M_Q^2\right)\left(M_Q^2 - 2M_{\gamma'}^2\right)$	$(M_Q^4 + 4M_{\gamma'}^2 M_{g'}^2)\, t_{f\bar{f}}^{(edge)}$
	$-\left(M_Q^2 - 2M_{\gamma'}^2\right)$	$M_Q^2\, t_{f\bar{f}}^{(edge)}$
	$\left(2M_{g'}^2 - M_Q^2\right)$	$M_Q^2\, t_{f\bar{f}}^{(edge)}$
	-1	$t_{f\bar{f}}^{(edge)}$

Fig. 12.9. The resulting differential decay-width distributions corresponding to the various possibilities discussed in Table 12.1. The mass scales are in units of $M_{g'}$. The left pane corresponds to $M_Q/M_{\gamma'} = 2$ and the right one has $M_Q/M_{\gamma'} = 1.2$. Notice the change in the slope for the VFV and SFV models as this mass ratio is changed.

Then, either all three partners, g', Z' and γ', are vector-bosons, or all three are scalars. Hence, with a single spin measurement of the Z', such as described in Refs. [14, 25, 28, 30, 31], one can lift this two-fold ambiguity and determine the spin of all the particles in the event. This optimistic picture is probably far from what will be possible in practice, however, it sharply illustrates the utility of the slope at distinguishing between different possible spin assignments.
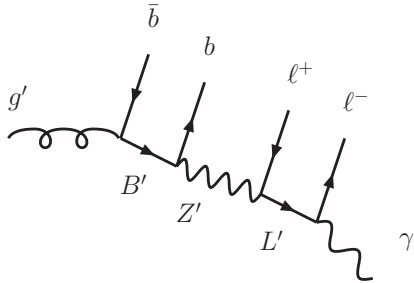
Fig. 12.10.   A long cascade decay in scenarios with same-spin partners. As explained in the text, a knowledge of the angular correlations between the $b\bar{b}$ pair and dilepton $\ell^-\ell^+$ may contain enough information to determine the spin of all the particles in the event, including g', Z' and γ'.

There is no question of reconstruction and no need for any charge asymmetry. The most urgent challenge is to identify the correct pairing. Realistic simulations and experimental input will go a long way to shed some light on the issue. Also, the ability to tag the charge of the outgoing particles in the decays discussed above could be of use. A study which will quantitatively clarify how does the signal deteriorate when such information is only partially available (b tagging) or altogether missing (jets) is in need. This will be helpful for assessing the prospects for spin determination at the LHC if matter partners are light enough to be present in the spectrum.

12.7. Off-Shell Decays

As was discussed in Ref. [25] and elaborated upon in Ref. [36], if a decay proceeds through an off-shell fermion (consider Fig. 12.8 again, but with $\bar{f}'$ being off-shell), angular correlations are guaranteed because such a fermion is inevitably polarized. This can be understood by considering the fermionic propagator for a Dirac fermion,

$$\Delta(p) = \frac{\not{p} + M}{p^2 - M^2} \, . \tag{12.13}$$

For $M \gg \not{p}$, the propagator favors one helicity structure over the other or in other words the intermediate particle is polarized. In SUSY, the intermediate particle is a scalar and no correlations are expected. The decay's kinematics are then governed by 3-body phase-space and the resulting differential decay-width is shown in Fig. 12.11. This is contrasted with the
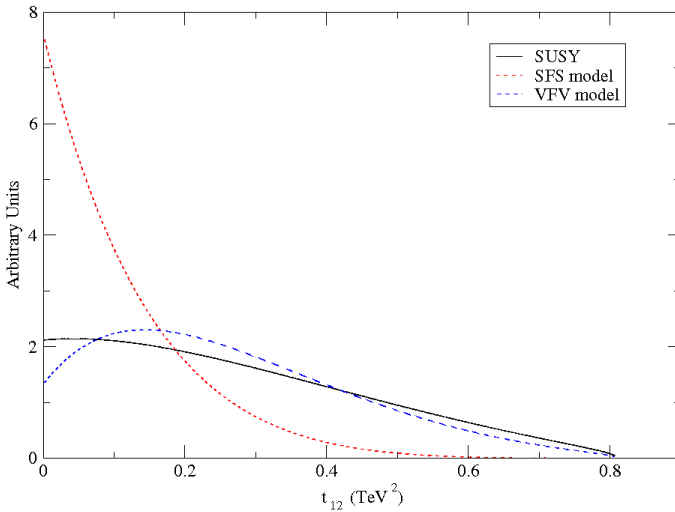
Fig. 12.11. Theoretical curves for the differential decay-width in decays of the type shown in Fig. 12.2 as a function of $t_{12} = (p_1 + p_2)^2$ for an off-shell intermediate state. The graphs are normalized to unit area. We contrast SUSY against two type of same-spin models. In SUSY, the intermediate particle is a scalar whereas the decaying particle and the LSP are Majoranna fermions i.e. the gluino and neutralino. In VFV (SFS) scenario, the intermediate particle is a Dirac fermion and the external partners are vector-bosons (scalars).

same-spin scenario where the polarized intermediate fermion affects the distribution and causes it to deviate from the phase-space prediction.

A simple example of such a decay is realized in scenarios where the matter partners are heavy, but the gluon partner can be produced directly (for an extreme realization of such a setup see Ref. [37]). It will then decay into neutral matter through an off-shell matter partner as in Fig. 12.8 (though, in the case of an intermediate off-shell state, one must be careful to include the crossed diagrams as well).

On top of the experimental difficulties mentioned above, there is one additional difficulty that must be recognized. A brief look at the distributions in Fig. 12.11 reveals that the real discrepancy between the different scenarios is concentrated in the low t_{12} region. This corresponds to the outgoing quarks being close by in real space. It is therefore susceptible to ΔR and isolation cuts and it is not even clear that such quarks will be tagged as two different jets by the jet algorithms. These effects can carve out the entire low t_{12} region and reduce the sensitivity of this observable to

spin information. These effects have been included in the study of Ref. [36], but since no jet algorithm was used, it would be important to reanalyze this channel with a more realistic simulation.

12.7.1. *Simulation tools to study spin correlations*

The amplitude for a single process is represented at tree level by several topologically distinct Feynman diagrams. The denominator for the amplitude correspodning to each diagram comes in the form of a product of simple poles. The numerator on the other hand takes into account the helicity structure of the diagram and can be written as the sum of several terms. To obtain an accurate simulation of the process one must square the full amplitude and include all the interference terms. Simulators such as CompHEP [38] and MadGraph [39] achieve exactly that albeit through slightly different routes (CompHEP offers in addition an analytic expression for the squared amplitude).

However, when interested in events with multiple final states (more than 4 or 5), it becomes too computationally demanding to proceed without an approximation. If the intermediate states within each diagram can go on-shell they will do so since such configurations receive strong support from the pole structure of the denominator. In this case, the interference terms between denominators with different poles are suppressed with respect to the leading singularities. It is then possible to approximate the full amplitude by a reduced one in which the intermediate states are set on-shell and any interference is neglected. This is the well-known narrow-width approximation and is utilized by the most widely used generators: PYTHIA [40] and Herwig [41]. This approximation of course breaks down near a threshold or when the width becomes large compared with the mass difference (in which case the notion of an isolated pole identified as a particle is meaningless to begin with). It goes without saying that in the case of an off-shell decay such an approximation is altogether invalid.

As we just saw that the narrow-width approximation ignores interference terms between topologically distinct Feynman diagrams. There may still be additional interference effects associated with the different polarizations of intermediate particles in individual Feynman diagrams. PYTHIA and Herwig differ in the way they treat these effects. In consequence of the narrow-width approximation the propagator of intermediate states is reduced to the sum over polarization and we can describe a generic matrix

element involving one propagator schematically as,

$$\langle out|prop|in\rangle = \sum_\lambda \langle out|\lambda\rangle\langle\lambda|in\rangle \tag{12.14}$$

where the sum is over the different intermediate polarizations λ. The event-generator is interested in the squared amplitude which corresponds to the probability,

$$|\langle out|prop|in\rangle|^2 = \sum_{\lambda\lambda'} \langle out|\lambda\rangle\langle\lambda'|out\rangle\langle\lambda|in\rangle\langle in|\lambda'\rangle$$

$$\equiv \sum_{\lambda\lambda'} \langle in|\lambda'\rangle \, D_{\lambda\lambda'} \, \langle\lambda|in\rangle. \tag{12.15}$$

In the last stage we defined the spin density matrix $D_{\lambda\lambda'}$ which embodies all the information carried by the numerator. Now, the spin of the initial and final state is presumably known either because we must average or sum over it. The question is what is being assumed about the density matrix and wether it is to be calculated. PYTHIA simply ignores it all together setting it to the identity matrix properly normalized. Herwig uses a clever algorithm and computes it stochastically [42, 43]. It therefore maintains full coherence as far as the spin is concerned. It was recently extended to include heavy on-shell vector-bosons (such as KK gluon states etc.) and the details are described in Ref. [25].

As mentioned above the problem in using fully coherent event generator is that it is computationally prohibitively expensive when the number of external particles exceeds a few. Events which result in many final states are unwieldy using this scheme. Recently, a new and useful tool called Bridge [44] was developed to deal with longer decay chains by making use of the narrow-width approximation. Unlike PYTHIA, Bridge does not ignore the density matrix altogether, but rather try to approximate it by computing the diagonal elements, $D_{\lambda\lambda}$, in a particular reference frame. This results in a fairly good approximation in certain cases when one of the elements is much larger than the others (such as in Top decay through an intermediate W-boson). However, it should not be expected to hold in general. In particular, since the density matrix is not Lorentz invariant, while the approximation may be valid in one reference frame it is not necessarily so in all frames. Which frame is optimal cannot be answered in full generality. It may prove useful to try and incorporate the algorithm for maintaining spin coherence used in Herwig into Bridge.

12.8. Conclusion and Outlook

We have reviewed methods of measuring the spin of new physics particles at the LHC. Such measurements are crucial in distinguishing qualitatively different classes of new physics scenarios, such as supersymmetry and Little Higgs or extra-dimensional models.

For given masses, new physics particles with similar gauge quantum numbers but different spin will typically have very different production rates.   Therefore, combining with independent measurements of their masses, their production cross-sections provide a quick determination of their spin, with minimal model assumptions. However, due to the existence of neutral stable massive particle at the end of the decay chain in many new physics scenarios, absolute mass measurement is challenging. Moreover, model dependent factors, such as decay branching ratios, have to be taken into account to extract total production rate. New method of utilizing the rate of information, such as combining production rates in several channels and using certain kinematical features which are sensitive to the overall mass scale, needs to be developed. Several new approaches of measuring absolute mass scales have been proposed recently. Their effectiveness in providing additional information in spin measurement need to be accessed.

We focus on direct and model independent ways of measuring spin using angular correlation among decay products of the new physics particles. Due to the difficulties in fully reconstructing of the restframe of the new physics particle from its decay products is difficult, we have to use Lorentz invariant combinations of momenta of the observable particles, which encode the spin information of the intermediate particles in the decay chain. We survey the potential of extracting spin information in a large class of different decay topologies. In each case, we present specific observables and discuss the conditions under which spin correlations are in principle observable.

We considered two classes of new physics particles: partners of the Standard Model gauge-bosons and partners of the Standard Model matter fermions. In both cases, understanding the masses of particles and the chiral structure of their couplings is crucial in extracting the spin information. Details of exclusive decay chains must be well understood so that the appropriate variables can be used and interpreted correctly. As illustrated in the text these issues apply directly to the gauge-boson partners. In the case of fermionic Standard Model matter partners The couplings are always chiral when the spectrum is non-degenerate. In the more subtle degenerate case the existence of spin effects depends on additional parameters. In particular

we concluded that the UED model always leads to angular correlations as a result of five-dimensional Lorentz invariance. Moreover, the slope of the resulting distributions contains additional information regarding the spin of the external particles. Its determination requires knowledge of the masses of those particles. Building on these findings, we also propose a way of measuring in principle the spin of every new physics particles in the decay chain. In the case of an off-shell decay with an intermmediate fermion, angular correlations are always present. This is an interesting direction which deserves further detailed investigation.

Since both the existence and the interpretation of the spin correlation at the LHC depends strongly on the parameters of the model under consideration, such as the mass spectrum and couplings. Therefore, we need to explore potentially useful channels and observables as much as possible. Viable strategies of extracting spin information at the LHC can only be finalized with our measurements of masses and couplings of the new physics particles. It is important to keep as much viable frameworks in mind as possible while we only have incomplete information about the new physics discovered at the LHC.

References

[1] S. Dimopoulos and H. Georgi, Softly broken supersymmetry and su(5), *Nucl. Phys.* **B193**, 150, (1981).

[2] D. J. H. Chung et al., The soft supersymmetry-breaking lagrangian: Theory and applications, *Phys. Rept.* **407**, 1–203, (2005).

[3] T. Appelquist, H.-C. Cheng, and B. A. Dobrescu, Bounds on universal extra dimensions, *Phys. Rev.* **D64**, 035002, (2001).

[4] N. Arkani-Hamed, A. G. Cohen, and H. Georgi, Electroweak symmetry breaking from dimensional deconstruction, *Phys. Lett.* **B513**, 232–240, (2001).

[5] M. Schmaltz and D. Tucker-Smith, Little higgs review, *Ann. Rev. Nucl. Part. Sci.* **55**, 229–270, (2005).

[6] N. Arkani-Hamed, A. G. Cohen, and H. Georgi, (de)constructing dimensions, *Phys. Rev. Lett.* **86**, 4757–4761, (2001).

[7] H.-C. Cheng, C. T. Hill, S. Pokorski, and J. Wang, The standard model in the latticized bulk, *Phys. Rev.* **D64**, 065007, (2001).

[8] H.-C. Cheng, C. T. Hill, and J. Wang, Dynamical electroweak breaking and latticized extra dimensions, *Phys. Rev.* **D64**, 095003, (2001).

[9] H.-C. Cheng and I. Low, Tev symmetry and the little hierarchy problem, *JHEP.* **09**, 051, (2003).

[10] H.-C. Cheng and I. Low, Little hierarchy, little higgses, and a little symmetry, *JHEP.* **08**, 061, (2004).

[11] I. Low, T parity and the littlest higgs, *JHEP.* **10**, 067, (2004).

[12] H.-C. Cheng, I. Low, and L.-T. Wang, Top partners in little higgs theories with t-parity, *Phys. Rev.* **D74**, 055001, (2006).

[13] M. R. Buckley, H. Murayama, W. Klemm, and V. Rentala, Discriminating spin through quantum interference. (2007).

[14] M. Battaglia, A. Datta, A. De Roeck, K. Kong, and K. T. Matchev, Contrasting supersymmetry and universal extra dimensions at the clic multi-tev e+ e- collider, *JHEP.* **07**, 033, (2005).

[15] A. J. Barr, Measuring slepton spin at the lhc, *JHEP.* **02**, 042, (2006).

[16] A. Datta, G. L. Kane, and M. Toharia, Is it susy? (2005).

[17] P. Meade and M. Reece, Top partners at the lhc: Spin and mass measurement, *Phys. Rev.* **D74**, 015010, (2006).

[18] H.-C. Cheng, J. F. Gunion, Z. Han, G. Marandella, and B. McElrath, Mass determination in susy-like events with missing energy, *JHEP.* **12**, 076, (2007).

[19] W. S. Cho, K. Choi, Y. G. Kim, and C. B. Park, Gluino stransverse mass. (2007).

[20] B. Gripaios, Transverse observables and mass determination at hadron colliders. (2007).

[21] A. J. Barr, B. Gripaios, and C. G. Lester, Weighing wimps with kinks at colliders: Invisible particle mass measurements from endpoints. (2007).

[22] W. S. Cho, K. Choi, Y. G. Kim, and C. B. Park, Measuring superparticle masses at hadron collider using the transverse mass kink. (2007).

[23] G. G. Ross and M. Serna, Mass determination of new states at hadron colliders. (2007).

[24] M. M. Nojiri, G. Polesello, and D. R. Tovey, A hybrid method for determining susy particle masses at the lhc with fully identified cascade decays. (2007).

[25] L.-T. Wang and I. Yavin, Spin measurements in cascade decays at the lhc, *JHEP.* **04**, 032, (2007).

[26] J. M. Smillie, Spin correlations in decay chains involving w bosons, *Eur. Phys. J.* **C51**, 933–943, (2007).

[27] A. Hook, L. Wang, and I. Yavin, to be published.

[28] A. J. Barr, Using lepton charge asymmetry to investigate the spin of supersymmetric particles at the lhc, *Phys. Lett.* **B596**, 205–212, (2004).

[29] P. Richardson, Spin correlations in monte carlo simulations, *JHEP.* **11**, 029, (2001).

[30] J. M. Smillie and B. R. Webber, Distinguishing spins in supersymmetric and universal extra dimension models at the large hadron collider, *JHEP.* **10**, 069, (2005).

[31] A. Datta, K. Kong, and K. T. Matchev, Discrimination of supersymmetry and universal extra dimensions at hadron colliders, *Phys. Rev.* **D72**, 096006, (2005).

[32] C. Athanasiou, C. G. Lester, J. M. Smillie, and B. R. Webber, Distinguishing spins in decay chains at the large hadron collider, *JHEP.* **08**, 055, (2006).

[33] H.-C. Cheng, K. T. Matchev, and M. Schmaltz, Bosonic supersymmetry? getting fooled at the lhc, *Phys. Rev.* **D66**, 056006, (2002).

[34] A. Alves, O. Eboli, and T. Plehn, It's a gluino, *Phys. Rev.* **D74**, 095010, (2006).

[35] C. Kilic, L.-T. Wang, and I. Yavin, On the existence of angular correlations in decays with heavy matter partners, *JHEP.* **05**, 052, (2007).

[36] C. Csaki, J. Heinonen, and M. Perelstein, Testing gluino spin with three-body decays, *JHEP.* **10**, 107, (2007).

[37] N. Arkani-Hamed and S. Dimopoulos, Supersymmetric unification without low energy supersymmetry and signatures for fine-tuning at the lhc, *JHEP.* **06**, 073, (2005).

[38] E. Boos et al., Comphep 4.4: Automatic computations from lagrangians to events, *Nucl. Instrum. Meth.* **A534**, 250–259, (2004).

[39] F. Maltoni and T. Stelzer, Madevent: Automatic event generation with madgraph, *JHEP.* **02**, 027, (2003).

[40] T. Sjostrand, S. Mrenna, and P. Skands, Pythia 6.4 physics and manual, *JHEP.* **05**, 026, (2006).

[41] G. Corcella et al., Herwig 6.5 release note. (2002).

[42] J. C. Collins, Spin correlations in monte carlo event generators, *Nucl. Phys.* **B304**, 794, (1988).

[43] I. G. Knowles, Spin correlations in parton - parton scattering, *Nucl. Phys.* **B310**, 571, (1988).

[44] P. Meade and M. Reece, Bridge: Branching ratio inquiry / decay generated events. (2007).

This page intentionally left blank

Chapter 13

Anticipating a New Golden Age

Frank Wilczek

Center for Theoretical Physics
Department of Physics
Massachusetts Institute of Technology
Cambridge, MA 02139

The standard model of fundamental interactions is remarkably success-ful, but it leaves an unfinished agenda. Several major questions seem ripe for exploration in the near future. I anticipate that the coming decade will be a Golden Age of discovery in fundamental physics.

13.1. Where We Stand

13.1.1. *Celebrating the standard model*

At present, the standard model of particle physics stands triumphant. It has survived testing far beyond the range of energies for which it was crafted, and to far greater precision.

Even the "ugly" parts look good. Unlike the gauge part of the standard model, whose parameters are few in number (namely, three) and have a beautiful geometric interpretation, the part dealing with fermion masses and mixings contains many parameters (about two dozen in the minimal model) that appear merely as abstract numbers describing the magnitudes of Yukawa-type couplings of one or more hypothetical Higgs fields. In the present state of theory all these numbers must be taken from experiment. Nevertheless, the framework is very significantly constrained and predictive. From the underlying hypotheses of renormalizable local quantum field theory, and three generation structure, we derive that a 3×3 unitary matrix, the CKM (Cabibbo, Kobayashi, Maskawa) matrix, must describe a multitude of *a priori* independent decay rates and mixing phenomena, including several manifestations of CP violation.

The first figure gives some sense of the rigor and power of these predictions.

Fig. 13.1.   Quantitative tests of the CKM framework, presented graphically. From [1].

Phenomena associated with neutrino masses, and with gravity, are commonly regarded as beyond, or at least outside, the standard model. Of course, where one draws the boundary of the standard model is largely a matter of taste. But it's appropriate to emphasize that our working descriptions both of neutrino masses and of gravity fit smoothly and naturally into the conceptual framework associated with the "core" standard model of strong and electroweak interactions. Specifically, neutrino masses can be accommodated using dimension 5 operators, and gravity through the

Einstein-Hilbert curvature term and minimal coupling to matter (we can also include a cosmological term). The deep guiding principles that underlie the standard model, to wit local quantum field theory based on operators of the lowest available mass dimension, also work to give theories of neutrino masses and of gravity that describe all existing observations in terms of a small number of parameters.

Altogether, the standard model supplies an economical, precise and — we now know — extraordinarily accurate description of an enormous range of phenomena. It supplies, in particular, firm and adequate foundations for chemistry (including biochemistry), materials science, and most of astrophysics. We should be very proud of what we, as a community stretching across continents and generations, have accomplished.

13.1.2. *An unfinished agenda*

But the success of the standard model, while imposing, is not complete. The standard model has esthetic shortcomings, and there are phenomena that lie beyond its scope. That combination of flaws is, ironically, full of promise. We may hope that by addressing the esthetic shortcomings, we will bring in the missing phenomena. I'll be discussing several concrete examples of that kind.

More generally, by drawing the boundaries of the known sharply, the standard model gives shape and definition to the unknown. Here is an agenda of questions that arise out of our present combination of knowledge and ignorance:

- What drives electroweak symmetry breaking?
- Do the gauge interactions unify?
- What about gravity?
- What is the dark matter?
- What is the dark energy?
- How can we clean up the messy bits?
- What else is out there?

Thanks to generous investment by the international community, and heroic work by many talented individuals, we will soon have a magnificent new tool, the Large Hadron Collider (LHC), to address many of these questions.

Of course, I don't know what we'll be finding, but I think it's possible to make some intelligent guesses, and that is what I'll be doing here. Returning to the agenda, I've highlighted in **boldface** the questions that seem ripe for decisive progress, and in *italic* the questions I think are ripe for significant progress, and left the truly obscure questions plain. These judgments emerge from the considerations that follow.

- **What drives electroweak symmetry breaking?**
- **Do the gauge interactions unify?**
- *What about gravity?*
- *What is the dark matter?*
- What is the dark energy?
- How can we clean up the messy bits?
- *What else is out there?*

13.2. Electroweak Symmetry Breaking

13.2.1. *The cosmic superconductor*

The success of the electroweak sector of the standard model teaches us that what we perceive as empty space is in reality a cosmic superconductor — not, of course, for electromagnetic fields and currents, but for the currents that couple to W and Z bosons. We do not know the mechanism or the substrate — i.e., what plays the role, for this cosmic superconductivity, that Cooper pairs play for ordinary metallic superconductivity. No presently known form of matter can play that role, so there must be more.

13.2.2. *Minimal model and search*

The most economical assumption about what's missing, measured by degrees of freedom, is incorporated in the minimal standard model. In this minimal model, besides the known fermion and gauge fields, we introduce a complex scalar $SU(2)$ doublet "Higgs" field. Of the four quanta this complex doublet brings in, three have been observed: the longitudinal components of the W^+, W^- and Z bosons. The remaining $\frac{1}{4}$ of the quartet is the so-called Higgs particle.

The Higgs particle has been a target of experimental search for many years now, so elaborate discussion is superfluous here. Let me just present an icon (Fig. 13.2):
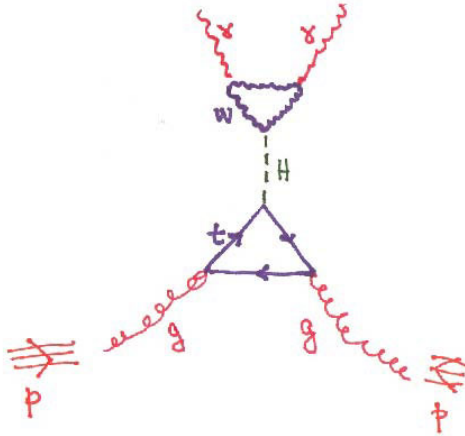
Fig. 13.2. A proposed mechanism for production and observation of the Higgs particle. It is a purely quantum-mechanical process that brings in every portion of the standard model.

This figure depicts an important search mode for the Higgs particle: production through gluon fusion, followed by decay into two photons. The phrase "Yesterday's sensation is today's calibration" conveys the pioneering ethos that is a glory of our community, but it is good on occasion to step back and appreciate how far we have come. The description of this process, leading from colliding protons to resonant $\gamma\gamma$ production, brings in every sector of the standard model, including such profundities as the gluon structure of protons, the universal color coupling of QCD, the basic Higgs couplings proportional to mass, and the electroweak Yang-Mills vertex. Moreover, this process is purely quantum-mechanical, twice over. Each of its two loops indicates that a quantum fluctuation has occurred; interaction with virtual particles is essential both for the production and for the decay. Yet we claim to understand this rare, involved, and subtle process well enough that we can calculate its rate, and distinguish it from many conceivable backgrounds. It is an impressive calibration, indeed. With any luck, it will become tomorrow's sensation!

13.3. Unification and Supersymmetry

13.3.1. *Unification of charges*

The structure of the gauge sector of the standard model gives powerful suggestions for its further development.

The salient features of the gauge sector of the standard model are displayed in Fig. 13.3.

Fig. 13.3.   The groups and multiplets of the standard model. Esthetic defects: there are three separate gauge groups, and corresponding couplings; five independent fermion multiplets (not counting family triplication); and peculiar hypercharge assignments tailored to experiment.

The gauge theories of strong and electroweak interactions successfully describe a vast amount of data quantitatively, in terms of a very small number of input parameters (i.e., just three continuous ones). Thus these theories are economical, as well as precise and accurate. They appear to represent Nature's last word, or close to it, on an enormous range of phenomena.

Yet there is room for improvement. The product structure $SU(3) \times SU(2) \times U(1)$, the reducibility of the fermion representation, and the peculiar values of the hypercharge assignments all suggest the possibility of a larger symmetry, that would encompass the three factors, unite the representations, and fix the hypercharges. The devil is in the details, and it is not at all automatic that the observed, complex pattern of matter will fit

neatly into a simple mathematical structure. But, to a remarkable extent, it does. The smallest simple group into which $SU(3) \times SU(2) \times U(1)$ could possibly fit, that is $SU(5)$, fits all the fermions of a single family into two representations $(\mathbf{10} + \mathbf{\bar{5}})$, and the hypercharges click into place.

As displayed in Fig. 13.4, a larger symmetry group, $SO(10)$, fits these and one additional $SU(3) \times SU(2) \times U(1)$ singlet particle into a single representation, the spinor $\mathbf{16}$. That additional particle is actually quite welcome. It has the quantum numbers of a right-handed neutrino, and it plays a crucial role in the attractive "seesaw" model of neutrino masses. (See below, and for a more extended introduction to these topics see [2].)

Perhaps most remarkably, according to this extended symmetry hypercharge assignments are no longer arbitrary and unrelated to the color and weak charges. The formula

$$Y \;=\; -\frac{1}{6}(R + W + B) + \frac{1}{4}(G + P) \tag{13.1}$$

relating hypercharge Y, color charges R, W, B and weak charges G, P is a consequence of the symmetry. With it, the loose end hypercharge assignments of the standard model join the central thread of unification.

13.3.2. *Unification of couplings*

Unification of charges within $SO(10)$, or alternative (closely related) symmetry groups, displays a marvelous correspondence between the physically real and the mathematically ideal. At first sight, however, its application to reality seems to fail quantitatively. For the unification of quantum numbers, though attractive, remains purely formal until it is embedded in a physical model. To do that, one must realize the enhanced symmetry in a local gauge theory. But nonabelian gauge symmetry requires universality. The $SO(10)$ symmetry requires that the relative strengths of the $SU(3) \times SU(2) \times U(1)$ couplings must be equal, which is not what's observed.

Fortunately, there is a compelling way to save the situation. If the higher symmetry is broken at a large energy scale (equivalently, a small distance scale), then we observe interactions at smaller energies (larger distances) whose intrinsic strength has been affected by the physics of vacuum polarization, and those distorted couplings need not be equal. The running of couplings is an effect that can be calculated rather precisely, in favorable cases (basically, for weak coupling). Given a definite hypothesis about the particle spectrum, we get a definite prediction for the distortion of couplings, which we can compare with observation. In this way we can test,

Fig. 13.4. The extended symmetry $SO(10)$ incorporates $SU(3) \times SU(2) \times U(1)$ as a subgroup. The five disparate fermion representations of the standard model gauge sector are united within a single internal-space spinor **16**. The spinor contains one additional degree of freedom, which plays an important role in the theory of neutrino masses. Hypercharge assignments are now related to weak and strong color charges.

quantitatively, the idea that the observed couplings derive from a single unified value.

Results from these calculations are tantalizing. If we include vacuum polarization from the particles we know about in the minimal standard model, we find approximate unification [3]. This is displayed in Fig. 13.5.

Though the general trends are encouraging, the different couplings do not become equal within the experimental uncertainty. Were we to follow
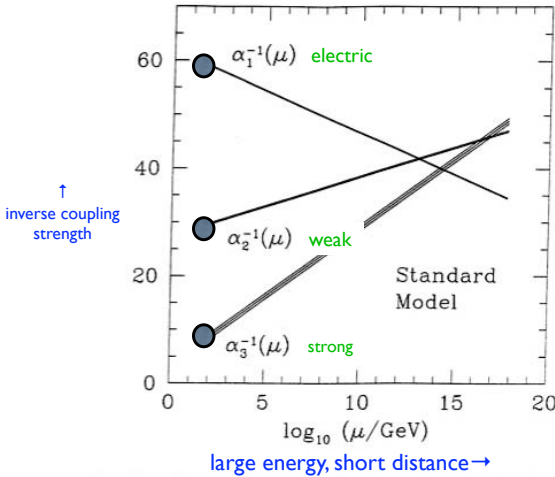
Fig. 13.5. Running of couplings, taking into account vacuum polarization due to standard model fields. The width of the lines indicates the uncertainty in the measured values.

the philosophy of Sir Karl Popper, according to which the goal of science is to produce falsifiable theories, we could at this point declare victory. For we turned the idea of unification of charge, schematically indicated in Fig. 13.6, into a theory that was not merely falsifiable, but actually false.

13.3.3. *Unification ♡ SUSY*

Our response is quite different: we are not satisfied with the hollow victory of falsification. Having a beautiful idea that nearly succeeds, we look to improve it, by finding a still more beautiful version that works in detail. We seek *truthification*.

There is a possibility of another kind of symmetry, supersymmetry (SUSY), that enables further unification in the other direction, as indicated schematically in Fig. 13.7.

If we include vacuum polarization from the particles needed to expand the standard model to include supersymmetry, softly broken at the TeV scale, we find accurate unification [4], as shown in Fig. 13.8.

Within this circle of ideas, called "low-energy supersymmetry," we predict the existence of a whole new world of particles with masses in the TeV range. There must be supersymmetric partners of all the presently known particles, each having the same quantum numbers as known analogue but

electron ⟷ quarks

photon ⟷ gluons

Fig. 13.6.   Schematic indication of the unification of charge. Gauge particles, notably including photons and gluons, are unified within a common representation, as are fermions, notably including electrons and quarks.

electron ⟷ quarks

photon ⟷ gluons

Fig. 13.7.   Schematic indication of unification including SUSY. Now particles of different spins fall into common multiplets.

differing in spin by $\frac{1}{2}$, and of course with different mass. Thus there are spin-$\frac{1}{2}$ gauginos, including gluino partners of QCD's color gluons and wino, zino, and photino partners of W, Z, γ, spin-0 squarks and sleptons, and more (Higgsinos, gravitinos, axinos). Some of these particles ought to become accessible as the Large Hadron Collider (LHC) comes into operation.
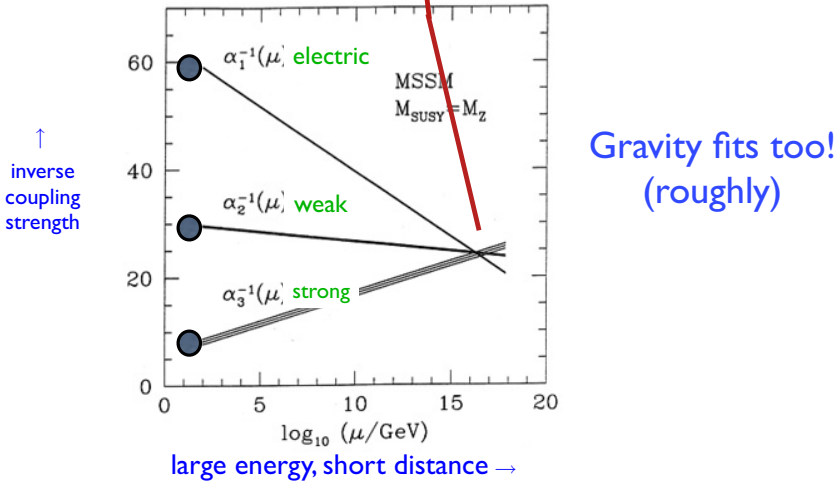
Fig. 13.8.   Running of couplings, taking into account vacuum polarization due to all the fields involved in the minimal extension of the standard model to include supersymmetry, starting at a mass scale ~ 1 GeV. The width of the lines indicates the uncertainty in the measured values. Gravity runs classically. It is ridiculously small at accessible scales, but we extrapolate to its (rough) equality with the other interactions at a common unification scale.

On the other hand, many proposals for physics beyond the standard model at the TeV scale (Technicolor models, large extra dimension scenarios, generic brane-world scenarios) corrupt the foundations of the unification of couplings calculation, and would render its success accidental.

13.3.3.1. *Importance of the emergent scale*

The unification occurs at a very large energy scale $M_{\text{unification}}$, of order 10^{16} GeV. This success is robust against small changes in the SUSY breaking

scale, and is not adversely affected by incorporation of additional particle multiplets, so long as they form complete representations of $SU(5)$.

Running of the couplings allows us to infer, based entirely on low-energy data, an enormously large new mass scale, the scale at which unification occurs. The disparity of scales arises from the slow (logarithmic) running of inverse couplings, which implies that modest differences in observed couplings must be made up by a long interval of running.

The appearance of a very large mass scale is profound, and welcome on several grounds:

- Earlier we discussed the accommodation of neutrino masses and mixings within the standard model, through use of nonrenormalizable couplings. With unification, we can realize those couplings as low-energy approximations to more basic couplings that have better high-energy behavior, analogous to the passage from the Fermi theory to modern electroweak theory.

  Indeed, right-handed neutrinos can have normal, dimension-four Yukawa couplings to the lepton doublet. In $SO(10)$ such couplings are pretty much mandatory, since they are related by symmetry to those responsible for charge-$\frac{2}{3}$ quark masses. In addition, since right-handed neutrinos are neutral under $SU(3) \times SU(2) \times U(1)$ they, unlike the fermions of the standard model, can have a Majorana type self-mass without violating those low-energy symmetries. We might expect the self-mass to arise where it is first allowed, at the scale where $SO(10)$ breaks (or, in other models of unification, its moral equivalent). Masses of that magnitude remove the right-handed neutrinos from the accessible spectrum, but they have an important indirect effect. In second-order perturbation theory the ordinary left-handed neutrinos, through their ordinary Yukawa couplings, make virtual transitions to their right-handed relatives and back. (Alternatively, one substitutes

  $$\frac{1}{\not{p} - M_{\nu_R}} \quad \rightarrow \quad \frac{1}{-M_{\nu_R}} \tag{13.2}$$

  in the appropriate propagator.) This generates non-zero masses for the ordinary neutrinos that are much smaller than the masses of other leptons and quarks.

  The masses predicted in this way are broadly consistent with the tiny observed neutrino masses. That is, the mass scale associated with the effective nonrenormalizable coupling, that we identified earlier, roughly

coincides with the unification scale deduced from coupling constant unification. Many, though certainly not all, concrete models of $SO(10)$ unification predict $M_{\nu_R} \sim M_{\text{unification}}$. No more than order-of-magnitude success can be claimed, because relevant details of the models are poorly determined.

- Unification tends to obliterate the distinction between quarks and leptons, and hence to open up the possibility of proton decay. Heroic experiments to observe this process have so far come up empty, with limits on partial lifetimes approaching 10^{34} years for some channels. It is very difficult to assure that these processes are sufficiently suppressed, unless the unification scale is very large. Even the high scale indicated by running of couplings and neutrino masses is barely adequate. Interpreting this state of affairs positively, we reckon that experiments to search for proton decay remain a most important and promising probe into unification physics.

- Similarly, it is difficult to avoid the idea that unification brings in new connections among the different families. Experimental constraints on strangeness-changing neutral currents and lepton number violation are especially stringent. These and other exotic processes that must be suppressed, and that makes a high scale welcome.

- Axion physics requires a high scale of Peccei-Quinn (PQ) symmetry breaking, in order to implement weakly coupled, "invisible" axion models. (See below.) Existing observations only bound the PQ scale from below, roughly as $M_{\text{PQ}} > 10^9$ GeV. Again, a high scale is welcome. Indeed many, though certainly not all, concrete models of PQ symmetry suggest $M_{\text{PQ}} \sim M_{\text{unification}}$.

- The unification of electroweak interactions with gravity becomes much more plausible. Newton's constant has units of mass^{-2}, so it runs even classically. Or, to put it less technically, because gravity responds directly to energy-momentum, gravity appears stronger to shorter-wavelength, higher-energy probes.

  Because gravity starts out extremely feeble compared to other interactions on laboratory scales, it becomes roughly equipotent with them only at enormously high scales, comparable to the Planck energy $\sim 10^{18}$ GeV. This is not so different from $M_{\text{unification}}$. That numerical coincidence might be a fluke; but it's prettier to think that it betokens the descent of all these interactions from a common source. Note that all these couplings have closely similar geometric interpretations, as measures of the resistance of fields (gauge or metric) to curvature.

13.3.4. *SUSY as calibration*

If low-energy supersymmetry is a feature of our world, several of its particles
will be discovered at the LHC. That would, of course, be a great discovery
in itself. As we've seen, it would also be a most encouraging vindication
of compelling suggestions for unification of the laws of physics, and for
the bold extrapolation of the laws of quantum mechanics and relativity far
beyond their empirical origins.

But tomorrow's sensation is the day-after-tomorrow's calibration, and
we can look forward to *using* the super-world as a tool for further explo-
ration:

- Some superpartner masses and couplings should, like the gauge couplings,
  derive from unified values distorted in calculable ways by vacuum polar-
  ization. See Fig. 13.9 and [5]. Pursuing these relations could grow the
  "one-off" success of unification of gauge couplings into a thriving ecology.
- There is currently no consensus regarding the mechanism of supersym-
  metry breaking. It is a vast and unsettled subject, that I will not engage
  seriously here. But as Fig. 13.10 indicates, the leading ideas about the
  mechanism of SUSY breaking invoke exciting new physics, and predict
  distinctive signatures.
- Many model implementations of low-energy supersymmetry include a
  particle that is extremely long-lived, interacts very feebly with ordinary
  matter, and is abundantly produced as a relic of the big bang. Such a
  particle is a candidate to provide the dark matter that astronomers have
  observed. This aspect deserves, and will now receive, a section of its own.

13.4. Dark Matter

13.4.1. *Dark matter from supersymmetry*

The multiplicative quantum number $R \equiv (-1)^{3B+L+2S}$, where B, L, and
S are baryon number, lepton number, and spin respectively, is $+1$ for all
standard model particles, and will be -1 for their superpartners. Since
B, L and S are to a very good approximation conserved, one expects that
R parity is to a very good approximation conserved. Therefore the lightest
R-odd particle is likely to be highly stable. In many models of low-energy
supersymmetry — though, as we'll discuss shortly, by no means all — this
particle is stable on cosmological scales.

Given a detailed model of low-energy supersymmetry, we can calculate
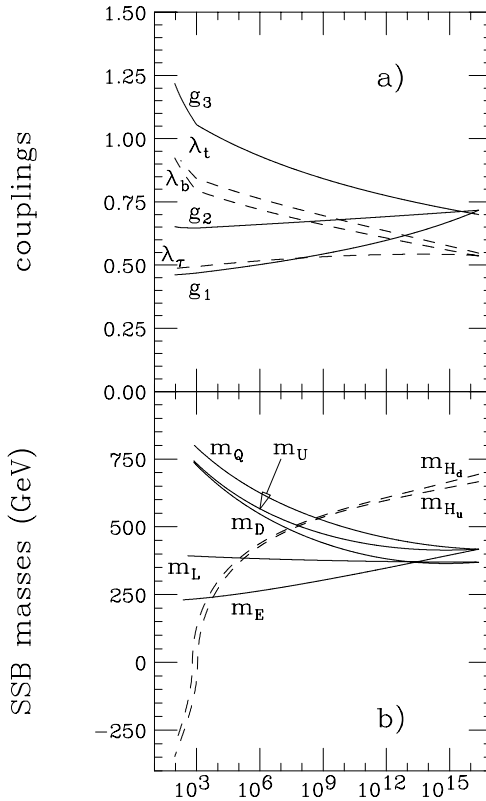the thermal history of the universe through the big bang, and estimate the

Fig. 13.9.   Many models of low-energy supersymmetry incorporate sources of mass, or couplings, that are constrained by the unified gauge symmetry. The logic of running gauge couplings likewise predicts numerical relations among the observed values of these masses and couplings.

surviving relic density of cosmologically stable particles. Over a healthy range of parameters, the lightest R odd particle is produced roughly in the right abundance to provide the dark matter, and also has the required property of interacting very feebly with ordinary matter. This is illustrated in Fig. 13.11.

13.4.2.   *"Mission accomplished"?*

It is all too easy to extrapolate a desired result from encouraging preliminary data.
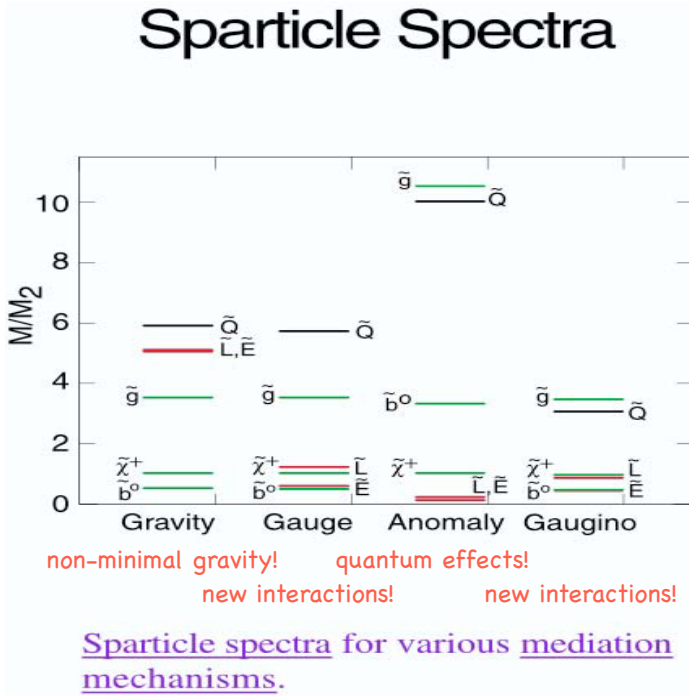
Fig. 13.10. Leading speculations about SUSY breaking invoke profound extensions of the known laws of physics. They also predict distinctive spectra. From [6]; see also [7].

If low-energy supersymmetry and a dark matter candidate are discovered at the LHC, it will be a great enterprise to check whether the detailed properties of the particle, processed through the big bang, lead to the observed dark matter density. That check is by no means a formality, because there are live, theoretically attractive alternatives to having the lightest R-parity odd particle observed at the LHC supply the cosmological density. Both "too much" and "too little" SUSY dark matter are consistent with well-motivated, important physical ideas, as I will now explain.

13.4.2.1. *Too much? — Superwimps*

There is a vast gap between decay lifetimes that can be detected at LHC and the age of the universe. Thus a particle could *appear* to be stable at the LHC, and *calculated* to be abundant in the present universe, but absent in reality, because it decays on sub-cosmological time scales.
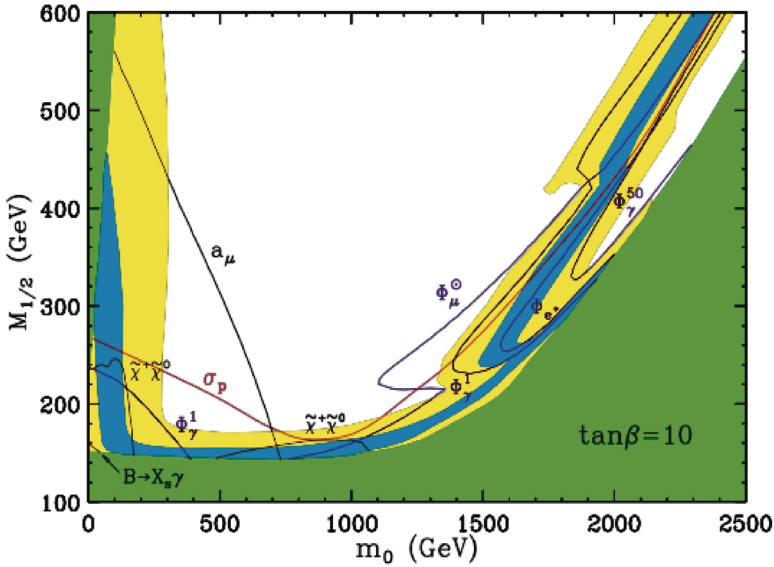
Fig. 13.11.   Many model implementations of low-energy supersymmetry produce a dark
matter candidate. Here, from Ref. [8], is displayed the production of cosmologically
stable particles in minimal supergravity-mediated models with $\tan\beta = 10$ and a range
of universal scalar and gaugino masses $m_0, m_{\frac{1}{2}}$. The green region is ruled out because the
stable particle is electrically charged, while in the upper white region it is overproduced
and in the lower right region production is cosmologically negligible. In the yellow
region there is a cosmologically interesting contribution to the dark matter, and in the
blue region a dominant contribution. See Ref. [8] for more details, and immediately
below for some qualifications.

That possibility is not as bizarre or contrived as it might sound at first
hearing, for the following reason. Superpartners of extremely feebly inter-
acting particles, such as gravitinos or axinos, couple so feebly to ordinary
matter that they are not accessible to observation at the LHC. Yet they
have odd R-parity. Thus the lightest *observed* R-odd particle might well
decay into a lighter *unobserved* R-odd particle with a lifetime that falls
within the gap. Since there is no good argument that the lightest stan-
dard model superpartner must be lighter than gravitinos, axinos, or other
possible "hidden sector" particles (see below), this is a very much a live
possibility.

So if the dark matter candidate observed at the LHC appears to provide
too much dark matter, or if it is electrically charged or otherwise cosmo-
logically dangerous, a plausible interpretation is available.

13.4.2.2. *Too little? — Axions*

Given its extensive symmetry and the tight structure of relativistic quantum field theory, the definition of QCD only requires, and only permits, a very restricted set of parameters — the quark masses, a coupling parameter, and one more, the θ parameter. Physical results depend periodically upon θ, so that effectively it can take values between $\pm\pi$. The discrete symmetries P and T are violated unless $\theta \equiv 0 \pmod{\pi}$. We don't know the actual value of the θ parameter, but only a limit, $|\theta| < 10^{-9}$. Values outside this small range are excluded by experimental results, principally the tight bound on the electric dipole moment of the neutron. Since there are P and T violating interactions in the world, the θ parameter can't be set to zero by any strict symmetry. So understanding its smallness is a challenge — and an opportunity.

Peccei and Quinn discovered that if one imposed a certain asymptotic symmetry, and if that symmetry is broken spontaneously, then an effective value $\theta \approx 0$ results. Weinberg and I explained that the approach $\theta \to 0$ could be understood as a relaxation process, whereby a very light field, corresponding quite directly to θ, settles into its minimum energy state. This is the axion field, and its quanta are called axions.

The phenomenology of axions is essentially controlled by one parameter, F, with dimensions of mass. It is the scale at which Peccei-Quinn symmetry breaks.

Axions, if they exist, have major cosmological implications, as I will now explain briefly. Peccei-Quinn symmetry is unbroken at temperatures $T \gg F$. When this symmetry breaks the initial value of the order parameter's phase is random beyond the then-current horizon scale. One can analyze the fate of these fluctuations by solving the equations for a scalar field in an expanding Universe.

The main general results are as follows. There is an effective cosmic viscosity, which keeps the field frozen so long as the Hubble parameter $H \equiv \dot{R}/R \gg m$, where R is the expansion factor and m the axion mass. In the opposite limit $H \ll m$ the field undergoes lightly damped oscillations, which result in an energy density that decays as $\rho \propto 1/R^3$. Which is to say, a comoving volume contains a fixed mass. The field can be regarded as a gas of nonrelativistic particles in a coherent state, i.e. a Bose-Einstein condensate. There is some additional damping at intermediate stages. Roughly speaking we may say that the axion field, or any scalar field in a classical regime, behaves as an effective cosmological term for $H \gg m$ and as cold

dark matter for $H \ll m$. Inhomogeneous perturbations are frozen in while their length-scale exceeds $1/H$, the scale of the apparent horizon, then get damped as they enter the horizon.

If we ignore the possibility of inflation, then there is a unique result for the cosmic axion density, given the microscopic model. The criterion $H \sim m$ is satisfied for $T \sim \sqrt{\frac{M_{\text{Planck}}}{F}} \Lambda_{\text{QCD}}$. At this point (and even more so at present) the horizon-volume contains many horizon-volumes from the Peccei-Quinn scale, but it still contains only a negligible amount of energy by contemporary cosmological standards. Thus in comparing to current observations, it is appropriate to average over the starting amplitude a/F statistically. If we don't fix the baryon-to-photon ratio, but instead demand spatial flatness, as inflation suggests we should, then $F \sim 10^{12}$ GeV correspond to the observed dark matter density, while for $F > 10^{12}$ GeV we get too much, and the relative baryon density we infer is smaller than what we observe.

If inflation occurs before the Peccei-Quinn transition, this analysis remains valid. But if inflation occurs after the transition, things are quite different.

For if inflation occurs after the transition, then the patches where a is approximately homogeneous get magnified to enormous size. Each one is far larger than the presently observable Universe. The observable Universe no longer contains a fair statistical sample of a/F, but some particular "accidental" value. Of course there is a larger region, which Martin Rees calls the Multiverse, over which the value varies, but we sample only a small part of it.

Now if $F > 10^{12}$ GeV, we could still be consistent with cosmological constraints on the axion density, so long as the starting amplitude satisfies $(a/F)^2 \sim (10^{12} \text{ GeV})/F$. The actual value of a/F, which controls a crucial regularity of the observable Universe, the dark matter density, is contingent in a very strong sense. Indeed, it takes on other values at other locations in the multiverse.

Within this scenario, the anthropic principle is demonstrably correct and appropriate [9]. Regions having large values of a/F, in which axions by far dominate baryons, seem likely to prove inhospitable for the development of complex structures. Axions themselves are weakly interacting and essentially dissipationless, and they dilute the baryons, so that these too stay dispersed. In principle laboratory experiments could discover axions with $F > 10^{12}$ GeV. If they did, we would have to conclude that the vast
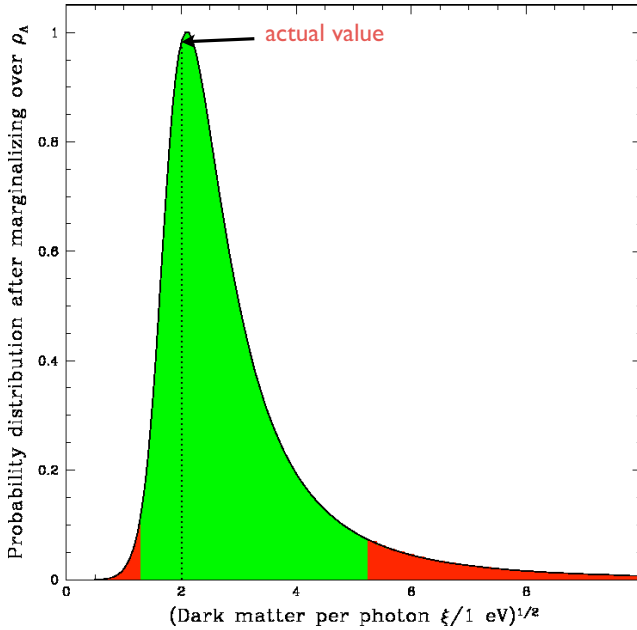
Fig. 13.12. In post-inflationary axion cosmology, the ratio of axion dark density to ordinary baryonic density varies over very large scales, and is subject to selection effects. The prior is determined, as is the microphysics, so it is possible to take these effects into account with some semblance of rationality [10]. One finds that the dark matter density we actually observe is remarkably close to the most probable value.

bulk of the Multiverse is inhospitable to intelligent life. And we'd be forced to appeal to the anthropic principle to understand the anomalously modest axion density in our Universe.

Though experiment does not make it compulsory, we are free to analyze the cosmological consequences of $F \gg 10^{12}$ GeV. Recently Tegmark, Aguirre, Rees and I carried out such an analysis [10]. We concluded that although the overwhelming *volume* of the Multiverse contains a much higher ratio of dark matter, in the form of axions, from what we observe, the typical *observer* is likely to see a ratio similar to what we observe. See Fig. 13.12.

This post-inflationary axion cosmology is attractive in many ways. It avoids the annoying axion string problem of traditional axion cosmology. It relieves us of the necessity of bringing in a new scale: now F could be the unification scale, or the Planck scale. It has a potential cosmological

signature, accessible in upcoming microwave background anisotropy measurements, as it provides a plausible source for isocurvature fluctuations that are larger in amplitude than gravitational wave fluctuations [11].

And post-inflationary axion cosmology will happily generate the right amount of cosmological dark matter for us, if low-energy SUSY provides too little. So if the dark matter candidate observed at the LHC appears to provide too little dark matter, and in particular if the lightest appreciably coupled R-odd particle decays into light species or into ordinary matter at a faster-than-cosmological rate, a plausible alternative source is available.

13.5. Hidden Sectors and Portals

13.5.1. *Might the LHC see nothing?*

Let me begin the discussion of hidden sectors in what I trust will be a provocative way, with that question. The usual answer is "No, the LHC must discover new particles or new strong interactions in the vacuum channel, in order to avoid a crisis in quantum mechanics (loss of unitarity)." The correct answer, however, is "Yes," as I'll now demonstrate.

13.5.1.1. *Division and dilution*

Consider, to begin, adding to the standard model a singlet real scalar "phantom" field η. All the couplings of gauge fields to fermions, and of both to the Higgs field, remain as they were in the original standard model. This is enforced by gauge symmetry and renormalizability. The Higgs potential is modified, however, to read

$$V(\phi, \eta) \;=\; -\mu_1^2 \phi^\dagger \phi + \lambda_1 (\phi^\dagger \phi)^2 - \mu_2^2 \eta^2 + \lambda_2 \eta^4 - \kappa \phi^\dagger \phi \eta^2 \,. \qquad (13.3)$$

The only communication between η and the standard model consistent with general principles is this κ coupling to the Higgs field.

The upshot of this simple cross-coupling is that when ϕ and η acquire vacuum expectation values, the mass eigenstates (i.e., the observable particles) are created by mixtures of the conventional Higgs field and the phantom field. The phantom component contributes nothing to the amplitude for production from conventional particles sources, i.e. quarks and gluons. Thus the same overall production rate of Higgs particle is now divided between two lines. Instead of finding a signal-to-noise ratio $S/N = 2$, for the same exposure you'll get two channels with $S/N = 1$, which is not as good.

Of course, it's easy to generalize this model. With more phantom fields, one has more division of strength. And whereas 1 5σ signal is a discovery, as a practical matter 5 independent 1 σ signals are worthless.

It gets worse. The phantoms might actually be the "Higgs fields" of an entire new sector, that has its own gauge fields and matter. Then the Higgs-phantom mixtures might also decay into particles of the new sector, which are effectively invisible. So not only is production divided, but also decay is diluted.

These effects of division and dilution could easily render the Higgs sector effectively invisible, whilst barely affecting any other aspect of phenomenology.

The good news: If we start from the minimal standard model, which contains just a single Higgs doublet field — and thus, after electroweak symmetry breaking, just a single neutral scalar — the Higgs portal might be quite challenging to exploit. Given a richer Higgs sector, including charged fields (as in low-energy SUSY), or more if "Higgs particles" appear as decay products of particles that are more identifiable, it could be much easier. In any case, a new world would be open to exploration.

13.5.1.2. *An example: Mass from quantum mechanics*

Let us add, in the spirit of counting, an $SU(4)$ symmetry to the standard model, so that the gauge group becomes

$$G \;=\; SU(4) \times SU(3) \times SU(2) \times U(1)\,.$$

In the spirit of coupling unification, we suppose that $SU(4)$ is a super-strong interaction. It can support spontaneous chiral symmetry breaking, which we represent by some sort of σ model. In the simplest version the new $\vec{\sigma}$ field is a 4-component vector; but it could also be some more elaborate matrix. Assuming all the fields charged under $SU(4)$ are $SU(3) \times SU(2) \times U(1)$ singlets, the important modification to the standard model will come through a modified effective potential, generalizing Eq. (13.3):

$$V(\phi, \eta) \;=\; -\mu_1^2 \phi^\dagger \phi + \lambda_1 (\phi^\dagger \phi)^2 - \mu_2^2 \vec{\sigma}^2 + \lambda_2 (\vec{\sigma}^2)^2 - \kappa \phi^\dagger \phi \vec{\sigma}^2. \quad (13.4)$$

The κ coupling will induce mixing, as before. The non-Goldstone field σ_0, that encodes the magnitude of $\vec{\sigma}$, will decay into the massless phantom Nambu-Goldstone "pions." So we get dilution, as well.

It is entertaining to imagine $\mu_1^2 = 0$. Then we have an underlying model in which there is no classical mass parameter anywhere. Electroweak

symmetry breaking is induced from nonperturbative, intrinsically quantum-mechanical chiral symmetry breaking in the phantom sector, through the cross-coupling κ. In this indirect way we implement the vision that inspires technicolor models, while avoiding the usual phenomenological difficulties of such models. Those difficulties arise because the new strongly interacting sector is not hidden (that is, if it does not consist of $SU(3) \times SU(2) \times U(1)$ singlets), and more specifically because the super-strong condensate itself breaks $SU(2) \times U(1)$.

13.5.2. *Motivations for hidden sectors*

The two little models we've discussed are not uninteresting in themselves. Moreover, they illustrate possibilities that are more broadly motivated. Here are some other reasons to consider the possibility of hidden sectors seriously:

Hippocratic oath: At the opening of their Hippocratic Oath, prospective doctors promise to "abstain from whatever is deleterious and mischievous." Hidden $SU(3) \times SU(2) \times U(1)$ singlet sectors, unlike many other speculative extensions of the standard model, do little harm. They do not spoil the successful unification of couplings, nor do they open a Pandora's box of flavor violation.

Stacks and throats: In string theory, hidden sectors easily arise from far-away (in the extra dimensions) stacks of D-branes or orbifold points. The original $E_8 \times E_8$ heterotic string contains an early incarnation of a hidden sector.

Plays well with SUSY: Hidden sectors are invoked in several mechanisms of SUSY breaking. And the next-to-minimal supersymmetric standard model (NMSSM), which introduces an extra $SU(3) \times SU(2) \times U(1)$ singlet chiral superfield, has been advocated on phenomenological grounds. It eases some "naturality" problems.

Flavor and axions: It is tempting to think that the complicated pattern of quark and lepton masses and mixings reflects a complicated solution to simpler basic equations; specifically, that the more fundamental equations have a flavor symmetry, which is spontaneously broken. Phenomenology seems to require that flavor-symmetry breaking dynamics occurs at a high mass scale. Therefore the order parameter fields must be $SU(3) \times SU(2) \times U(1)$ singlets, and they constitute a hidden sector in our sense. Axion physics embodies this idea in a compelling way for one aspect of the quark mass matrix, i.e. its overall phase.

13.5.3. *Bringing method to the madness*

Possible forms of communication between hidden sectors can be considered more abstractly, in the style of effective field theory. We seek low-dimension operators suitable for inclusion in the world-Lagrangian that contain both standard model and hidden sector fields. We assume these operators must be gauge and Lorentz invariant. The simplest cases correspond to coupling in spin 0, $\frac{1}{2}$, or 1 hidden sector fields, building up dimension 4:

Spin 1: An $SU(3) \times SU(2) \times U(1)$ vector V^μ can couple in three different ways to make a dimension 4 invariant operators. It can couple to fermion $\bar{f}\gamma_\mu f$ currents. This possibility has been much discussed under the rubric "Z' bosons." It can couple to the hypercharge gauge curvature $B_{\mu\nu}$ through the current $\overleftarrow{\partial}^\nu B_{\mu\nu}$. This gives "kinetic mixing." (It might also couple through the dual current $\overleftarrow{\partial}^\nu \tilde{B}_{\mu\nu}$, to give a form of θ-parameter mixing, but this appears to be of little consequence.) Finally, V^μ might couple in through the Higgs field, appearing within the co-variant derivative in $(\nabla^\nu \phi^\dagger)(\nabla_\nu \phi)$. As the Higgs field condenses, this leads to mixing between V^μ and standard model gauge bosons at the level of mass eigenstates. In general, in both kinetic and mass mixing, the hidden sector particles will acquire electric charges that need not be commensurate with the familiar unit (and presumably must be much smaller).

Spin $\frac{1}{2}$: An $SU(3) \times SU(2) \times U(1)$ spin-$\frac{1}{2}$ fermion ξ can make a dimension 4 invariant operator by coupling in to the dimension $\frac{5}{2}$ singlet $\phi^\dagger L$, where L is a left-handed lepton doublet. If such an interaction occurs with a very small coefficient, it leads to a massive Dirac neutrino; if the coefficient is moderate, but ξ has a large intrinsic mass, we integrate out ξ to get the familiar see-saw mechanism to generate small physical neutrino masses.

Spin 0: An $SU(3) \times SU(2) \times U(1)$ spin-$\frac{1}{2}$ spin 0 particle can couple in through the dimension 2 singlet $\phi^\dagger \phi$. This opens the Higgs portal to the hidden sector, as we discussed above.

Evidently this framework helps to organize several old ideas, and puts the Higgs portal idea in proper context.

13.6. **Summary and Conclusions**

With the LHC, we will expand the frontiers of fundamental physics.

- We will learn, through a *tour de force* of physics, what makes empty space function as a cosmic superconductor.
- We will learn whether existing indications for unification and supersymmetry have been Nature teaching us or Nature teasing us.
- If indeed the superworld opens up, it will probably supply a good candidate for the dark matter. It will then be a great enterprise to establish or disprove that candidate.
- Hidden sectors are entirely possible. They could complicate things in the short run, but would teach us even more in the long run.

It will lead to a new Golden Age, that could also be enriched by discoveries in precision low-energy physics (elementary electric dipole moments), rare processes (proton decay), and cosmology (primordial isocurvature or gravitational wave fluctuations).

References

[1] A. Hocker and Z. Ligeti, to appear in *Annual Reviews of Nuclear and Particle Science*, [hep-ph/0605217].

[2] F. Wilczek, The Universe is a strange place, *Nucl. Phys. Proc. Supp.* **B134** 3-12 (2004), [astro-ph/0401347].

[3] H. Georgi, H. Quinn, and S. Weinberg, Hierarchy of Interactions in Unified Gauge Theories, *Phys. Rev. Lett.* **33**, 451 (1974).

[4] S. Dimopoulos, S. Raby, and F. Wilczek, Supersymmetry and the Scale of Unification, *Phys. Rev.* **D24**, 1681 (1981); S. Dimopoulos, S. Raby, and F. Wilczek, Unification of couplings, *Physics Today* **44, Oct.** 25 (1991).

[5] G. L. Kane, C. Kolda, L. Roszkowski, and J. D. Wells, Predictions for constrained minimal supersymmetry with bottom tau mass unification, *Phys. Rev.* **D49**, 6173 (1994), [hep-ph/9404253].

[6] Figure from M. Peskin, modified to include exclamations.

[7] M. Peskin, The Experimental investigation of supersymmetry breaking, *Prog. Theor. Phys. Suppl.* **123** 507-537 (1996), [hep-ph/9604339].

[8] J. Feng, K. Matchev, and F. Wilczek, Prospects for indirect detection of neutralino dark matter, *Phys. Rev.* **D63**, 4502-4504 (2001), [astro-ph/0008115].

[9] A. Linde, Inflation and axion cosmology, *Phys. Lett.* **B201** 437 (1988).

[10] M. Tegmark, A. Aguirre, M. Rees, and F. Wilczek, Dimensionless constants, cosmology and other dark matters, *Phys. Rev.* **D73** 023505 (2006), [astro-ph/0511774].

[11] M. Hertzberg and F. Wilczek, paper in preparation, and references therein.

This page intentionally left blank

Chapter 14

Strongly Interacting Electroweak Theories and Their Five-Dimensional Analogs at the LHC

Alex Pomarol

IFAE, Universitat Autònoma de Barcelona
08193 Bellaterra, Barcelona, Spain
alex.pomarol@uab.cat

Strongly interacting theories of electroweak (EW) symmetry breaking provide an elegant solution to the hierarchy problem. In these models the EW symmetry can either be broken without a Higgs or by means of a composite Higgs boson. These scenarios have been recently investigated in the framework of 5-dimensional warped models that, according to the AdS/CFT correspondence, have a 4-dimensional holographic interpretation in terms of strongly coupled field theories. We describe the minimal Higgsless and composite Higgs model and show how they can successfully pass all the electroweak precision tests and solve the flavor problems. We explore the implications of these models at the LHC.

14.1. Introduction

Introducing a Higgs boson is a simple and economical way to break spontaneously the electroweak gauge symmetry of the Standard Model (SM) [a] and cure the bad high-energy behaviour of its scattering amplitudes, thus allowing one to extrapolate the theory up to very high energies. It is hard to believe that Nature is not using such a simple mechanism to give us a UV-completed theory of electroweak interactions. Nevertheless, naturalness criteria suggest that the Higgs mechanism is unlikely to be just the last ingredient to be incorporated in the SM at the electroweak scale. Why the Higgs mass, which determines the scale of electroweak symmetry breaking, is so small compared to the Planck scale?

---

[a] In this chapter we will refer as SM only the fermion and gauge sector (the only particles discovered so far). Therefore the Higgs will not be included in our definition of SM particles.

   To answer this question dynamically one must postulate new physics, such as supersymmetry , and hence new particles around the TeV, making the simplicity of the Higgs mechanism for UV-completing the SM just a theoretical curiosity. At this point, one might think that there is no need for the Higgs particle, and look for other ways to unitarize the SM scattering amplitudes. An example can be found in QCD, where pion-pion scattering is unitarized by the additional resonances that arise from the $SU(3)_c$ strong dynamics. A replica of QCD at energies $\sim$ TeV that breaks the EW symmetry can then be an alternative for a UV-completion of the SM. This is the so-called Technicolor model [1] (TC). In TC there is no Higgs particle and the SM scattering amplitudes are unitarized, as in QCD, by infinite heavy resonances. One of the main obstacle to implement this approach has arisen from electroweak precision tests (EWPT) that has disfavored this type of models. The reason has been the following. Without a Higgs, we expect the new particles responsible for unitarizing the SM amplitudes to have a mass at around 1 TeV. These same resonances give large tree-level contributions to the electroweak observables.

   There has been two different alternatives to overcome this problem. Either one assumes that (1) there are extra contributions to the electroweak observables that make the model consistent with the experimental data, or (2) assumes that the strong sector does not break the EW symmetry but it just deliver a composite pseudo-Goldstone scalar, the Higgs. This Higgs gets a potential at the one-loop level and triggers EWSB at lower energies.

   In the first case, the Higgsless approach, EWPT are satisfied thanks to additional contributions to the electroweak observables that can come from extra scalars or fermions of the TC model [2], or from vertex corrections. As we will see, the cancellations needed to pass the EWPT are not large, making this possibility not so unconceivable.

   In the second case, the Higgs plays the role of *partly* unitarizing the SM scattering amplitudes. Compared to theories without a Higgs, we will have now that the scale at which new dynamics is needed can be delayed, and therefore the extra resonances that ultimately unitarize the SM amplitudes can be heavier. In this case EWPT will be under control. This is the approach of the composite Higgs models, first considered by Georgi and Kaplan [3]. In these theories a light Higgs arises as a Pseudo-Goldstone boson (PGB) of a strongly interacting theory, in a very similar way as pions in QCD.

   Although these scenarios offer an interesting completion of the SM, the difficulty to calculate within strongly coupled theories has been a deterrent

from fully exploring them. Nevertheless, the situation has changed in the last years. Inspired by the AdS/CFT correspondence [4], a new approach to build realistic and predictive Higgsless and composite Higgs models has been developed. The AdS/CFT correspondence states that weakly coupled five-dimensional theories in Anti-de-Sitter (AdS) have a 4D holographic description in terms of strongly coupled conformal field theories (CFT). Such correspondence gives a definite prescription on how to construct 5D theories that have the same physical behaviour and symmetries of the desired strongly coupled 4D theory. This has allowed to propose concrete Higgsless [5–7] and composite Higgs [8–10] models that not only are consistent with the experimental constraints, but also give clear predictions for the physics at the LHC.

In this chapter we will proceed in the following way. In Sec. 14.2 we will discuss the Higgsless approach. We will first introduce the original TC model and show its main problems. Next, we will describe a 5D Higgsless model with similar properties of the TC model but with the advantage of calculability. This will help to discuss possible solutions to the TC problems. In Sec. 14.3 we will analyze the composite Higgs idea, focusing in a realistic 5D example. Finally, in Sec. 14.4 we will study the implications of these models at the LHC.

14.2. Higgsless Models

14.2.1. *The original technicolor model. Achievements and pitfalls*

Technicolor models [1] of EWSB consists of a new strong gauge sector, SU(N) or SO(N), that it is assumed to confine at a low-scale $\mu_{IR} \sim$ TeV. In addition, the model contains (at least) two flavors of techni-quarks $T_L^{u,d}$, $T_R^{u,d}$ transforming in the fundamental representation of the strong group and as ordinary quarks under the EW group. As it occurs in QCD, this implies that the strong sector has a global $G = \mathrm{SU}(2)_L \times \mathrm{SU}(2)_R \times \mathrm{U}(1)_X$ symmetry under which $T_L^{u,d}$ transforms as a $(\mathbf{2}, \mathbf{1})_{\mathbf{1/6}}$ and $T_R^{u,d}$ transforms as a $(\mathbf{1}, \mathbf{2})_{\mathbf{1/6}}$ (the hypercharge is given by $Y = T_3^R + X$). Assuming that the TC-quarks condensate, $\langle \bar{T}_L T_R \rangle \sim \mu_{IR}^3$, the global symmetry of the strong sector G is broken down to $H = \mathrm{SU}(2)_V \times \mathrm{U}(1)_X$. The EW symmetry is then broken given mass to the SM gauge boson. Fermion masses are assumed to arise from higher-dimensional operators such as $\bar{q}_L u_R \bar{T}_R T_L / M^2$ that can be induced from an extended heavy gauge sector (ETC). After the TC-quark condensation, SM fermions get masses $m_u \sim \mu_{IR}^3 / M^2$.

If the number of colors N of the TC group is large enough, the strong sector can be described by an infinite number of resonances [11]. The masses and couplings of the resonances depend on the model. Nevertheless, as in QCD, we can expect vector resonances transforming as a triplet of SU(2)$_V$; the TC-rho of mass $m_\rho \sim \mu_{IR}$. In order to see the implications of these resonances on the SM observables, it is useful to write the low-energy Lagrangian of the SM fields obtained after integrating out the strong sector (the equivalent of the QCD chiral Lagrangian). It is convenient to express this Lagrangian in a SU(2)$_L \times$SU(2)$_R \times$U(1)$_X$-symmetric way. To do so, we promote the elementary SM fields to fill complete representations of SU(2)$_L \times$SU(2)$_R \times$U(1)$_X$. For the bosonic sector, this means to introduce extra non-dynamical vectors, i.e. spurions, to complete the corresponding adjoint representations W_μ^L, W_μ^R and B_μ. Having the Goldstone multiplet U parametrizing the coset SU(2)$_L \times$SU(2)$_R$/SU(2)$_V$, the bosonic low-energy Lagrangian is given by

$$\mathcal{L}_{\text{eff}} = f_\pi^2 \left[\frac{1}{4}|D_\mu U|^2 + \frac{c_S}{m_\rho^2}\text{Tr}[W_{\mu\nu}^L U W^{R\,\mu\nu} U^\dagger] + \cdots \right] \qquad (14.1)$$

where $D_\mu U = \partial_\mu U + i W_\mu^L U - i U W_\mu^R$ and f_π is the analog of the pion decay constant that scales as $f_\pi \sim \sqrt{N}/(4\pi) \times m_\rho$ [11]. In Eq. (14.1) we have omitted terms of order $(DU)^4$ that do not contribute to the SM gauge boson self-energies, and terms of order $f_\pi^2 D^2/m_\rho^4$ that are subleading for physics at energies below m_ρ. The c_S is an order one coefficient that in QCD takes the value $c_S = L_{10}m_\rho^2/f_\pi^2 \simeq -0.4$. The mass of the SM W arises from the kinetic term of U that gives $M_W^2 = g^2 f_\pi^2/4$ from which we can deduce

$$f_\pi \simeq 246 \text{ GeV} \quad \text{and} \quad m_\rho \simeq 2\sqrt{\frac{3}{N}} \text{ TeV}. \qquad (14.2)$$

14.2.1.1. *Flavour changing neutral current (FCNC) and the top mass*

If the SM fermion masses arise from an ETC sector that generate the operator $\bar{q}_L^i u_R^j \bar{T}_R T_L/M^2$, this sector also will generate FCNC of order $\bar{q}_L^i u_R^j \bar{q}_L^k u_R^l/M^2$ that are larger than experimentally allowed. Also the top mass is too large to be generated from a higher dimensional operator. Solutions to these problems have been proposed [12]. Nevertheless most of the solutions cannot successfully pass the electroweak precision tests.

14.2.1.2. *Electroweak precision tests*

The most important corrections to the electroweak observables coming from TC-like models are universal corrections to the SM gauge boson self-energies, $\Pi_{ij}(p)$, and non-universal corrections to $Zb\bar{b}$, $\delta g_b/g_b$. The universal corrections to the SM gauge bosons can be parametrized by four quantities: $\widehat{S}$, $\widehat{T}$, W and Y [13]. The first two, the only relevant ones for TC models [14], are defined as

$$\widehat{S} = g^2 \Pi'_{W_3 B}(0) \ , \quad \widehat{T} = \frac{g^2}{M_W^2} \left[\Pi_{W_3 W_3}(0) - \Pi_{W^+ W^-}(0) \right] . \qquad (14.3)$$

From the Lagrangian Eq. (14.1) only $\widehat{S}$ is generated giving a contribution

$$\widehat{S} = -g^2 c_S \frac{f_\pi^2}{m_\rho^2} \simeq 2.3 \cdot 10^{-3} \left(\frac{N}{3} \right) , \qquad (14.4)$$

where we have extracted the result from QCD. Extra contributions to $\widehat{S}$, beyond those of the SM, are constrained by the experimental data. They must be smaller than [b] $\widehat{S} \lesssim 2 \cdot 10^{-3}$ at 99% CL. We see that the contribution Eq. (14.4) is at the edge of the allowed value. Models with N larger than 3 or with an extra generation of TC-quarks, needed for realistic constructions (ETC models), are therefore ruled out. The bound $\widehat{S} \lesssim 2 \cdot 10^{-3}$ can be saturated only if $\widehat{T}$ receive extra positive contributions $\sim 5 \cdot 10^{-3}$ beyond those of the SM. Although the custodial $SU(2)_V$ symmetry of the TC models guarantees the vanishing of the TC contributions to the $\widehat{T}$-parameter, one-loop contributions involving both the top and the TC sector are nonzero. Nevertheless, in strongly interacting theories we cannot reliably calculate these contributions and know whether they give the right amount to $\widehat{T}$.

As we said before, the generation of a top mass around the experimental value is difficult to achieve in TC models and requires new strong dynamics beyond the original sector [12]. Even if a large enough top mass is generated, an extra difficulty arises from $Zb\bar{b}$. On dimensional grounds, assuming that $t_{L,R}$ couples with equal strength to the TC sector responsible for EWSB, we have the estimate $\delta g_b/g_b \sim m_t/m_\rho \gtrsim 0.07$ that overwhelms the experimental bound $|\delta g_b/g_b| \lesssim 5 \cdot 10^{-3}$. Similar conclusions are reached even if $t_{L,R}$ couples with different strength to the TC sector [9]. Only a custodial O(3) symmetry in the top sector seems to avoid this problem [15] (see below), but no TC model with this symmetry has been constructed so far.

[b]Since TC models do not have a Higgs, we are taking the result of Ref. [13] for $m_H \simeq 1$ TeV.

It is clear that although TC models are plague with phenomenological problems, the main obstacle that stops us from making progress is the lack of predictability in strongly coupled theories.

14.2.2. *5D Higgsless models*

Five-dimensional models can give rise to predictive Higgsless scenarios [5–7]. We will concentrate in AdS$_5$ geometries since they also give an explanation to the $M_{\mathrm{Pl}} - M_W$ hierarchy [16]. [c] The 5D spacetime metric will be given by

$$ds^2 = \frac{L^2}{z^2} \left(\eta_{\mu\nu} \, dx^\mu dx^\nu - dz^2 \right) , \qquad (14.5)$$

where z represents the coordinate for the fifth dimension and L is the AdS curvature radius. The spacetime will have two boundaries, one at $z = L_0 \equiv L \sim 1/M_{\mathrm{Pl}}$ (UV-boundary), and another at $z = L_1 \sim \mu_{\mathrm{IR}} \sim 1/\mathrm{TeV}$ (IR-boundary). The theory is thus defined on the line segment $L_0 \leq z \leq L_1$. The symmetry patterns are assumed to be

$$
\begin{aligned}
\mathrm{UV - boundary:} \qquad & G_{\mathrm{SM}} \equiv \mathrm{SU(2)_L \times U(1)_Y \times SU(3)_c} \\
\mathrm{5D\ Bulk:} \qquad & \mathrm{SU(2)_L \times SU(2)_R \times U(1)_X \times SU(3)_c} \\
\mathrm{IR - boundary:} \qquad & \mathrm{SU(2)_V \times U(1)_X \times SU(3)_c}.
\end{aligned}
$$

We also assume that the bulk and IR-boundary are invariant under the parity P_{LR} that interchanges $L \leftrightarrow R$. We will see later that this discrete symmetry is crucial to avoid large contributions to $Zb\bar{b}$. In the fermion sector, each SM generation is identified with the lightest Kaluza-Klein (KK) mode of a set of 5D bulk multiplets. For the up-quark sector, these 5D fields are chosen to be

$$
\xi_q = \left[(\mathbf{2}, \mathbf{2})_{\mathbf{L}}^{\mathbf{q}} = \begin{bmatrix} q'_L(-+) \\ q_L(++) \end{bmatrix} , \ (\mathbf{2}, \mathbf{2})_{\mathbf{R}}^{\mathbf{q}} = \begin{bmatrix} q'_R(+-) \\ q_R(--) \end{bmatrix} \right] ,
$$
$$
\xi_u = \left[(\mathbf{1}, \mathbf{1})_{\mathbf{L}}^{\mathbf{u}} = u_L(--) , \ (\mathbf{1}, \mathbf{1})_{\mathbf{R}}^{\mathbf{u}} = u_R(++) \right] , \qquad (14.6)
$$

with X-charge equal to 2/3. Chiralities under the 4D Lorentz group have been denoted by L, R, and $(\pm, \pm)$ is a shorthand notation to denote Neumann $(+)$ or Dirichlet $(-)$ boundary conditions on the two boundaries. The bulk masses of the 5D fields $\xi_{q,u}$, in units of $1/L$, will be denoted by $c_{q,u}$. Localized on the IR-boundary, we can have mass terms invariant under

---

[c] As far as physics at the TeV is concerned, 5D flat space or other geometries give similar predictions [7].

$SU(2)_V \times U(1)_X \times SU(3)_c$:

$$\widetilde{M}_u \, \bar{q}_L u_R + h.c. \tag{14.7}$$

For $c_q > 1/2$ and $c_u < -1/2$, the wave functions of the lightest KK of the 5D fermion fields are peaked towards the UV-boundary, and therefore their projection on the IR-boundary, where the EWSB masses Eq. (14.7) resides, are small [17]. This implies that small fermion masses can be easily generated in these models [17, 18]. For the top we will require $|c_{q,u}| \lesssim 1/2$ such that the wave function of the lightest $t_{L,R}$ mode is peaked towards the IR-boundary and a large mass can be generated. The SM down-quark and lepton masses can arise similarly.

To study the implications of this 5D model it is convenient to use the holographic approach, instead of the more convencional KK decomposition. The holographic procedure consists in separating the UV-boundary fields $A(z = L_0, x)$ from the bulk fields $A(z \neq L_0, x)$ and treating them as distinct variables. If we integrate out the bulk with fixed values of the fields on the UV-boundary, we obtain a 4D (non-local) theory defined on the UV-boundary. For the transverse gauge bosons at the quadratic level and in momentum space, this is given by

$$\mathcal{L}_{\text{eff}} = \frac{P_{\mu\nu}}{2} \left\{ \text{Tr}[V_\mu \Pi_V(p) V_\nu + A_\mu \Pi_A(p) A^\nu] + B_\mu \Pi_B(q) B^\nu \right\}, \tag{14.8}$$

where $A = (W^L - W^R)/\sqrt{2}$, $V = (W^L + W^R)/\sqrt{2}$, $P_{\mu\nu} = \eta_{\mu\nu} - p_\mu p_\nu/p^2$ and

$$\Pi_{V,A}(p) = -M_5 L \frac{p}{L_0} \frac{Y_0(pL_0)J_{0,1}(pL_1) - Y_{0,1}(pL_1)J_0(pL_0)}{Y_1(pL_0)J_{0,1}(pL_1) - Y_{0,1}(pL_1)J_1(pL_0)}, \tag{14.9}$$

where J_n, Y_n are Bessel functions and $\Pi_B = M_5^B \Pi_V/M_5$ (M_5 and M_5^B are the inverse squared of the 5D gauge couplings of the $SU(2)_{L,R}$ and $U(1)_X$ groups respectively). From Eq. (14.9) we can obtain the W mass

$$M_W^2 = \frac{g^2}{4} f_\pi^2 \quad \text{where} \quad f_\pi^2 = 2\Pi_A(0) = \frac{4M_5 L}{L_1^2}, \tag{14.10}$$

and the $\widehat{S}$ parameter

$$\widehat{S} = \frac{g^2}{4}[\Pi_V'(0) - \Pi_A'(0)] = \frac{3g^2}{8} M_5 L = 3 \cdot 10^{-3} \left(\frac{\tilde{N}}{3} \right), \tag{14.11}$$

where we have defined $\tilde{N} \equiv 16\pi^2 M_5 L$ that corresponds to the inverse of our 5D expansion parameter (only for $1/\tilde{N} \ll 1$ we have a weakly coupled

description of our 5D theory). Eq. (14.11) indicates that (marginal) agreement with data can only be obtained in the region where $\tilde{N} \sim 2$; too small to trust the 5D calculation of $\widehat{S}$. If we want to stay in the 5D perturbative regime, we need extra negative contributions to $\widehat{S}$ to reduce its value. Possible extra contributions to $\widehat{S}$ can come from the fermion sector [19, 20].[d] Assuming a cancellation in $\widehat{S}$ such that its value is reduced a 1/4 (this will allow a $\tilde{N} \sim 8$), the mass of the lowest vector KK is

$$ m_\rho \simeq \frac{3\pi}{4L_1} \simeq 1.3 \sqrt{\frac{8}{\tilde{N}}} \text{ TeV} , \qquad (14.12) $$

where for the numerical value we have used Eqs. (14.10) and (14.11). The detection of this vector KK (the equivalent of the TC-rho) can therefore be accessible at the LHC.

Contrary to TC, this 5D model is safe from large corrections to $\delta g_b/g_b$. It can be shown [15] that the P_{LR} discrete symmetry together with the custodial $\mathrm{SU}(2)_V$ protect the coupling $Zb\bar{b}$ from tree-level corrections.

14.2.2.1. *Holographic 4D interpretation of the 5D Higgsless models and the size of FCNC*

Using the AdS/CFT dictionary [4], the above 5D model can be interpreted as a 4D strongly interacting theory [9]. This gives a very useful description of the 5D models as 4D theories. The correspondence goes as follows. The 5D bulk and IR-boundary corresponds to a CFT with a mass gap at the infrared scale $\mu_{\mathrm{IR}} \sim 1/L_1$, responsible for the formation of resonances (corresponding to the KK states). The value of $\tilde{N}$ corresponds to the number of colors N of the CFT. The global symmetry of the CFT is $G = \mathrm{SU}(3)_c \times \mathrm{SU}(2)_L \times \mathrm{SU}(2)_R \times \mathrm{U}(1)_X$, spontaneously broken down to $H = \mathrm{SU}(3)_c \times \mathrm{SU}(2)_V \times \mathrm{U}(1)_X$. The SM gauge bosons and fermions are elementary fields external to the strongly interacting CFT. They corresponds to the UV-boundary fields $A(z = L_0, x)$. The SM gauge bosons couple to the CFT through its conserved currents, gauging the subgroup $\mathrm{SU}(3)_c \times \mathrm{SU}(2)_L \times \mathrm{U}(1)_Y$ contained in G. The SM fermions ψ_i couple linearly to the strong sector through a single operator $\mathcal{O}_i$ made of CFT fields: $\mathcal{L} = \lambda_i \bar{\psi}_i \mathcal{O}_i + h.c.$ [22]. The running coupling $\lambda_i(\mu)$ obeys the RG equation

$$ \mu \frac{d\lambda_i}{d\mu} = \gamma_i \lambda_i + a \frac{N}{16\pi^2} \lambda_i^3 + \cdots , \qquad (14.13) $$

---

[d]In Ref. [21] has been claimed that $\widehat{S}$ can be small or even negative for certain geometries of the 5D space. Nevertheless, one must check that the curvature of those geometries is not larger than the cut-off scale of the model such that does not invalidate the calculation.

where the dots stand for terms subleading in the large-N limit, and a is an $\mathcal{O}(1)$ positive coefficient. The first term in Eq. (14.13) drives the energy scaling of λ_i as dictated by the anomalous dimension $\gamma_i = \mathrm{Dim}[\mathcal{O}_i] - 5/2$, $\mathrm{Dim}[\mathcal{O}_i]$ being the conformal dimension of the operator $\mathcal{O}_i$. The second term originates instead from the CFT contribution to the fermion wave-function renormalization. The low-energy value of λ_i is determined by γ_i. For $\gamma_i > 0$, the coupling of the elementary fermion to the CFT is irrelevant, and λ_i decreases with the energy scale μ. Below μ_{IR}, we have

$$\lambda_i \sim \left(\frac{\mu_{\mathrm{IR}}}{\Lambda} \right)^{\gamma_i} , \qquad (14.14)$$

where $\Lambda \sim M_{\mathrm{Pl}}$ is the UV-cutoff of the CFT. Therefore, fermions with $\gamma_i > 0$ will have a small mixing with the CFT bound states, and thus small fermion masses. For the up-quarks we will have

$$m_u \sim \lambda_q \lambda_u \frac{f_\pi^2}{m_\rho} \sim \frac{\sqrt{N}}{4\pi} \left(\frac{\mu_{\mathrm{IR}}}{\Lambda} \right)^{\gamma_q + \gamma_u} 246 \text{ GeV} . \qquad (14.15)$$

For $\gamma_i < 0$, the coupling is relevant and λ_i flows at low energy to the fixed-point value

$$\lambda_i = \frac{4\pi}{\sqrt{N}} \sqrt{-\frac{\gamma_i}{a}} . \qquad (14.16)$$

In this case the mixing between ψ_i and the CFT is large, and sizable SM fermion masses can be generated for not too large values of N. The values of γ_i are related to the 5D fermion masses c_i according to [22]:

$$\gamma_q = \left| c_q + \frac{1}{2} \right| - 1 , \qquad \gamma_u = \left| c_u - \frac{1}{2} \right| - 1 . \qquad (14.17)$$

Therefore the requirement $\gamma_{q,u} > 0$ for the light fermions implies $c_q > 1/2$ and $c_u < -1/2$, while for the top $\gamma_{q,u} \lesssim 0$ implies $|c_{q,u}| \lesssim 1/2$.

In this 4D description it is easy to see why FCNC effects in these models are not in conflict with the experiments. FCNC operators induced by the CFT such as $(\bar{\psi}_i \psi_j)^2$ are proportional to $\lambda_i^2 \lambda_j^2 f_\pi^2 / m_\rho^4 \sim m_i m_j / (f_\pi^2 m_\rho^2)$. This suppression factor allow us to pass all experimental constraints with no large tuning in the parameters [17, 18].

The 4D holographic model is then described by the Lagrangian:

$$\mathcal{L} = \mathcal{L}_{\text{CFT}} + \mathcal{L}_{\text{SM}} + J_{\text{CFT}}^{a_L\,\mu} W_\mu^{a_L} + J_{\text{CFT}}^{Y\,\mu} B_\mu + \lambda_i\, \bar{\psi}_i \mathcal{O}_i + \text{h.c.} \,. \qquad (14.18)$$

14.3. Composite Higgs Models

By enlarging the group G, while keeping qualitatively the same properties of the Higgsless models described above, we are driven to a different scenario in which the strong or extra dimenional sector, instead of breaking the EW symmetry, contains a light Higgs in its spectrum that will be the responsible for EWSB. These scenarios, named Composite Higgs models, were first proposed in the eighties [3]. Nevertheless, these first examples lacked several ingredients. First, they did not incorporate a heavy top (since its mass was not known at that time), and the largest SM contribution to the Higgs potential was that of the SM weak bosons. Since the latter always leads to an electroweak-preserving vacuum, the authors of Ref. [3] had to enlarge the SM gauge group in order to trigger EWSB. Second, flavor was not successfully incorporated and the corrections to the EW precision observables were not possible to be calculated.

Five-dimensional theories allow us to obtain realistic and predictive models of composite Higgs. Here we want to present the minimal 5D composite Higgs [9, 10]. The 5D geometry is the same as in the Higgsless case, Eq. (14.5). Nevertheless, the gauge symmetry is in this case given by

$$\text{UV} - \text{boundary}: \qquad \text{SU(2)}_\text{L} \times \text{U(1)}_\text{Y} \times \text{SU(3)}_\text{c}$$
$$\text{5D Bulk}: \qquad \text{SO(5)} \times \text{U(1)}_\text{X} \times \text{SU(3)}_\text{c}$$
$$\text{IR} - \text{boundary}: \qquad \text{O(4)} \times \text{U(1)}_\text{X} \times \text{SU(3)}_\text{c}.$$

Since the symmetry-breaking pattern of the bulk and IR-boundary is given by $\text{SO(5)}\rightarrow\text{O(4)}$, we expect four Goldstone bosons parametrized by the $\text{SO(5)}/\text{SO(4)}$ coset [9]:

$$\Sigma = \langle\Sigma\rangle e^{\Pi/f_\pi}\,, \qquad \langle\Sigma\rangle = (0,0,0,0,1)\,, \qquad \Pi = \begin{pmatrix} 0_4 & H \\ -H^T & 0 \end{pmatrix}\,, \quad (14.19)$$

where H is a real 4-component vector, which transforms as a doublet under SU(2)_L. This is identified with the Higgs. In the fermion sector, each SM generation is identified with the zero mode of 5D bulk multiplets transforming as fundamentals of SO(5). For the up-quark sector these 5D fields

are [10]

$$
\xi_q = (\Psi_{qL}, \Psi_{qR}) = \begin{bmatrix} (\mathbf{2,2})_{\mathbf{L}}^{\mathbf{q}} = \begin{bmatrix} q_L'(-+) \\ q_L(++) \end{bmatrix} & , & (\mathbf{2,2})_{\mathbf{R}}^{\mathbf{q}} = \begin{bmatrix} q_R'(+-) \\ q_R(--) \end{bmatrix} \\ (\mathbf{1,1})_{\mathbf{L}}^{\mathbf{q}}(--) & , & (\mathbf{1,1})_{\mathbf{R}}^{\mathbf{q}}(++) \end{bmatrix} ,
$$

$$
\xi_u = (\Psi_{uL}, \Psi_{uR}) = \begin{bmatrix} (\mathbf{2,2})_{\mathbf{L}}^{\mathbf{u}}(+-) & , & (\mathbf{2,2})_{\mathbf{R}}^{\mathbf{u}}(-+) \\ (\mathbf{1,1})_{\mathbf{L}}^{\mathbf{u}}(-+) & , & (\mathbf{1,1})_{\mathbf{R}}^{\mathbf{u}}(+-) \end{bmatrix} , \tag{14.20}
$$

where $\xi_{q,u}$ transform as $\mathbf{5}_{2/3}$ of $SO(5) \times U(1)_X$. In Eq. (14.20) we have grouped the fields of each multiplet $\xi_{q,u}$ in representations of $SU(2)_L \times SU(2)_R$, and used the fact that a fundamental of $SO(5)$ decomposes as $\mathbf{5} = (\mathbf{2,2}) \oplus (\mathbf{1,1})$. Localized on the IR-boundary, we consider the most general set of mass terms invariant under $O(4) \times U(1)_X$:

$$
\widetilde{m}_u \, \overline{(\mathbf{2,2})}_{\mathbf{L}}^{\mathbf{q}} (\mathbf{2,2})_{\mathbf{R}}^{\mathbf{u}} + \widetilde{M}_u \, \overline{(\mathbf{1,1})}_{\mathbf{R}}^{\mathbf{q}} (\mathbf{1,1})_{\mathbf{L}}^{\mathbf{u}} + \text{h.c.} . \tag{14.21}
$$

At energies below the mass of the KK-states, m_ρ, the spectrum corresponds to that of the SM with a Higgs. The low-energy theory for the PGB Higgs Σ, written in a $SO(5)$-invariant way, is given by

$$
\mathcal{L}_{\text{eff}} = f_\pi^2 \left[\frac{1}{2} (D_\mu \Sigma)(D^\mu \Sigma)^T + \frac{c_Y}{m_\rho} \bar{\Psi}_{qL}^i \Sigma^i \Sigma^j \Psi_{uR}^j \right.
$$
$$
\left. + \frac{c_S}{m_\rho^2} \Sigma F_{\mu\nu} F^{\mu\nu} \Sigma^T + V(\Sigma) + \dots \right] . \tag{14.22}
$$

From the kinetic term of Σ we obtain $M_W^2 = g^2 (s_h f_\pi)^2/4$ where we have defined $s_h \equiv \sin h/f_\pi$. This implies

$$
v \equiv \epsilon f_\pi = s_h f_\pi = 246 \text{ GeV} . \tag{14.23}
$$

The value of ϵ can vary between 0 (no EWSB) and 1 (maximal EWSB) and we will discuss later how it is determined. The second term of Eq. (14.22), in which Ψ_{qL} (Ψ_{uR}) transforms as a $\mathbf{5}_{2/3}$ and contains the SM q_L (u_R) plus spurions, is responsible for the fermion masses:

$$
m_u = c_Y \frac{f_\pi^2}{m_\rho} s_h c_h , \tag{14.24}
$$

where $c_Y \sim \lambda_q \lambda_u$ with $\lambda_{q,u}$ scaling as in the Higgsless case — see Eqs. (14.14), (14.16) and (14.17). FCNC in this model are under control as in the Higgsless case. It is important to notice from Eq. (14.24) that to generate non-zero fermion masses we must require $0 < s_h c_h < 1$, i.e. $0 < \epsilon < 1$. Therefore, maximal EWSB $\epsilon = 1$ is not allowed.

From the third term of Eq. (14.22) we can derive the the Peskin-Takeuchi $\widehat{S}$-parameter. The value of c_S does not differ from the Higgsless case and therefore we have [9]

$$\widehat{S} = \frac{3g^2}{128\pi^2}\tilde{N}\epsilon^2\,,\tag{14.25}$$

The 99% CL experimental bound [13] [e] $\widehat{S} \lesssim 3 \cdot 10^{-3}$ then translates into

$$\epsilon^2 \lesssim \frac{1}{4}\left(\frac{10}{\tilde{N}}\right)\,.\tag{14.26}$$

Contrary to the Higgsless case, we see that the composite Higgs model can satisfy the constraint from $\widehat{S}$ (with a large value of $\tilde{N}$ to trust the 5D result) if ϵ is small. Later we will see the region of the parameter space in which Eq. (14.26) is satisfied. Eq. (14.26) is the only constraint from EW precision tests, since $\widehat{T}$ and $\delta g_b/g_b$ are both protected by the custodial $O(3) \simeq SU(2)_V \times P_{LR}$ symmetry [15] and therefore are only generated at the loop-level, being small enough [23]. We can then conclude that in composite Higgs models the lowest vector KK can be as light as

$$m_\rho \simeq \frac{3\pi}{4L_1} \simeq 2.4\sqrt{\frac{10}{\tilde{N}}}\text{ TeV}\,.\tag{14.27}$$

14.3.1. *Higgs potential and vacuum misalignment*

The last term of Eq. (14.22) corresponds to the PGB Higgs potential that it is induced at the loop level. This potential can be calculated in two steps following the holographic prescription: we first integrate out (at tree-level) the bulk fields as a function of the UV-boundary fields. This leaves a 4D theory in which the Higgs potential can be calculated following Coleman-Weinberg. In this second step the dominant contribution to this Higgs potential comes at the one-loop level from the virtual exchange of the $SU(2)_L$ gauge bosons and top quark, and it is given by

$$V(h) = \int \frac{d^4p}{(2\pi)^4}\left\{-\frac{9}{2}\log \Pi_W + 2N_c[\log \Pi_{b_L} + \log(p^2\Pi_{t_L}\Pi_{t_R} - \Pi_{t_L t_R}^2)]\right\}\,,\tag{14.28}$$

---

[e]We are taking the value from Ref. [13] with $m_h \sim 120$ GeV, since in composite Higgs scenarios, as we will see later, the Higgs is light.

where $N_c = 3$ and

$$\Pi_W = \Pi_0 + \frac{s_h^2}{4}\,\Pi_1\,,$$

$$\Pi_{t_L t_R} = \frac{s_h c_h}{\sqrt{2}}\,M_1^u\,,$$

$$\Pi_{b_L} = \Pi_0^q\,,$$

$$\Pi_{t_L} = \Pi_0^q + \frac{s_h^2}{2}\,\Pi_1^q\,,$$

$$\Pi_{t_R} = \Pi_0^u + c_h^2\,\Pi_1^u\,. \qquad (14.29)$$

The Π_i are complicated momentum-dependent form factors that can be found in Ref. [10]. Apart from a constant piece, the potential of Eq. (14.28) is finite, since the form factors Π_1 and M_1 drop exponentially for $p \gg 1/L_1$. This fast decrease with the momentum allows us to expand the logarithms in Eq. (14.28) and write the approximate formula

$$V(h) \simeq \alpha\, s_h^2 - \beta\, s_h^2 c_h^2\,, \qquad (14.30)$$

where α and β are integral functions of the form factors. For $\alpha < \beta$ and $\beta \geqslant 0$ we have that the electroweak symmetry is broken: $\epsilon \neq 0$. If $\beta > |\alpha|$, the minimum of the potential is at

$$s_h = \epsilon = \sqrt{\frac{\beta - \alpha}{2\beta}}\,, \qquad (14.31)$$

while for $\beta < |\alpha|$ the minimum corresponds to $c_h = 0$, and the EWSB is maximal: $\epsilon = 1$. As we said before, this latter case leads to zero fermion masses and must be discarded. The gauge contribution gives $\alpha > 0$ and tends to align the vacuum along the $(\mathrm{SU}(2)_L)$-preserving direction. A misalignment of the vacuum, however, can come from the top loops, which can give $\alpha < 0$ and $\beta > 0$. The physical Higgs mass is given by

$$m_h^2 \simeq \frac{8\beta s_h^2 c_h^2}{f_\pi^2} \sim \frac{8 N_c}{\tilde{N}}\, m_t^2\,, \qquad (14.32)$$

and, for moderate values of $\tilde{N} \sim 10$, it can be above the experimental bound $m_h > 114$ GeV.

What is the allowed region of the 5D parameter space of the model that gives EWSB ($\epsilon \neq 0$) and satisfy the constraint Eq. (14.26) from precision tests? To answer this question we first notice that the only relevant 5D parameters are those related to the top quark and gauge sector since they give the dominant contribution to the Higgs potential. These parameters are

$$\tilde{N}\,,\ c_q\,,\ c_u\,,\ \widetilde{m}_u\,,\ \widetilde{M}_u\,. \qquad (14.33)$$

Here $\widetilde{m}_u$, $\widetilde{M}_u$, c_q and c_u denote the mass parameters of the top quark, $q_L = (t_L, b_L)$ and $u_R = t_R$. The scale L_1 has been traded for v.
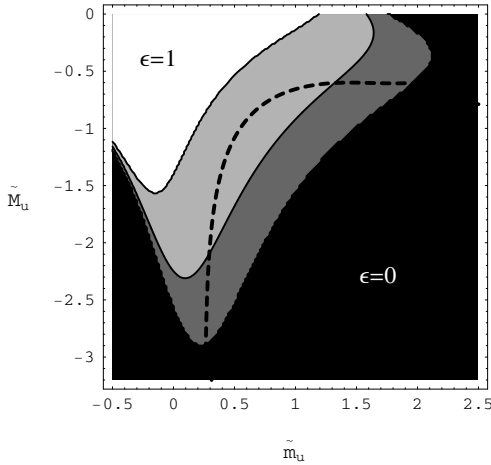
Fig. 14.1. Contour plots in the plane $(\widetilde{m}_u, \widetilde{M}_u)$ with $c_q = 0.35$, $c_u = 0.45$, $\tilde{N} = 8$. The black (white) area denotes the region with $\epsilon = 0$ ($\epsilon = 1$). The gray intermediate area with $0 < \epsilon < 1$ is the region with EWSB and non-zero fermion masses. Its lighter gray portion is excluded by Eq. (14.26). The dashed black line represents the curve with $m_t^{\overline{\mathrm{MS}}}(2\,\mathrm{TeV}) = 150\,\mathrm{GeV}$, equivalent to $m_t^{\mathrm{pole}} = 173\,\mathrm{GeV}$.

Figure 14.1 gives an example of the allowed and excluded region of the parameter space. One can see that, although the constraint Eq. (14.26) excludes a portion of the parameter space, there is still a sizable portion allowed, showing that no large fine tuning is required to pass the electroweak tests. Thus, this model can give a realistic account of the EWSB and fermion masses without conflict with experiments.

14.3.2. *Fermionic resonances*

A crucial prediction of the 5D composite Higgs model is that the requirement of a large top quark mass always forces some of the fermionic KK resonances to be lighter than their gauge counterpart. The reason is the following. The embedding of t_L and t_R into SO(5) bulk multiplets implies that some of their SO(5) partners have $(\pm, \mp)$ boundary conditions, an assignment that is necessary to avoid extra massless states (see Eqs. (14.20)). Consider for example the case in which the left-handed chirality of the 5D field is $(+, -)$, (hence the right-handed one is $(-, +)$): for values of the 5D mass $c_i > 1/2$, the lightest KK mode — we will denote it by q^* — has its left-handed chirality exponentially peaked on the UV-boundary, while its
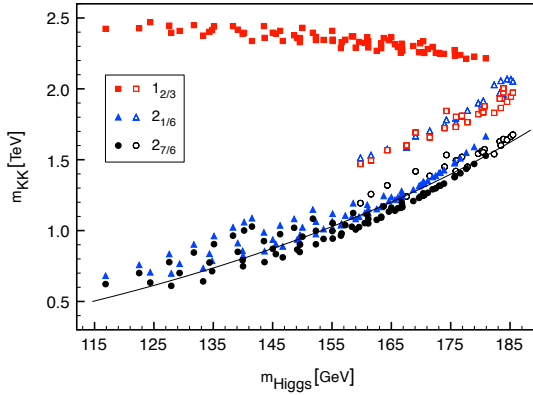
Fig. 14.2.   Masses of the lightest colored KK fermions. Different symbols denote KKs with different quantum numbers under $SU(2)_L \times U(1)_Y$. We have fixed $\epsilon = 0.5$, $\tilde{N} = 8$, and varied $0.28 < c_q < 0.38$, $0 < c_u < 0.41$, $0.32 < \tilde{m}_u < 0.42$, $-3.5 < \widetilde{M}_u < -2.2$ (filled points), or $0.2 < c_q < 0.35$, $-0.25 < c_u < -0.42$, $-1.3 < \tilde{m}_u < 0.2$, $0.1 < \widetilde{M}_u < 2.3$ (empty points). The black continuous line is the fit to the mass of the lightest resonance [10].

right-handed is localized on the IR-boundary. This implies that the mass of q^* is exponentially suppressed. In the opposite limit $c_i < -1/2$, both chiralities are localized on the IR-boundary and the mass of q^* is of the same order as that of the other KKs: $m_{q^*} \simeq m_\rho$. In the intermediate region $-1/2 < c_i < 1/2$, the one we chose for top quark bulk fields, one finds that m_{q^*} is given by [24]

$$m_{q^*} \simeq \frac{2}{L_1} \sqrt{\frac{1}{2} - c_i}, \qquad (14.34)$$

which means that it is still parametrically smaller than m_ρ by a factor $\sqrt{1/2 - c_i}$. Analogous results hold in the case of a $(+, -)$ right-handed chirality, but for $c_i \to -c_i$.

Let us concentrate on the region $-1/2 < c_u < 1/2$ and $c_q > 0$. From the argument above and by inspecting Eq. (14.20), one finds that the lightest KK modes are those arising from the $(\mathbf{2}, \mathbf{2})^{\mathbf{u}}$ component of the bulk multiplet ξ_u. This field contains two $SU(2)_L$ doublets of hypercharge $Y = 7/6$ and $Y = 1/6$. Figure 14.2 shows the spectrum of the lowest fermionic KK states. The lightest states are those predicted. Their mass is around $500 - 1500$ GeV for $\epsilon = 1/2$ and $\tilde{N} = 8$, much smaller than that of the lightest gauge KK, $m_\rho \simeq 2.6$ TeV, and of other fermionic excitations.
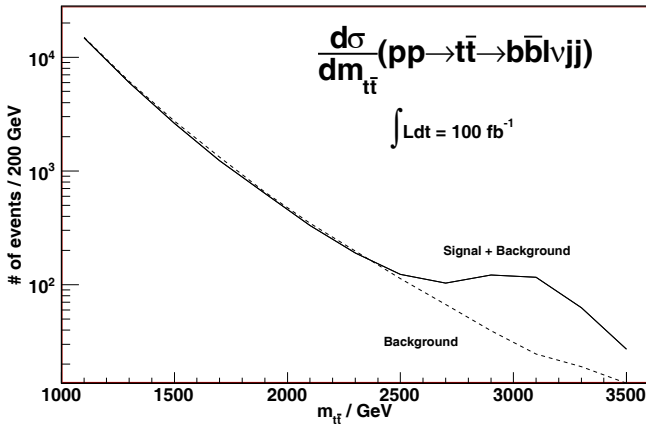
Fig. 14.3.   Invariant $t\bar{t}$ mass distribution for a gluon resonance of 3 TeV produced at the LHC [28].

14.4. LHC Phenomenology

14.4.1. *Heavy resonances at the LHC*

The universal feature of strongly coupled theories of EWSB or their extra dimensional analogs is the presence of vector resonances, triplet under $SU(2)_V$, of masses in the range $0.5 - 2.5$ TeV; they are the TC-rho or KK of the W. They can either be produced in a $q\bar{q}$ Drell-Yan scattering or via weak boson fusion. These vector resonances will mostly decay into pairs of longitudinally polarized weak bosons (or, if possible, to a weak boson plus a Higgs), and to pairs of tops and bottoms. Studies at the LHC has been devoted to a very light TC-rho, $m_\rho \lesssim 600$ GeV, that will be able to be seen for an integrated luminosity of 4 fb^{-1} [25] (see also Ref. [26]). Recent studies suggest that one can go up to masses of 2 TeV for 100 fb^{-1} [27].

Another more interesting signal from extra dimensional models (but also present in top-assited TC models [12]) is the detection of heavy gluon resonances. The dominant production mechanism at the LHC is through $u\bar{u}$ or $d\bar{d}$ annihilation, decaying mostly in top pairs. The signal will be then a bump in the invariant $t\bar{t}$ mass distribution -see Fig. 14.3. For an integrated luminosity of 100 fb^{-1} the reach of the gluon resonances can be up to masses of 4 TeV [28].

The most promising way to unravel the 5D warped models described above is by detecting the lowest fermionic KKs at the LHC. In particular, for

the composite Higgs model, detecting heavy fermions with electric charge $5/3$ ($q^*_{5/3}$) that arise from the $\mathbf{2}_{7/6}$ multiplet of $SU(2)_L \times U(1)_Y$, would be the smoking-gun signature of the model. For not-too-large values of its mass $m_{q^*_{5/3}}$, roughly below 1 TeV, these new particles will be mostly produced in pairs, via QCD interactions,

$$q\bar{q}, gg \to q^*_{5/3}\,\bar{q}^*_{5/3}\,, \tag{14.35}$$

with a cross section completely determined in terms of $m_{q^*_{5/3}}$. Once produced, $q^*_{5/3}$ will mostly decay to a (logitudinally polarized) W^+ plus a top quark. The final state of the process Eq. (14.35) consists then mostly of four W's and two b-jets:

$$q^*_{5/3}\,\bar{q}^*_{5/3} \to W^+ t\, W^- \bar{t} \to W^+ W^+ b\, W^- W^- \bar{b}\,. \tag{14.36}$$

Using same-sign dilepton final states we could discover these particles for masses of 500 GeV (1 TeV) for an integrated luminosity of 100 pb^{-1} (20 fb^{-1}) [29]. The same final state also comes from pair production of KKs with charge $-1/3$. A way to discriminate between the two cases, consists in reconstructing the electric charge of the resonance. For example, one could look for events with two highly-energetic leptons of the same sign, coming from the leptonic decay of two of the four W's, plus at least six jets, two of which tagged as b-jets. Demanding that the invariant mass of the system of the two hadronically-decaying W's plus one b-jet equals $m_{q^*_{5/3}}$ then identifies the process and gives evidence for the charge $5/3$ of the resonance. Furthermore, indirect evidence in favor of $q^*_{5/3}$ would come from the non-observation of the decays to Zb, Hb that is allowed for resonances of charge $-1/3$.

For increasing values of $m_{q^*_{5/3}}$ the cross section for pair production quickly drops, and single production might become more important. The relevant process is tW fusion [30], where a longitudinal W radiated from one proton scatters off a top coming from the other proton. The analogous process initiated by a bottom quark, bW fusion, has been studied in detail in the literature and shown to be an efficient way to singly produce heavy excitations of the top quark [31–33]. To prove that the same conclusion also applies to the case of tW fusion a dedicated analysis is required. The main uncertainty and challenge comes from the small top quark content of the proton, which however can be compensated by the large coupling involved.

Besides $q^*_{5/3}$, the other components of the $\mathbf{2}_{1/6}$ and $\mathbf{2}_{7/6}$ multiplets of $SU(2)_L \times U(1)_Y$ are also predicted to be light. The states of electric charge $2/3$ or $-1/3$ could also be produced in pairs via QCD interactions or singly

via bW or tW fusion. They will decay to a SM top or bottom quark plus a longitudinally polarized W or Z, or a Higgs. When kinematically allowed, a heavier resonance will also decay to a lighter KK accompanied with a W_{long}, Z_{long} or h. Decay chains could lead to extremely characteristic final states. For example, in one of the models of Ref. [10], the KK with charge 2/3 from $\mathbf{3}_{2/3}$ is predicted to be generally heavier than $q_{5/3}^*$. If pair produced, they can decay to $q_{5/3}^*$ leading to a spectacular six W's plus two b-jets final state:

$$q_{2/3}^* \, \bar{q}_{2/3}^* \to W^- q_{5/3}^* \, W^+ \bar{q}_{5/3}^* \to W^- W^+ W^+ b \, W^+ W^- W^- \bar{b} \,. \qquad (14.37)$$

To fully explore the phenomenology of the fermionic resonances in composite Higgs models a detailed analysis is necessary. Existing studies in the literature have focussed on the production and detection of $\text{SU}(2)_L$ singlets of hypercharge $Y = 2/3$ [33, 34], since this is a typical signature of Little Higgs theories. In composite Higgs models, however, the singlet is not predicted to be light, except for specific regions of the parameter space. In conclusion, our brief discussion shows that there are characteristic signatures predicted by these models that will distiguish them from other extensions of the SM. While certainly challenging, these signals will be extremely spectacular, and will provide an indication of a new strong dynamics responsible for electroweak symmetry breaking.

14.4.2. *Experimental tests of a composite Higgs*

Alternative to the detection of the KK-states, the composite Higgs scenario can also be tested by measuring the couplings of the Higgs and seeing differences from those of a SM point-like Higgs. For small values of $\epsilon^2 \equiv \xi$, as needed to satisfy Eq. (14.26), we can expand the low-energy Lagrangian in powers of h/f_π and obtain in this way the following dimension-6 effective Lagrangian involving the Higgs field doublet H:

$$\mathcal{L}_{\text{SILH}} = \frac{c_H}{2f^2} \partial^\mu \left(H^\dagger H \right) \partial_\mu \left(H^\dagger H \right) + \frac{c_T}{2f^2} \left(H^\dagger \overleftrightarrow{D^\mu} H \right) \left(H^\dagger \overleftrightarrow{D}_\mu H \right)$$
$$- \frac{c_6 \lambda}{f^2} \left(H^\dagger H \right)^3 + \left(\frac{c_y y_f}{f^2} H^\dagger H \bar{\psi}_L H \psi_R + \text{h.c.} \right) . \qquad (14.38)$$

Equation (14.38) will be refer as the Strongly Interacting Light Higgs (SILH) Lagrangian [35]. We have neglected operators suppressed by $1/m_\rho^2$ that are subleading versus those of Eq. (14.38) by a factor $f_\pi^2/m_\rho^2 \sim N/(16\pi^2)$, or operators that do not respect the global symmetry G and

therefore are only induced at the one-loop level with extra suppression factors — see Ref. [35]. Out of the four operators of Eq. (14.38), only the coefficient of the second one (c_T) is highly constrained by the experimental data, since it contributes to the $\widehat{T}$-parameter. As explained above, however, composite Higgs models give small contributions to $\widehat{T}$, and therefore to c_T, consistently with the experimental bounds. The other operators are only measurable in Higgs physics. Their coefficients, in the 5D composite Higgs described above, are [35]: $c_H = c_y = 1$ and $c_6 = 0$. They modify the Higgs decay widths according to

$$\Gamma(h \to f\bar{f})_{\text{SILH}} = \Gamma(h \to f\bar{f})_{\text{SM}}[1 - \xi(2c_y + c_H)]$$
$$\Gamma(h \to WW)_{\text{SILH}} = \Gamma(h \to WW^{(*)})_{\text{SM}}[1 - \xi c_H]$$
$$\Gamma(h \to ZZ)_{\text{SILH}} = \Gamma(h \to ZZ^{(*)})_{\text{SM}}[1 - \xi c_H]$$
$$\Gamma(h \to gg)_{\text{SILH}} = \Gamma(h \to gg)_{\text{SM}}[1 - \xi\,\text{Re}(2c_y + c_H)] \quad (14.39)$$
$$\Gamma(h \to \gamma\gamma)_{\text{SILH}} = \Gamma(h \to \gamma\gamma)_{\text{SM}}\left[1 - \xi\,\text{Re}\left(\frac{2c_y + c_H}{1 + J_\gamma/I_\gamma} + \frac{c_H}{1 + I_\gamma/J_\gamma}\right)\right]$$
$$\Gamma(h \to \gamma Z)_{\text{SILH}} = \Gamma(h \to \gamma Z)_{\text{SM}}\left[1 - \xi\,\text{Re}\left(\frac{2c_y + c_H}{1 + J_Z/I_Z} + \frac{c_H}{1 + I_Z/J_Z}\right)\right].$$

The loop functions I and J are given in Ref. [35]. Notice that the contribution from c_H is universal for all Higgs couplings and therefore it does not affect the Higgs branching ratios, but only the total decay width and the production cross section. The measure of the Higgs decay width at the LHC is very difficult and it can only be reasonably done for a rather heavy Higgs, well above the two gauge boson threshold, that is not the case of a composite Higgs. However, for a light Higgs, LHC experiments can measure the product $\sigma_h \times BR_h$ in many different channels: production through gluon, gauge-boson fusion, and top-strahlung; decay into b, τ, γ and (virtual) weak gauge bosons. In Fig. 14.4, we show the prediction of the 5D composite Higgs for the relative deviation from the SM expectation in the main channels for Higgs discovery at the LHC. At the LHC with about 300 fb^{-1}, it will be possible to measure Higgs production rate times branching ratio in the various channels with 20–40 % precision [36], although a determination of the b coupling is quite challenging [37]. This will translate into a sensitivity on $|c_H\xi|$ and $|c_y\xi|$ up to 0.2–0.4, at the edge of the theoretical predictions. Since the Higgs coupling determinations at the LHC will be limited by statistics, they can benefit from a luminosity upgrading, like the SLHC. At a linear collider, like the ILC, precisions on $\sigma_h \times BR_h$ can reach the percent level [38], providing a very sensitive probe
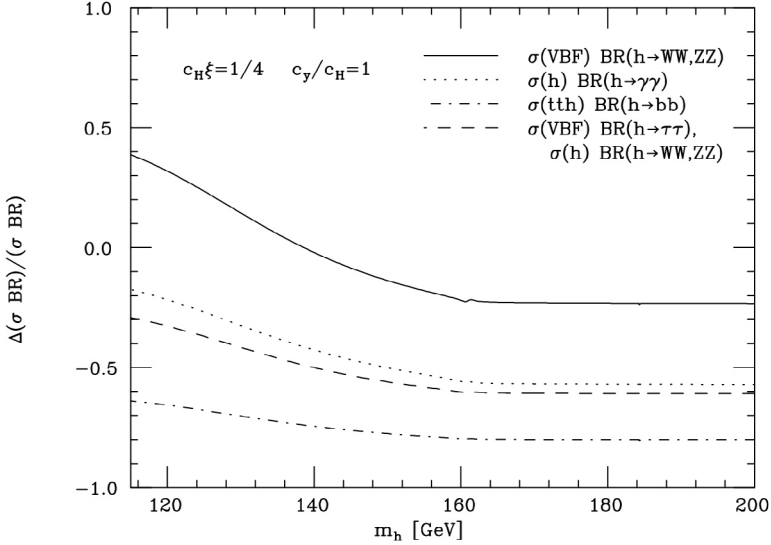
Fig. 14.4.   The deviations from the SM predictions of Higgs production cross sections (σ) and decay branching ratios (BR) defined as $\Delta(\sigma\,BR)/(\sigma\,BR) = (\sigma\,BR)_{\mathrm{SILH}}/(\sigma\,BR)_{\mathrm{SM}} - 1$. The predictions are shown for some of the main Higgs discovery channels at the LHC with production via vector-boson fusion (VBF), gluon fusion (h), and topstrahlung (tth).

on the scale f_π. Moreover, a linear collider can test the existence of c_6, since the triple Higgs coupling can be measured with an accuracy of about 10% for $\sqrt{s} = 500$ GeV and an integrated luminosity of 1000 fb^{-1} [39].

   Deviations from the SM predictions of Higgs production and decay rates, could be a hint towards models with strong dynamics. Nevertheless, they do not unambiguously imply the existence of a new strong interaction. The most characteristic signals of the SILH Lagrangian have to be found in the very high-energy regime. Indeed, a peculiarity of the SILH Lagrangian is that, in spite of a light Higgs, longitudinal gauge-boson scattering amplitudes grow with energy and the corresponding interaction can become sizable. Indeed, the extra Higgs kinetic term proportional to $c_H \xi$ in Eq. (14.38) prevents Higgs exchange diagrams from accomplishing the exact cancellation, present in the SM, of the terms growing with energy in the amplitudes. Therefore, although the Higgs is light, we obtain strong WW scattering at high energies.

   From the operator $O_H \equiv \partial^\mu(H^\dagger H)\partial_\mu(H^\dagger H)$ in Eq. (14.38), using the equivalence theorem [40], it is easy to derive the following high-energy limit

of the scattering amplitudes for longitudinal gauge bosons

$$\mathcal{A}(Z_L^0 Z_L^0 \rightarrow W_L^+ W_L^-) = \mathcal{A}(W_L^+ W_L^- \rightarrow Z_L^0 Z_L^0) = -\mathcal{A}(W_L^\pm W_L^\pm \rightarrow W_L^\pm W_L^\pm),$$

$$\mathcal{A}\left(W_L^\pm W_L^\pm \rightarrow W_L^\pm W_L^\pm\right) = -\frac{c_H s}{f^2}, \tag{14.40}$$

$$\mathcal{A}\left(W^\pm Z_L^0 \rightarrow W^\pm Z_L^0\right) = \frac{c_H t}{f^2}, \mathcal{A}\left(W_L^+ W_L^- \rightarrow W_L^+ W_L^-\right) = \frac{c_H(s+t)}{f^2}, \tag{14.41}$$

$$\mathcal{A}\left(Z_L^0 Z_L^0 \rightarrow Z_L^0 Z_L^0\right) = 0. \tag{14.42}$$

The growth with energy of the amplitudes in Eqs. (14.40)–(14.42) is strictly valid only up to the maximum energy of our effective theory, namely m_ρ. The behaviour above m_ρ depends on the specific model realization. For example, in 5D composite Higgs models the growth of the elastic amplitude will be softened by KK exchange. Notice that the result in Eqs. (14.40)–(14.42) is exactly proportional to the scattering amplitudes obtained in a Higgsless SM [40]. Therefore, in theories with a SILH Lagrangian, the cross section at the LHC for producing longitudinal gauge bosons with large invariant masses can be written as

$$\sigma\left(pp \rightarrow V_L V_L' X\right)_{c_H} = (c_H \xi)^2 \sigma\left(pp \rightarrow V_L V_L' X\right)_{\cancel{H}}, \tag{14.43}$$

where $\sigma(pp \rightarrow V_L V_L' X)_{\cancel{H}}$ is the cross section in the SM without Higgs, at the leading order in $s/(4\pi v)^2$. With about 200 fb^{-1} of integrated luminosity, it should be possible to identify the signal of a Higgsless SM with about 30–50% accuracy [41–43]. This corresponds to a sensitivity up to $c_H \xi \simeq 0.5$–0.7.

Another generic prediction of the SILH Lagrangian is that the strong gauge boson scattering is accompanied by strong production of Higgs pairs. Indeed we find that, as a consequence of the $O(4)$ symmetry of the H multiplet, the amplitudes for Higgs pair-production grow with the center-of-mass energy as Eq. (14.40),

$$\mathcal{A}\left(Z_L^0 Z_L^0 \rightarrow hh\right) = \mathcal{A}\left(W_L^+ W_L^- \rightarrow hh\right) = \frac{c_H s}{f^2}. \tag{14.44}$$

Using Eqs. (14.40), (14.41) and (14.44), we can relate the Higgs pair production rate at the LHC to the longitudinal gauge boson cross sections

$$2\sigma_{\delta,M}\left(pp \rightarrow hhX\right)_{c_H} = \sigma_{\delta,M}\left(pp \rightarrow W_L^+ W_L^- X\right)_{c_H}$$
$$+ \frac{1}{6}\left(9 - \tanh^2 \frac{\delta}{2}\right) \sigma_{\delta,M}\left(pp \rightarrow Z_L^0 Z_L^0 X\right)_{c_H}. \tag{14.45}$$

Here all cross sections $\sigma_{\delta,M}$ are computed with a cut on the pseudorapidity separation between the two final-state particles (a boost-invariant quantity) of $|\Delta\eta| < \delta$, and with a cut on the two-particle invariant mass $\hat{s} > M^2$. The sum rule in Eq. (14.45) is a characteristic of the SILH Lagrangian. However, the signal from Higgs-pair production at the LHC is not so prominent. It was suggested that, for a light Higgs, this process is best studied in the channel $b\bar{b}\gamma\gamma$ [44], but the small branching ratio of $h \rightarrow \gamma\gamma$ makes the rate unobservable. Nevertheless, one can take advantage of the growth of the cross section with energy. It may be possible that, with sufficient luminosity, the signal of $b\bar{b}b\bar{b}$ with high invariant masses could be distinguished from the SM background. Notice however that, because of the high boost of the Higgs boson, the b jets are often not well separated. The case in which the Higgs decays to two real W's appears more promising for detection. The cleanest channel is the one with two like-sign leptons, where $hh \rightarrow \ell^{\pm}\ell^{\pm}\nu\nu$ jets, studied in Refs. [44, 45].

Acknowledgments

References

[1] S. Weinberg, Phys. Rev. D **13** (1976) 974; Phys. Rev. D **19** (1979) 1277; L. Susskind, Phys. Rev. D **20** (1979) 2619.

[2] See for example, M. J. Dugan and L. Randall, Phys. Lett. B **264** (1991) 154.

[3] D. B. Kaplan and H. Georgi, Phys. Lett. B **136** (1984) 183; D. B. Kaplan, H. Georgi and S. Dimopoulos, Phys. Lett. B **136** (1984) 187; H. Georgi, D. B. Kaplan and P. Galison, Phys. Lett. B **143** (1984) 152; H. Georgi and D. B. Kaplan, Phys. Lett. B **145** (1984) 216; M. J. Dugan, H. Georgi and D. B. Kaplan, Nucl. Phys. B **254** (1985) 299.

[4] J. M. Maldacena, Adv. Theor. Math. Phys. **2** (1998) 231; S. S. Gubser, I. R. Klebanov and A. M. Polyakov, Phys. Lett. B **428** (1998) 105; E. Witten, Adv. Theor. Math. Phys. **2** (1998) 253.

[5] C. Csaki, C. Grojean, L. Pilo and J. Terning, Phys. Rev. Lett. **92** (2004) 101802.

[6] G. Burdman and Y. Nomura, Phys. Rev. D **69**, 115013 (2004).

[7] R. Barbieri, A. Pomarol and R. Rattazzi, Phys. Lett. B **591** (2004) 141.

[8] R. Contino, Y. Nomura and A. Pomarol, Nucl. Phys. B **671** (2003) 148.

[9] K. Agashe, R. Contino and A. Pomarol, Nucl. Phys. B **719** (2005) 165.

[10] R. Contino, L. Da Rold and A. Pomarol, Phys. Rev. D **75**, 055014 (2007).

[11] G. 't Hooft, Nucl. Phys. B **72** (1974) 461; E. Witten, Nucl. Phys. B **160** (1979) 57.

[12] See for example, K. Lane, arXiv:hep-ph/0202255, and references therein.

[13] R. Barbieri, A. Pomarol, R. Rattazzi and A. Strumia, Nucl. Phys. B **703** (2004) 127.

[14] M. E. Peskin and T. Takeuchi, Phys. Rev. Lett. **65**, 964 (1990); Phys. Rev. D **46**, 381 (1992).

[15] K. Agashe, R. Contino, L. Da Rold and A. Pomarol, Phys. Lett. B **641** (2006) 62.

[16] L. Randall and R. Sundrum, Phys. Rev. Lett. **83** (1999) 3370.

[17] T. Gherghetta and A. Pomarol, Nucl. Phys. B **586** (2000) 141.

[18] S. J. Huber and Q. Shafi, Phys. Lett. B **498** (2001) 256; K. Agashe, G. Perez and A. Soni, Phys. Rev. Lett. **93** (2004) 201804; Phys. Rev. D **71** (2005) 016002.

[19] G. Cacciapaglia, C. Csaki, C. Grojean and J. Terning, Phys. Rev. D **71** (2005) 035015.

[20] R. Sekhar Chivukula, E. H. Simmons, H. J. He, M. Kurachi and M. Tanabashi, Phys. Rev. D **72** (2005) 015008.

[21] J. Hirn and V. Sanz, Phys. Rev. Lett. **97** (2006) 121803.

[22] R. Contino and A. Pomarol, JHEP **0411** (2004) 058.

[23] M. Carena, E. Ponton, J. Santiago and C. E. M. Wagner, arXiv:hep-ph/0607106.

[24] K. Agashe and R. Contino, Nucl. Phys. B **742** (2006) 59.

[25] P. Kreuzer, CMS note, 2006/135.

[26] A. Birkedal, K. Matchev and M. Perelstein, Phys. Rev. Lett. **94** (2005) 191803.

[27] K. Agashe *et al.*, Phys. Rev. D **76** (2007) 115015.

[28] K. Agashe, A. Belyaev, T. Krupovnickas, G. Perez and J. Virzi, Phys. Rev. D **77** (2008) 015003.

[29] R. Contino and G. Servant, arXiv:0801.1679 [hep-ph].

[30] S. S. D. Willenbrock and D. A. Dicus, Phys. Rev. D **34** (1986) 155.

[31] T. Han, H. E. Logan, B. McElrath and L. T. Wang, Phys. Rev. D **67** (2003) 095004.

[32] M. Perelstein, M. E. Peskin and A. Pierce, Phys. Rev. D **69** (2004) 075002.

[33] G. Azuelos *et al.*, Eur. Phys. J. C **39S2** (2005) 13.

[34] J. A. Aguilar-Saavedra, Phys. Lett. B **625** (2005) 234 [Erratum-ibid. B **633** (2006) 792]; PoS **TOP2006** (2006) 003; arXiv:hep-ph/0603200.

[35] G. F. Giudice, C. Grojean, A. Pomarol and R. Rattazzi, JHEP **0706** (2007) 045.

[36] M. Dührssen, ATL-PHYS-2003-030.

[37] S. Cucciarelli *et al.*, CMS Note 2006/119.

[38] J. A. Aguilar-Saavedra *et al.* [ECFA/DESY LC Physics Working Group], arXiv:hep-ph/0106315.

[39] V. Barger, T. Han, P. Langacker, B. McElrath and P. Zerwas, Phys. Rev. D **67** (2003) 115001.

[40] M. S. Chanowitz and M. K. Gaillard, Nucl. Phys. B **261** (1985) 379.

[41] J. Bagger *et al.*, Phys. Rev. D **52** (1995) 3878 .

[42] J. M. Butterworth, B. E. Cox and J. R. Forshaw, Phys. Rev. D **65** (2002) 096014.

[43] E. Accomando, A. Ballestrero, A. Belhouari and E. Maina, arXiv:hep-ph/0603167.

[44] U. Baur, T. Plehn and D. L. Rainwater, Phys. Rev. D **69** (2004) 053004.

[45] A. Pierce, J. Thaler and L. T. Wang, arXiv:hep-ph/0609049.

Chapter 15

How to Find a Hidden World at the LHC

James D. Wells

CERN, Theory Division, CH-1211 Geneva 23, Switzerland
and
MCTP, University of Michigan, Ann Arbor, MI 48109
James.Wells@cern.ch

I discuss how the Large Hadron Collider era should broaden our view of particle physics research, and apply this thinking to the case of Hidden Worlds. I focus on one of the simplest representative cases of a Hidden World, and detail the rich implications it has for LHC physics, including universal suppression of Higgs boson production, trans-TeV heavy Higgs boson signatures, heavy-to-light Higgs boson decays, weakly coupled exotic gauge bosons, and Higgs boson decays to four fermions via light exotic gauge bosons. Some signatures may be accessible in the very early stages of collider operation, whereas others motivate a later high-lumonosity upgrade.

15.1. Particle Physics in the LHC Era

The annals of particle physics are replete with exhortations to solve the hierarchy problem, the flavor problem, the baryon asymmetry problem, the dark matter problem, the unification problem, etc. Much of our efforts go into constructing the simplest solution to one of these problems. There is a premium on taut constructions narrowly tailored to solve our most precious problems.

With the coming of the LHC era, electroweak symmetry breaking and naturalness become the central focus for at least the initial phase of running. Our community has had many ideas, the simplest being that a single scalar boson condenses to break the electroweak symmetry and simultaneously gives mass to all elementary particles. Although a logical possibility,

few believe the Higgs boson alone is a viable option since it is so delicate to quantum corrections. For thirty years the beyond-the-Standard Model community has pursued various scenarios that support and protect the Higgs boson from these destabilizing tendencies (supersymmetry, CFT, extra dimension, etc.), or have banished the offending fundamental scalar from nature (technicolor, compositeness, higgsless models, etc.), while other ideas have found ways to push the problem to higher scales (little Higgs theories, etc.).

Of course there are too many ideas out there for all to be correct. Nevertheless, if there are a thousand ideas and only one is right, it does not mean that the others were useless, just as when a thousand rescue volunteers are looking for a little girl lost in the woods and one finds her, it does not mean the others were useless. It may be argued that the only useless ideas are ones not grounded in rigor or are incompatible with past observations. This criteria for the worth of an idea is somewhat looser than the criteria we normally apply to theory in deciding what is good work. Normally, we give our highest esteem to efforts that solve problems. We value invention over unmoored creativity. I once heard an inventor describe what he does as first asking "What sucks?" and then working day and night to make it better. That is what we mostly do in physics. We worship inventions. We dislike the SM Higgs boson and its quantum instability. This leads us to invent technicolor, supersymmetry, extra dimensions, etc. and then further invent solutions to their iatrogenic illnesses. This formula is rather human-centric because we care most about *our* problems – at the core, they are the problems associated with understanding the particles that make up our bodies. Surely, there is more to the universe than that.

A more universalist approach asks rather "what's possible?" There is great danger in this approach, since a whole lot more things are possible than are even probable. What then can discipline us? A new answer to this question is the Large Hadron Collider. The LHC era beckons us to approach physics less as an inventor and more humbly as a universalist. The beckoning is due to the filtering opportunity of experiment, and the impertinent susurrations that we shall fall short if we only take seriously our inventions. Agreeing to the LHC as the primary disciplinarian of our creativity can yield a deeper interpretation of the data and perhaps may lead to new discoveries that were not anticipated.

Thus, it is the existence of the LHC that propels me to write about hidden worlds, or hidden sectors [1–6]. I could argue some second-order problem-solving explanation for why we must all care about this issue,

by telling you that many ideas of physics beyond the SM have sectors in addition to the SM that are hard to get rid of. I could also describe why landscape studies imply the existence of even hundreds of possible new sectors [7] that have nothing directly to do with solving any deep problem in nature that we recognize. No, instead, despite the motivating paralepsis, the physics of this chapter has but one core reason for cogitation: it can be discovered at the LHC.

15.2. Hidden Worlds

The definition of "hidden" that I use here is the collection of particles that are not the SM, that are not charged under SM gauge groups, and that do not couple via gauge interactions to SM particles. The possibilities are numerous. We can envision analogous copies of the SM charged under new gauge groups $SU(3)'_c \times SU(2)'_L \times U(1)'_Y$. We can envision pure singlet states. We can envision gauge fields of exotic gauge groups of large dimensionality. Very little experimental data bears on the question of whether such sectors exist.

It is not assured that we shall be able to discern the existence of a hidden world. All we can do is identify opportunities and explore them. Of course, any gauge invariant and Lorenz invariant operator of the SM $\mathcal{O}^{inv}_{SM}$ can be paired with a similar operator from the hidden sector $\mathcal{O}^{inv}_{hid}$ to form $\mathcal{O}^{inv}_{SM}\mathcal{O}^{inv}_{hid}$. If this resulting operator is irrelevant (dimension > 4) it will be suppressed by some unknown scale M_*. We have no *a piori* idea what scale M_* should be; however, we know that if it is above a few TeV it is unlikely we shall see evidence of this interaction due to decoupling.

The SM however does have two operators that are gauge-invariant and relevant (dimension < 4): the hypercharge field strength tensor $B_{\mu\nu}$ and the Higgs modulus squared $|H_{SM}|^2$. These two operators give us hope that we can couple to a hidden sector in a relevant or marginal way (dimension ≤ 4), thereby enabling a search for a hidden world via the hypercharge gauge boson or the Higgs boson of the SM.

Indeed, both of these operators can be exploited in the above-stated way to explore the simplest, non-trivial hidden sector that couples to $B_{\mu\nu}$ and $|\Phi_{SM}|^2$: $U(1)_X$ gauge theory with a complex Higgs boson Φ_H that breaks the symmetry upon condensation. We call this simple model the "Hidden Abelian Higgs Model" or HAHM, and explore the rich phenomenology that it implies for the LHC.

15.3. Hidden Abelian Higgs Model (HAHM)

In this section I define precisely what I mean by HAHM. First, we have the afore-mentioned extra $U(1)_X$ factor in addition to the SM gauge group. The only coupling of this new gauge sector to the SM is through kinetic mixing with the hypercharge gauge boson B_μ. The kinetic energy terms of the $U(1)_X$ gauge group are

$$\mathcal{L}_X^{KE} = -\frac{1}{4}\hat{X}_{\mu\nu}\hat{X}^{\mu\nu} + \frac{\chi}{2}\hat{X}_{\mu\nu}\hat{B}^{\mu\nu} , \qquad (15.1)$$

where we comment later that $\chi \ll 1$ is helpful to keep precision electroweak predictions consistent with experimental measurements.

We introduce a new Higgs boson Φ_H in addition to the usual SM Higgs boson Φ_{SM}. Under $SU(2)_L \otimes U(1)_Y \otimes U(1)_X$ we take the representations $\Phi_{SM} : (2, 1/2, 0)$ and $\Phi_H : (1, 0, q_X)$, with q_X arbitrary. The Higgs sector Lagrangian is

$$\mathcal{L}_\Phi = |D_\mu\Phi_{SM}|^2 + |D_\mu\Phi_H|^2 + m_{\Phi_H}^2|\Phi_H|^2 + m_{\Phi_{SM}}^2|\Phi_{SM}|^2$$
$$-\lambda|\Phi_{SM}|^4 - \rho|\Phi_H|^4 - \kappa|\Phi_{SM}|^2|\Phi_H|^2, \qquad (15.2)$$

so that $U(1)_X$ is broken spontaneously by $\langle\Phi_H\rangle = \xi/\sqrt{2}$, and electroweak symmetry is broken spontaneously as usual by $\langle\Phi_{SM}\rangle = (0, v/\sqrt{2})$.

One can diagonalize the kinetic terms by redefining $\hat{X}_\mu, \hat{Y}_\mu \to X_\mu, Y_\mu$ with

$$\begin{pmatrix} X_\mu \\ Y_\mu \end{pmatrix} = \begin{pmatrix} \sqrt{1-\chi^2} & 0 \\ -\chi & 1 \end{pmatrix} \begin{pmatrix} \hat{X}_\mu \\ \hat{Y}_\mu \end{pmatrix}.$$

The covariant derivative is then

$$D_\mu = \partial_\mu + i(g_X Q_X + g'\eta Q_Y)X_\mu + ig'Q_Y B_\mu + igT^3 W_\mu^3 . \qquad (15.3)$$

where $\eta \equiv \chi/\sqrt{1-\chi^2}$.

After a $GL(2, R)$ rotation to diagonalize the kinetic terms followed by an $O(3)$ rotation to diagonalize the 3×3 neutral gauge boson mass matrix, we can write the mass eigenstates as (with $s_x \equiv \sin\theta_x$, $c_x \equiv \cos\theta_x$)

$$\begin{pmatrix} B \\ W^3 \\ X \end{pmatrix} = \begin{pmatrix} c_W & -s_W c_\alpha & s_W s_\alpha \\ s_W & c_W c_\alpha & -c_W s_\alpha \\ 0 & s_\alpha & c_\alpha \end{pmatrix} \begin{pmatrix} A \\ Z \\ Z' \end{pmatrix} , \qquad (15.4)$$

where the usual weak mixing angle and the new gauge boson mixing angle are

$$s_W \equiv \frac{g'}{\sqrt{g^2 + g'^2}} ; \quad \tan(2\theta_\alpha) = \frac{-2s_W\eta}{1 - s_W^2\eta^2 - \Delta_Z} , \qquad (15.5)$$

with $\Delta_Z = M_X^2/M_{Z_0}^2$, $M_X^2 = \xi^2 g_X^2 q_X^2$, $M_{Z_0}^2 = (g^2 + g'^2)v^2/4$. M_{Z_0} and M_X are masses before mixing. The photon is massless (i.e., $M_A = 0$), and the two heavier gauge boson mass eigenvalues are

$$M_{Z,Z'} = \frac{M_{Z_0}^2}{2}\Big[\left(1 + s_W^2\eta^2 + \Delta_Z\right)$$
$$\pm \sqrt{\left(1 - s_W^2\eta^2 - \Delta_Z\right)^2 + 4s_W^2\eta^2}\Big], \qquad (15.6)$$

valid for $\Delta_Z < (1 - s_W^2\eta^2)$ ($Z \leftrightarrow Z'$ otherwise). Since we assume that $\eta \ll 1$, mass eigenvalues are taken as $M_Z \approx M_{Z_0} = 91.19$ GeV and $M_{Z'} \approx M_X$.

The two real physical Higgs bosons ϕ_{SM} and ϕ_H mix after symmetry breaking, and the mass eigenstates h, H are

$$\begin{pmatrix} \phi_{SM} \\ \phi_H \end{pmatrix} = \begin{pmatrix} c_h & s_h \\ -s_h & c_h \end{pmatrix} \begin{pmatrix} h \\ H \end{pmatrix}.$$

Mixing angle and mass eigenvalues are

$$\tan\left(2\theta_h\right) = \frac{\kappa v\xi}{\rho\xi^2 - \lambda v^2} \qquad (15.7)$$
$$M_{h,H}^2 = \left(\lambda v^2 + \rho\xi^2\right) \mp \sqrt{(\lambda v^2 - \rho\xi^2)^2 + \kappa^2 v^2\xi^2}. \qquad (15.8)$$

In summary, the model has been completely specified above. The effect of HAHM on LHC phenomenology is to introduce two extra physical states Z' and H. Z' is an extra gauge boson mass eigenstate that interacts with the SM fields because of gauge-invariant, renormalizable kinetic mixing with hypercharge, and H is an extra Higgs boson that interacts with the SM fields because of renormalizable modulus-squared mixing with the SM Higgs boson.

The Feynman rules are obtained from a straightforward expansion of the above lagrangian in terms of mass eigenstates. Some of the Feynman rules most relevant for LHC studies are given below [4].

<u>Fermion couplings:</u> Couplings to SM fermions are

$$\bar{\psi}\psi Z : \frac{ig}{c_W}\left[c_\alpha(1 - s_W t_\alpha\eta)\right]\left[T_L^3 - \frac{(1 - t_\alpha\eta/s_W)}{(1 - s_W t_\alpha\eta)}s_W^2 Q\right]$$
$$\bar{\psi}\psi Z' : \frac{-ig}{c_W}\left[c_\alpha(t_\alpha + \eta s_W)\right]\left[T_L^3 - \frac{(t_\alpha + \eta/s_W)}{(t_\alpha + \eta s_W)}s_W^2 Q\right] \qquad (15.9)$$

where $Q = T_L^3 + Q_Y$ and $t_\alpha \equiv s_\alpha/c_\alpha$. The photon coupling is as in the SM and is not shifted.

<u>Triple gauge boson couplings:</u> We $\mathcal{R}$ being the coupling relative to the corresponding SM, one finds $\mathcal{R}_{AW^+W^-} = 1$, $\mathcal{R}_{ZW^+W^-} = c_\alpha$ and

$\mathcal{R}_{Z'W^+W^-} = -s_\alpha$ (the last is compared to the SM ZW^+W^- coupling). We will normally assume rather small kinetic mixing and so to leading order we have $c_\alpha \approx 1$, $s_\alpha \ll 1$.

<u>Higgs couplings</u>: The Higgs couplings are

$$
\begin{aligned}
hff &: -ic_h\frac{m_f}{v} , \qquad hWW : 2ic_h\frac{M_W^2}{v} , \\
hZZ &: 2ic_h\frac{M_{Z_0}^2}{v}(-c_\alpha + \eta s_W s_\alpha)^2 - 2is_h\frac{M_X^2}{\xi}s_\alpha^2 , \\
hZ'Z' &: 2ic_h\frac{M_{Z_0}^2}{v}(s_\alpha + \eta s_W c_\alpha)^2 - 2is_h\frac{M_X^2}{\xi}c_\alpha^2 , \\
hZ'Z &: 2ic_h\frac{M_{Z_0}^2}{v}(-c_\alpha + \eta s_W s_\alpha)(s_\alpha + \eta s_w c_\alpha) - 2is_h\frac{M_X^2}{\xi}s_\alpha c_\alpha .
\end{aligned}
\tag{15.10}
$$

15.4. Precision Electroweak

Generally speaking HAHM does not have significant disruptions of the precision electroweak predictions compared to the SM to cause undo worry. In other words, a vast region of parameter space is completely compatible with the precision electroweak data. However, it is useful to review some of the issues [2, 3].

First, when the X gauge boson mixes with hypercharge there will be a shift in the precision electroweak observables compared to the SM. For example, from hypercharge-X mixing, the Z mass eigenvalue is further shifted relative to the $W^\pm$ mass. These effects can be computing in an effective Peskin-Takeuchi parameter analysis [8–10]. One finds that the three most important observables for constraining new physics by precision electroweak observables are

$$\Delta m_W = (17\,\text{MeV})\,\Upsilon \tag{15.11}$$

$$\Delta\Gamma_{l^+l^-} = -(80\,\text{keV})\,\Upsilon \tag{15.12}$$

$$\Delta\sin^2\theta_W^{eff} = -(0.00033)\,\Upsilon \tag{15.13}$$

where

$$\Upsilon \equiv \left(\frac{\eta}{0.1}\right)^2\left(\frac{250\,\text{GeV}}{m_X}\right)^2 . \tag{15.14}$$

Experimental measurements [11] imply that $|\Upsilon| \lesssim 1$. Kinetic mixing at the level of $\eta \lesssim \mathcal{O}(0.1)$ is not constrained if M_X is greater than a few hundred GeV, and there is essentially no constraint if M_X is greater than about a

TeV. This is consistent with the PDG analysis of constraints on other Z' bosons [12]. For lighter M_X, which we will also concern ourselves with, the constraint is not difficult to satisfy as long as $\eta \lesssim \mathcal{O}(0.01)$.

A pure singlet Higgs boson causes no concern for precision electroweak observables, but after mixing the coupling of the Higgs to the gauge bosons is shared by two states of different masses. The leading order way to account for this is to first recognize that in the SM the Higgs boson mass constraints is succinctly summarized as [11]

$$\log\left(M_{\text{Higgs}}/1 \text{ GeV}\right) = 1.93^{+0.16}_{-0.17}. \tag{15.15}$$

When two states, such as ours, mix and share the electroweak coupling, this constraint becomes to leading order

$$c_h^2 \log\left(\frac{M_h}{1 \text{ GeV}}\right) + s_h^2 \log\left(\frac{M_H}{1 \text{ GeV}}\right) \simeq 1.93^{+0.16}_{-0.17} . \tag{15.16}$$

There is very little difficulty in exploring large regions of parameter space where the precision electroweak implications of this multi-Higgs boson theory are in agreement with all data [3].

Other constraints, such as perturbative unitarity and vacuum stability have been analyzed elsewhere [3] and also can be accomodated easily within the theory.

15.5. Example LHC Phenomena of HAHM

How do we find evidence for HAHM at colliders? The main implication of HAHM is the different spectrum it implies compared to the SM spectrum of states:

- The existence of a new gauge boson Z' that couples to SM states according to the strength of the kinetic mixing parameter.
- The existence of two CP-even Higgs boson mass eigenstates, both of which couple to SM states by virtue of the mixing of the HAHM Higgs boson with the SM Higgs boson.

These two simple qualitative facts, combined with the details of the HAHM langrangian enable us to explore many possible interesting implications for the LHC.

In the next few paragraphs I shall discuss a few of these implications. The reader should keep in mind that not all cases are simultaneously allowed by the theory. Each phenomenological manifestation I discuss can

be considered the dominant interesting signal in a subset of the parameter space, not in all of parameter space.

Signal #1: Universal suppression of Higgs boson signal

Let us suppose that the two Higgs bosons mix, such that the lightest Higgs boson is mostly SM, and the heavier Higgs boson eigenstate is mostly singlet. Let us further suppose that the additional Z' Higgs boson is sufficiently heavy or weakly coupled that is has no role in the phenomenology. In this case, the primary signal will be that the light Higgs mass eigenstate couples to the SM states in exactly the same way as the SM Higgs except there is a universal suppression of all interactions due to the mixing angle.

Thus the cross-section is reduced by a factor of

$$\sigma(VV \to h)(m_h) = c_h^2 \sigma(VV \to h_{SM})(m_h). \tag{15.17}$$

This implies that no state in the spectrum of Higgs bosons has a production cross-section as large as the SM Higgs boson, making production, and thus detection, more difficult.

Production is only half of the story when discussing detectability. One must also consider how the branching fraction changes. Of course, if there is only a universal suppression of couplings, the branching fractions will be identical to those of the SM Higgs boson. However, if there are exotic matter states in the HAHM model in addition to just the X boson and its associated symmetry-breaking Φ_H boson, the lightest Higgs might decay into them. If the exotic states are stable on detector time scales it would contribute to the invisible width of the Higgs boson Γ^{hid}, which depends on exotic sector couplings, m_h and s_h^2. The branching fraction into visible states is then reduced and computed by

$$B_i(h) = \frac{c_h^2 \Gamma_i^{SM}(m_h)}{c_h^2 \Gamma_i^{SM}(m_h) + \Gamma^{hid}(m_h)}. \tag{15.18}$$

The effect of this universal suppression was studied in the context of hidden sectors [1] and also in a related context of extra-dimensional theories [13]. Of course, this signal is not unique to the HAHM, as any singlet Higgs boson that gets a vacuum expectation value could mimic it. However, a singlet with a vacuum expectation value is likely to have gauge charge, but it is not necessary that it be exclusively abelian and kinetic mix with hypercharge. Thus, the universal suppression of the Higgs boson phenomenology is more general than just HAHM.
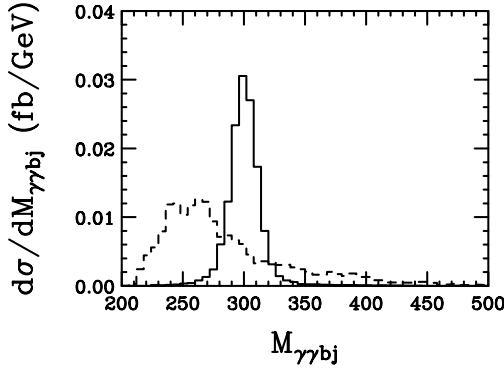
Fig. 15.1. Differential cross-section [3] as a function of $b\bar{b}\gamma\gamma$ invariant mass in $H \rightarrow hh \rightarrow b\bar{b}\gamma\gamma$ production.

Signal #2: $H \rightarrow hh$

Another broad implication of mixing with a singlet Higgs boson is the existence of a heavier Higgs boson that couples to SM states and can decay into a pair of lighter Higgs bosons. This has been discussed in detail in the context of HAHM [3]. There, an example model was studied where

$$m_H = 300 \, \text{GeV}, \quad m_h = 115 \, \text{GeV}, \quad c_h^2 = \frac{1}{2}. \tag{15.19}$$

Thus, the decay of $H \rightarrow hh$ is kinematically allowed in this case, and the relevant branching fraction is $B(H \rightarrow hh) = 1/3$.

One of the most useful signals to find this decay chain is when one light Higgs decays to $h \rightarrow b\bar{b}$, which it is most apt to do, and the other decays to the rarer $h \rightarrow \gamma\gamma$. The signal is reduced substantially by requiring this lower probability $b\bar{b}\gamma\gamma$ final state, but the background is reduced by even more. It is found that with $30 \, \text{fb}^{-1}$ the total expected signal event rate after relevant cuts and identification criteria are applied [3] is 8.2 on a background of 0.3. Fig. 15.1 shows the differential cross-section as a function of invariant mass of $b\bar{b}\gamma\gamma$ for these events.

In the above example the lighter higgs boson is light – right at the edge of the current SM limits – and decays preferentially to $b\bar{b}$. If the lighter Higgs boson is heavier than this, the decay to WW starts to become dominant. The cross-over point where $B(b\bar{b}) = B(W^+W^-)$ is about $m_h = 130 \, \text{GeV}$. For this case of $m_h \gtrsim 130 \, \text{GeV}$, it is more fruitful to exploit the $4W \rightarrow 4\ell+$ missing E_T signature. An analysis of this final state has been shown [3] to be a promising approach to finding $H \rightarrow hh$ at the LHC.

Signal #3: Trans-TeV Narrow Higgs Boson

Within the SM the Higgs boson becomes so broad when its mass is above about $700\,\mathrm{GeV}$ that it starts to become meaningless to even call it a particle. There is no sense in which a trans-TeV Higgs boson resonance can be found within standard Higgs boson phenomenology at the LHC. However, in the mixed boson sector induced by HAHM, we find that a Higgs boson just like the SM can exist, except its couplings are universally suppressed by a factor of s_h^2 compared to the SM Higgs boson. Thus, a reasonably narrow trans-TeV Higgs boson can be in the spectrum, and can be searched for at the LHC.

The narrowness of the Higgs boson is also correlated with a low production cross-section, and so the biggest challenge is simply getting enough events to even analyse. Once they are produced, distinguishing them from background is made possible by the very high energy invariant mass and transverse mass reconstructions. For example, in Fig. 15.2 the invariant mass distribution of $l\nu jj$ (missing E_T vector used for ν) is plotted for the signal ($H \to WW \to l\nu jj$) of a $m_H = 1.1\,\mathrm{TeV}$ Higgs boson and compared to the distributions of the most significant backgrounds from $WWjj$ and $t\bar{t}jj$. The cuts we applied were

$$p_T(e,\mu) > 100\,\mathrm{GeV} \text{ and } |\eta(e,\mu)| < 2.0$$

$$\text{Missing } E_T > 100\,\mathrm{GeV}$$

$$p_T(j,j) > 100\,\mathrm{GeV} \text{ and } m_{jj} = m_W \pm 20\,\mathrm{GeV}$$

$$\text{"Tagging jets" with } |\eta| > 2.0$$

With $100\,\mathrm{fb}^{-1}$ the signal gives 13 events in the invariant mass range between 1.0 and 1.3 TeV, compared to a background of 7.7 events. This is obviously not "early phase" LHC signal, and it highlights the challenges in finding evidence of heavy Higgs bosons from a hidden sector. Nevertheless, it is possible to find evidence for it with enough integrated luminosity, which the LHC should attain in time. The signal significance will increase when all possible channels are included.

An even more challenging final state to consider is $H \to ZZ \to ll\nu\nu$. The most significant background is $ZZjj$. The cuts we applied were

$$p_T(l^+,l^-) > 100\,\mathrm{GeV} \text{ and } |\eta(l^+,l^-)| < 2.0$$

$$m_{ll} = m_Z \pm 5\,\mathrm{GeV}$$

$$\text{Missing } E_T > 100\,\mathrm{GeV}$$

$$\text{"Tagging jets" with } |\eta| > 2.0$$
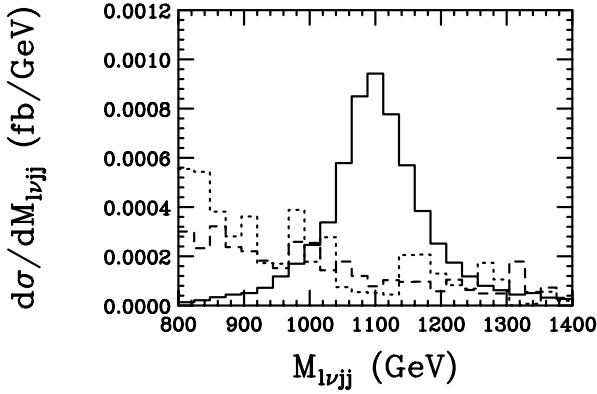
Fig. 15.2. Differential cross-section [3] as a function of invariant mass of $\ell\nu_T jj$ for the signal $H \to WW \to \ell\nu jj$ (solid) and two main backgrounds, $WWjj$ (dashed) and $t\bar{t}jj$ (dotted).

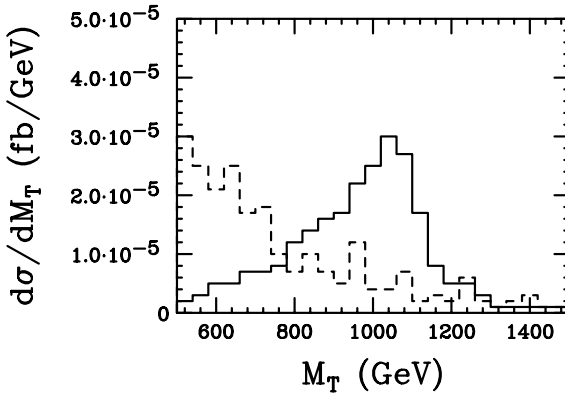
Fig. 15.3. Differential cross-section [3] of transverse mass of Z and missing E_T for the signal $H \to \ell\ell\nu\nu$ (solid) and the main background $ZZjj$ (dashed).

Figure 15.3 shows the transverse mass of Z with missing E_T for a different signal topology ($H \to ZZ \to \ell\ell\nu\nu$) and compared with the most significant background, $ZZjj$. If we restrict ourselves to $0.8\,\text{TeV} < M_T < 1.4\,\text{TeV}$ with $500\,\text{fb}^{-1}$ there are 3.9 signal events compared to 1.4 background events. Again, this is not early stage LHC physics. Finding and studying this kind of trans-TeV Higgs boson physics should be considered a strong motivation for the high-luminosity phase of the LHC.
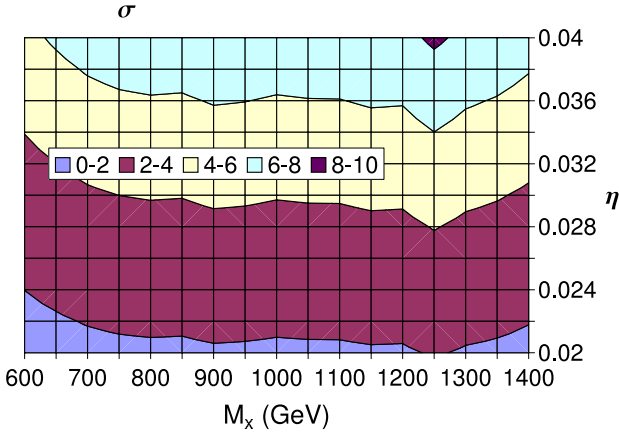
Fig. 15.4.   LHC detection prospects [2] in $\eta - M_X$ plane for $100\,\mathrm{fb}^{-1}$ integrated luminosity at the LHC. Signal significance exceeds 5 only when $\eta \gtrsim 0.03$.

Signal #4: Searching for Z' resonance

When the exotic X boson mixes with hypercharge via kinetic mixing, the resulting mass eigenstates picks up couplings with the SM states. At the LHC one can look for resonance production and decay of this new Z' boson. One of the best approaches expeimentally to finding evidence for such a Z' is to investigate the $\mu^+\mu^-$ invariant mass spectrum.

There is a staggeringly large literature on the search for Z' bosons at colliders [14], but usually little emphasis is put on treating the overall coupling strength as a free parameter that could be very small [15]. Indeed, the kinetic mixing is normally expected to be maybe loop level for theories of this kind, which would imply a rather small coupling of the Z' to SM states. We studied some of the implications of very weakly coupled Z' physics for the LHC [2]. The summary graph of this study is Fig. 15.4 where it was determined that it is very hard for the LHC to probe lower than $\eta \sim 10^{-2}$, which is not particularly constraining to the theory given expectations.

Signal #5: $h \to Z'Z' \to 4l$

In the previous discussion we noted that values of $\eta \lesssim 10^{-2}$ are not very well constrained by the data, nor will they be easily constrained at the LHC. Nevertheless, even a tiny value of η has important phenomenological implications to collider physics. Since a tiny value of $\eta \lesssim 10^{-2}$ may even

be more motivated, it becomes interesting to ask what effect it could still have on LHC phenomenology. In a recent paper [4], we showed that a light Z' boson with $\eta \sim 10^{-4}$ could lead to large branching fractions of $h \to Z'Z' \to 4f$, where the first step $h \to Z'Z'$ is accomplished by Higgs mixing and a sufficiently light Z' mass, and the last step $Z' \to f\bar{f}$ is allowed merely because $\eta \neq 0$ and the Z' must decay.

The branching fractions of the Z' depend on several factors in the theory, but to illustrate they are shown in Fig. 15.5 for $c_h^2 = 0.5$ and $\eta = 10^{-4}$. The branching fraction into four leptons is high enough to exploit its clean signatures at the LHC. Looking for various invariant mass peaks and making various kinematic cuts on the data, the prospects of finding this signature at the LHC with only a few fb^{-1} are excellent [4] provided the two Higgs bosons mix significantly and $h \to Z'Z'$ is kinematically accessible. This may even be the channel where the light Higgs boson mass is first discovered, since it is an easy "gold-plated channel". Compare that with the very difficult normal searches of the Higgs boson with mass $\sim 120\,\mathrm{GeV}$, which is made even more difficult when its production cross-section is reduced, by 50% in this case.

15.6. Beyond the Standard Model and the Hidden World

The discussion in this chapter has all been about physics that attaches itself to the SM relevant operators. However, there are many reasons to believe that the SM sector cannot stand alone in the operation of symmetry breaking and mass generation. We expect new non-hidden particles, such as superpartners and KK excitations, etc., that solve the problems we have identified with the SM. Some people wish that we will discover something totally new and unexpected. However, it would necessitate a shift in our philosophical approach to frontier basic science.

The LHC is just as much a philosophy experiment as a physics experiment. The impacting issue is "To what degree can humans discern nature from pure thought?" Arguably we have had some success already in the past, but would anything in the past compare, for example, to postulating that supersymmetry cures the hierarchy problem if it turns out to be correct? It would certify that humans can see around the corner and discern deep new principles into the energy frontier. If we get that right, no idea would be too esoteric, and no scale would be too remote or inaccessible for humans to discuss with confidence and expectation for understanding.
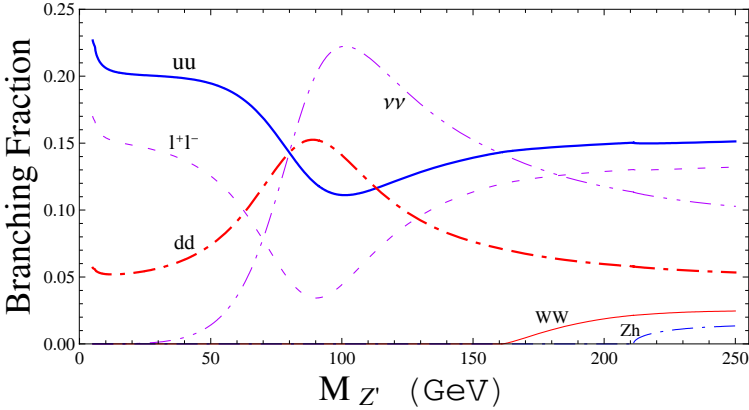
Fig. 15.5. The branching ratio [4] of the Z' boson as a function of its mass for the parameters $c_h = 0.5$ and $\eta = 10^{-4}$.

Thus, I hope and expect that we find new physics that explains by principle the stability of the electroweak scale from ideas that we have already developed. How does this impact the HAHM discussion presented above? First, if it is supersymmetry then it is likely to merely complicate the discussion above, as many new states will be produced and will decay in the detector, and the number of Higgs bosons will be greater, making simple mixing angle factors such as c_h from our 2×2 matrix into more complicated combinations of mixing angles such as $c_{\theta_1} c_{\theta_2} s_{\theta_3}$. The origin of the "hidden sector" higgs mixing with MSSM Higgs is most likely to be from the renormalizable coupling in the superpotential: SH_uH_d, which yields $|S|^2|H_i|^2$-type couplings in the F-term lagrangian directly analogous to the $|\Phi_H|^2|\Phi_{SM}|^2$ mixing terms we have discussed here. Thus, the basic ideas shine through in the Higgs sector and analyses similar to those discussed above can be applicable.

Of course, if the stability of the electroweak scale is explained by the banishment of all fundamental scalars from nature, then additional Higgs boson mixing may not be relevant, but perhaps an effective Higgs boson mixing theory with composite Higgs bosons would be a useful description. This would be highly model dependent, and the data from LHC will have to guide us to decide if there is a path by which we can interpret electroweak symmetry breaking by effective Higgs boson scalars. If so, looking for a Hidden World then would be possible again via couplings to this effective Higgs boson.

Acknowledgments

References

[1] R. Schabinger and J. D. Wells, A minimal spontaneously broken hidden sector and its impact on Higgs boson physics at the Large Hadron Collider, *Phys. Rev. D* **72**, 093007 (2005) [arXiv:hep-ph/0509209].

[2] J. Kumar and J. D. Wells, LHC and ILC probes of hidden-sector gauge bosons, *Phys. Rev. D* **74**, 115017 (2006) [arXiv:hep-ph/0606183].

[3] M. Bowen, Y. Cui and J. D. Wells, Narrow trans-TeV Higgs bosons and H → h h decays: Two LHC search paths for a hidden sector Higgs boson, *JHEP* **0703**, 036 (2007) [arXiv:hep-ph/0701035].

[4] S. Gopalakrishna, S. Jung and J. D. Wells, Higgs boson decays to four fermions through an abelian hidden sector, arXiv:0801.3456 [hep-ph].

[5] M. J. Strassler and K. M. Zurek, Echoes of a hidden valley at hadron colliders, *Phys. Lett. B* **651**, 374 (2007) [arXiv:hep-ph/0604261].
M. J. Strassler, Why Unparticle Models with Mass Gaps are Examples of Hidden Valleys, arXiv:0801.0629.

[6] R. Barbieri, T. Gregoire and L. J. Hall, Mirror world at the Large Hadron Collider, arXiv:hep-ph/0509242.
Z. Chacko, Y. Nomura, M. Papucci and G. Perez, Natural little hierarchy from a partially Goldstone twin Higgs, *JHEP* **0601**, 126 (2006) [arXiv:hep-ph/0510273].
B. Patt and F. Wilczek, Higgs-field portal into hidden sectors, arXiv:hep-ph/0605188.
J. March-Russell, S. M. West, D. Cumberbatch and D. Hooper, Heavy Dark matter through the higgs portal, arXiv:0801.3440 [hep-ph].

[7] See, e.g., sec. 5.4 of T. P. T. Dijkstra, L. R. Huiszoon and A. N. Schellekens, Supersymmetric standard model spectra from RCFT orientifolds, *Nucl. Phys. B* **710**, 3 (2005) [arXiv:hep-th/0411129].

[8] M. E. Peskin and T. Takeuchi, Estimation of oblique electroweak corrections, *Phys. Rev. D* **46**, 381 (1992).

[9] B. Holdom, Oblique Electroweak Corrections And An Extra Gauge Boson, *Phys. Lett. B* **259**, 329 (1991).

[10] K. S. Babu, C. F. Kolda and J. March-Russell, Implications of generalized Z Z' mixing, *Phys. Rev. D* **57**, 6788 (1998) [arXiv:hep-ph/9710441].

[11] LEP Electroweak Working Group, A combination of preliminary electroweak measurements and constraints on the standard model, arXiv:hep-ex/0511027; arXiv:hep-ex/0612034; arXiv:0712.0929.

[12] W. M. Yao *et al.* [Particle Data Group], Review of particle physics, *J. Phys. G* **33**, 1 (2006).

[13] J. D. Wells, Extra dimensions and the universal suppression of Higgs boson observables at high energy colliders, arXiv:hep-ph/0205328.

[14] See, e.g., these reviews and the references therein: T. G. Rizzo, Z' phenomenology and the LHC, arXiv:hep-ph/0610104.
P. Langacker, The Physics of Heavy Z' Gauge Bosons, arXiv:0801.1345 [hep-ph].

[15] For examples of narrow Z' searches, see W. F. Chang, J. N. Ng and J. M. S. Wu, A very narrow shadow extra Z-boson at colliders, *Phys. Rev. D* **74**, 095005 (2006) [arXiv:hep-ph/0608068] and *Phys. Rev. D* **75**, 115016 (2007) [arXiv:hep-ph/0701254].

Chapter 16

B Physics at LHCb

Monica Pepe Altarelli[*] and Frederic Teubert[†]

CERN, PH Department, CH-1211 Genève 23, Switzerland
[*]Monica.Pepe.Altarelli@cern.ch
[†]Frederic.Teubert@cern.ch

LHCb is a dedicated detector for b physics at the LHC. In this article we present a concise review of the detector design and performance together with the main physics goals and their relevance for a precise test of the Standard Model and search of New Physics beyond it.

16.1. Introduction

LHCb is a dedicated b and c-physics precision experiment at the LHC that will search for New Physics (NP) beyond the Standard Model (SM) through the study of very rare decays of charm and beauty-flavoured hadrons and precision measurements of CP-violating observables. At present, one of the most mysterious facts in particle physics is that, on the one hand, NP is expected in the TeV energy range to solve the hierarchy problem, but, on the other hand, no signal of NP has been detected through precision tests of the electroweak theory at LEP, SLC, Tevatron or through flavour-changing and/or CP-violating processes in K and B decays. In the last decade, experiments at B factories have confirmed the validity of the SM within the accuracy of the measurements. The domain of precision experiments in flavour physics has been extended from the rather limited kaon sector to the richer and better computable realm of B decays. The main conclusion of the first generation of B-decay experiments can be expressed by saying that the Cabibbo-Kobayashi-Maskawa (CKM) description [1, 2] of flavour-changing processes has been confirmed in $b \rightarrow d$ transitions at the level of 10–20% accuracy [3]. However, NP effects can still be large in $b \rightarrow s$ transitions, modifying the B_s mixing phase ϕ_s measured from

$B_s \to J/\psi(\mu\mu)\phi$ decays [4], or in channels dominated by other loop dia-grams, like, for example, the very rare decay $B_s \to \mu^+\mu^-$, e.g. via Higgs penguin diagrams [5, 6]. Therefore, the challenge of the future b experi-ments is to widen the range of measured decays, reaching channels that are strongly suppressed in the SM and, more generally, to improve the precision of the measurements to achieve the necessary sensitivity to NP effects in loops. LHCb will extend the b-physics results from the B factories by studying decays of heavier b hadrons, such as B_s or B_c, which will be copiously produced at the LHC. It will complement the direct search of NP at the LHC by providing important information on the NP flavour structure through a dedicated detector, optimized for this kind of physics.

The main physics goals, which will be addressed in this review, include:

- Precision measurements of the CKM matrix elements including a search for possible inconsistencies in measurements of the angles and sides of the unitarity triangles using suitable decays, which proceed through different types of diagrams. A comparison of results from decays dominated by tree-level diagrams with those that start at loop level can probe the validity of the SM.
- Measurements of processes that are strongly suppressed in the SM and are poorly constrained by existing data, particularly in $b \to s$ transitions. Such processes, which could be enhanced through the impact of NP, include measurements of the B_s mixing phase ϕ_s and of the very rare decay $B_s \to \mu^+\mu^-$.

16.2. *b* Physics at the LHC: Environment, Background, General Trigger Issues

The LHC will be the world's most intense source of b hadrons. In proton-proton collisions at $\sqrt{s} = 14$ TeV, the $b\bar{b}$ cross section is expected to be ~ 500 μb producing $10^{12}b\bar{b}$ pairs in a standard (10^7s) year of running at the LHCb operational luminosity of 2×10^{32} cm^{-2} sec^{-1}. The large centre of mass energy means that a complete spectrum of b hadrons will be available, including $B_{(s)}$, $B_{(c)}^+$ mesons and Λ_b baryons. However, less than 1% of all inelastic events contain b quarks, hence triggering is a critical issue.

At the nominal LHC design luminosity of 10^{34} cm^{-2} sec^{-1}, multiple pp collisions within the same bunch crossing (so-called pile-up) would signifi-cantly complicate the b production and decay-vertex reconstruction. For

this reason the luminosity at LHCb will be locally controlled by appropriately focusing the beam to yield a mean value within L = 2–5 × 10^{32} cm^{-2} sec^{-1}, at which most events have a single pp interaction. This matches well with the expected LHC conditions during the start-up phase. Furthermore, running at relatively low luminosity reduces the detector occupancy of the tracking systems and limits radiation damage effects.

The dominant $b\bar{b}$ production mechanism at the LHC is through gluon fusion in which the momenta of the incoming partons are strongly asymmetric in the laboratory frame. As a consequence, the centre of mass energy of the produced $b\bar{b}$ pair is boosted along the direction of the higher momentum gluon, and both b hadrons are produced in the same forward (or backward) direction. The detector is therefore designed as a single arm forward spectrometer covering the pseudorapidity range $1.9 < \eta < 4.9$, which ensures a high geometric efficiency for detecting all the decay particles from one b hadron together with a decay particle from the accompanying b hadron to be used as a flavour tag. A modification to the LHC optics, displacing the interaction point by 11.25 m from the centre, has permitted maximum use to be made of the existing cavern by freeing 19.7 m for the LHCb detector components.

A detector design based on a forward spectrometer offers further advantages: b hadrons are expected to have a hard momentum spectrum in the forward region; their average momentum is ~ 80 GeV/c, corresponding to approximately 7 mm mean decay distance, which facilitates the separation between primary and decay vertices. This property, coupled to the excellent vertex resolution capabilities, allows proper time to be measured with a few percent uncertainty, which is crucial for studying CP violation and oscillations with B_s mesons, because of their high oscillation frequency. Furthermore, the forward, open geometry allows the vertex detector to be positioned very close to the beams and facilitates detector installation and maintenance. In particular, the silicon detector sensors, housed, like Roman pots, in a secondary vacuum, are positioned within ~ 8 mm from the beam during stable running conditions. They are split in two halves that are retracted by ~ 3 cm during injection.

Figure 16.1 illustrates the LHCb acceptance in the plane (η, p_T) of the b hadrons in comparison to that of ATLAS and CMS: ATLAS and CMS cover a pseudorapidity range of $|\eta| < 2.5$ and rely on high-p_T lepton triggers. LHCb relies on much lower p_T triggers, which are efficient also for purely hadronic decays. Most of the ATLAS and CMS b-physics programme will be pursued during the first few years of operation, for luminosities of order
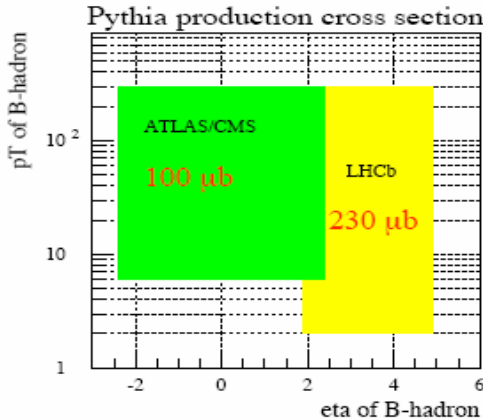
Fig. 16.1. *b* hadron transverse momentum p_T as a function of the pseudorapidity η, showing the (η, p_T) regions covered by ATLAS and CMS, compared to that covered by LHCb.

$10^{33} \, \mathrm{cm}^{-2} \, \mathrm{sec}^{-1}$. Once LHC reaches its design luminosity, *b* physics will become exceedingly difficult for ATLAS and CMS due to the large pile-up ($\sim$ 20 interactions per bunch crossing, on average), except for very few specific channels characterized by a simple signature, like $B_s \to \mu\mu$.

16.3. Detector Description and Performance

The key features of the LHCb detector are:

- A versatile trigger scheme efficient for both leptonic and hadronic final states, which is able to cope with a variety of modes with small branching fractions;
- Excellent vertex and proper time resolution;
- Precise particle identification (ID), specifically: hadron π/K separation, and lepton e/μ ID;
- Precise invariant mass reconstruction to efficiently reject background due to random combinations of tracks. This implies a high momentum resolution.

A schematic layout is shown in Fig. 16.2. It consists of a vertex locator (VELO) [7, 8], a charge particle tracking system with a large aperture dipole magnet [9], aerogel and gas Ring Imaging Cherenkov counters (RICH) [8, 10], electromagnetic (ECAL) and hadronic (HCAL) calorimeters [11]
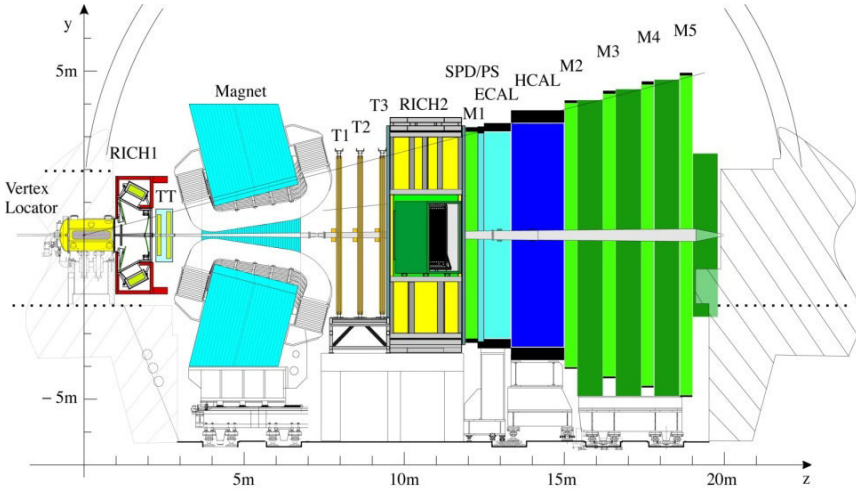
Fig. 16.2. Side view of the LHCb detector showing the Vertex Locator (VELO), the dipole magnet, the two RICH detectors, the four tracking stations TT and T1-T3, the Scintillating Pad Detector (SPD), Preshower (PS), Electromagnetic (ECAL) and Hadronic (HCAL) calorimeters, and the five muon stations M1-M5.

and a muon system [12]. In the following, the most salient features of the LHCb detector are described in more detail.

16.3.1. *Trigger*

One of the most critical elements of LHCb is the trigger system [13]. At the chosen LHCb nominal luminosity, taking into account the LHC bunch crossing structure, the rate of events with at least two particles in the LHCb acceptance is $\sim$ 10 MHz (instead of the nominal 40 MHz LHC crossing rate). The rate of events containing b quarks is $\sim$ 100 kHz while the rate of events containing c quarks is much larger ($\sim$ 600 kHz). However the rate of 'interesting' events is just a very small fraction of the total rate ($\sim$ Hz), hence the need for a highly selective and efficient trigger.

The LHCb trigger exploits the fact that b hadrons are long-lived, resulting in well separated primary and secondary vertices, and have a relatively large mass, resulting in decay products with large p_T.

The LHCb trigger consists of two levels: Level0 (L0) and High Level Trigger (HLT). L0, implemented on custom boards, is designed to reduce the input rate to 1 MHz at a fixed latency of $4\,\mu$s. At this rate, events are sent to a computer farm with up to $\sim$ 2000 multi-processor boxes where

several HLT software algorithms are executed. The HLT, which has access to the full detector information, reduces the rate from 1 MHz to ~ 2 kHz.

L0, based on calorimeter and muon chamber information, selects muons, electrons, photons or hadrons above a given p_T or E_T threshold, typically in the range 1 to 4 GeV. A pile-up trigger system is also foreseen: two dedicated silicon disks located upstream of the VELO are used to reconstruct the longitudinal position of the interaction vertices and reject events with two or more such vertices, thus reducing the processing time on the remaining events as well as simplifying the offline analysis. However, if two muon candidates are found with $\Sigma p_T > 1.3$ GeV/c, the pile-up is overridden; for this reason the L0 efficiency for B decays with two muons is very high independently of the instantaneous luminosity. The L0 hadron trigger occupies most of the bandwidth (~ 700 kHz) and is unique within the LHC experiments. The muon triggers (single and double) select ~ 200 kHz, while the rest of the bandwidth is due to the electromagnetic calorimeter triggers. Typically, the L0 efficiency is $\sim 50\%$ for hadronic channels, $\sim 90\%$ for muon channels and $\sim 70\%$ for radiative channels, normalized to offline selected events.

The HLT algorithms are designed to be fast and simple to understand in terms of systematic uncertainties. This is realized by reconstructing for each trigger only a few tracks, which are used for the final decision. The HLT comprises several paths (alleys) to confirm and progressively refine the L0 decision, followed by inclusive and exclusive selections. The choice of the alley depends on the L0 decision. For instance, if L0 triggers because of a hadron candidate (L0-h), a unique feature of LHCb, the trigger rate is further reduced by confirming the L0-h using the VELO. The candidate is then matched to a segment in the tracking stations and if it has p_T and impact parameter above given thresholds, the event is sent to the inclusive/exclusive HLT selections. If these conditions are not satisfied, but a second 'companion' track is found in the VELO, which forms a good secondary vertex with the previous candidate, the event is also sent to the inclusive/exclusive HLT selections. Similar algorithms are applied to the other L0 decisions: L0-μ, L0-e and L0-γ. The average execution time is few ms, which matches with the expected size of the CPU farm. The total trigger rate after the HLT is ~ 2 kHz, a relatively high rate that also includes calibration samples to be used to understand the detector performance. The total rate can be approximately subdivided in ~ 200 Hz from the exclusive selections, ~ 300 Hz from the inclusive D^* selection, also usable for particle identification efficiency studies, ~ 600 Hz from the

inclusive di-muon selection without impact parameter cuts, also usable to calibrate the proper time distribution, and ~ 900 Hz from the inclusive muon selection for calibration of the trigger and tagging performance.

Overall, the combined trigger efficiency (L0 + HLT) is expected to be $\sim 30\%$ for hadronic channels ($B_{(s)} \to hh$, $B_s \to D_s h$, etc.), $\sim 40\%$ for channels with photons ($B \to K^* \gamma$, $B_s \to \phi \gamma$, etc.), $\sim 70\%$ for channels with muons ($Bs \to J/\phi(\mu\mu)\phi$, etc.), and $\sim 90\%$ for simple channels as $B_s \to \mu\mu$, normalized to offline selected events.

16.3.2. *VELO and tracking system*

The LHCb tracking system consists of a warm dipole magnet, which generates a magnetic field integral of ~ 4 Tm, four tracking stations [14, 15] and the VELO. The first tracking station located upstream of the magnet consists of four layers of silicon strip detectors. The remaining three stations downstream of the magnet are each constructed from four double-layers of straw tubes in the outer region, covering most ($\sim 98\%$) of the tracker area, and silicon strips in the area closer to the beam pipe ($\sim 2\%$). However, $\sim 20\%$ of the charged particles traversing the detector go through the silicon inner tracker, due to the forward-peaked multiplicity distribution. The expected momentum resolution, displayed in Fig. 16.3(a) as a function of momentum, increases from $\delta p/p \sim 0.35\%$ for low momentum tracks to 0.55% at the upper end of the momentum spectrum.
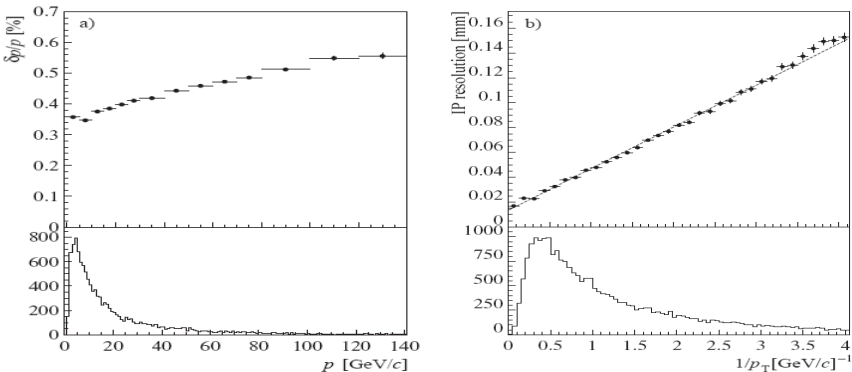

Fig. 16.3. Resolution of the reconstructed track parameters at the track production vertex: (a) momentum resolution as a function of track momentum, (b) impact parameter resolution as a function of $1/p_T$. For comparison, the p and $1/p_T$ spectra of b-decay particles are also shown in the bottom plots.

This translates into an invariant mass resolution of $\delta M \sim 20$ MeV/c^2 for $B_{(s)}$ decays into two charged tracks, like $B_s \rightarrow \mu\mu$, substantially better than in the General-Purpose detectors at LHC.

The VELO consists of 21 stations, each made of two silicon half disks, which measure the radial and azimuthal coordinates. The VELO has the unique feature of being located at a very close distance from the beam line (~ 0.8 cm), inside a vacuum vessel, separated from the beam vacuum by a thin aluminum foil. This allows an impressive vertex resolution to be achieved, translating, for instance, in a proper time resolution of ~ 36 fs for the decay $B_s \rightarrow J/\psi \ (\mu\mu)\phi$, i.e. a factor of ten smaller than the B_s oscillation period and a factor of two better than in the General-Purpose detectors. The resolution on the impact parameter can be parameterized as $\Delta IP \sim 14\mu\text{m} + 35\mu\text{m}/p_T$, as shown in Fig. 16.3(b).

16.3.3. *Particle identification*

Particle identification is provided by the two RICH detectors and the Calorimeter and Muon systems. The RICH system is one of the crucial components of the LHCb detector. The first RICH, located upstream of the magnet, employs two radiators, C_4F_{10} gas and aerogel, ensuring a good π/K separation in the momentum range from 2 to 60 GeV/c. A second RICH in front of the calorimeters, uses a CF_4 gas radiator and extends the momentum coverage up to ~ 100 GeV/c. The calorimeter system comprises a pre-shower detector consisting of 2.5 radiation length lead sheet sandwiched between two scintillator plates, a 25 radiation length lead-scintillator electromagnetic calorimeter of the shashlik type and a 5.6 interaction length iron-scintillator hadron calorimeter. The muon detector consists of five muon stations equipped with multiwire proportional chambers, with the exception of the centre of the first station, which uses triple-GEM detectors.

Electrons, photons and π^0s are identified using the Calorimeter system. The average electron identification efficiency in the ECAL acceptance extracted from $J/\psi \rightarrow e^+e^-$ decays is $\sim 95\%$ for a pion misidentification rate of $\sim 0.7\%$. Muons are identified using the muon detector with an average efficiency in the acceptance extracted from $J/\psi \rightarrow \mu\mu$ decays of $\sim 93\%$ for a pion misidentification rate of $\sim 1\%$.

The RICH system provides a clean separation of hadron types, as well as some separation between leptons and hadrons, which is used to improve the overall particle identification performance. An example of the ability to
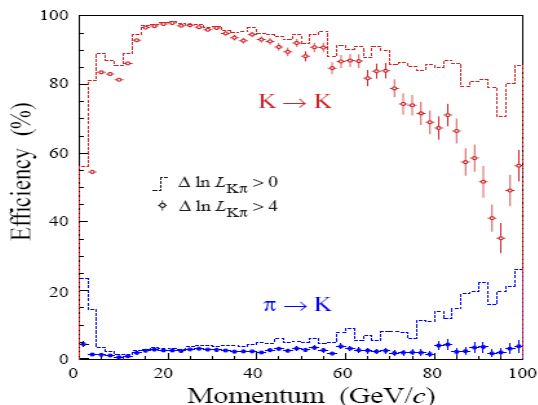
Fig. 16.4. Kaon identification efficiency and pion misidentification rate as a function of momentum, for two different values of $\Delta \ln L_{K\pi}$, indicated by histograms and points, respectively.

identify kaons using the RICH system is shown in Fig. 16.4. By changing the cut on the likelihood difference between the "K hypothesis" and the "π hypothesis," the pion misidentification rate can be reduced, thus improving the purity of the selected sample, at the cost of some loss in the kaon identification efficiency. The trade-off between efficiency and purity can be adjusted according to the needs of individual analyses. For instance, a strong reduction in pion contamination is crucial to be able to separate the decay $B_s \to D_s K$ from the 15 times more abundant $B_s \to D_s \pi$.

16.4. Physics Objectives

The objective of the earliest running phase is to complete the commissioning of the sub-detectors and of the trigger, which includes time and space alignment, calibration of momentum, energy and particle identification. An integrated luminosity of ~ 0.5 fb^{-1}, which should be collected during the first year of physics running, will already allow LHCb to perform a number of very significant measurements, with the potential of revealing NP effects, such as the measurement of the B_s mixing phase ϕ_s, or the search of the decay $B_s \to \mu\mu$ beyond the limit set by CDF and D0. In subsequent years, the experiment will develop its full physics programme, and plans are to accumulate an integrated luminosity of ~ 10 fb^{-1}. Such a data sample will, for example, allow LHCb to improve the error on the CKM angle γ by a factor of $\sim$ five, and probe NP in rare B meson decays with electroweak,

radiative and hadronic penguin modes. In the following, after a brief introduction of the necessary formalism, some selected physics highlights are reviewed that are of particular relevance for NP discovery. A description of the other LHCb physics goals and sensitivity can be found in Ref. [8].

16.4.1. *Introduction of formalism*

In the SM the unitary matrix V_{CKM} arises from a misalignment of the flavour and mass eigenstate basis [1, 2]: $D' = V_{CKM}D$, where

$$V_{CKM} = \begin{pmatrix} V_{ud} & V_{us} & V_{ub} \\ V_{cd} & V_{cs} & V_{cb} \\ V_{td} & V_{ts} & V_{tb} \end{pmatrix}$$

and $D'^T = (d', s', b')$ and $D^T = (d, s, b)$ are the flavour and mass eigenstates, respectively. After applying unitarity constraints and using the freedom of redefining the relative quark phases, the matrix V_{CKM} depends on three mixing angles and one phase, which is the unique source of CP violation in the SM. The unitarity of the matrix implies $\sum_i V_{ij}V_{ik}^* = 0$ for $j \neq k$. Each of these six unitarity constraints can be seen as the sum of three complex numbers, closing a triangle in the complex plane. One of these relations, for $j = d$ and $k = b$ (db unitarity triangle) is of particular interest as it applies directly to b decays and is given by: $V_{ud}V_{ub}^* + V_{cd}V_{cb}^* + V_{td}V_{tb}^* = 0$. This relation defines the angles α, β and γ commonly used in the literature. Their general expression is:

$$\alpha = \arg\left(\frac{-V_{td}V_{tb}^*}{V_{ud}V_{ub}^*}\right), \quad \beta = \arg\left(\frac{-V_{cd}V_{cb}^*}{V_{td}V_{tb}^*}\right) \quad \text{and} \quad \gamma = \arg\left(\frac{-V_{ud}V_{ub}^*}{V_{cd}V_{cb}^*}\right).$$

The unitarity relation with $j = u$ and $k = t$ (ut unitarity triangle) is of special relevance for the physics of the B_s mesons, of particular interest for the LHCb experiment: $V_{ud}V_{td}^* + V_{us}V_{ts}^* + V_{ub}V_{tb}^* = 0$. It defines a triangle with angles very similar to those of the db unitarity triangle, except for a small shift: $\beta + \beta_s$ and $\gamma - \beta_s$, where β_s is defined as:

$$\beta_s = \arg\left(\frac{-V_{cb}V_{cs}^*}{V_{tb}V_{ts}^*}\right).$$

A useful parameterization of the CKM matrix for phenomenological applications is that of Wolfenstein [16]. This parameterization corresponds to an expansion in terms of $\sin\theta_c = \lambda \sim 0.22$, where θ_c is the Cabibbo angle, with three additional real parameters ρ, η, A. If one takes this expansion

up to $O(\lambda^4)$, only three CKM elements have an imaginary part: V_{td}, V_{ts} and V_{ub} and in the SM all phases are proportional to η. One has:

$$\beta \approx -\arg(V_{td}) \approx \arctan\left(\frac{\eta(1-\lambda^2/2)}{1-\rho(1-\lambda^2/2)}\right)$$

$$\beta_s \approx \arg(V_{ts}) - \pi \approx \lambda^2\eta$$

$$\gamma \approx -\arg(V_{ub}) \approx \arctan\left(\frac{\eta}{\rho}\right) .$$

In the SM the $B_{(s)} - \bar{B}_{(s)}$ transitions arise from box diagrams; the off-diagonal elements of the mass matrix $M_{12} = M_{21}^*$ (in the $B_{(s)}$, $\bar{B}_{(s)}$ basis) are given by the box diagram amplitude and are dominated by t-quark exchange. Additional contributions from NP are not excluded and could make the result deviate from the SM prediction. On the other hand, the off-diagonal element of the width matrix Γ_{12} is given by the absorptive part of the box diagram amplitude and is dominated by real final states to which both $B_{(s)}$ and $\bar{B}_{(s)}$ can decay and is less sensitive to NP. In the SM and adopting the Wolfenstein parameterization, the phase of M_{12} reduces to the box diagram phase $\phi_d = -2\arg\left(V_{td}^* V_{tb}\right) \approx 2\beta$ for the B system, and $\phi_s = 2\arg\left(V_{ts} V_{tb}^*\right) \approx -2\beta_s$ for the B_s system. The SM values of $\phi_{d,s}$ are precisely predicted, therefore any significant deviation from the SM value would be a signal of NP. The decays of the neutral $B_{(s)}$ mesons to CP eigenstates like $B \to J/\psi K_s$ or $B_s \to J/\psi\phi$, which are dominantly produced by the $b \to c$ tree transition, are perfectly suited to measure the phase $\phi_{d,s}$ in the box diagram, as the only complex coupling involved is $V_{td(s)}$. Processes like $B \to D^{*\pm}\pi^\mp$ or $B_s \to D_s^\pm K^\mp$ measure the sum of the mixing phase $\phi_{d,s}$ and the V_{ub} phase, i.e. the angle γ, through interference between the decays where the $B_{(s)}$ has or not oscillated.

These measurements will be illustrated in some more detail in the following sections.

16.4.2. *Measurement of the B_s mixing phase ϕ_s*

The most promising channel [4] to measure the B_s mixing phase ϕ_s is $B_s \to J/\psi \left(\to l^+ l^-\right) \phi \left(\to K^+ K^-\right)$. The final state $f = J/\psi\phi$ can be a CP eigenstate with eigenvalue $\eta_f = \pm 1$. The 'plus' sign applies to an orbital angular momentum $l = 0$ or 2, while the 'minus' sign is for $l = 1$. What is to be measured is the time-dependent CP violating asymmetry defined as:

$$A_f^{CP}(t) = \frac{\Gamma_{\bar{B}\to f}(t) - \Gamma_{B\to f}(t)}{\Gamma_{\bar{B}\to f}(t) + \Gamma_{B\to f}(t)} .$$
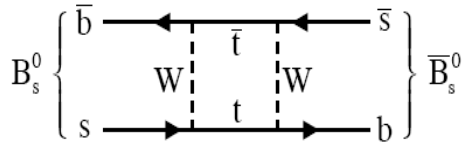
Fig. 16.5. Box diagram contributing to the B_s mixing in the SM.

A tagging method is needed to attribute each event to either B_s or $\bar{B}_s$ decays. The time t is the proper time of the decaying B_s or $\bar{B}_s$ counted from the production time of the pair at $t = 0$. The two interfering amplitudes are for a B_s ($\bar{B}_s$) to decay directly into f or to first mix into $\bar{B}_s$ (B_s) (see Fig. 16.5) and then decay. The complex parameter that determines the interference pattern is $\lambda_f \equiv \frac{q}{p}\frac{\bar{A}_f}{A_f}$, where q and p are the complex numbers describing the state mixing, while A_f and $\bar{A}_f$ are the decay amplitudes. For this particular process, $|q/p| = 1$ (i.e. no CP violation in the $B_s - \bar{B}_s$ oscillations) and $|\bar{A}_f/A_f| = 1$ (i.e. no CP violation in the decay amplitudes) with very good approximation, so that λ_f is a pure phase. In the SM, the decay phase ϕ_d from the ratio $\bar{A}_f/A_f$ is negligible, because the dominant contribution is from a diagram that is real. The remaining phase from q/p is determined from the box diagram and is given by $\lambda_f \approx \eta_f e^{-i\phi_s}$ (CP violation in the interplay between the mixing and decay amplitudes). In this case the time-dependent CP violation amplitude reduces to:

$$A_{CP}(t) = -\frac{\eta_f \sin\phi_s \sin(\Delta m_s t)}{\cosh(\Delta\Gamma_s t/2) - \eta_f \cos\phi_s \sinh(\Delta\Gamma_s t/2)},$$

where Δm_s and $\Delta\Gamma_s$ are the difference between the mass and widths of the two B_s mass eigenstates, following the sign conventions of [17].

Flavour tagging dilutes the measured CP asymmetry through a factor $D = (1 - 2\omega_{tag})$, where ω_{tag} is the probability of having the wrong identification ($\omega_{tag} = 1/2$ if there is no tag). Flavour tagging is performed reconstructing the charge of the b hadron accompanying the B meson under study (opposite side tag) from its decay products, i.e. leptons, kaons, as well as the charge of the inclusive secondary vertex. Moreover B_s (B) mesons can be tagged by exploiting the correlation with charged kaons (pions) produced in the fragmentation decay chain (same side tag). These taggers are combined in a neural network. The effective tagging efficiency ($\varepsilon_{eff} = \varepsilon_{tag}D^2$), which is the figure of merit for the tagging power, varies between 7–9% for B_s (4–5% for B) [18].

The $J/\psi\phi$ final state is a sum of CP eigenstates and each contribution can be disentangled on a statistical basis. This is realized by performing an analysis based on the so-called transversity angle, defined as the angle between the positive lepton and the ϕ decay plane in the J/ψ rest frame [4]. The phase ϕ_s is determined through a simultaneous fit to the proper time and transversity angle distributions, as well as to the proper time distribution of a control sample of $B_s \to D_s\pi$ decays, which is used to extract Δm_s and the tagging efficiency. Recently, the CDF and D0 collaborations have reported a first indication of the mixing phase: $\phi_s \in [0.32, 2.82]$ at 68% C.L. and $\phi_s = 0.57^{+0.24}_{-0.30}$ using ~ 2k $B_s \to J/\psi\phi$ signal candidates at CDF and D0 [19, 20]. The combined result [21] deviates from the SM prediction ($\phi_s = -0.04$ radians) by $\sim 3\sigma$. LHCb expects [22] approximately 130k $B_s \to J/\psi\phi$ signal events in 2 fb^{-1} of data with a background over signal ratio $B/S \sim 0.1$. The phase ϕ_s can also be extracted from pure CP eigenstates, such as $B_s \to J/\psi\,\eta$ or $B_s \to \eta_c\phi$, which do not require an angular analysis, but for which the statistics is much lower. Combining all these modes, the expected statistical sensitivity on ϕ_s is 0.021 (0.009) radians with 2(10) fb^{-1} of data [22, 23], i.e. one (five) nominal year(s), which corresponds to a $\sim 2\sigma$ ($\sim 4\sigma$) measurement assuming the SM value.

16.4.3. $B_s \to \phi\phi$ as a probe for new physics

The discussion of the process $B_s \to \phi\phi$ proceeds along similar lines as for $B_s \to J/\psi\phi$. The final state f is again a sum of different CP eigenstates with $\eta_f = \pm 1$ and the relevant complex parameter is of the form $\lambda_f \equiv \frac{q}{p}\frac{\bar{A}_f}{A_f}$, where p and q are the same as before, while A_f refers to the amplitude for $f = \phi\phi$. The crucial difference is however that in this case the dominant decay amplitude A_f is a penguin diagram with top exchange (as shown in Fig. 16.6), so that the decay phase ϕ_d is not negligible. Indeed it turns out
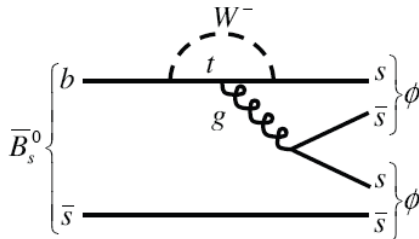

Fig. 16.6. Penguin diagram contributing to the $B_s \to \phi\phi$ decay in the SM.

that in the SM there is a complete cancellation between ϕ_s and ϕ_d (for the dominant penguin with top exchange) [24]:

$$\phi_S^{SM}(B_S \to \phi\phi) \approx 2\arg(V_{ts}^* V_{tb}) - \arg(V_{tb}V_{ts}^*/V_{tb}^*V_{ts}) = 0\,.$$

Therefore this process is particularly sensitive to NP, which can introduce new CP-violating phases in the penguin decay and/or B_s mixing. When combining with the decay $B_s \to J/\psi\phi$, one can disentangle NP contributions in B_s mixing and decay. LHCb expects approximately 3.1k signal events in 2 fb^{-1} of data with a background over signal ratio $B/S < 0.8$ at 90% C.L. From the time-dependent angular distribution of flavour-tagged events, the phase ϕ_s can be measured with a statistical precision $\sigma(\phi_s) = 0.11\ (0.05)$ with $2(10)$ fb^{-1} of data [25].

16.4.4. *Measurement of the weak decay-phase γ from tree-level processes*

The weak phase $\gamma + \phi_s$ can be measured at LHCb from a time-dependent CP asymmetry analysis of the decay $B_s \to D_s^{\mp}K^{\pm}$ (see Fig. 16.7) [26]. As a B_s and a $\overline{B}_s$ can both decay as $D_s^+K^-$, there is interference between the B_s decays where the B_s has or not oscillated. The intrinsic theoretical uncertainty in the extraction of γ is estimated to be $\sim 0.1\%$, so that this is not a limiting factor for the measurement. Contrary to the equivalent channel in the B system, i.e. $B \to D^{(*)+}\pi^-$, the decay amplitudes for the $b \to c$ and $b \to u$ transitions are both of $O(\lambda^3)$ and their ratio can be extracted from data, allowing a clean determination of the CP angle $\phi_s + \gamma$. The main issue is separating the decay $B_s \to D_s^{\mp}K^{\pm}$ from the very similar decay $B_s \to D_s^{\mp}\pi^{\pm}$, with a ~ 15 times larger branching ratio. Here, use of the RICH system crucially allows the background contamination to be reduced down to $\sim 15\%$. The unique capability of the LHCb trigger to select
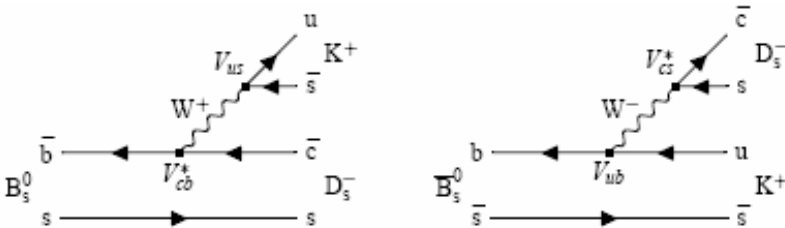

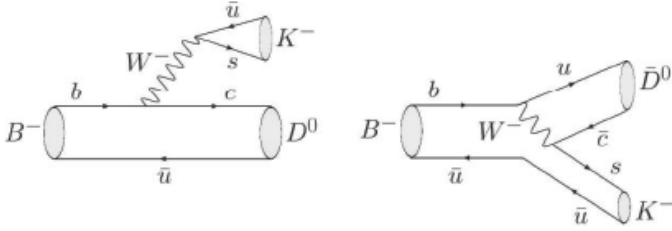Fig. 16.7.   Feynman diagrams for $B_s \to D_s^- K^+$ and $\bar{B}_s \to D_s^+ K^-$ in the SM.

Fig. 16.8. Feynman diagrams for $B^- \to DK^-$ and $B^- \to \bar{D}K^-$ in the SM. In the left diagram all colourless configurations of the s and $\bar{u}$ are allowed (coloured-favoured diagram). In the right diagram the W^- decay products are split to form the $\bar{D}$ and K^- and therefore the colour is constrained by the colour of the initial b and $\bar{u}$ quarks (colour-suppressed diagram).

hadronic decays is instrumental to collecting a sufficient statistics. It is estimated that LHCb will select 31k events for 10 fb^{-1} with a combinatorial background to signal ratio $B/S < 0.2$. The estimated precision on γ for the same integrated luminosity is $\sim 4.6°$ (i.e. a $\sim 7\%$ uncertainty), assuming that ϕ_s is known from the measurements described in the previous section [27, 28].

Alternatively, γ can be extracted from $B^\pm$ decays to open charm, as done by BaBar and Belle, where a precision of $\sim 20°$ was achieved through this method [29, 30]. From the experimental point of view, this analysis is much simpler as no flavour tagging or time-dependent analysis is required. Various methods using $B^\pm \to (D/\bar{D})K^\pm$ decays have been proposed. All of them are based on two key observations: (1) The decay $B^\pm \to (D/\bar{D})K^\pm$ can produce neutral D mesons of both flavours via colour-favoured or colour-suppressed decays (see Fig. 16.8). (2) Neutral D and $\bar{D}$ mesons can decay to a common final state, for example through Cabibbo-favoured or doubly Cabibbo-suppressed Feynman diagrams (ADS method) [31] or through decays to CP eigenstates such as K^+K^- or $\pi^+\pi^-$ (GLW method) [32–34]. In the ADS case, the reversed suppression between B and D decays results in very similar amplitudes leading to a high sensitivity to γ. The relative phase between the two interfering amplitudes for $B^+ \to DK^+$ and $B^+ \to \bar{D}K^+$ is the sum of the strong and weak interaction phases, while in the case of $B^- \to DK^-$ and $B^- \to \bar{D}K^-$ the relative phase is the difference between the strong phase and γ. Therefore both phases can be extracted by measuring the two charge conjugate modes. The feasibility of this measurement crucially depends on the size of the ratio: $r_B = |A(B^+ \to DK^+)|/|A(B^+ \to \bar{D}K^+)|$. The r_B value is given by

the ratio of the CKM matrix elements involved $|V_{ub}^* V_{cs}|/|V_{cb}^* V_{us}|$ times a colour suppression factor, and is estimated to be in the range 0.1–0.2. The three-body final state of the D meson can also be used through a Dalitz plot analysis that allows one to obtain all information required for the determination of γ with a single decay mode [35, 36]. In particular, LHCb has studied the $B^\pm \rightarrow D/\bar{D}(K\pi)K^\pm$ and $B^\pm \rightarrow D/\bar{D}(K\pi\pi)K^\pm$ modes. Assuming $r_B \sim 0.15$, $\sim 300\text{k}$ (2.5k) events are selected for 10 fb^{-1} in the favoured (suppressed) modes, with $B/S \sim 0.3(\sim 2)$. From these modes LHCb estimates a precision on γ in the range $(2\text{–}6)^\circ$, depending on the D strong phase, with 10 fb^{-1} of data [37–39].

A similar precision can be achieved with the neutral B-decay modes $B \rightarrow \bar{D}(K\pi)K^*(K\pi)$, $B \rightarrow D_{CP}(KK/\pi\pi)K^*(K\pi)$ and their charge conjugate modes, where D_{CP} denotes the CP even eigenstate mode. These modes are self-tagged, as the B flavour is determined by the K charge in the K^* decay, while the D flavour is determined by the K charge in the D decay. It is expected [40] that the experiment will select $\sim 19\text{k}$ events from the $B \rightarrow \bar{D}K^*$ mode summing over the four possible flavour combinations (with $B/S \sim 0.4\text{–}10$) and $\sim 3\text{k}$ events from the CP eigenstate channel ($B/S <\sim 4$), assuming $r_B \sim 0.4$, with 10 fb^{-1} of data.

Combining all these different techniques, the final LHCb precision on γ is expected to be $\sim 2.4^\circ$, with 10 fb^{-1} of data [41].

Figure 16.9 shows the direct measurement of γ from the B factories ($\gamma = 83^\circ \pm 19^\circ$) and the indirect determination [27] from the rest of the CP measurements available in 2006 ($\gamma = 64.1^\circ \pm 4.6^\circ$), as well as a future
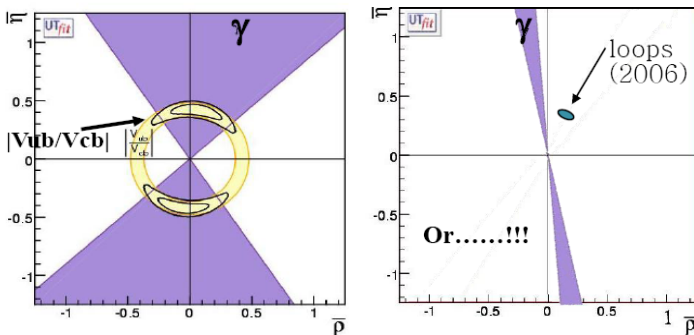

Fig. 16.9. (a) Direct measurements of γ using only "tree diagrams" as measured recently. (b) Comparison of a hypothetical LHCb direct measurement of γ and a recent indirect determination. A discrepancy would indicate the presence of NP in loops affecting the indirect determination.
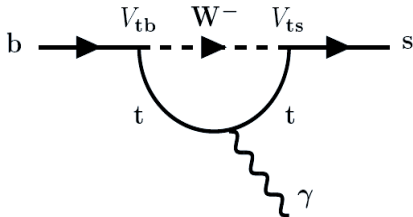
Fig. 16.10.   Example of Feynman diagram for $b \to s\gamma$.

scenario where the precision achieved by LHCb reveals NP effects as a disagreement between these two determinations.

16.4.5. *Example of radiative penguins*: $B_s \to \phi\gamma$

The flavour-changing neutral current transition $b \to s\gamma$ (see Fig. 16.10) is among the most valuable probes of NP models, in particular those where the flavour-violating chiral transition of the amplitude is not suppressed [42–44]. Inclusive measurements of $B \to X_s\gamma$, which can be computed using perturbation theory, cannot be performed at LHCb. However, many exclusive measurements, like $B_s \to \phi(K^+K^-)\gamma$, are well suited to the LHCb detector capabilities. The CP asymmetry for this decay can be expressed as:

$$A_{CP}(t) = -\frac{C\cos(\Delta m_s t) + S\sin(\Delta m_s t)}{A^\Delta \sinh(\Delta\Gamma_s t/2) + \cosh(\Delta\Gamma_s t/2)} \, ,$$

The prediction for S is dominated by the electromagnetic dipole operator, and precisely known in the SM: $S_{\phi\gamma} = -0.1 \pm 0.1\%$. BaBar and Belle have measured a similar quantity in the $B \to K^*(K_s\pi^0)\gamma$ decay and it is consistent with the SM prediction [45, 46], however with large uncertainties: $\Delta S_{K\gamma} \sim 40\%$ with samples of ~ 150 events. LHCb expects [47] to collect 36k (6k) events per fb^{-1} in $B \to K^*(K^+\pi^-)\gamma$ ($B_s \to \phi(K^+K^-)\gamma$) decays with $B/S \sim 0.7$ (0.9). In LHCb the $B \to K^*\gamma$ decays can be used as control channel, while the time-dependent CP asymmetry, which is sensitive to the photon polarization, can be measured in $B_s \to \phi\gamma$ decays, provided that the proper time resolution is sufficient to resolve the B_s oscillations. The proper time resolution depends on the kinematics and topology of the particular B_s candidates: mainly on the opening angle between kaons from the ϕ decay. LHCb should be able to measure $S_{\phi\gamma}$ with a precision of $\Delta S_{\phi\gamma} \sim 5\%$ with 10 fb^{-1} of data [48].
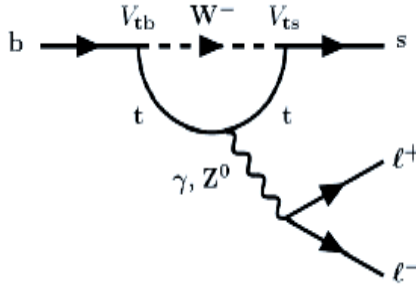
Fig. 16.11.   Example of Feynman diagram of $b \to sl^+l^-$.

16.4.6.   *Example of an electroweak penguin*: $B \to K^*\mu\mu$

In the SM, the decays $b \to sl^+l^-$ cannot occur at tree level but only through electroweak penguin diagrams with small branching fractions, e.g. $\mathrm{BR}(B \to K^*\mu\mu) \sim 1.2 \times 10^{-6}$ (see Fig. 16.11). The $B \to K^*\mu\mu$ channel is well suited to searches for NP, because most NP scenarios make definite predictions for the forward-backward asymmetry A_{FB} of the angular distribution of the μ relative to the B direction in the di-muon rest frame as a function of the di-muon invariant mass $m_{\mu\mu}$. In particular, the value of $m_{\mu\mu}$ for which A_{FB} becomes zero is predicted with small theoretical uncertainties and may thus provide a stringent test of the SM [49]. The B factory experiments BaBar and Belle have succeeded in measuring several observables for this exclusive decay: branching fraction, di-lepton angular asymmetry A_{FB} vs di-lepton q^2, K^* longitudinal polarization vs di-lepton q^2 and fits of the $d^2\Gamma/d\cos\theta dq^2$ distribution to extract the relevant Wilson coefficients, with a precision comparable to what LHCb can do with ~ 0.07 fb^{-1} of data.

This exclusive decay can be triggered and reconstructed in LHCb with high efficiency [50], because of the clear di-muon signature and K/π separation provided by the RICH detectors. Moreover, the invariant mass of the di-muon system is measured with an excellent resolution ($\sigma \sim 14$ MeV/c^2). The selection criteria including the trigger have an efficiency of $\sim 1\%$, leading to an expectation of ~ 7k signal events for an integrated luminosity of 2 fb^{-1} and a background over signal ratio of ~ 0.5 in a ± 50 MeV/c^2 mass window around the B mass and ± 100 MeV/c^2 window around the K^* mass. About half of the background is estimated from an upper limit to the (not yet observed) non-resonant $B \to K^+\pi^-\mu^+\mu^-$ decay, which constitutes an
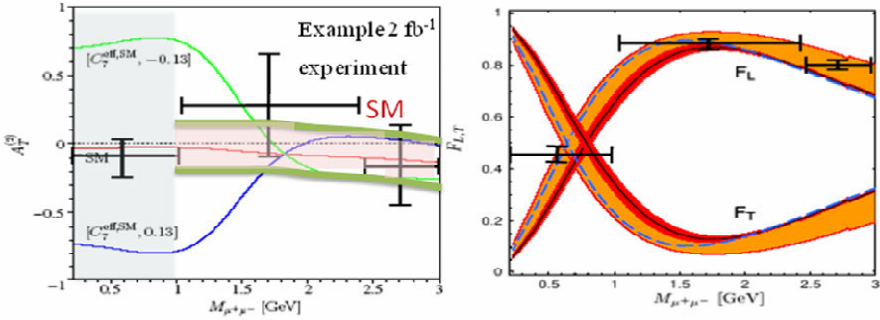
Fig. 16.12. $A_T^{(2)}$ (left) and $F_{L,T}$ (right) as a function of the di-muon mass. Also shown on the left plot is the SM NLO prediction for $A_T^{(2)}$ with its uncertainty (horizontal band), and the predictions from the MSSM with MFV and $\tan\beta = 5$ (green and blue lines). The grey-shaded region is excluded as theory is not reliable at low q^2. The right plot shows the SM prediction for $F_{L,T}$ and its uncertainty.

irreducible background, while the other half originates from events with two semileptonic B decays.

In addition to measuring A_{FB} [51], LHCb will have enough statistics to extract the transversity amplitudes [52, 53] A_0, $A_\parallel$ and $A_\perp$, through differential distribution defined in terms of q^2, the invariant mass square of the di-muon candidates, θ_l, the angle between the μ^+ and the B in the di-muon rest frame, θ_K, the angle between the K and the B in the $K\pi$ rest frame, and ψ, the angle between the normal to the planes defined by the di-lepton and $K\pi$ systems in the B rest frame. Figure 16.12 shows an example of the LHCb sensitivity to the measurements of $A_T^{(2)}(q^2) = (|A_\perp|^2 - (|A_\parallel|^2)/(|A_\perp|^2 + (|A_\parallel|^2)$, which is sensitive to new sources of right-handed currents, and the fraction of K^* polarization: $F_L(q^2) = |A_0|^2/(|A_0|^2 + |A_\perp|^2 + (|A_\parallel|^2)$. Figure 16.12 also shows the SM NLO prediction with its uncertainty, and the predictions from the MSSM with Minimal Flavour Violation (MFV) and $\tan\beta = 5$. The fact that these measurements are sensitive to SUSY with low $\tan\beta$ values shows the complementarity with the $B_s \to \mu\mu$ measurement, which is sensitive to models with large $\tan\beta$, as explained in the next section. Unfortunately, in the more sensitive region $q^2 < 1$ $(\text{GeV}/c^2)^2$ the theory is not very reliable. In the theoretically favoured region, away from the photon pole, $q^2 > 1$ $(\text{GeV}/c^2)^2$, and below the charm resonances, $q^2 < 6$ $(\text{GeV}/c^2)^2$, the resolution in $A_T^{(2)}$ is 0.42 (0.16) and the resolution in F_L is 0.016 (0.007) with 2 fb^{-1} (10 fb^{-1}) of integrated luminosity [54].
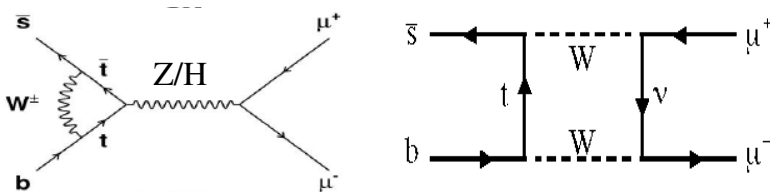
Fig. 16.13.   Examples of Feynman diagram for $B_s \to \mu^+\mu^-$.

16.4.7. *Example of a Higgs-penguin*: $B_s \to \mu^+\mu^-$

The decay $B_s \to \mu^+\mu^-$ has been identified as a very interesting poten-
tial constraint on the parameter space of models for physics beyond the
SM [5, 6]. The upper limit to the $B_s \to \mu^+\mu^-$ branching ratio measured
at the Tevatron [55, 56] is 4.7×10^{-8} at 90% C.L. The SM prediction
is computed [57] to be $\mathrm{BR}(B_s \to \mu^+\mu^-) = (3.35 \pm 0.32)10^{-9}$ using
the latest measurement of the B_s oscillation frequency at the Tevatron
($\Delta M_s = 17.8 \pm 0.1$ ps^{-1}) [58], which significantly reduces the uncer-
tainties in the SM prediction. Within the SM, this decay is dominated
by a "Z/Higgs-penguin" diagram (Fig. 16.13(left)), while the contribu-
tion from the "box" diagram (Fig. 16.13(right)) is suppressed by a fac-
tor $\sim (M_w/m_t)^2$. Moreover, the decay is helicity suppressed by a factor
$\sim (m_l/m_{Bs})^2$, hence it is very sensitive to any NP with new scalar or
pseudoscalar interactions, in particular to any model with an extended
Higgs sector.

   In the MSSM this branching ratio is known to increase as the sixth
power of $\tan\beta = v_u/v_d$, the ratio of the two Higgs vacuum expectation
values. Any improvement to this limit is therefore particularly important
for models with large $\tan\beta$. For instance, Fig. 16.14 shows the values
of $\tan\beta$ and M_A, the mass of the CP odd neutral Higgs, preferred by a
global fit to several measurements within one particular realization [59] of
the MSSM. The best fit position is largely dominated by the present 3.4σ
discrepancy in the measured anomalous magnetic moment of the muon. As
a consequence, if such a discrepancy is not due to a statistical fluctuation,
a sizable enhancement of the branching ratio is expected in this model, i.e.
$\mathrm{BR}(B_s \to \mu^+\mu^-) \sim 10^{-8}$.

   The large background expected in the search for the decay $B_s \to \mu^+\mu^-$
is largely dominated by random combinations of two muons originating from
two distinct b decays. This background can be kept under control by ex-
ploiting the excellent tracking and vertexing capabilities of LHCb. Specific
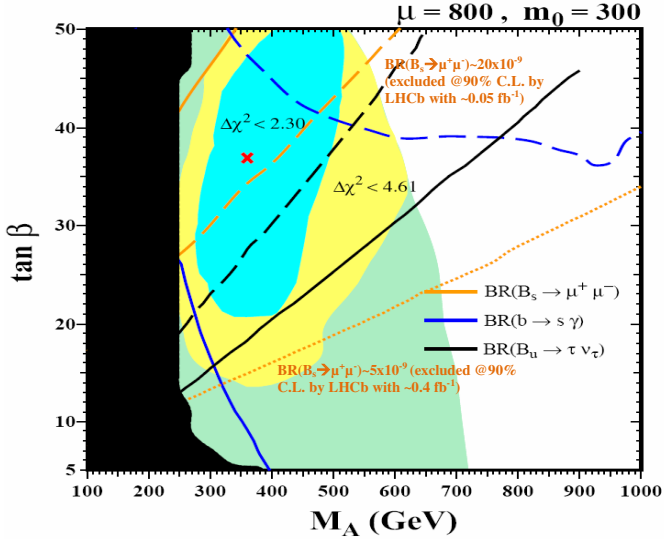
Fig. 16.14.   Best fit and χ^2 contours in the plane $(M_A, \tan\beta)$ from the fit in Ref. [59] to several observables, including the anomalous magnetic moment of the muon. The orange lines indicate the excluded region when $\text{BR}(B_s \to \mu^+\mu^-) < 10^{-7}$ $(2\,10^{-8})$ $(5\,10^{-9})$.

decays, such as $B_{(s)} \to h^+h^-$, where the hadrons (h) are misidentified as μ, or $B_c \to J/\psi(\mu^+\mu^-)\mu\nu$, do not contribute to the background at a significant level, compared to the combinatorial background, due to the very low μ misidentification rate $(\sim 0.5\%)$ and excellent invariant mass resolution $(\sigma \sim 20\ \text{MeV}/c^2)$. The LHCb trigger selects the signal very efficiently: the total trigger efficiency, L0 + HLT, is larger than 90%, normalized to the offline selected events.

The expected reach for exclusion at 90% C.L. of a given branching ratio if only background is observed, is also shown in Fig. 16.14. LHCb has the potential to exclude the interesting region with very little luminosity $(\sim 0.4\ \text{fb}^{-1})$, and to make a 3σ (5σ) observation (discovery) of the SM prediction with $\sim 2\ \text{fb}^{-1}$ $(\sim 6\ \text{fb}^{-1})$ of data [60].

16.5. Conclusions and Outlook

The large $b\bar{b}$ production cross section at the LHC provides a unique opportunity to study in detail CP violation and rare b decays. In particular, production of B_s mesons could play a crucial role in disentangling CP

violation effects originating from NP. LHCb is an experiment characterized by a flexible and robust trigger system, sensitive to many b decays, including those with no lepton in the final state. It has a RICH system that allows a clean π/K separation over a wide momentum range, and a powerful vertex detector providing excellent decay-time resolution. LHCb can nicely complement the direct search of NP performed by ATLAS and CMS. If, as we all hope, NP phenomena will be observed directly by ATLAS and CMS, LHCb will become essential for elucidating the dynamics of such phenomena by looking for signals of virtual effects in flavour-changing and CP-violating processes.

Acknowledgments

References

[1] N. Cabibbo, *Phys. Rev. Lett.* **10**, 531 (1963).
[2] M. Kobayashi and T. Maskawa, *Prog. Theor. Phys.* **49**, 652–657 (1973).
[3] Y. Nir, arXiv:hep-ph/0208080 (2002).
[4] A. S. Dighe, I. Dunietz, H. J. Lipkin and J. L. Rosner, *Phys. Lett. B* **369**, 144–150 (1996).
[5] A. Dedes, H. K. Dreiner and U. Nierste, *Phys. Rev. Lett.* **87**, 251804 (2001).
[6] C. Huang, L. Wei, Q. Yan and S. Zhu, *Phys. Rev. D* **63**, 114021 (2001).
[7] LHCb Collaboration, LHCb VELO TDR CERN-LHCC-2001-011 (2001).
[8] LHCb Collaboration, LHCb Reoptimized Detector, Design and Performance, LHCC-2003-030 (2003).
[9] LHCb Collaboration, LHCb Magnet TDR, LHCC-2000-07 (2000).
[10] LHCb Collaboration, LHCb RICH TDR, LHCC-2000-037 (2000).
[11] LHCb Collaboration, LHCb Calorimeters TDR, LHCC-2000-036 (2000).
[12] LHCb Collaboration, LHCb Muon System TDR, LHCC-2001-010 (2001).
[13] LHCb Collaboration, LHCb Trigger System, LHCC-2003-031 (2003).
[14] LHCb Collaboration, LHCb Inner Tracker, LHCC-2002-029 (2002).
[15] LHCb Collaboration, LHCb Outer Tracker, LHCC-2001-024 (2001).
[16] L. Wolfenstein, *Phys. Rev. Lett.* **51**, 1945 (1983).
[17] I. Dunietz, R. Fleischer and U. Nierste, *Phys. Rev. D* **63**, 114015 (2001).
[18] M. Calvi, O. Leroy and M. Musy, CERN-LHCb-2007-058 (2007).

[19] T. Aaltonen *et al.* (CDF Collaboration), arXiv:hep-ex/0712.2397 (2007).
[20] V. M. Abazov *et al.* (D0 Collaboration), arXiv:hep-ex/0802.2255 (2008).
[21] M. Bona *et al.* (UTfit Collaboration), arXiv:hep-ph/0803.0659 (2008).
[22] L. Fernandez, CERN-LHCb-2006-047 (2006).
[23] D. Volyanskyy and J. van. Tilburg, CERN-LHCb-2007-027 (2007).
[24] M. Raidal, *Phys. Rev. Lett.* **89**, 231803 (2002).
[25] S. Amato, J. McCarron, F. Muheim, B. Souza de Paula and Y. Xie, CERN-LHCb-2007-047 (2007).
[26] R. Aleksan, I. Dunietz and B. Kayser, *Z. Phys. C* **54**, 653 (1992).
[27] J. Borel, L. Nicolas, O. Schneider and J. Van Hunen, CERN-LHCb-2007-017 (2007).
[28] S. Cohen, M. Merk and E. Rodrigues, CERN-LHCb-2007-041 (2007).
[29] J. Charles *et al.* (CKMfitter Collaboration), *Eur. Phys. J. C* **41**, 1 (2005), hep-ph/0406184.
[30] M. Bona *et al.* (UTfit Collaboration), *JHEP* **0507**, 28 (2005), hep-ph/0501199.
[31] D. Atwood, I. Dunietz and A. Soni, *Phys. Rev. Lett.* **78**, 3257 (1997).
[32] M. Gronau and D. London, *Phys. Lett. B* **253**, 483 (1991).
[33] M. Gronau and D. Wyler, *Phys. Lett. B* **265**, 172 (1991).
[34] M. Gronau, *Phys. Rev. D* **58**, 037301 (1998).
[35] D. Atwood, I. Dunietz and A. Soni, *Phys. Rev. D* **63**, 036005 (2001).
[36] A. Giri, Y. Grossman, A. Soffer and J. Zupan, *Phys. Rev. D* **68**, 054018 (2003).
[37] M. Patel, CERN-LHCb-2006-066 (2006).
[38] A. S. Powell, CERN-LHCb-2007-004 (2007).
[39] M. Patel, CERN-LHCb-2007-043 (2007).
[40] K. Akiba and M. Gandelman, CERN-LHCb-2007-050 (2007).
[41] G. Buchalla *et al.*, arXiv:0801.1833 (2008).
[42] T. Hurth and T. Mannel, hep-ph/0109041 (2001).
[43] K. Kiers, A. Soni and G. H. Wu, *Phys. Rev. D* **62**, 116004 (2000).
[44] D. Atwood, M. Gronau and A. Soni, *Phys. Rev. Lett.* **79**, 185 (1997).
[45] B. Aubert *et al.*, *Phys. Rev. D* **72**, 051103 (2005).
[46] K. Abe *et al.*, hep-ph/0507059 (2005).
[47] L. Shchutska, A. Golutvin and I. Belyaev, CERN-LHCb-2007-030 (2007).
[48] L. Shchutska, Y. Xie, A. Golutvin, V. Egorychev, V. Shevchenko and I. Belyaev, CERN-LHCb-2007-147 (2007).
[49] A. Ali, P. Ball, L. T. Handoko and G. Hiller, *Phys. Rev. D* **61**, 074024 (2000).
[50] J. Dickens, V. Gibson, C. Lazzeroni and M. Patel, CERN-LHCb-2007-038 (2007).
[51] J. Dickens, V. Gibson, C. Lazzeroni and M. Patel, CERN-LHCb-2007-039 (2007).
[52] F. Kruger and J. Matias, *Phys. Rev. D* **71**, 094009 (2005).
[53] E. Lunghi and J. Matias, arXiv:0612166 (2007).
[54] U. Egede, CERN-LHCb-2007-057(2007).
[55] B. Aubert *et al.* (D0 Collaboration), http://wwwd0.fnal.gov/Run2Physics/WWW/results/b.htm (2006).

[56] A. Abulencia *et al.* (CDF Collaboration), Note 8176,
     http://www-cdf.fnal.gov/physics/new/bottom/060316.blessed-bsmumu3
     (2006).
[57] M. Blanke, A. J. Buras, D. Guadagnoli and C. Tarantino, *JHEP* **0610**, 003
     (2006).
[58] A. Abulencia *et al.*, *Phys. Rev. Lett.* **97**, 242003 (2006).
[59] J. Ellis, T. Hahn, S. Heinemeyer, K. A. Olive and G. Weiglein,
     arXiv:0709.0098 (2007).
[60] D. Martinez, J. A. Hernando and F. Teubert, CERN-LHCb-2007-033 (2007).

Chapter 17

The LHC and the Universe at Large

Pierre Binétruy

APC*, Université Paris-Diderot, Bâtiment Condorcet,
10, rue Alice Domont et Léonie Duquet
F-75205 Paris Cedex 13, France

I discuss here some of the deeper connections between the physics studied at the LHC (electroweak phase transition, physics beyond the Standard Model, extra dimensions) and some of the most important issues in the field of particle astrophysics and cosmology (dark matter, primordial gravitational waves, black holes,...).

17.1. Introduction

The Standard Model, which we hope to fully probe with the long awaited discovery of the Higgs particle at the LHC, not only provides a complete theory of microscopic physics. It serves also as a basis for a complete picture of the Universe: as one goes back in time towards the big bang, the symmetries which rule the submicroscopic world (electroweak symmetry, supersymmetry, grand unification,...) become apparent, towards an ultimate unification of all interactions, probably described by a string theory. Needless to say that this scenario may be disproved or modified at each stage of its experimental verification, the first one being provided by LHC. It remains true that, until now, such a global scheme has been comforted by several decisive observations: the best illustration is provided by the inflation scenario, first devised in the context of grand unification, which has successfully predicted that our space is flat, i.e. that the energy density in the universe is the critical energy density $\rho_c \sim 10^{-26}$ kg.m^{-3}.

Putting to test this general picture is particularly exciting at a time where, on one hand, LHC will confirm or infirm the Standard Model and,

---

*Université Paris Diderot, CNRS/IN2P3, CEA/DSM, Observatoire de Paris.

on the other hand, one expects decisive results from cosmology and particle astrophysics observations in the next decade. It is this rich interplay that I will try to explore in what follows, by taking some specific examples such as dark matter, gravitational waves, and extra spatial dimensions.

The discovery of the Higgs particle at the LHC would be the first observation of a fundamental scalar particle. Besides providing a spectacular confirmation of the Standard Model, it would have far reaching consequences for the physics of the early universe. Indeed, scalar fields are to this date the best remedy to cure some of the most fundamental cosmological problems. For example, most models of inflation (proposed to cure the flatness, horizon and monopole problems) involve one or more scalar fields. Similarly, dark energy (invoked to understand the recent acceleration of the expansion of the universe) is often attributed to a scalar component. And models with extra spatial dimensions have a dynamics where the size of the compact dimensions is the value of a scalar field (a modulus).

One of the reason for invoking scalar fields in a cosmological context is that scalars tend to resist to gravitational clustering. More quantitatively, the speed of sound

$$c_s^2 = \delta p / \delta \rho \tag{17.1}$$

measures how the pressure p of the field resists gravitational clustering. In the generic case of a scalar field evolving in its potential, c_s is of the order of the speed of light c. Thus, scalar fields easily provide candidates for a very diffuse background.

17.2. The Dark Side of LHC

What can the LHC tell us about the dark components of the Universe, which represent 95% of the energy content of the Universe?

There is little, if any, hope to detect directly dark energy at LHC or any future collider: in the example of quintessence, the scalar field which constitutes dark matter is extremely light (its mass is provided by the Hubble constant H_0, see for example [2], which is 10^{-33} eV) and must have sub-gravitational strength couplings to ordinary matter; otherwise, its exchangewould generate a new long range force. On the other hand, since dark energy is leading the recent cosmological evolution of the Universe, it may have some indirect consequences on the way we may interpret from cosmological point of view some of results of LHC. We will return to this point at the end of this section.

The situation is quite different for dark matter. It is well-known that models of particle physics provide candidates for dark matter, under the form of a Weakly Interacting Massive Particle (WIMP). The best known is the neutralino of supersymmetric models.There is in fact a deep connection between the question of the naturalness of the electroweak scale and the presence of a WIMP in a theory.

Let us start by recalling what is the naturalness problem (see for example the contribution of G. Giudice in this volume [1]). As is well-known, the Higgs squared mass m_h^2 receives quadratically divergent corrections. In the context of an effective theory valid up to a cut-off scale Λ where a more fundamental theory takes over, Λ is the mass of the heavy degrees of freedom of the fundamental theory. Their contribution in loops, quadratic in their mass, destabilizes the Higgs mass and thus the electroweak scale ($m_h^2 \sim \lambda v^2$ where λ is the scalar self-coupling and $v \sim 1/(G_F \sqrt{2})^{1/2} \sim 250$ GeV is the Higgs vacuum expectation value. More precisely, we have at one loop

$$\delta m_h^2 = \frac{3m_t^2}{2\pi^2 v^2}\Lambda_t^2 - \frac{6M_W^2 + 3M_z^2}{8\pi^2 v^2}\Lambda_g^2 - \frac{3m_h^2}{8\pi^2 v^2}\Lambda_h^2 \ , \qquad (17.2)$$

where for completeness we have assumed different cut-offs for the top loops (Λ_t), the gauge loops (Λ_g) and the scalar loops (Λ_h) [3]. The naturalness condition states that the order of magnitude of the Higgs mass is not destabilized by the radiative corrections i.e. $\left|\delta m_h^2\right| < m_h^2$. This translates into the conditions:

$$\Lambda_t > \sqrt{\frac{2}{3}}\,\frac{\pi v}{m_t}m_h \sim 3.5 m_h \ , \qquad (17.3)$$

$$\Lambda_g > \frac{2\sqrt{2}\pi v}{\sqrt{6M_W^2 + 3M_z^2}}m_h \sim 3.5 m_h \ , \qquad (17.4)$$

$$\Lambda_h > \frac{2\sqrt{2}\pi v}{\sqrt{3}}m_h \sim 1.3 \text{ TeV} \ . \qquad (17.5)$$

Thus one should introduce new physics at a scale Λ_t or raise m_h to the 400 GeV range (in which case we have a theory that makes sense only up to the scale Λ_h). We will illustrate our argument with three examples: supersymmetry, extra dimensions, and the inert doublet model recently proposed by Barbieri, Hall and Rychkov [3]. In the first two cases, one introduces new physics at the scale Λ_t (supersymmetric particles or Kaluza-Klein modes). In the latter case, one introduces a second Higgs doublet H_2 which is not coupled to fermions (through a symmetry $H_2 \to -H_2$): this allows to raise the ordinary Higgs mass to the 400 GeV level.

Typically, these models require the presence of a symmetry that prevents direct coupling between the Standard Model (SM) fermions and the new fields that one has introduced: otherwise, such couplings introduce new mixing patterns incompatible with what is observed in flavor mixings (compatible with the Standard Model). This symmetry is usually a parity (i.e. a discrete symmetry) which is the low energy remnant of a continuous symmetry which operates at the level of the underlying fundamental theory: SM fermions are even under this parity whereas the new fields are odd. Among these new fields, the lightest odd-parity particle (we will refer to it as the LOP) is stable: it cannot decay into SM fermions because of the parity; it cannot decay into the new fields because it is the lightest. It is massive and weakly interacting. It thus provides an adequate candidate for a WIMP.

Let us take our examples in turn. In the case of supersymmetry, the parity operation is R-parity (which usually proceeds from a continuous R-symmetry broken by gaugino masses i.e. supersymmetry breaking). And the LOP is the Lightest Supersymmetric Particle, the famous LSP, the lightest neutralino in the simplest models.

In the case of extra dimensions, say a 5-dimensional model, the local symmetry is 5-dimensional Lorentz invariance. It ensures conservation of the Kaluza-Klein levels: if $A^{(n)}$ is the nth Kaluza-Klein mode of the massless 5-dimensional field A (in other words, the 4-dimensional field with mass $m = n/R$, where R is the radius of the 5th dimension), then in the reaction $A^{(n)} + B^{(p)} \to C^{(q)} + D^{(r)}$, we have $n + p = q + r$. At energies smaller than R^{-1}, this turns into a Kaluza-Klein parity $(-1)^n$. The LOP is then the lightest Kaluza-Klein mode, usually $B^{(1)}$, the first mode of the $U(1)_Y$ gauge boson [4].

In the final example of the inert doublet model [3], the parity operation is $H_2 \leftrightarrow -H_2$, the new fields are the inert scalars i.e. the components of this H_2 doublet and the LOP is the lightest inert scalar.

In all cases, one may compute the relic density (see for example [2]) in terms of the average annihilation cross-section times velocity $\langle \sigma_{\mathrm{ann}} v \rangle$:

$$\Omega_{\mathrm{LOP}} h_0^2 \sim \frac{10^9 \ \mathrm{GeV}^{-1}}{g^{*1/2} M_P} \frac{x_f}{\langle \sigma_{\mathrm{ann}} v \rangle} \ , \tag{17.6}$$

where g^* is the number of degrees of freedom at the time of decoupling, $x_f \sim 25$. Since the LOP mass is of the order of the electroweak mass M_{EW}, we have $\langle \sigma_{\mathrm{ann}} v \rangle \sim \alpha_{EW} / M_{EW}^2$ and thus $\Omega_{\mathrm{LOP}} h_0^2$ is of order 10^{-1} to 1 to be compared with the WMAP result: $\Omega_{\mathrm{DM}} h_0^2 = 0.1099 \pm 0.00062$ [12].

In realistic models, there is often the possibility that other odd-parity fields are almost degenerate in mass with the LOP. This leads to the possibility of co-annihilations, that is annihilations of the LOP against these almost degenerate fields. This leads to a modification of the relic density in the corresponding region of parameter space (a decrease in the supersymmetric case, an increase in the Kaluza-Klein case, as illustrated in Fig. 17.1).
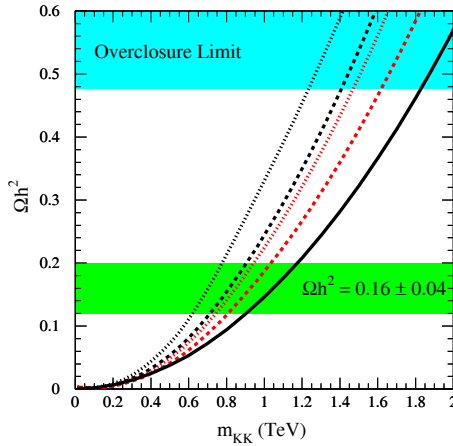

Fig. 17.1. Prediction for $\Omega_{B^{(1)}} h_0^2$. The solid line is the case for $B^{(1)}$ alone, and the dashed and dotted lines correspond to the case in which there are one (three) flavors of nearly degenerate $e_R^{(1)}$. There are several curves associated with various values of the mass difference between the $e_R^{(1)}$ and $B^{(1)}$ [4].

The search at LHC is based on the missing energy signal corresponding to the LOP (see top panel of Fig. 17.2). Since LOP are produced in pairs, they are difficult to reconstruct in all generality [7]. But, in the case of a specific model, one may be able to reconstruct the mass of the LSP as well as the relic density, as shown on Fig. 17.3 for the case of supersymmetry [8]. In parallel, one may search for the LOP through direct detection (see bottom panel of Fig. 17.2).

If a possible candidate for dark matter is detected at the LHC, we will find ourselves in an interesting situation because we have at least two other sources of information:

- Direct detection of particles forming the halo: the next generation of experiments will provide a senstivity allowing to probe regions of parameter space similar to the one made accessible by the LHC (for example in the case of supersymmetry).
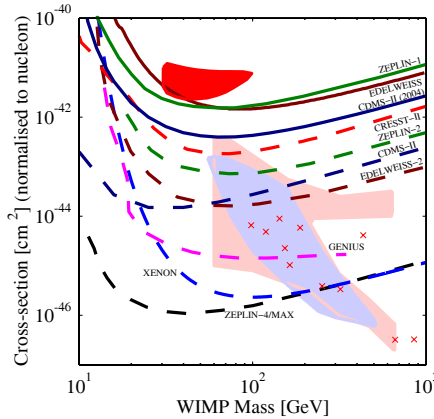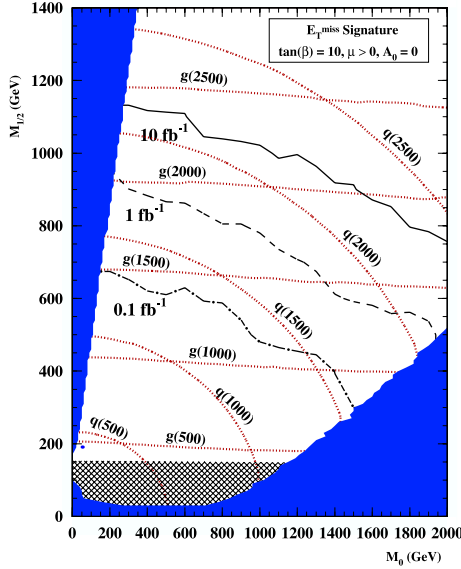
Fig. 17.2.   (Top) Contours in a parameter space of supersymmetry models for the discovery of the missing energy plus jets signature of new physics by the ATLAS experiment at the LHC. The three sets of contours correspond to levels of integrated luminosity at the LHC (in fb^{-1}), contours of constant squark mass, and contours of constant gluino mass [5]. (Bottom) Sensitivities of some running and planned direct detection dark matter experiments to the spin-independent elastic scattering cross-section. Full curves correspond to limits from existing experiments, dashed curves to predicted sensitivities of future experiments. The full dark (red) region corresponds to the 3 σ allowed region from the DAMA experiment. The full light regions correspond to predictions in the light of WMAP data. The crosses correspond to neutralino masses and cross-sections predicted for post-LEP benchmark CMSSM models [6].
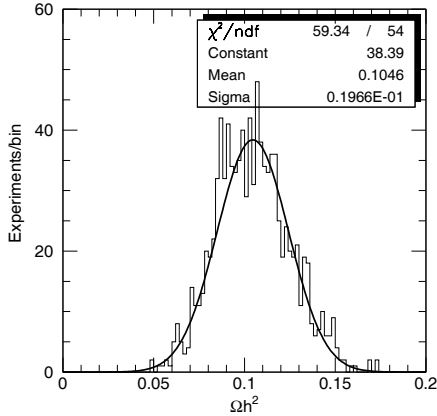
Fig. 17.3. Distribution of the predicted relic density $\Omega_\chi h_0^2$ for the SPA benchmark model incorporating the experimental errors (the uncertainty on the position of the $\tau\tau$ edge is assumed to be 5 GeV) [8].

- the rather precise knowledge of dark matter energy density provided by cosmology [12]: $\Omega_{\mathrm{DM}} h_0^2 = 0.1099 \pm 0.00062$

I have not included in this list indirect detection of dark matter. Observations in the recent past have shown that it is difficult to disentangle production of particles through dark matter annihilation from production from standard (or non-standard) astrophysical sources. One may cite the observation by INTEGRAL of an intense 511 keV line in the galactic bulge which implies the annihilation of some 10^{43} positrons per second. Such a large production of positrons seemed difficult to account for with standard astrophysical sources. A possible alternative is the annihilation of a new form of light scalar dark matter [9]. Also, an excess found by EGRET in the galactic diffuse gamma ray flux [10] has been interpreted as resulting from dark matter annihilation, more specifically in a supersymmetric context, the annihilation of neutralinos in the 50 to 100 GeV mass range [11].

Let us now for illustration consider the case where a WIMP candidate χ of mass m_χ is found at LHC, and direct detection identifies a WIMP candidate η of mass m_η (possibly identical to χ, in which case obviously $m_\eta = m_\chi$. The detailed study of χ interactions may LHC may provide an order of magnitude of its annihilation cross-section[a] and thus, through

---

[a]Not more than an order of magnitude since not all channels may be identified. In the supersymmetric case, one may think of identifying the LSP content (in terms of Higgsinos and gauginos) but this will be difficult in ageneric case. I thank Leonardo Sala for detailed discussions of this issue.

Table 17.1.   The most probable solutions to the identity of the dark matter based on outcomes at the LHC and direct searches.

	$\Omega_\chi < \Omega_{DM}$	$\Omega_\chi \sim \Omega_{DM}$	$\Omega_\chi > \Omega_{DM}$
$m_\chi < m_\eta$	Several DM components $(\chi, \eta, \cdots)$	Why no direct detection of χ?	Late inflation
$m_\chi \sim m_\eta$	Non-standard cosmology (kination?)	**Standard case** $\chi = \eta$ **is dark matter**	Late inflation
$m_\chi > m_\eta$	χ decays invisibly (compute Ω_η)	χ and η DM components but $\langle\sigma_{\text{ann}}v\rangle_\eta \gg \langle\sigma_{\text{ann}}v\rangle_\chi$	χ decays invisibly (compute Ω_η)

(17.6), of the corresponding relic density Ω_χ. We might find ourselves in the following situations:

- within experimental errors, m_χ is larger, equal or smaller than m_ϕ,
- Ω_χ is much larger, much smaller or of the same order of magnitude as the observed Ω_{DM}.

Table 17.1 summarizes the most probable solutions for each of the possible cases.

We may illustrate the discussion for the case $m_\chi \sim m_\eta$ and $\Omega_\chi < \Omega_{DM}$. Most probably, χ and η are identical and form the dark matter. It remains to explain why the relic density computed using (17.6) does not coincide with the observed value Ω_{DM}. The most plausible explanation is that the cosmological evolution at the dark matter freeze-out transition is non-standard. For example, if a quintessence field is the source of dark energy, it could be that, at freeze-out, we are in a phase dominated by the kinetic energy of the quintessence field (which decreases with the cosmic scale factor $a(t)$ as a^{-6}, thus becoming rapidly subdominant with respect to radiation which scales as a^{-4}). This tends to increase the estimation of the dark matter density Ω_χ [14], possibly by several orders of magnitude [13].

17.3. The Gravitational Side of LHC

If the LHC is associated with tests of the three fundamental gauge interactions, its association with the gravitational interaction is not immediate. There are however remarkable connections. I will discuss two: how the space interferometer LISA may probe the electroweak phase transition and

more generally may provide an investigation of the terascale region truely complementary to LHC; how the LHC may probe the formation and evaporation of black holes.

17.3.1. *Phase transitions at the terascale:*
the LHC-LISA connection

The energy reach of the LHC is perfectly suited to study the breaking of the electroweak symmetry and, in all probability, to discover the Higgs particle. We should know by the beginning of the next decade the details of the electroweak symmetry breaking sector, and whether it is described by the Standard Model or by a more complex theory.

There is a corresponding phase transition in the evolution of the Universe at $T \sim 100$ GeV. How could we observe it? Direct observation using photons is hopeless: the Universe was opaque until recombination, which happened much later ($T \sim 0.26$ eV). The Universe on the other hand is "transparent" to gravitons. As we will now see, it turns out that gravitons produced at the electroweak phase transition fall precisely in the LISA frequency window. Hence, LISA may provide the way to study the details of the electroweak phase transition.

LISA is a space interferometer designed to detect gravitational waves in the frequency window $[10^{-4}, 10^{-1}]$ Hz. It will allow to study black holes with high precision. It will observe how massive black holes form and interact over the entire history of galaxy formation. It will also record the inspirals and mergers of binary black holes and allow precision measurements of these systems. And it will study in detail thousands of compact binary stars, which provides a new window into reconstructing the history of stars in our galaxy.

The case for LISA as an observer for cosmology has become stronger in recent years. As we will see in what follows, this rests on the fact that LISA provides a unique way to test theories in the Terascale region.

Gravitational waves provide an ideal means to study the primordial universe because they are a fossil radiation: gravitons decoupled very early from the thermal evolution of the Universe.

If gravitons were in thermal equilibrium, their spectrum would be, just as photons, a blackbody spectrum (at a slightly different temperature [15]: $T \sim 0.91$ K). One easily checks however that they cannot be thermally coupled beyond the Planck era. Indeed, their interaction rate scales like G_N^2 and is thus on dimensional grounds $\Gamma \sim G_N^2 T^5 \sim T^5/m_P^2$. This should be

compared with the expansion rate $H \sim T^2/m_P$ (in the radiation-dominated era). Thus

$$\frac{\Gamma}{H} \sim \frac{T^3}{m_P^3} \ . \tag{17.7}$$

Thus gravitons are decoupled from the thermal evolution ($\Gamma < H$) past the Planck era.

Gravitons produced at a later stage, say at temperature T_*, will not evolve, except for their frequency being redshifted by the expansion of the Universe: if it is f_* at T_* (cosmic scale factor a_*), it is observed presently ($T_0 = 2.7$ K, $a = a_0$) at f where $f/f_* = a_*/a_0 \sim T_0/T_*$. More precisely, assuming that the original wavelength λ_* is a fraction ϵ of the horizon length ($\lambda_* = \epsilon H_*^{-1}$ or $f_* = H_*/\epsilon$), we have [16]

$$f = 1.65 \ 10^{-7} \ \text{Hz} \ \frac{1}{\epsilon} \left(\frac{T_*}{1 \ \text{GeV}}\right) \left(\frac{g_*}{100}\right)^{1/6} \ , \tag{17.8}$$

where g_* is the effective number of degrees of freedom. We see that $T_* \sim$ 1 TeV with $g_* \sim 100$ and $\epsilon \sim 1$ yields $f \sim 1$ mHz, right in the LISA frequency window. Hence LISA is the ideal gravitational detector to probe the terascale region, and in particular the electroweak phase transition.

The next question is thus the production of gravitons in a phase transition. If the phase transition is second order, it is smooth and there is basically no production of energy in the form of gravitational waves. On the other hand, a first order phase transition proceeds through the nucleation of true vaccum bubbles inside the false vacuum. The collision of bubbles and the turbulent motion that it causes lead to the production of gravitational waves.

The two relevant parameters to discuss this production are (i) the ratio α of energy density available in the false vacuum to the radiation energy density at transition, (ii) the time variation beta of the bubble nucleation rate (β^{-1} measures the duration of the phase transition). Detection of the gravitons produced requires a phase transition which is strongly first order ($\alpha > 1$) and long enough ($\beta^{-1} > 10^{-3}H^{-1}$).

Let us now review the possible phase transitions in the Terascale region. We start with the electroweak phase transition. In the context of the Standard Model, the constraint that $m_H > 72$ GeV tells us that the transition is not first order. In the MSSM, it requires a light stop, which is almost ruled out. It is however possible to recover a strong first order phase transition by including non-renormalizable terms of order H^6 in the

Higgs potential [17] (such terms appear in effective theories and may be significant if the scale of the underlying theory is just above the TeV scale) or by going to non-minimal supersymmetric models (such as the nearly Minimal Supersymmetric Standard Model or nMSSM [18]). If it is found out at LHC that the phase transition is indeed first order, then LISA would provide a remarkable complementary means of testing the phase transition with gravitational waves!

Even if the electroweak phase transition is not first order, we know that the phase transition associated with baryogenesis must be so: one of the Sakharov conditions for baryon number generation is to be out of equilibrium, which favors first order phase transitions over second order ones. The corresponding frequency at which one expects gravitational waves depends mainly on the scale at which the corresponding phase transition occurs, as can be seen from (17.8).

In fact, LISA reach is even higher than LHC and one may expect to probe phase transitions in the 10 TeV range. An example is provided by the Randall Sundrum I model [19], where the phase transition is thought to be strongly first order [20]. This phase transition can be probed for Kaluza-Klein scales as large as a few tens of TeV [21].

17.3.2. *Black hole physics and the LHC*

The proposal that there exists some large extra special dimensions allows to consider the (remote) possibility to produce mini black holes at LHC, thus giving a unique possibility to study the physics of black holes (production, Hawking radiation,...). We recall that, in theories with n extra spatial dimensions of same radius R (to simplify), the 4-dimensional Planck mass $(G_N = m_P^{-2})$ is given in terms of the more fundamental $(D = 4+n)$-dimensional gravitational constant $(G_D = M_D^{2-D})$ as

$$m_P^2 = M_D^{2+n} R^n \ . \tag{17.9}$$

Taking R large enough allows to decrease M_D to the TeV range. This usually occurs for values of R which have been probed by non-gravitational interactions at colliders. Since the search for extra dimensions at high energy colliders has been negative, this means that, if they exist, these extra dimensions should only be probed by gravitational interactions.[b] It turns out that string theory provides models of spacetime where non-gravitational

---

[b]The law of gravitational attraction (in r^{-2} as is characteristic of 3 space dimensions) has been probed only down to the mm to μm range.

interactions are localized on dynamical surfaces known as p-branes (p stands for the number of space dimensions of the brane). In the case of a 3-brane, the non-gravitational interactions are localized in the 3-dimensional space of the brane; only gravitational interactions probe the extra dimensions.

In the case where M_D is in the TeV range, we are in the lucky situation where LHC is going to experimentally probe the gravitational realm. This means quite a dramatic departure from Standard phenomenology. In particular, collisions may lead to a such a localization of energy that black holes are formed [22, 23], just as in the primordial universe where energy fluctuations generate primordial black holes[c]. More precisely, the relevant scale for a collision at energy $E \gg M_D$ is the Schwarzschild radius:

$$r_S \sim \frac{1}{M_D} \left(\frac{E}{M_D} \right)^{1/1+n} .$$
(17.10)

A black hole forms in the collision if the impact parameter is smaller than r_S. A lower bound for the mass M_{BH} is typically $0.7E$. The cross section (at the parton level) is

$$\sigma = \pi r_S^2 .$$
(17.11)

The semi-classical approximation used to derive the formulas above is valid for a minimal black hole mass $(M_{BH})_{min} \equiv x_{min} M_D$. Taking $x_{min} = 5$ and $M_D = 1$ TeV, the minimum parton energy E is around 7 TeV. Corresponding cross-sections are in the 10^3 fb range [24]: one black hole produced every minute for a nominal LHC luminosity of 10^{34} cm^{-2}.s^{-1}.

Just as primordial black holes eventually disappear because of Hawking evaporation, the black holes produced evaporate rapidly. Hawking radiation is characterized by the temperature:

$$T_H = \frac{n+1}{4\pi r_S} .$$
(17.12)

The energy loss scales like $dE/dt \propto T_H^{4+n}$. Thus the black hole lifetime is typically

$$\tau_{BH} \sim \frac{1}{M_D} \left(\frac{M_{BH}}{M_D} \right)^{3+n/1+n} .$$
(17.13)

Black holes decay visibly to SM particles with: (i) a large multiplicity ($N \sim M_{BH}/(2T_H)$), (ii) a large total transverse energy, (iii) a characteristic ratio of hadronic to leptonic activity of 5 : 1.

[c]As originally studied by Penrose in the case of vanishing impact parameter, the collision forms a closed trapped surface which, according to the area theorem of general relativity, corresponds to the formation of a black hole.

For what concerns us here, there is a complementarity of searches at colliders (LHC) and in high energy cosmic rays. In the Pierre Auger Observatory, one is precisely looking for the highest energy cosmic rays. It is thus of interest to try to search for signals of black hole production. More precisely, in order to overcome the QCD background, one is looking for such a production by high energy neutrinos (found more frequently in horizontal showers since those are the ones that travel through more atmosphere). Fig. 17.4 gives, for $n = 6$ extra dimensions, the discovery reach for the LHC in the plane (M_D, x_{min}), to be compared with the region of parameter space excluded at 95% C.L. if no neutrino shower induced by black holes is observed at Pierre Auger observatory in 5 years.
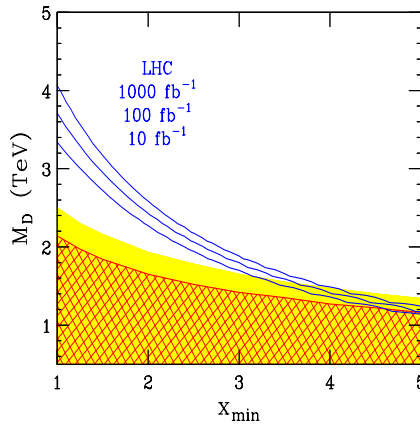

Fig. 17.4. Comparison of the regions covered by LHC (with respective integrated luminosities 1000, 100 and 10 fb^{-1}) and the Pierre Auger Observatory in 5 years in the plane (M_D, x_{min}) [25].

17.4. Conclusion

The experimental checklist of the decade 2008-2017 might read as such:

- light Higgs, heavy Higgs or no Higgs observed,
- observation or absence of supersymmetric partners,
- observation or absence of Kaluza-Klein modes, of microscopic black holes,
- direct detection of WIMPs, or limit on its mass; indirect signal of WIMP annihilation or no clear signal; detection of other kinds of dark matter; astrophysical observations pointing towards another solution of the dark matter problem (MOND,...),

- detection or not of a gravitational background in CMB experiments; detection or not of a stochastic background of primordial gravitational waves at space or ground interferometers,
- cosmological observation of some dynamical behaviour of dark energy or consistency of all observations with a cosmological constant,

and so on. There exists a standard scenario which has been alluded to in the introduction (supersymmetric version of the SM as a low energy effective theory of a string/brane theory valid at the Planck scale). In this scenario, one expects a light Higgs, supersymmetric partners, no low energy Kaluza-Klein modes; one is likely to detect a WIMP, directly and indirectly, but no background of gravitational waves. With such a variety of data expected, there are however many ways to deviate from such a scenario. This is why the decade that we are entering is an exciting time for the fields of particle and astroparticle physics and cosmology, LHC being the lead actor in the play that is about to begin.

References

[1] G. Giudice, Naturally speaking: the naturalness criterion and physics at the LHC, this volume, arXiv:0801.2562 [hep-ph]

[2] P. Binétruy, *Supersymmetry: Theory, experiment and cosmology*, (Oxford University Press, Oxford, UK, 2006).

[3] R. Barbieri, L.J. Hall and V.S. Rychkov, Improved naturalness with a heavy Higgs: An alternative road to LHC physics *Phys. Rev. D* **74**, 015007 (2006) [arXiv:hep-ph/0603188].

[4] G. Servant and T.M.P. Tait, Is the lightest Kaluza-Klein particle a viable dark matter candidate?, *Nucl. Phys. B* **650**, 391 (2003) [arXiv:hep-ph/0206071].

[5] D.R. Tovey, Inclusive SUSY searches and measurements at ATLAS, *Eur. Phys. J. direct C* **4**, N4 (2002).

[6] M. Battaglia, I. Hinchliffe and D. Tovey, Cold dark matter and the LHC, *J. Phys. G* **30**, R217 (2004) [arXiv:hep-ph/0406147].

[7] M. Battaglia and M.E. Peskin, The Role of the ILC in the study of cosmic dark matter, [arXiv:hep-ph/0509135].

[8] M. M. Nojiri, G. Polesello and D. R. Tovey, Constraining dark matter in the MSSM at the LHC, *JHEP* **0603**, 063 (2006) [arXiv:hep-ph/0512204].

[9] C. Boehm, D. Hooper, J. Silk, M. Cassé and J. Paul, MeV dark matter: Has it been detected? *Phys. Rev. Lett.* **92** (2004) 101301.

[10] S.D. Hunter at al., EGRET observations of the diffuse gamma-ray emission from the galactic plane. *Astrophys. J.* **481** (1997) 205.

[11] W. de Boer et al., The Supersymmetric interpretation of the EGRET excess of diffuse galactic gamma rays, *Phys. Lett. B* **636**, 13 (2006) [arXiv:hep-ph/0511154]

[12] J. Dunkley *et al.* [WMAP Collaboration], Five-Year Wilkinson Microwave Anisotropy Probe (WMAP) Observations: Likelihoods and Parameters from the WMAP data, arXiv:0803.0586 [astro-ph]

[13] D. Chung, L. Everett, K. Kong and K.T. Matchev, Connecting LHC, ILC and quintessence, *JHEP* **0710**, 016 (2007), arXiv:0706:2375 [hep-ph].

[14] P. Salati, Quintessence and the relic density of neutralinos, *Phys. Lett. B* **571**, 121 (2003) [arXiv:astro-ph/0207396].

[15] R. Kolb and M. Turner, The early Universe, *Frontiers in Physics* **69** 1–547 (1990).

[16] M. Maggiore, Gravitational wave experiments and early universe cosmology, *Phys. Rep.* 331, 283 (2000).

[17] C. Grojean, G. Servant and J. D. Wells, First-order electroweak phase transition in the standard model with a low cutoff, *Phys. Rev. D* **71** (2005) 036001 [arXiv:hep-ph/0407019].

[18] A. Menon, D. E. Morrissey and C. E. M. Wagner, Electroweak baryogenesis and dark matter in the nMSSM, *Phys. Rev. D* **70** (2004) 035005 [arXiv:hep-ph/0404184].

[19] L. Randall and R. Sundrum, A large mass hierarchy from a small extra dimension, *Phys. Rev. Lett.* **83** (1999) 3370 [arXiv:hep-ph/9905221].

[20] P. Creminelli, A. Nicolis and R. Rattazzi, Holography and the electroweak phase transition, *JHEP* **0203** (2002) 051 [arXiv:hep-th/0107141].

[21] L. Randall and G. Servant, Gravitational Waves from Warped Spacetime, *JHEP* **0705** (2007) 054 [arXiv:hep-ph/0607158].

[22] T. Banks and W. Fischler, A model for high energy scattering in quantum gravity, [arXiv:hep-th/9906038].

[23] S. B. Giddings and E. Katz, Effective theories and black hole production in warped compactifications, *J. Math. Phys.* **42** (2001) 3082 [arXiv:hep-th/0009176].

[24] S. B. Giddings, High-energy black hole production, *AIP Conf. Proc.* **957** (2007) 69, arXiv:0709.1107 [hep-ph].

[25] L.A. Anchordoqui, *et al.* Inelastic black hole production and large extra dimensions, *Phys. Lett. B* **594**, 363 (2004) [arXiv:hep-ph/0311365].